Polymeric Drug Delivery Systems for Biological Antimicrobial Agents

Chongyu Zhu

A thesis submitted in partial fulfilment of the requirements of the degree of Doctor of Philosophy in Chemistry

Department of Chemistry

University of Warwick

April 2017

Table of Contents

List of Figures

List of Tables

List of Schemes

Abbreviations

aaPEG	acetic acid terminated poly (ethylene glycol) methyl ether
ABCD	amphotericin B colloidal dispersion
AmBd	amphotericin B micellar deoxycholate complex, Fungizone™
ABLC	amphotericin B lipid complex
ACN	acetonitrile
AcOH	acetic acid
AEE	2-(2-aminoethoxy) ethanol
AmB	amphotericin B
APPEGA	poly(poly(ethylene glycol) methyl ether acrylate) with an acrylate end-group
ATRP	atom transfer radical polymerisation
BHT	butylated hydroxytoluene
BMPAA	2-(2-bromo-2-methylpropanoyloxy) acetic acid
Boc	*tert*-butyloxycarbonyl
Boc_2O	di-*tert*-butyl dicarbonate
$B_{pin}A$	4-(4,4,5,5-tetramethyl-1,3-dioxolan-2-yl)benzyl acrylate
BzA	benzyl acrylate
CAMHB	cation-adjusted Mueller-Hinton broth
CCK-8	cell count kit-8
$CDCl_3$	deuterated chloroform
CHCA	α-cyano-4-hydroxycinnamic acid
CFU	colony-forming unit
CMC	critical micelle concentration
CMS	colistimethate sodium

col	colistin
CP-LRP	copper-mediated photoinduced living radical polymerisation
CRP	controlled radical polymerisation
$CuBr_2$	copper(II) bromide
Cys	cysteine
Đ	dispersity
D_2O	deuterated water
Dab	2,4-diaminobutyric acid
DCC	*N*,*N'*-dicyclohexylcarbodiimide
DCTB	*trans*-2-[3-(4-*tert*-butylphenyl)-2-methyl-2-propenylidene] malononitrile
DCM	dichloromethane
DF-PEG	4-formylbenzoic acid difunctionalised poly(ethylene glycol)
DIPEA	*N*,*N*-diisopropylethylamine
DMAP	4-dimethylaminopyridine
DMF	dimethylformamide
DMSO	dimethyl sulfoxide
DP	degree of polymerisation
EBiB	ethyl α-bromoisobutyrate
EDC·HCl	*N*-(3-dimethylaminopropyl)-*N*'-ethylcarbodiimide hydrochloride
EPR	enhanced permeability and retention
ESI-MS	electrospray ionisation-mass spectrometry
FBA	4-formylbenzoic acid
FPLC	fast protein liquid chromatography

FTIR	Fourier transform infrared spectrometry
FPy	2-formylpyridine
F/S MQH_2O	filtered and sterilised Milli-Q grade water
G'	storage modulus
G''	loss modulus
GO	graphene oxide
GPC	gel permeation chromatography
HBA	4-(hydroxymethyl)phenylboronic acid
HCl	hydrochloride
HEA	2-hydroxyethyl acrylate
HG-5/10	hydrogels formed from 3% w/w glycol chitosan solution and either 5% or 10% w/w DF-PEG solution
HOBt	1-hydroxybenzotriazole
HPLC	high performance liquid chromatography
I	intergration
IE	ion-exchange
K_2CO_3	potassium carbonate
K_a/K_b	acid/base dissociation constant
L-AmB	amphotericin B liposome, i.e., AmBisome®
LC_{20}	the lethal concentration of 20% cell death
LiBr	lithium bromide
LPS	lipopolysaccharide
MA	methyl acrylate
MALDI-ToF MS	matrix-assisted laser desorption/ionisation-time of flight mass spectrometry

MDR	multidrug resistant
Me_6TREN	tris[2-(dimethylamino)ethyl]amine
MeOH	methanol
$MgSO_4$	magnesium sulfate
MIC	minimum inhibitory concentration
M_n	number average molar mass
mPEG	poly(ethylene glycol) methyl ether
mPEG-FBA	FBA modified mPEG
MS/MS	tandem mass spectrometry
Na_2CO_3	sodium carbonate
Na_2SO_4	sodium sulphate
Na_2HPO_4	disodium hydrogen phosphate
NaAc	sodium acetate
$NaBH_3CN$	sodium cyanoborohydride
$NaHCO_3$	sodium bicarbonate
NaH_2PO_4	sodium dihydrogen phosphate
NaOMe	sodium methoxide
NHS	*N*-hydroxysuccinimidyl
NMR	nuclear magnetic resonance
Nys	nystatin
OD	optical density
PBA	phenylboronic acid
PBS	phosphate buffered saline
$PB_{pin}A$	poly(4-(4,4,5,5-tetramethyl-1,3-dioxolan-2-yl)benzyl acrylate)
PBzA	poly(benzyl acrylate)

PAA	poly(acrylic acid)
PAM	polyacrylamide
PAMPS	poly(2-(acrylamido)-2-methylpropanesulfonic acid
PEG	poly(ethylene glycol)
PEGA	poly(ethylene glycol) methyl ether acrylate
PEGMA	poly(ethylene glycol) methyl ether methacrylate
PHEMA	poly(2-hydroxyethyl methacrylate
PHPMA	poly(*N*-(2-hydroxypropyl) methacrylamide
p*Ka*	acid dissociation constant at logarithmic scale
PMAA	poly(methacrylic acid)
PMMA	poly(methyl methacrylate)
PNIPAM	poly(*N*-isopropylacrylamide)
Pol-SH	$Thr^{10} \rightarrow$ Cys polymyxin B
PPEGA	poly(poly(ethylene glycol) methyl ether acrylate)
PPEGMA	poly(poly(ethylene glycol) methyl ether methacrylate)
PVA	poly(vinyl alcohol)
PVP	poly(vinylpyrrolidone)
PREP HPLC	preparative high performance liquid chromatography
RAFT	reversible addition−fragmentation chain transfer polymerisation
saPEG	succinic acid functional mPEG
SD	standard deviation
SET-LRP	single-electron transfer living radical polymerisation
T	time
tBuOH	*tert*-butanol

tBuOK	potassium *tert*-butoxide
TCEP	tris(2-carboxyethyl)phosphine
TEA	triethylamine
TEM	transmission electron microscopy
TFA	trifluoroacetic acid
THF	tetrahydrofuran
Thr	threonine
TLC	thin layer chromatography
Vis	visible
UV	ultraviolet
ZoI	zone of inhibition

Acknowledgements

I would like to thank my supervisor, Prof. David M. Haddleton, for helping me on my scholarship and giving me the opportunity to be a member of Haddleton group. Great appreciation toward your encouragement and support throughout my PhD. I am really grateful for your influence on me through your positive attitude to science and life (‘just do it’), inspiring thoughts and communication skills.

Specially thanks go to Prof. Lei Tao, not only for his recommendation to initiate my PhD with Dave, but also the continuous helps and supports on my work and life during my PhD. Thank you for the prompt replies, helpful discussions and advices and quick tests for my work. Working with you has been very happy and inspiring and will have great impact on my future life and career.

I also would like to express my gratitude to Dr. Kristian Kempe and Dr. Paul Wilson, my ‘senior’ friends who have got involved and contributed a lot to my work and provide endless ideas and help. Many thanks for your delicated and careful ideas for my work and your kind words and suggestions whenever I felt depressed.

Enormous thanks go to our Monash collaborators (Prof. Jian Li, Prof. Thomas P. Davis, Dr. Tony Velkov, Dr. Jiping Wang, Dr. Michael Whittaker, Heidi Yu, Jinxin Zhao, and Elena K. Schneider) and our Tsinghua research team (Prof. Lei Tao, Prof. Xing Wang, Dr. YalingZhang, Guoqiang Liu) from the other side of the world. Despite the physical distance and the time difference, your expertise and passion to my work have been delivered successfully through countless emails and calls. Speical thanks to Prof. Jian Li and Dr. Michael Whittaker for the warmest welcome and the thoughtful arrangement for my two-month stay in MIPS.

I would also like to thank all my colleagues from the polymer groups for accompanying with me over the years. Firstly, as Danielle said, 'Everyone is the best. Especially Danielle.' Special thanks to my 'lunch-mates' and 'squash teammates', Danielle, Nuttapol and Sam who have been providing me laughters all the times with interesting talks. Secondly, huge thanks to Dr. Alex Simula, Dr. Daniel Lester, Dr. Jennifer Collins, Emma Tombs and Dr. Monika Prokesova for the instruments and lab maintenances in our lab during my PhD. Thirdly, thanks to Richard and Dr. Vasiliki Nikolaou for the discussion and help on the polymerisation of my 'special' monomers. Fourthly, many thanks to my former colleagues, Jenny K. Kiviaho, Dr. Olivier Bertrand, and Dr. Gabit Nurumbetov all the good memories and grateful help. Finally, to all my Chinese colleagues (Prof. Qiang Zhang, Dr. Muxiu Li, Zaidong Li), especially Muxiu, thank you for the guidances and the helps on both my work and life.

I would also like to thank Prof. Sebastien Perrier, Prof. Stefan Bon and Prof. Matthew I. Gibson for the advice and guidance they have provided during my PhD.

Special thanks to our great technicians and experts in our department, especially Dr. Lijiang Song (mass spectrometry) and Dr. Ivan Prokes (NMR), for the careful analysis and helpful instructions on my tricky samples with great patience and no complaints. Great appreciation to Jason Noone for the quick responses for all my IT problems, Philip Aston for explaining these comprehensive mass spectrometry training in an easy way, Peter Brindley for the quick fabrication of the perfect glass equipments, Dr. Richard Beanland and Dr. Houari Amari for the prompt TEM training and analysis and Dr. Hasan Imam for the detail explanations and great help on FPLC analysis. Huge thanks to the store staffs (Steve, Phil, David and Gemma) for being extremely nice to meet my needy requests and help to find my countless orders.

I would also like to thank all my colleagues and friends who are a great support to my PhD. My ‘reference libraries’ (Dr. Yunqing Zhu, Dr. Ming Gong, and Shiqi Wang), my ‘personal IT technician’ (Junyi Yi), my own Monash-Warwick alliance (Prof. Jinming Hu and Dr. Qiuming Liu), my ‘polymer buddies’ (Dr. Yan Kang, Dr. Liang Sun, Dr. Xin Li, and Dr. Zengchao Tang, Junliang Zhang, and Sangho Won), the ‘badminton gang’ (Dr. Victor Quan, Wei Yu, Zan Hua and Yujie Xie), ‘Manchester squad’ (Manrui Zhang and Ziyi Wang) and all the members of ‘Shangdong tearoom’ (especially Dr. Guohui Zhang and Mi Yi) for all the helps, memorable times and delicious food.

Last but not least, I would like to thank my family and all my friends in China for all the patience, encouragement, supports and love to me for so many years. Thank you all for making my life colourful and enjoyful. This work would not have been done without your companion throughout the years.

Declaration

Experimental work contained in this thesis is original research carried out by the author, unless otherwise stated, in the Department of Chemistry at the University of Warwick, October 2013 and April 2017. No material contained herein has been submitted for any other degree, or at any other institution.

Results from other authors are referenced in the usual manner throughout the text.

Date:

_____

Chongyu Zhu

Abstract

The objective of this work was to develop suitable delivery systems for biological agents that have antimicrobial activities using biocompatible polymers, aiming to reduce their toxicity when administered. Two biological agents, colistin as an antibacterial agent and nystatin (Nys) as an antifungal agent, are the focus of this thesis as they are potent treatments for current pathogen infections, especially to the multidrug-resistant (MDR) bacteria/fungi, but have potential toxicity to human. Polymeric drug delivery systems, including prodrug, hydrogel and micelle formulations, have been developed and discussed for their potential as topical and systemic regimes.

The majority of the work was focused on the effect of the covalently attachment of synthetic polymers onto the biological agents upon their antimicrobial activities and the toxicity. The conjugation between colistin and polymers was achieved successfully through either irreversible or releasable linkages. Although irreversible polymer modifications on colistin showed no antimicrobial activity (chapter 2), an acceptable antibacterial activity was observed from the polymer-colistin conjugates with a releasable linkage through either 'grafting-to' (chapter 3) or 'grafting-from' (chapter 4) approaches. On the other hand, even though the pure polymer-Nys conjugate with a releasable imine linkage cannot be obtained due to the nature of the labile imine bond, the crude conjugate showed an excellent antifungal activity and a reduced toxicity compared to the native Nys (chapter 6).

Other polymeric delivery systems were also discussed in this thesis. The incorporation of colistin within a developed hydrogel delivery system as an antibacterial patch for burn infections was investigated through *in vitro* and *in vivo*

studies, showing a similar antibacterial activity as the native colistin solution against MDR Gram-negative bacteria with no systemic toxicity (chapter 5). Finally, an amphiphilic polymer containing boronic acid groups on the side chains was synthesised and used to target the hydroxyl groups on Nys, expecting to build up an environmental responsive micelle through dynamic boronate ester bond (chapter 7). Although more work is still needed, this system showed a potential to improve Nys solubility.

Chapter 1 *Introduction*

1.1 Biological Antimicrobial Agents

Biological antimicrobial agents are the biomolecules that are generated or discovered from a living organism or its products which can be used for human therapeutics against pathogenic microorganisms. Ever since the very first biological antimicrobial agent, penicillin,[1] was discovered by Alexander Fleming in 1928 and then applied clinically to treat infectious diseases, the long drawn fight between the micro-world and humans has not relented.[2, 3] Over the last decades, the infections caused by microorganisms, especially bacterial and fungal infections, remain a great physical and financial burden to all human beings.[4-11] Unfortunately, due to the increased use of these antimicrobial agents in recent years, more and more of these microorganisms have developed resistance to them. The emergence of multidrug-resistant (MDR) strains of bacteria/fungi has become a worrying prospect for all humanity.[7-9, 11, 12] While there is an urgent need for more novel antimicrobial agents, the development of new drugs normally takes years.[10, 13-15] Thus, some 'old' antimicrobial agents, e.g. colistin as an antibacterial agent and amphotericin B (AmB)/nystatin (Nys) as an antifungal agent, have now been reappraised and reused as 'last-line' treatments for microbial infections.[16-19] These agents are effective and incidents to resistance, to date, have been rare.[20] However, the use of these drugs is limited by concerns regarding systemic toxicity in humans, especially to the kidney, during administration.[21-23] Therefore, methods to reduce their toxicity while retaining activity were developed and discussed in this thesis.

1.1.1 MDR Gram-negative bacteria infections and colistin

Bacterial infections, especially drug-resistant infections are a major global health issue.[7-11, 19] The emergence of MDR Gram-negative 'superbugs' including *Pseudomonas aeruginosa, Acinetobacter baumanii, and Klebsiella pneumoniae*, threatens to undermine the efficacy of treatments in both the developed and developing world.[24-26] These problematic bacteria can easily spread within confined environments such as hospitals to immunodeficient patients,[27, 28] making the treatment of these patients more complex and problematic. A recent report suggests failing to control drug-resistant infections may cause in excess of 10 million deaths per year and cost up to US$ 100 trillion by 2050.[11] *P. aeruginosa*, for example, is a particularly problematic pathogen that is of concern worldwide.[26-30] These 'superbugs' are particularly difficult to treat due to the nature of their robust outer membrane.[31] Polymyxin, a type of anitibacterial lipopeptide, are one of the only few effective treatment options for these MDR Gram-negative infections.[32-35]

1.1.1.1 Chemical structure and the related activity of colistin

Colistin (polymyxin E), one important member of the polymyxin family, is a peptide-based antibiotic produced by Gram-positive bacteria such as *Paenibacillus polymyxa*.[20] It was first discovered in 1949 and had been used clinically in a salt form of colistin sulfate or in a prodrug form of colistimethate sodium (CMS) from the 1950s.[20, 36] Although it was later banned for use since in the 1980s due to the high incidence of nephrotoxicity,[34] it is now applied as a last-line therapy against infections, as a result of increased cases of resistance in less toxic therapeutics and limited discovery of new antibiotics.[33]

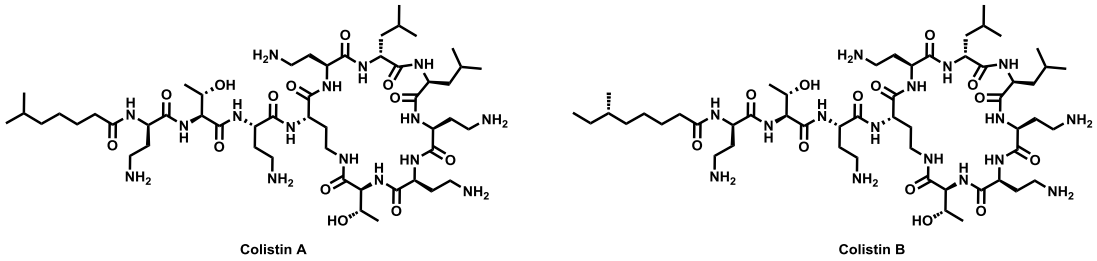

Figure 1.1 The chemical structure of the two major subgroups of colistin, colistin A (left) and colistin B (right).

Colistin is a cyclic lipopeptide constructed of an intramolecular hydrophilic peptide-based loop with a *N*-terminal fatty acyl group.[33, 37] The commercial colistin source contains two major active components, colistin A and colistin B, of which the only difference is on the *N*-terminal fatty acyl group; a 6-methyloctanoic acid for colistin A and isooctanoic acid for colistin B (Figure 1.1).[38] Both compounds are biologically active against Gram-negative bacteria, therefore, the mixture of colistin A and B are used directly in clinical colistin treatments.

The mechanism of colistin activity takes place at the bacterial outer membrane of the Gram-negative bacteria. The insertion of colistin can disrupt the barrier function of the Gram-negative outer membrane that ultimately cause the cell death.[18, 20, 37, 39] The amphiphilic structure formed by the hydrophilic amino acid residues (2,4-diaminobutyric acid (Dab) and threonine (Thr) residues) and two hydrophobic domains (the *N*-terminal fatty acyl group and the two hydrophobic residues) on colistin helps it to fold into a more compacted surfactant-like structure to achieve a better binding to the bacterial outer membrane. The five primary amine groups on the Dab residues of colistin, which are protonated under physiological condition, can recognise and electrostatically interact with the phosphorylated sugars on the lipid A component of the lipopolysaccharide (LPS), the major constituent of the outer membrane of Gram-negative bacteria. This interaction will displace the divalent cations (Mg^{2+} and

Ca^{2+}) within the LPS, causing the disruption of the bacteria outer membrane, further leading to bacteria lysis.

1.1.1.2 Potential toxicity of colistin

Even though colistin is a potent antibiotic against most Gram-negative bacteria, the potential toxicity is always of concern.[40-42] The major adverse effects of the administration of colistin are neurotoxicity (~7%) and nephrotoxicity (15-55%), particularly acute renal failure. Most patients that experience neurotoxicity are likely to have also had renal failure. Thus, many studies have focused on colistin nephrotoxicity to elucidate its mechanism. So far, several pathways including oxidative damage and inflammatory caspase (Caspase 1) have been reported to be involved in the nephrotoxicity mechanism.[42] The main cause of toxicity is considered to be closely related to its antimicrobial activity, with the five primary amine groups on the Dab residues and the *N*-terminal fatty acyl group of colistin being implicated. Although the clearance pathway of colistin is not fully understood, it is believed that colistin undergoes renal tubular reabsorption during the the clearance process, where it can also bind and be inserted into the tubular epithelial cell membrane. Thus, it would increase the permeability of the cell membrane causing cell swelling and cell lysis.

However, it is still possible to maintain the colistin antimicrobial activity and reduce its potential nephrotoxicity. One straightforward method is to alter the structure of colistin. Thanks to the development of automated solid-phase peptide synthesis, many polymyxin analogues have been synthesised and screened for their activity and toxicity.[37] Unfortunately, it was found many analogues possessed no or low antibacterial activity, indicating the interaction between colistin and the bacterial outer

membrane is crucially influenced by the chemical structure of colistin. Due to the small molecular weight of colistin as well as most functional groups are involved during the binding process, a single change on one residue can cause a dramatic change on the binding affinity, and result in a loss of its activity. To evaluate the effect of polymer modification on colistin, several approaches have been developed and will be discussed in chapter 2.

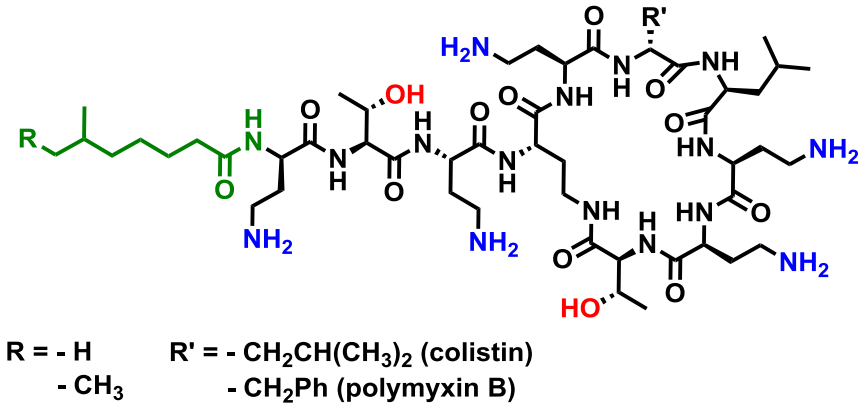

Figure 1.2 The possible modification sites for polymyxins, Dab amines (blue), hydroxyl groups (red), and terminal amine (green).

In order to modify the chemical structure of colistin while maintaining its activity, an alternative approach involves formulation of polymyxins into prodrugs.[43] The possible modification sites, terminal amine, Dab amines and hydroxyl groups, have been labelled in different colours in Figure 1.2. The terminal amine on colistin can be recovered through enzyme degradation on the *N*-terminal fatty acyl group.[44] The resultant polymyxin nonapeptide analogue exhibits a much lower toxicity with an acceptable antibacterial acitivty.[37] Therefore, it can be potentially fabricated into a prodrug.[45] However, the polymyxin nonapeptide analogue itself has a lower antibacterial activity compared to the native polymyxins, thus, no clinical product has been developed. The modification on polymyxin Dab residues is also possible and CMS, or colistimethate sodium, is one successful example. As an FDA approved

prodrug of colistin, it can be used intravenously in the clinic.[36] The prodrug is prepared by modification of the five primary amines to form methanesulfonate groups, which reduce the possibility of the interactions between colistin and the healthy human cells during the delivery process, making it is less toxic compared to the native colistin.[46] Despite this CMS still has some limitations that will be elaborated in chapter 3. To date, this is the only FDA approved colistin-based prodrug therapy available for clinic use. Another possible modification site that has been underestimated is to modify the hydroxyl groups on polymyxins. Although no prodrug has been developed through the hydroxyl group modification, the chemical engineering on polymyxin hydroxyl group(s) can potentially become a useful tool for formulation into a prodrug and has some advantages compared the other two modification methods. To demonstrate this possibility, two approaches for the development of polymeric colistin prodrugs have been addressed in chapter 3 and 4.

As nephrotoxicity is dose-dependant, an alternative approach to reducing the risk is to lower the dosage and therefore the overall systematic colistin concentration.[40, 42, 47] Owing to the differences between the bacteria and human cell membrane, it is possible to kill the bacteria at a low enough colistin concentration to avoid or limit the toxicity. The clinical studies suggested the potential risk of colistin nephrotoxicity can be suppressed by lowing the dose of colistin (in CMS prodrug form) during the administration, while the colistin concentration remains effective against the infection.[35] Alternatively, delivery of colistin through a topical delivery system in principle may also help to reduce the overall systematic colistin concentration while keeping the local colistin concentration high enough to kill the bacteria. To explore this concept, a hydrogel-based localised delivery system is developed in this thesis as well, which will be elaborated in chapter 5.

1.1.2 Fungal infection and polyene antimycotics

Although a large population of fungal species (> 5 million species) lives on the Earth,[48] less than 2 per mille (around 600 species) of them are considered to be human pathogens.[23] Some fungal infections (i.e., superficial and cutaneous infections) are mild and easy to treat thanks to the development of antifungal treatments, however, other fungal infections can sometimes be life-threatening.[23, 49-52] For example, *Candida albicans*, one of the most common fungi pathogens in clinic, is able to infect every human organ through the bloodstream, causing severe systematic damage to the patients.[53] Furthermore, the opportunistic invasive fungal infections, especially by Canadida pathogens, can easily cause cross-infection in immunocompromised patients in hospitals, which burdens the medical care and increases the cost of treatment.[54]

Before the other less-toxic synthetic antifungal drugs such as azoles and pyrimidine analogues have been developed over the last decades, the natural product polyene drugs, AmB in particular, was the standard treatment against these pathogens like *Candida* species.[23]

1.1.2.1 Structure and pharmaceutical behaviours of polyene antimycotics

Polyene antifungal agents are primarily produced by *Streptomyces* bacteria, a genus of *actinomycete* Gram-positive bacteria.[21, 23, 55-57] Although there are more than 200 analogues that have a similar antifungal activity, amongst them, AmB and Nys are the two most widely used polyene antifungal agents because of their acceptable clinical toxicity.[23] Both compounds are cyclic amphiphilic macrolides containing eight hydroxyl groups, a carboxyl group and a glycoside group on the main ring (Figure 1.3).[58, 59] The difference of the two structures is that AmB is a heptaene macrolide

(seven conjugated double bonds within the main ring) with two hydroxyl residues on position 5 and 6 while Nys is tetraene diene macrolide (two sets of conjugated double bonds, two and four, within the main ring) with two hydroxyl residues on position 4 and 7.

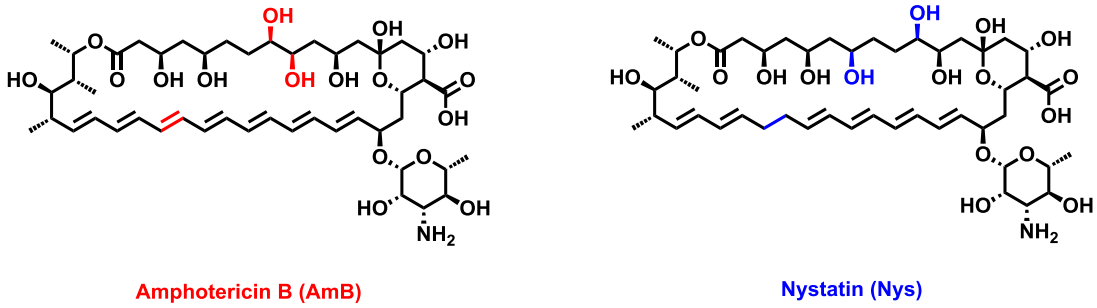

Figure 1.3 The difference between the chemical structures of the two polyene antifungal agents, AmB and Nys.

The colour difference between the two compounds (AmB has an orange colour while Nys is light yellow) is likely caused by the difference in the conjugation double bonds system of Nys, the similar chemical structure of AmB and Nys instils in them a similar physical and biological behaviour, i.e., low solubility in aqueous media, similar antifungal activity and mode of action.[60, 61]

Although different models have been suggested to explain the mechanism, which can vary in some fungal strains, it is widely accepted that the binding to ergosterol, the major sterol component of the fungal membrane, is very crucial to this process.[23, 56, 62] Thanks to the hydrophobic polyene structure and the polar glycoside group, AmB and Nys can target and bind ergosterol on the fungal membrane.[61, 62] Their amphiphilic structures can further help AmB and Nys insert into the cell membrane, disrupting the integrity of the cell membrane, resulting in changes in permeability and cell lysis.[23, 61] Thus, both drugs have a broad antifungal activity

although AmB is more effective in most cases which is attributed to its rigid structure.[60]

1.1.2.2 Current available formulation of polyene drugs to improve their solubility and reduce toxicity

Due to the similar structure between ergosterol and cholesterol (the sterol existence on human cell membrane), these polyene drugs also have an affinity, albeit lower, towards cholesterol.[21, 23] It is considered to be one of the main reasons that these drugs produce a high toxicity, especially to human kidneys, when administrated. The solubility of AmB and Nys is also a big issue.[62, 63] In addition to the difficulties that arise in clinical applications, the low solubility of these polyene drugs will induce the non-selectively formation of aggregates onto both fungal and mammalian cells, resulting in unwanted cell damage.

In order to improve the solubility of AmB as well as to reduce its toxicity, it has been formulated with solubilizing agents prior to administration.[17, 56, 64-68] The common formulation includes of AmB micellar deoxycholate complex (AmBd, Fungizone™, solubiliser: sodium deoxycholate), lipid complex (ABLC, solubiliser: dimyristoylphosphatidylcholine and dimyristoyl phosphatidylglycerol), liposome (L-AmB, i.e., AmBisome®, solubiliser: hydrogenated soy phosphatidylcholine, cholesterol and distearoylphosphatidylglycerol) and AmB colloidal dispersion (ABCD, solubiliser: sodium cholesteryl sulfate).[56] The concept of formulating AmB into a prodrug has also been raised recently.[66, 69-71] The sugar amine and the carboxyl group on AmB are often targeted for site-specific modification. With various physical/biological behavior, all these formulations reduce the toxicity of AmB but retain all or part of its antifungal activity.[56, 64]

Conversley, formulation of Nys is not as well developed since it is mainly used as a topical treatment.[57, 60] Systemic administrations have been avoided due to the low systemic activity caused by the poor gastrointestinal absorption.[6, 60, 72] Of the two antimycotic agents, Nys is less active than AmB and is also less toxic. More interestingly, it shows activity against some *Candida* species that have resistance against AmB, suggesting its potential as an alternative to AmB in systemic administration.[53, 60, 73] Thus far, some initial studies have been developed on the formulation of Nys into a micelle or liposome to improve its aqueous solubility.[16, 60, 74-76]

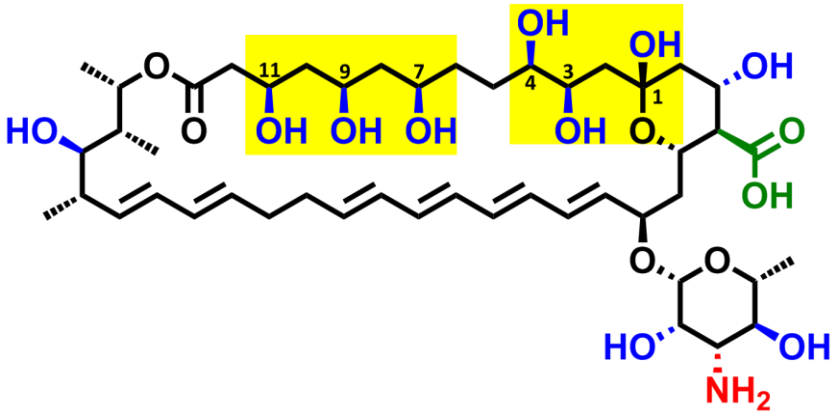

Figure 1.4 The possible modification sites for Nys, sugar amines (red), hydroxyl groups (blue), 1,2-/1,3- diols (highlighted) and carboxyl group (green).

Similarly to AmB, the sugar amine and the carboxyl group on Nys are also the possible modification sites for it to form a prodrug (Figure 1.4).[77] To emphasise the possibility of modifying Nys on its amine group with a polymer to improve its chemical and biological performances, a prodrug approach has been developed in chapter 6. Although the hydroxyl groups on Nys can also potentially be targeted (Figure 1.4), it has not been well-evaluated due to the multiple possible reaction sites. Fortunately, when applying the reversible covalent boronic acid-1,2/1,3-diol interaction,[78-80] the possible reaction sites can be in principle narrow down to two.

Through this environment-responsive interaction, Nys can be attached through a polymer delivery system with boronic acid units and can be released with stimuli, which will be discussed in chapter 7.

1.2 Polymer-Based Delivery System for Antimicrobial Biological Agents

As mentioned previously, the administration of these antimicrobial agents with the help of a suitable delivery system can increase their solubility, reduce their potential toxicity while maintaining their biological activity.[16, 17, 56, 60, 64-68, 74, 76, 77] However, unlike the delivery some other drugs such as antitumor agents, the initial concentration of the antimicroibial agents in the first few hours is crucial to their antimicrobial activity (especially against these MDR microorganisms) due to the fast (re)growth and resistance response of these microorganisms. Thus, the effective release of the antimicrobial agents is an important consideration when selecting an appropriate delivery system.

Two main approaches have been successfully applied in clinic: 1) reaction of the antimicrobial agents with some biocompatible (bio)molecules, formulating them into prodrugs;[81, 82] 2) encapsulating these drugs into macro/micro-carriers (i.e., hydrogels, emulsions, suspensions, and aerosols) or nano-complexes (i.e., micelles, vesicles/liposomes, and nanogels) ahead of administration.[83, 84] Although many small molecules such as sugars, lipids, and some other natural products have been successfully applied for drug delivery, more and more polymer-based drug delivery systems have been developed in order to benefit from the notable advantages of using polymers, especially synthetic polymer, over the small molecules.[85, 86] Due to the

diversification of polymer selection and the development of polymerisation techniques, cheap polymers with high functionality, low toxicity and higher chemo-/bio- stability can be synthesised and purified in economical ways.[81, 87, 88]

1.2.1 Biological agent-polymer conjugates

Although the biological agents are effective therapies, they normally have poor bioavailability. Unlike the common synthetic small molecular drugs, many peptide/protein-based drugs only have short half-lives in the human body due to the biodegradable nature caused by the proteolytic degradation.[81, 82, 89] The poor solubility of some of the biological agents like the polyene antimycotics and some lipopeptides is sometimes problematic and limits their use.[63, 66, 90, 91] Moreover, the functional groups on the biological agents may also trigger immune response, producing toxicity or other side effects.[82, 92] One approach that has been developed to address these limitation is to modify these therapeutic biological molecules with polymers and has attracted increasingly attention in the past few years.[81, 86]

1.2.1.1 Poly(ethylene glycol) (PEG) and PEGylation

Amongst all the polymers, poly(ethylene glycol) (PEG), a polymer approved by the FDA, is most well-studied conferring high stability and good biocompatibility in the human body.[81, 86, 89] Attachment of PEG to biological agents, known as PEGylation, can improve the pharmacokinetic and pharmacodynamic properties of these fragile biocompounds.[93] The PEG chains on these agents will help them bypass enzymatic recognition, avoiding antigenic/immunogenic recognition[92] and proteolytic degradation.[81] PEGylation of these biological drugs also increases the total hydrodynamic volume of these drugs, changing their bio-distribution in the human

body.[81, 89] Due to the unique structure of PEG, PEGylation can also prevent unnecessary fouling of these drugs during the delivery.[94] It can also, to some extent, reduce the toxicity caused by therapeutic biomolecules during the drug delivery.[93] Furthermore, PEG has a molecular weight-dependent clearance property in the human body,[81] which means that the PEG conjugated biological agents can have increased half-lives and circulation times can be controlled by tuning the size of the PEG attached. In addition, PEGylation is well studied since most PEG derivatives are commercial available or easily obtained. Up until now, a few PEGylated protein products like Adagen®, Oncospar®, and PEG-Intron® have been introduced to the market.[81]

1.2.1.2 Controlled radical polymerisation (CRP) and their conjugates with antimicrobial agents

Although PEGylation is a commonly used method to achieve biological antimicrobial agent conjugates, other synthetic functional polymers can provide more versatility and functionalisation.[95-100] Controlled radical polymerisation (CRP) is a powerful tool to synthesize biocompatible polymers, stimuli responsive polymers and other function polymers with controlled molecular weights and narrow dispersities (*Đ*). Examples include, but are not limited to, poly(poly(ethylene glycol) methyl ether (meth)acrylate) (PPEGA/PPEGMA),[97-99] poly(*N*-(2-hydroxypropyl) methacrylamide (PHPMA)),[100] poly(*N*-isopropylacrylamide) (PNIPAM)[95] and glycopolymers.[96] Furthermore, some CRP methods, such as reversible addition−fragmentation chain transfer (RAFT) polymerisation,[95, 101] atom transfer radical polymerisation (ATRP),[102, 103] single-electron transfer living radical polymerisation (SET-LRP),[104, 105] and copper-mediated photoinduced living radical polymerisation (CP-LRP)[106, 107] can

now be conducted in water, buffer, or even physiological environment, which make it possible to perform polymerisation and conjugation in one pot under biologically relevant conditions. Through careful selection of the initiator and by selecting the appropriate conditions, conjugates between biological agents and desired polymers with various architectures and high end-group fidelity can be achieved.[70] The biological agents can be attached on the end-group as well as the side chains of the polymers.

1.2.1.3 Polymer conjugation methods and sites

As the biological agents are usually complex structures with an array of functionality, the selection and control over the conjugation site is important during the modification. As amine groups are exist in many natural biological products, especially in peptides/proteins, it is the most commonly targeted site for the polymer conjugation.[66, 81, 98, 108] The high nucleophilicity of the amine groups allows the conjugation to proceed smoothly with high yields in aqueous media. Thus, numerous functional groups, including aldehyde, dichlorotriazine, carbonylimidazole and activated ester/carbonate (1-hydroxybenzotriazole ester or *N*-hydroxysuccinimidyl ester), have been developed for this type of conjugation.[81, 108] Other functional groups such as thiol, carboxyl and hydroxyl groups are also targeted as more specific alternatives.[81, 96, 97, 99]

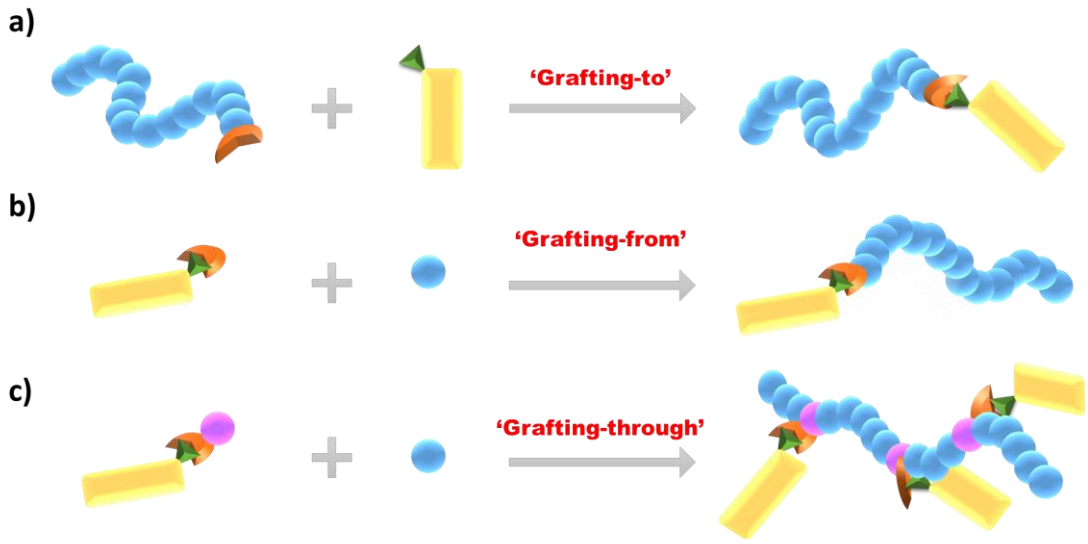

Figure 1.5 Three approaches for biological agent-polymer conjugation. a) 'Grafting-to' approach is the conjugation of polymer directly onto a biological agent. b) 'Grafting-from' approach is the polymerisation of monomers from the initiator derivative from a biological agent. c) 'Grafting-through' approach is the polymerisation of the monomers derivative from a biological agent.

Three approaches that are classified as 'grafting-from', 'grafting-to' and 'grafting-through' are mainly applied for the polymer conjugation (Figure 1.5).[109, 110] The 'grafting-to' approach has been widely explored to conjugate the biomolecules with α–functional polymers, especially PEG, typically through an efficient reaction (i.e., 'click' reaction) under a mild conditions such as water/buffer system at ambient temperature.[81, 89, 96, 98, 100, 101] However, the 'grafting-from' and 'grafting-through' approaches are more often used when combined with CRP techniques.[101, 103, 110] This is as the conjugation between the biological agent and a small molecule is usually much more efficient than between the biological agent and a polymer. In general, the 'grafting-from' polymerisation through CRP is with high yield and high end-group fidelity and the final polymer is easy to purify and characterise.[109, 110]

Although the covalently linked polymer modification can normally provide a good stability to the conjugate both *in vitro* and *in vivo*, a significant (or sometimes

complete) loss of the activity of the biomolecules has often been reported for many polymer-biomolecule conjugates following such modifications.[98, 111] This has mainly been attributed to blockage of the active site(s) or changes to the structure of the biological agent caused by the polymer. Thus, prodrugs based on traceless and/ or reversible conjugations have attracted significant attention.[112-116] These types of prodrugs usually stay as an inactive or less active derivative under normal (storage) conditions, but can be converted back to the active drug at the targeted site/ environment *in vitro*/ *in vivo*. Several dynamic covalent bonds, including 1,6-elimination,[113] thioester,[115] bicine,[114] azidomethyl-methylmaleic anhydride,[117] and disulphide bonds[115, 118-120] have been explored as releasable linkers.

1.2.2 Micellar delivery system of poorly soluble antimicrobial agents

Despite the benefits obtained from the polymeric prodrug formulation, some antimicrobial agents are very poorly soluble in water/buffer systems and sometimes even in organic media, making them difficult to be fabricated into prodrugs. Due to the low solubility, these drugs will also cause other clinic problems such as low bioavailability and unreliable absorption behaviour.[62, 63, 121] To disperse and stabilise these drugs in aqueous media on a nanometer scale, one approach is the formation of high-order self-assembled structure such as micelles as nano-carriers.[85, 122-124] Micelles are formed from the self-assembly of amphiphiles and have a spherical structure with a hydrophobic core and a hydrophilic shell. The core of the micelle can encapsulate hydrophobic antimicrobial drugs while the hydrophilic shell can stabilise the micelles, preventing the micelle-micelle/environment interactions.[124-126] Although it showed some potential in the research, the small molecule based micelles are rarely used in

clinic as the critical micelle concentration (CMC) of micelles is relatively high and is not stable in the human body.[127]

With the development of controlled polymerisation techniques, polymer micelles have received more attention.[124, 127] Self-assembled micelles with a narrow polydispersity can be prepared from well-defined and well-designed amphiphilic block copolymers.[128, 129] Compared to low molecular weight surfactant, the CMC of polymer micelles are normally several orders of magnitude lower, therefore, they are more stable when administered. There is a wide choices of polymers that are non-toxic and will not trigger the immune response or other adverse effect through the delivery. Through the design of the polymers, it is feasible to introduce functionality (i.e., pH/chemo-/thermo- response and (bio)degradability) onto the micelles.[79, 126, 129] Furthermore, the tunable hydrophobic/hydrophilic ratio and length of the polymer provide a precise control of the size of polymer micelles, which is important for cell uptake and the passive targeting delivery through the enhanced permeability and retention (EPR) effect.[130]

The major approach to load hydrophobic antimicrobial drugs into polymer micelles is to dissolve the drugs the same time with the polymers and co-assemble *via* solvent switch.[126] However, other methods including the incorporation of the drugs after the self-assembled micelle or the conjugation of the drugs onto the polymers side chains/end group(s) in advance of self-assembly are also possible to achieve a successful drug loading.

1.2.2.1 Cross-linked polymer micelle formulation

Unfortunately, most of the drug-loaded polymer micelles developed so far have not provided significant improvements compared to the original drug in vivo.[131, 132]

Through dilution from body fluid when administered, the micelles are no longer stable and thus disassembly into unimers can occur, which is unable to disperse and stablise the poorly soluble antimicrobial agents.

To avoid this, core or shell 'cross-linking' can be applied, preventing micelle disassembly *in vivo*.[131-134] By covalently cross-linking the hydrophobic part ('core cross-linking') or the hydrophilic part ('shell cross-linking') of the self-assembly of the amphiphilic polymer, the dynamic feature of the micelles is fixed. The cross-linker is normally a bi/multi-functional compound that can react with the micelle effectively. Other methods for cross-linking include polyelectrolyte complexation,[135] reduction/oxidation,[136] metal chelation[137] and photo-radiation.[138]

As drugs normally stay in the core (the hydrophobic domain) of the polymer micelles due to the strong hydrophobic interactions, one concern for the drug-loaded cross-linked polymer micelle is whether it is too stable for the release of the drugs. Thus, a trigger within the cross-linked polymer micelle system (i.e., cleavable polymer side chains or degradable cross-linkers) is normally required to achieve an efficient release.[80, 136]

1.2.3 Hydrogel formulation for water-soluble antimicrobial agents

Although systemic administration is a powerful method to deliver antimicrobial agents and it is necessary for severe or systemic infections, it is also costly and not always effective against some local infections (like surface infections). Thus, some localised drug delivery systems have been appraised and applied clinically.[139, 140] As these formulations are only applied topically, the local drug concentration can be high

enough against the microorganisms but not high enough to cause systemic toxicity to the human body.

Hydrogel formulation, as one of these topical formulations, is well accepted by the market and has been used as contact lenses, wound dressings, tissue engineering materials and superabsorbent hygiene products over the last few decades.[141] Hydrogels are cross-linked polymeric materials that are capable of capture water within the porous network.[142] The ones cross-linked chemically, also known as permanent hydrogels, are normally stable and have strong mechanical properties whilst the one cross-linked by physical interaction such as hydrogen bonding, electrostatic interaction and Van der Waals forces can sometimes be dissolved or reversible in response to the change of the surrounding environment.[141] Recent research area regarding hydrogels is the development of a covalent cross-linked hydrogel that can be responsive to some specific stimuli by introducing some photo-/chemo-cleavable linkers.[143]

Polymeric materials used to formulate hydrogels can be both synthetic polymers and natural biomacromolecules depends on application. Synthetic polymers such as PEG, PNIPAM, poly(vinyl alcohol) (PVA), poly(vinylpyrrolidone) (PVP), poly(2-hydroxyethyl methacrylate) (PHEMA), poly(acrylic acid) (PAA), poly(methacrylic acid) (PMAA), poly(2-(acrylamido)-2-methylpropanesulfonic acid) (PAMPS) and polyacrylamide (PAM) are favoured as they are normally with low cost and easy to fabricate and characterise.[142-144] The chemo-/bio-stability of synthetic polymers allows them to have a longer shelf life and stable performance. However, biomacromolecules also have their advantages such as good biocompatibility and biodegradability.[145, 146] As the solid content in hydrogels is normally quite low (< 10% w/w), the cost of using biomaterials is also acceptable.

1.2.3.1 Water-soluble antimicrobial agents in hydrogel formulations used in wound care

Thanks to the wide choices of hydrogels, this high-water-content, porous and soft material is particularly favoured in wound care.[142, 147-149] Generally, the high water content of the hydrogels ensures this three-dimensional material a good biocompatible and non-irritant property.[142] The incorporation of therapeutics in hydrogel formulations has been widely employed to facilitate and manage many wound-healing processes, particularly burn wounds.[147-151] In advance to other treatments, the application of hydrogels can prevent the loss of the body fluid, keep the wound surface hydrated, promote the healing process, and also act as a barrier against further infections.[152, 153] Furthermore, properties such as degradability,[154, 155] environmental responsiveness,[156, 157]and self-healing[158, 159] can be fine-tuned to support the curing process of specific wound types.

Chitosan, as a nature biomacromolecules, is of particular interests.[145] Chitosan is a linear polysaccharide generated by the deacetylation of chitin, a component obtained from the exoskeleton of crustaceans and insects. It is consisted of two monomer units, the deacetylated unit β-D-glucosamine (commercial product normally contains > 60%) and the acetylated unit *N*-acetyl-D-glucosamine. This unique structure allows it to form a hydrogel with other molecules through ionic interaction, hydrogen bonding, or/and Van de Waal interaction, providing various types of hydrogels for different applications. The sugar units make chitosan a stable hydrophilic backbone but also a responsive material to some enzymes. In addition to its biocompatibility and biodegradability, chitosan has the potential to induce faster wound healing and smoother scarring.[145, 160]

The combination of hydrogel and antimicrobial agents can protect the wound site and inhibit the growth of microorganisms at the same time.[150] There are three drug loading methods: 1) direct addition of the drug during the hydrogel formation; 2) Drug loading after the hydrogel formation; 3) Covalent attachment of the drug on the hydrogel.[145, 161] Amongst all these methods, the former two methods are more commonly used for water-soluble antimicrobial agents.[145, 161] Due to the high water content and the porous structure of hydrogels, a large capacity and high loading efficiency can be achieved. The release of these drugs can be promoted by the concentration exchange of the solution in the hydrogels and the environment, which could provide a high local initial concentration of the antimicrobial agents.

1.3 References

1. A. Fleming, *Brit. J. Exp. Pathol.*, 1929, **10**, 226-236.
2. D. M. Dixon, M. M. McNeil, M. L. Cohen, B. G. Gellin and J. R. La Montagne, *Public Health Rep.*, 1996, **111**, 226-235.
3. A. L. Demain and S. Sanchez, *J. Antibiot.*, 2009, **62**, 5-16.
4. P.-L. Shao, L.-M. Huang and P.-R. Hsueh, *Int. J. Antimicrob. Agents*, 2007, **30**, 487-495.
5. C.-C. Lai, C.-K. Tan, Y.-T. Huang, P.-L. Shao and P.-R. Hsueh, *J. Infect. Chemother.*, 2008, **14**, 77-85.
6. M. K. Kathiravan, A. B. Salake, A. S. Chothe, P. B. Dudhe, R. P. Watode, M. S. Mukta and S. Gadhwe, *Bioorg. Med. Chem.*, 2012, **20**, 5678-5698.
7. U. S. D. o. H. a. H. Services, available at: http://www.cdc.gov/drugresistance/pdf/ar-threats-2013-508.pdf, (accessed 9 September, 2016).
8. J. O'Neill, available at: https://amr-review.org/sites/default/files/Report-52.15.pdf, (accessed 9 September, 2016).
9. D. o. H. a. D. o. A. Australian Government, available at: https://www.health.gov.au/internet/main/publishing.nsf/Content/1803C433C71415C

ACA257C8400121B1F/$File/amr-strategy-2015-2019.pdf, (accessed 9 September, 2016).

10. C. L. Ventola, *Pharmacol. Ther.*, 2015, **40**, 277-283.

11. J. O'Neill, available at: http://amr-review.org/sites/default/files/160525_Final%20paper_with%20cover.pdf, (accessed 9 Septermber, 2016).

12. D. Sanglard, *Front. Med.*, 2016, **3**, 11.

13. A. Coates, Y. Hu, R. Bax and C. Page, *Nat. Rev. Drug Discov.*, 2002, **1**, 895-910.

14. B. Spellberg, J. H. Powers, E. P. Brass, L. G. Miller and J. E. Edwards, *Clin. Infect. Dis.*, 2004, **38**, 1279-1286.

15. S. R. Norrby, C. E. Nord and R. Finch, *Lancet Infect. Dis.*, 2005, **5**, 115-119.

16. F. Offner, V. Krcmery, M. Boogaerts, C. Doyen, D. Engelhard, P. Ribaud, C. Cordonnier, B. de Pauw, S. Durrant, J.-P. Marie, P. Moreau, H. Guiot, G. Samonis, R. Sylvester, R. Herbrecht and t. E. I. F. I. Group, *Antimicrob. Agents Chemother.*, 2004, **48**, 4808-4812.

17. M. D. Moen, K. A. Lyseng-Williamson and L. J. Scott, *Drugs*, 2009, **69**, 361-392.

18. T. Velkov, K. D. Roberts, R. L. Nation, P. E. Thompson and J. Li, *Future Microbiol.*, 2013, **8**, 711-724.

19. N. Cassir, J.-M. Rolain and P. Brouqui, *Front. Microbiol.*, 2014, **5**, 551.

20. M. E. Falagas, S. K. Kasiakou and L. D. Saravolatz, *Clin. Infect. Dis.*, 2005, **40**, 1333-1341.

21. B. E. Cohen, *Int. J. Pharm.*, 1998, **162**, 95-106.

22. H. Spapen, R. Jacobs, V. Van Gorp, J. Troubleyn and P. M. Honoré, *Ann. Intensive Care*, 2011, **1**, 14.

23. P. Vandeputte, S. Ferrari and A. T. Coste, *Int. J. Microbiol. Res.*, 2011, **2012**.

24. H. W. Boucher, G. H. Talbot, J. S. Bradley, J. E. Edwards, D. Gilbert, L. B. Rice, M. Scheld, B. Spellberg and J. Bartlett, *Clin. Infect. Dis.*, 2009, **48**, 1-12.

25. A. P. Zavascki, C. G. Carvalhaes, R. C. Picão and A. C. Gales, *Expert Rev. Anti. Infect. Ther.*, 2010, **8**, 71-93.

26. A. P. Magiorakos, A. Srinivasan, R. Carey, Y. Carmeli, M. Falagas, C. Giske, S. Harbarth, J. Hindler, G. Kahlmeter and B. Olsson‐Liljequist, *Clin Microbiol. Infect.*, 2012, **18**, 268-281.

27. E. A. Azzopardi, E. Azzopardi, L. Camilleri, J. Villapalos, D. E. Boyce, P. Dziewulski, W. A. Dickson and I. S. Whitaker, *PloS one*, 2014, **9**, e95042.

28. E. E. Tredget, H. A. Shankowsky, R. Rennie, R. E. Burrell and S. Logsetty, *Burns*, 2004, **30**, 3-26.

29. J. B. Lyczak, C. L. Cannon and G. B. Pier, *Microb. Infect.*, 2000, **2**, 1051-1060.

30. G. H. Talbot, J. Bradley, J. E. Edwards, D. Gilbert, M. Scheld and J. G. Bartlett, *Clin. Infect. Dis.*, 2006, **42**, 657-668.

31. R. J. Fair and Y. Tor, *Perspect. Medicin. Chem.*, 2014, **6**, 25-64.

32. J. Li, R. L. Nation, R. W. Milne, J. D. Turnidge and K. Coulthard, *Int. J. Antimicrob. Agents*, 2005, **25**, 11-25.

33. J. Li, R. L. Nation, J. D. Turnidge, R. W. Milne, K. Coulthard, C. R. Rayner and D. L. Paterson, *Lancet Infect. Dis.*, 2006, **6**, 589-601.

34. R. L. Nation and J. Li, *Curr. Opin. Infect. Dis.*, 2009, **22**, 535-543.

35. L. M. Lim, N. Ly, D. Anderson, J. C. Yang, L. Macander, A. Jarkowski, A. Forrest, J. B. Bulitta and B. T. Tsuji, *Pharmacother.*, 2010, **30**, 1279-1291.

36. P. J. Bergen, J. Li, C. R. Rayner and R. L. Nation, *Antimicrob. Agents Chemother.*, 2006, **50**, 1953-1958.

37. T. Velkov, P. E. Thompson, R. L. Nation and J. Li, *J. Med. Chem.*, 2009, **53**, 1898-1916.

38. K. D. Roberts, M. A. Azad, J. Wang, A. S. Horne, P. E. Thompson, R. L. Nation, T. Velkov and J. Li, *ACS Infect. Dis.*, 2015, **1**, 568-575.

39. R. L. Soon, T. Velkov, F. Chiu, P. E. Thompson, R. Kancharla, K. Roberts, I. Larson, R. L. Nation and J. Li, *Anal. Biochem.*, 2011, **409**, 273-283.

40. M. E. Falagas and S. K. Kasiakou, *Crit. Care*, 2006, **10**, R27-R27.

41. C. A. C. Mendes and E. A. Burdmann, *Rev. Assoc. Med. Bras.*, 2009, **55**, 752-759.

42. A. Ordooei Javan, S. Shokouhi and Z. Sahraei, *Eur. J. Clin. Pharmacol.*, 2015, **71**, 801-810.

43. E. Forde and M. Devocelle, *Molecules*, 2015, **20**, 1210-1227.

44. S. Chihara, T. Tobita, M. Yahata, A. Ito and Y. Koyama, *Agric. Biol. Chem.*, 1973, **37**, 2455-2463.

45. K. Marina, H. Tsubery, S. Kolusheva, A. Shames, M. Fridkin and R. Jelinek, *Biochem. J.*, 2003, **375**, 405-413.

46. J. Li, R. W. Milne, R. L. Nation, J. D. Turnidge and K. Coulthard, *Antimicrob. Agents Chemother.*, 2003, **47**, 1364-1370.

47. M. E. Falagas, K. N. Fragoulis, S. K. Kasiakou, G. J. Sermaidis and A. Michalopoulos, *Int. J. Antimicrob. Agents*, 2005, **26**, 504-507.

48. M. Blackwell, *Am. J. Bot.*, 2011, **98**, 426-438.

49. J. Perlroth, B. Choi and B. Spellberg, *Med. Mycol.*, 2007, **45**, 321-346.

50. M. W. Pound, M. L. Townsend, V. Dimondi, D. Wilson and R. H. Drew, *Med. Mycol.*, 2011, **49**, 561-580.

51. M. Beed, R. Sherman and S. Holden, *CEACCP*, 2013, **14**, 262-267.

52. P. Badiee and Z. Hashemizadeh, *Indian J. Med. Res.*, 2014, **139**, 195-204.

53. M. A. Pfaller, R. N. Jones, S. A. Messer, M. B. Edmond and R. P. Wenzel, *Diagn. Microbiol. Infect. Dis.*, 1998, **31**, 327-332.

54. C. R. Sims, L. Ostrosky-Zeichner and J. H. Rex, *Arch. Med. Res.*, 2005, **36**, 660-671.

55. H. A. Gallis, R. H. Drew and W. W. Pickard, *Rev. Infect. Dis.*, 1990, **12**, 308-329.

56. S. Hartsel and J. Bolard, *Trends Pharmacol. Sci.*, 1996, **17**, 445-449.

57. M. Bondaryk, W. Kurzątkowski and M. Staniszewska, *Postepy Dermatol. Alergol.*, 2013, **30**, 293-301.

58. K. C. Nicolaou, T. K. Chakraborty, Y. Ogawa, R. A. Daines, N. S. Simpkins and G. T. Furst, *J. Am. Chem. Soc.*, 1988, **110**, 4660-4672.

59. E. G. Brescansin, M. Portilho and F. B. T. Pessine, *Acta Sci. Health Sci.*, 2013, **35**, 215-221.

60. E. M. Johnson, J. O. Ojwang, A. Szekely, T. L. Wallace and D. W. Warnock, *Antimicrob. Agents Chemother.*, 1998, **42**, 1412-1416.

61. M. A. Ghannoum and L. B. Rice, *Clin. Microbiol. Rev.*, 1999, **12**, 501-517.

62. K. C. Gray, D. S. Palacios, I. Dailey, M. M. Endo, B. E. Uno, B. C. Wilcock and M. D. Burke, *Proc. Natl. Acad. Sci. U.S.A.*, 2012, **109**, 2234-2239.

63. P. Legrand, E. A. Romero, B. E. Cohen and J. Bolard, *Antimicrob. Agents Chemother.*, 1992, **36**, 2518-2522.

64. A. Wong-Beringer, R. A. Jacobs and B. J. Guglielmo, *Clin. Infect. Dis.*, 1998, **27**, 603-618.

65. M. Sedlák, V. r. Buchta, L. Kubicová, P. Šimůnek, M. Holčapek and P. Kašparová, *Bioorg. Med. Chem. Lett.*, 2001, **11**, 2833-2835.

66. C. D. Conover, H. Zhao, C. B. Longley, K. L. Shum and R. B. Greenwald, *Bioconjugate Chem.*, 2003, **14**, 661-666.

67. K. H. MA, J. Miah, S. Shanmugam, C. S. Yong, H.-G. Choi, J. A. Kim and B. K. Yoo, *Arch. Pharm. Res.*, 2007, **30**, 1344-1349.

68. M. Sedlák, M. Pravda, F. Staud, L. Kubicová, K. Týčová and K. Ventura, *Bioorg. Med. Chem.*, 2007, **15**, 4069-4076.

69. S. Matsuoka, N. Matsumori and M. Murata, *Org. Biomol. Chem.*, 2003, **1**, 3882-3884.

70. S. A. Davis, B. M. Vincent, M. M. Endo, L. Whitesell, K. Marchillo, D. R. Andes, S. Lindquist and M. D. Burke, *Nat. Chem. Biol.*, 2015, **11**, 481-487.

71. A. Halperin, Y. Shadkchan, E. Pisarevsky, A. M. Szpilman, H. Sandovsky, N. Osherov and I. Benhar, *J. Med. Chem.*, 2016, **59**, 1197-1206.

72. S. B. Zotchev, *Curr. Med. Chem.*, 2003, **10**, 211-223.

73. D. W. Denning and P. Warn, *Antimicrob. Agents Chemother.*, 1999, **43**, 2592-2599.

74. S. R. Croy and G. S. Kwon, *J. Control. Release*, 2004, **95**, 161-171.

75. T. P. Day, D. Sil, N. M. Shukla, A. Anbanandam, V. W. Day and S. A. David, *Mol. Pharm.*, 2010, **8**, 297-301.

76. M. Spulber, A. Fifere, D.-A. Anamaria and N. Fifere, *J. Incl. Phenom. Macrocycl. Chem.*, 2011, **71**, 87-93.

77. E. Bílková, A. Imramovský, V. Buchta and M. Sedlák, *Int. J. Pharm.*, 2010, **386**, 1-5.

78. S. D. Bull, M. G. Davidson, J. M. H. van den Elsen, J. S. Fossey, A. T. A. Jenkins, Y.-B. Jiang, Y. Kubo, F. Marken, K. Sakurai, J. Zhao and T. D. James, *Acc. Chem. Res.*, 2013, **46**, 312-326.

79. A. W. Jackson and D. A. Fulton, *Polymer Chemistry*, 2013, **4**, 31-45.

80. Y. Li, K. Xiao, W. Zhu, W. Deng and K. S. Lam, *Adv. Drug Deliv. Rev.*, 2014, **66**, 58-73.

81. M. J. Roberts, M. D. Bentley and J. M. Harris, *Adv. Drug Deliv. Rev.*, 2012, **64**, 116-127.

82. A. Grigoletto, K. Maso, A. Mero, A. Rosato, O. Schiavon and G. Pasut, *J. Drug Deliv. Sci. Technol.*, 2016, **32**, 132-141.

83. V. P. Torchilin, *Nat. Rev. Drug Discov.*, 2014, **13**, 813-827.

84. S. J. Buwalda, T. Vermonden and W. E. Hennink, *Biomacromolecules*, 2016, DOI: 10.1021/acs.biomac.6b01604.

85. R. Duncan, *Nat. Rev. Drug Discov.*, 2003, **2**, 347-360.

86. A. N. Zelikin, C. Ehrhardt and A. M. Healy, *Nat. Chem.*, 2016, **8**, 997-1007.

87. H. Chen, L. Yuan, W. Song, Z. Wu and D. Li, *Prog. Polym. Sci.*, 2008, **33**, 1059-1087.

88. M. A. Ward and T. K. Georgiou, *Polymers*, 2011, **3**, 1215-1242.

89. F. M. Veronese and G. Pasut, *Drug Discov. Today*, 2005, **10**, 1451-1458.

90. J. Bolard, P. Legrand, F. Heitz and B. Cybulska, *Biochemistry*, 1991, **30**, 5707-5715.

91. P. Zhang, J. Lu, Y. Huang, W. Zhao, Y. Zhang, X. Zhang, J. Li, R. Venkataramanan, X. Gao and S. Li, *AAPS J.*, 2014, **16**, 114-124.

92. A. Abuchowski, J. R. McCoy, N. C. Palczuk, T. van Es and F. F. Davis, *J. Biol. Chem.*, 1977, **252**, 3582-3586.

93. J. M. Harris and R. B. Chess, *Nat. Rev. Drug Discov.*, 2003, **2**, 214-221.

94. I. Banerjee, R. C. Pangule and R. S. Kane, *Adv. Mater.*, 2011, **23**, 690-718.

95. C. Boyer, V. Bulmus, J. Liu, T. P. Davis, M. H. Stenzel and C. Barner-Kowollik, *J. Am. Chem. Soc.*, 2007, **129**, 7145-7154.

96. J. Geng, G. Mantovani, L. Tao, J. Nicolas, G. Chen, R. Wallis, D. A. Mitchell, B. R. G. Johnson, S. D. Evans and D. M. Haddleton, *J. Am. Chem. Soc.*, 2007, **129**, 15156-15163.

97. G. Mantovani, F. Lecolley, L. Tao, D. M. Haddleton, J. Clerx, J. J. L. M. Cornelissen and K. Velonia, *J. Am. Chem. Soc.*, 2005, **127**, 2966-2973.

98. L. Tao, G. Mantovani, F. Lecolley and D. M. Haddleton, *J. Am. Chem. Soc.*, 2004, **126**, 13220-13221.

99. M. W. Jones, R. A. Strickland, F. F. Schumacher, S. Caddick, J. R. Baker, M. I. Gibson and D. M. Haddleton, *J. Am. Chem. Soc.*, 2012, **134**, 1847-1852.

100. P. K. Dhal, S. C. Polomoscanik, D. A. Gianolio, P. G. Starremans, M. Busch, K. Alving, B. Chen and R. J. Miller, *Bioconjugate Chem.*, 2013, **24**, 865-877.

101. V. Bulmus, *Polymer Chemistry*, 2011, **2**, 1463-1472.

102. S. Averick, A. Simakova, S. Park, D. Konkolewicz, A. J. D. Magenau, R. A. Mehl and K. Matyjaszewski, *ACS Macro Lett.*, 2012, **1**, 6-10.

103. D. J. Siegwart, J. K. Oh and K. Matyjaszewski, *Prog. Polym. Sci.*, 2012, **37**, 18-37.

104. Q. Zhang, M. Li, C. Zhu, G. Nurumbetov, Z. Li, P. Wilson, K. Kempe and D. M. Haddleton, *J. Am. Chem. Soc.*, 2015, **137**, 9344-9353.

105. Q. Zhang, P. Wilson, Z. Li, R. McHale, J. Godfrey, A. Anastasaki, C. Waldron and D. M. Haddleton, *J. Am. Chem. Soc.*, 2013, **135**, 7355-7363.

106. G. R. Jones, R. Whitfield, A. Anastasaki and D. M. Haddleton, *J. Am. Chem. Soc.*, 2016, **138**, 7346-7352.

107. A. Anastasaki, V. Nikolaou, Q. Zhang, J. Burns, S. R. Samanta, C. Waldron, A. J. Haddleton, R. McHale, D. Fox, V. Percec, P. Wilson and D. M. Haddleton, *J. Am. Chem. Soc.*, 2014, **136**, 1141-1149.

108. S. Zalipsky, *Adv. Drug Deliv. Rev.*, 1995, **16**, 157-182.

109. S. Averick, R. A. Mehl, S. R. Das and K. Matyjaszewski, *J. Control. Release*, 2015, **205**, 45-57.

110. I. Cobo, M. Li, B. S. Sumerlin and S. Perrier, *Nat. Mater.*, 2015, **14**, 143-159.

111. M. A. Gauthier and H.-A. Klok, *Polymer Chemistry*, 2010, **1**, 1352-1373.

112. J. Khandare and T. Minko, *Prog. Polym. Sci.*, 2006, **31**, 359-397.

113. R. B. Greenwald, K. Yang, H. Zhao, C. D. Conover, S. Lee and D. Filpula, *Bioconjugate Chem.*, 2003, **14**, 395-403.

114. H. Zhao, K. Yang, A. Martinez, A. Basu, R. Chintala, H.-C. Liu, A. Janjua, M. Wang and D. Filpula, *Bioconjugate Chem.*, 2006, **17**, 341-351.

115. J. Chen, M. Zhao, F. Feng, A. Sizovs and J. Wang, *J. Am. Chem. Soc.*, 2013, **135**, 10938-10941.

116. D. Filpula and H. Zhao, *Adv. Drug Deliv. Rev.*, 2008, **60**, 29-49.

117. X. Liu, P. Zhang, D. He, W. Rödl, T. Preiß, J. O. Rädler, E. Wagner and U. Lächelt, *Biomacromolecules*, 2016, **17**, 173-182.

118. L. Tao, J. Liu, J. Xu and T. P. Davis, *Org. Biomol. Chem.*, 2009, **7**, 3481-3485.

119. G. Saito, J. A. Swanson and K.-D. Lee, *Adv. Drug Deliv. Rev.*, 2003, **55**, 199-215.

120. L. Tao, J. Liu, J. Xu and T. P. Davis, *Chem. Commun.*, 2009, 6560-6562.

121. T. N. Thompson, *Med. Res. Rev.*, 2001, **21**, 412-449.

122. M. L. Adams, A. Lavasanifar and G. S. Kwon, *J. Pharm. Sci.*, 2003, **92**, 1343-1355.

123. K. Kataoka, A. Harada and Y. Nagasaki, *Adv. Drug Deliv. Rev.*, 2001, **47**, 113-131.

124. Y. Lu and K. Park, *Int. J. Pharm.*, 2013, **453**, 198-214.

125. G. S. Kwon and T. Okano, *Adv. Drug Deliv. Rev.*, 1996, **21**, 107-116.

126. U. Kedar, P. Phutane, S. Shidhaye and V. Kadam, *Nanomedicine*, 2010, **6**, 714-729.

127. V. P. Torchilin, *J. Control. Release*, 2001, **73**, 137-172.

128. A. W. York, S. E. Kirkland and C. L. McCormick, *Adv. Drug Deliv. Rev.*, 2008, **60**, 1018-1036.

129. H. Kakwere and S. Perrier, *Polymer Chemistry*, 2011, **2**, 270-288.

130. E. A. Azzopardi, E. L. Ferguson and D. W. Thomas, *J. Antimicrob. Chemother.*, 2013, **68**, 257-274.

131. M. Talelli, M. Barz, C. J. Rijcken, F. Kiessling, W. E. Hennink and T. Lammers, *Nano today*, 2015, **10**, 93-117.

132. R. K. O'Reilly, C. J. Hawker and K. L. Wooley, *Chem. Soc. Rev.*, 2006, **35**, 1068-1083.

133. C. F. van Nostrum, *Soft Matter*, 2011, **7**, 3246-3259.

134. E. S. Read and S. P. Armes, *Chem. Commun.*, 2007, 3021-3035.

135. J. V. M. Weaver, Y. Tang, S. Liu, P. D. Iddon, R. Grigg, N. C. Billingham, S. P. Armes, R. Hunter and S. P. Rannard, *Angew. Chem. Int. Ed.*, 2004, **43**, 1389-1392.

136. Y. Li, K. Xiao, J. Luo, W. Xiao, J. S. Lee, A. M. Gonik, J. Kato, T. A. Dong and K. S. Lam, *Biomaterials*, 2011, **32**, 6633-6645.

137. T. K. Bronich, P. A. Keifer, L. S. Shlyakhtenko and A. V. Kabanov, *J. Am. Chem. Soc.*, 2005, **127**, 8236-8237.

138. H. He, Y. Ren, Y. Dou, T. Ding, X. Fang, Y. Xu, H. Xu, W. Zhang and Z. Xie, *RSC Adv.*, 2015, **5**, 105880-105888.

139. M. E. Falagas, I. I. Siempos, P. I. Rafailidis, I. P. Korbila, E. Ioannidou and A. Michalopoulos, *Respir. Med.*, 2009, **103**, 707-713.

140. P. Krakowka, K. Traczyk, J. Walczak, H. Halweg, Z. Elsner and L. Pawlicka, *Tubercle*, 1970, **51**, 184-191.

141. E. Caló and V. V. Khutoryanskiy, *Eur. Polym. J.*, 2015, **65**, 252-267.

142. K. Pal, A. Banthia and D. Majumdar, *Des. Monomers Polym.*, 2009, **12**, 197-220.

143. M. C. Koetting, J. T. Peters, S. D. Steichen and N. A. Peppas, *Mater. Sci. Eng. R-Rep.*, 2015, **93**, 1-49.

144. K. Halake, M. Birajdar, B. S. Kim, H. Bae, C. Lee, Y. J. Kim, S. Kim, H. J. Kim, S. Ahn, S. Y. An and J. Lee, *J. Ind. Eng. Chem.*, 2014, **20**, 3913-3918.

145. N. Bhattarai, J. Gunn and M. Zhang, *Adv. Drug Deliv. Rev.*, 2010, **62**, 83-99.

146. K. Y. Lee and D. J. Mooney, *Prog. Polym. Sci.*, 2012, **37**, 106-126.

147. T. Vermonden, R. Censi and W. E. Hennink, *Chem. Rev.*, 2012, **112**, 2853-2888.

148. J. S. Boateng, K. H. Matthews, H. N. E. Stevens and G. M. Eccleston, *J. Pharm. Sci.*, 2008, **97**, 2892-2923.

149. M. Madaghiele, C. Demitri, A. Sannino and L. Ambrosio, *Burns & Trauma*, 2014, **2**, 153.

150. V. W. L. Ng, J. M. W. Chan, H. Sardon, R. J. Ono, J. M. García, Y. Y. Yang and J. L. Hedrick, *Adv. Drug Deliv. Rev.*, 2014, **78**, 46-62.

151. N. S. Goodwin, A. Spinks and J. Wasiak, *Int. Wound J.*, 2015.

152. G. Sun, X. Zhang, Y.-I. Shen, R. Sebastian, L. E. Dickinson, K. Fox-Talbot, M. Reinblatt, C. Steenbergen, J. W. Harmon and S. Gerecht, *Proc. Natl. Acad. Sci. U.S.A.*, 2011, **108**, 20976-20981.

153. T. Dai, M. Tanaka, Y.-Y. Huang and M. R. Hamblin, *Expert Rev. Anti. Infect. Ther.*, 2011, **9**, 857-879.

154. D. Seliktar, *Science*, 2012, **336**, 1124-1128.

155. P. M. Kharkar, K. L. Kiick and A. M. Kloxin, *Chem. Soc. Rev.*, 2013, **42**, 7335-7372.

156. P. Gupta, K. Vermani and S. Garg, *Drug Discov. Today*, 2002, **7**, 569-579.

157. Y. Qiu and K. Park, *Adv. Drug Deliv. Rev.*, 2001, **53**, 321-339.

158. A. Phadke, C. Zhang, B. Arman, C.-C. Hsu, R. A. Mashelkar, A. K. Lele, M. J. Tauber, G. Arya and S. Varghese, *Proc. Natl. Acad. Sci. U.S.A.*, 2012, **109**, 4383-4388.

159. Z. Wei, J. H. Yang, J. Zhou, F. Xu, M. Zrínyi, P. H. Dussault, Y. Osada and Y. M. Chen, *Chem. Soc. Rev.*, 2014, **43**, 8114-8131.

160. H. Ueno, H. Yamada, I. Tanaka, N. Kaba, M. Matsuura, M. Okumura, T. Kadosawa and T. Fujinaga, *Biomaterials*, 1999, **20**, 1407-1414.

161. T. R. Hoare and D. S. Kohane, *Polymer*, 2008, **49**, 1993-2007.

Chapter 2 *Approaches for the Development of Mono PEGylation on Polymyxins*

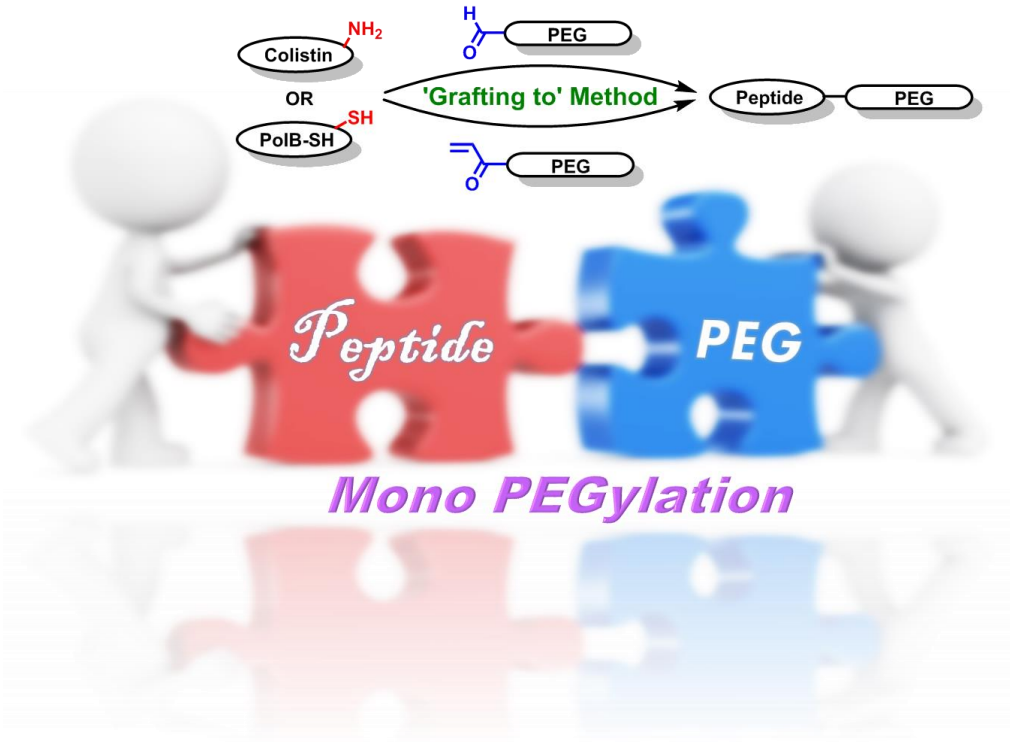

Two approaches for irreversibly PEGylated polymyxins have been developed using imine reduction and thiol-acrylate addition reactions. Both small molecule models and polymer modification were investigated in both approaches. Through the imine reduction reaction, the compositions of products from the modification of colistin can be tuned by varing the pH of the reaction while acrylate monomer or polymer can be selectively attached onto the Cys residue of an engineered polymyxin analogue (Pol-SH) in an atom-economic and efficient way under basic aqueous media without catalyst through the thiol-acrylate addition. Although both mono PEGylated conjugates failed to demonstrate an antimicrobial activity against the selected MDR Gram-negative bacteria, the chemistry developed in this work can still be applied in other polymer peptide conjugation that required a stable linker.

2.1 Introduction

As mentioned previously, the PEGylation of biomolecules may sometimes improve or hinder its biological performances.[1-3] Since the molecular weight of colistin is relatively low and the Dab residues on colistin are essential to its antibacterial activity, it remained unknown whether the activity of colistin would be retained when PEG, especially a single PEG chain, is irreversibly attached on Dab or other residue(s). Despite their antibiotic activity, the unique cyclic peptide structure of colistin is also attractive. As found in other cyclic peptides, this type of ring structures can be a potential unit for self-assembly and have some applications in gas separation,[4] drug delivery or other fields,[5, 6] of which normally require a more stable and defined modification. Furthermore, although there are many functional groups on colistin, the chemistry of the colistin modification, especially the attachment of PEG, has not been well studied in general. Because of the poor chemoselectivity among the five amine groups on colistin, it is not easy to achieve a selective modification or mono-modification through traditional chemistry. Thus, two approaches of the irreversible mono PEGylation of polymyxins were developed and discussed in this chapter.

To improve the selectivity on amines and reduce the potential multiple modification, a common approach to selectively modify peptide/protein terminal amine group presented by the five Dab residues present, was developed. The reductive amination has proven to have a good selectivity to amines, especially to terminal amines, at a suitable pH in aqueous solution. Through the adjustment of the reagent stoichiometry and reaction conditions, the multiple modification of colistin was greatly suppressed thanks to the pH-tunable activity of the imine reduction reaction and the steric hindrance caused by the addition of PEG. Although the side reactions

cannot be avoided and the yield of desired product is not very high, the 'pure' mono PEGylated products (at one of five undetermined Dab residues) can be obtained *via* the developed high performance liquid chromatography (HPLC) method.

As an alternative approach to mono PEGylation at undetermined reaction sites, PEGylation at a single site of a peptide can minimise the diversity of the products, providing a more precise modification. However, it is not practical for native colistin due to the similar activity of its functional groups. Thanks to the well-developed solid-phase peptide synthesis, an engineered peptide with a single site mutation can now be achieved in a relative easy way. Recently, a cysteine containing polymyxin analogue, $Thr^{10} \rightarrow$ Cys polymyxin B (Pol-SH) was successfully synthesised by our collaborator from Monash University. Through the 'thiol-acrylate' reaction with its thiol group, PEG with different size can be site-specifically modified onto this polymyxin analogue at ambient temperature without a catalyst in an aqueous solution.

2.2 Results and Discussion

2.2.1 Modification of colistin on Dab residues *via* reductive amination approach

Although the reductive amination has been widely applied for amine modification of peptides/proteins,[1, 7] it has not been used to modify colistin, which does not have a reactive *N*-terminal amine but does have five amines that are very similar in chemical structure, environment and reactivity. Taking into account the fact that the Dab amine has a larger base dissociation constant (K_b) than the terminal amine,[8, 9] it is more likely to be protonated in aqueous media, leading to a less stable

imine bond formation. Thus, it is uncertain whether this approach can modify colistin under the same conditions as that used for the terminal amine modification on other peptides/proteins. Thus, a better understanding of imine reduction reaction and the optimisation on the reaction condition are required for the polymer modification of the colistin.

2.2.1.1 Aqueous selectivity and stability analysis of imine bond via a small molecule model

Before using the imine reduction approach for colistin conjugation, the stability of imines in aqueous media was first tested through a small molecule model. 2-(2-aminoethoxy) ethanol (AEE) as a simplified model for colistin and 2-formylpyridine (FPy) as the water soluble aldehyde model were selected to investigate the stability of the formed imine under different pH conditions through nuclear magnetic resonance (NMR) (Figure 2.1). The heterocyclic aromatic ring on FPy was expected to increase the stability of the formed Schiff base so that it can be used as a motif to link the polymers with the colistin under physiological condition.

As shown in Figure 2.1, the aldehyde signal (δ = 9.89 ppm) belonged to FPy decreased while a new peak belonged to the imine bond (δ = 8.35 ppm) appeared and increased when the pH of the reaction mixture increased, indicating FPy can react with AEE smoothly in a neutral or basic condition. Although the yield of imine formation varies at different pH (Figure 2.2), in general, the higher pH helped the formation and the stability of the imine bond, which may be mainly attributed to the chemical equilibrium shift caused by the protonation of the amine at a lower pH.

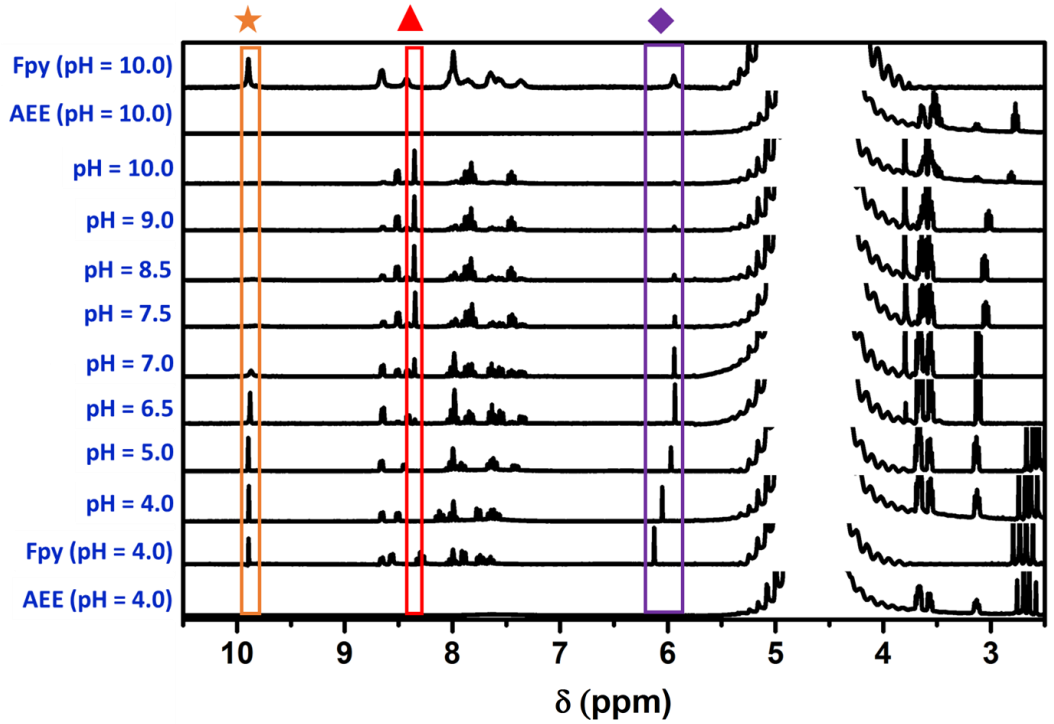

Figure 2.1 ^{1}H-NMR spectra of the FPy/AEE reaction mixture at different pH. The peaks belonged to aldehyde, imine and hydrate product are labled with ★, ▲, and ♦, repectively.

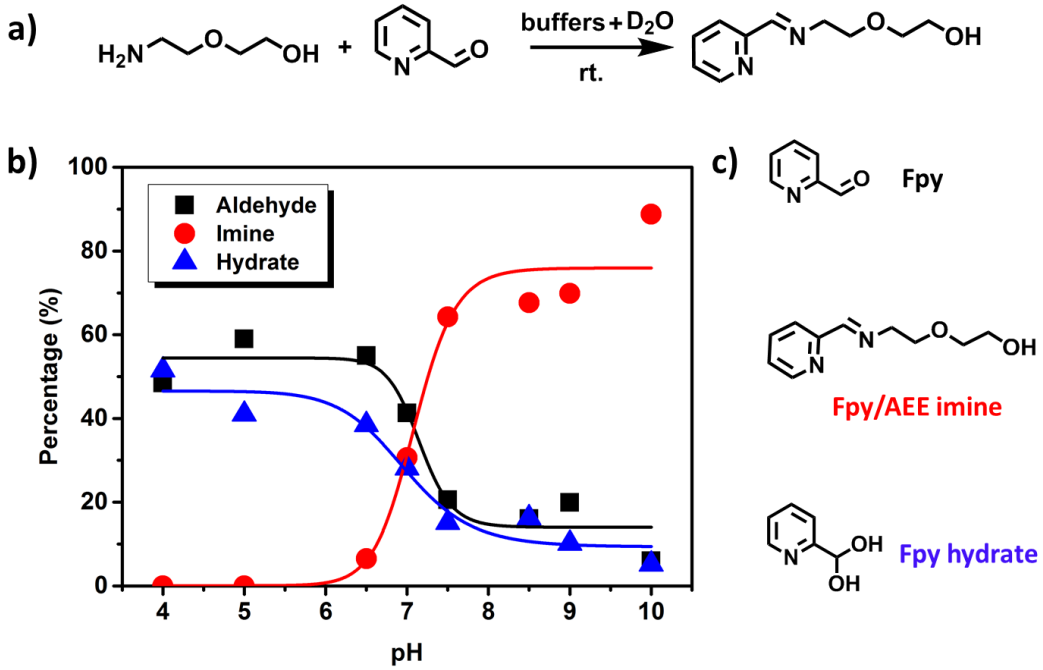

Figure 2.2 The stability test of the model Schiff base in different pH condition. a) Synthesis of the model Schiff base. b) The percentage of Schiff base and other product at different pH in the reaction mixture from ^{1}H-NMR spectra. c) Proposed structures of products at different pH for the corresponding signals from ^{1}H-NMR.

Notably, a side reaction forming FPy hydrate was also observed in the reaction mixture over the pH range tested due to the strong electron-withdrawing effect from the pyridine ring. Although suppressed at elevated pH, a significant amount of adduct (~ 20%) was formed at near physiological conditions. Thus, even though both of the amount of the FPy and FPy hydrate decreased dramatically from pH = 6 to pH = 8, there was only around 60% imine present in the reaction mixture under physiological condition (pH = 7.5).

2.2.1.2 Colistin modification using small molecule aldehyde model via the schiff base reaction

Although the imine bond is not so stable at physiological pH, the majority of the FPy was converted into imine at pH = 10 (Figure 2.2). Thus, an attempt to modify colistin linked through the imine formation using FPy directly without reduction was conducted. Interestingly, a precipitate formed immediately when FPy was added into the colistin solution at pH =10 (Figure 2.16), indicating a chemical reaction between FPy and colistin had taken place. Through the imine bond formation, FPy was attached onto the amine groups present in colistin, reducing the overall hydrophilicity, resulting in the precipitation of the formed FPy-colistin conjugates. To confirm this, the precipitate was collected and analysed by matrix-assisted laser desorption/ionisation-time of flight mass spectrometry (MALDI-ToF MS) (Figure 2.3).

As the native peptide is water-soluble and should remain in the solution rather than in precipitate, it was surprising to see the typical double-peak pattern of native colistin A and B at a mass of 1177.7 and 1191.8 Da from the MALDI-ToF MS. Although no further solid data can be obtained so far, this might be due to the breakage

of the relatively unstable imine bond during the ionisation process of the MALDI-ToF MS.

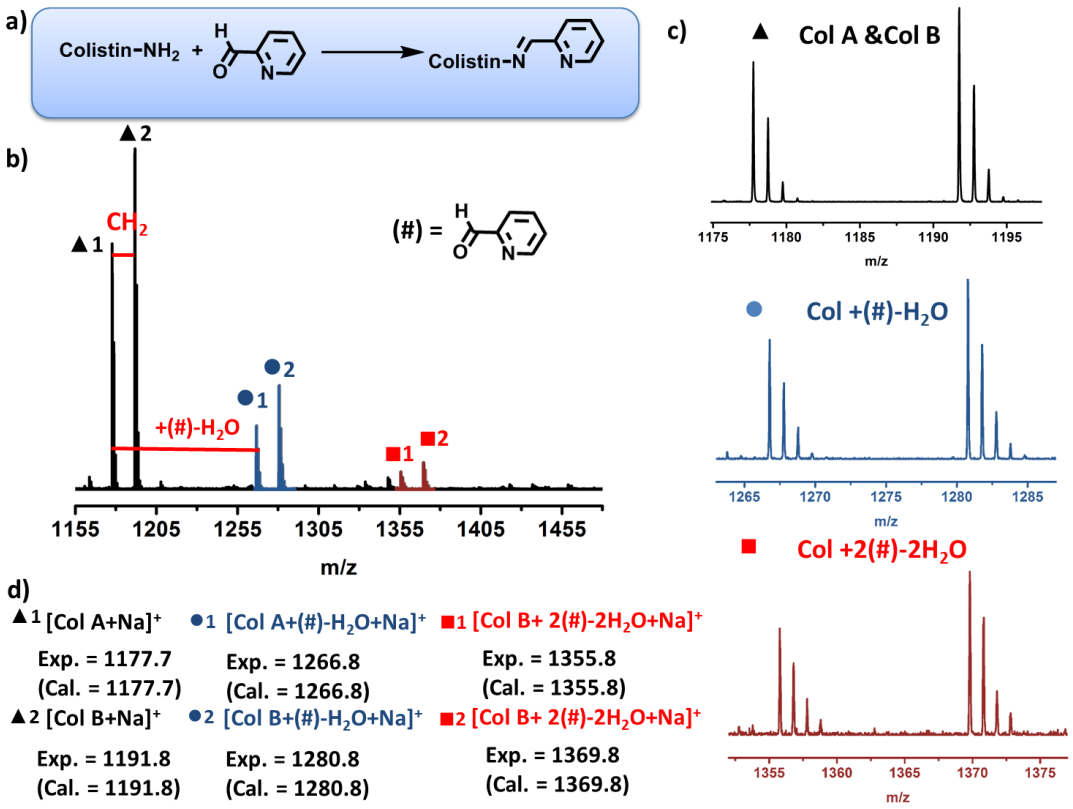

Figure 2.3 MALDI-ToF MS analysis of the colistin-FPy Schiff base from the mixture. a) Synthesis of the colistin-FPy Schiff base. b) MALDI-ToF MS analysis of the reaction mixture. c) The set of peaks for colistin and the Schiff base conjugate.

Apart from the colistin double-peak pattern, the similar double-peak patterns of the mono-adduct and double-adduct on both colistin A and B were also clearly observed from the MALDI-ToF MS spectrum at a distance of 89 Da (Figure 2.3). Other signals that may be contributed to colistin with more FPy modification is also observable even though the quality of signal is too poor to be confirmed as suppressed by the unexpected high signals of the unmodified colistin A and B. Although it is not clear that the precipitate was composed of a complete modification of FPy on all five amines of colistin, all the data suggested FPy could be successfully attached onto colistin amines through the formation of the dynamic imine bond.

Given the fact that the imine bond is relatively unstable towards hydrolysis under physiological conditions, FPy has been shown the potential to conjugate onto colistin without the reducing agent. However, the direct polymer conjugation to colistin *via* the imine formation will be troublesome and difficult to characterise due to the dynamic nature of the linkage coupled to the dispersity present in the polymer. Thus, the imine reduction approach was tested, initially using a small molecule model. With the help of the reducing agents, i.e., sodium cyanoborohydride ($NaBH_3CN$), the formed imine bond can be converted into a secondary amine *in situ* which is stable under physiological condition to the hydrolysis.

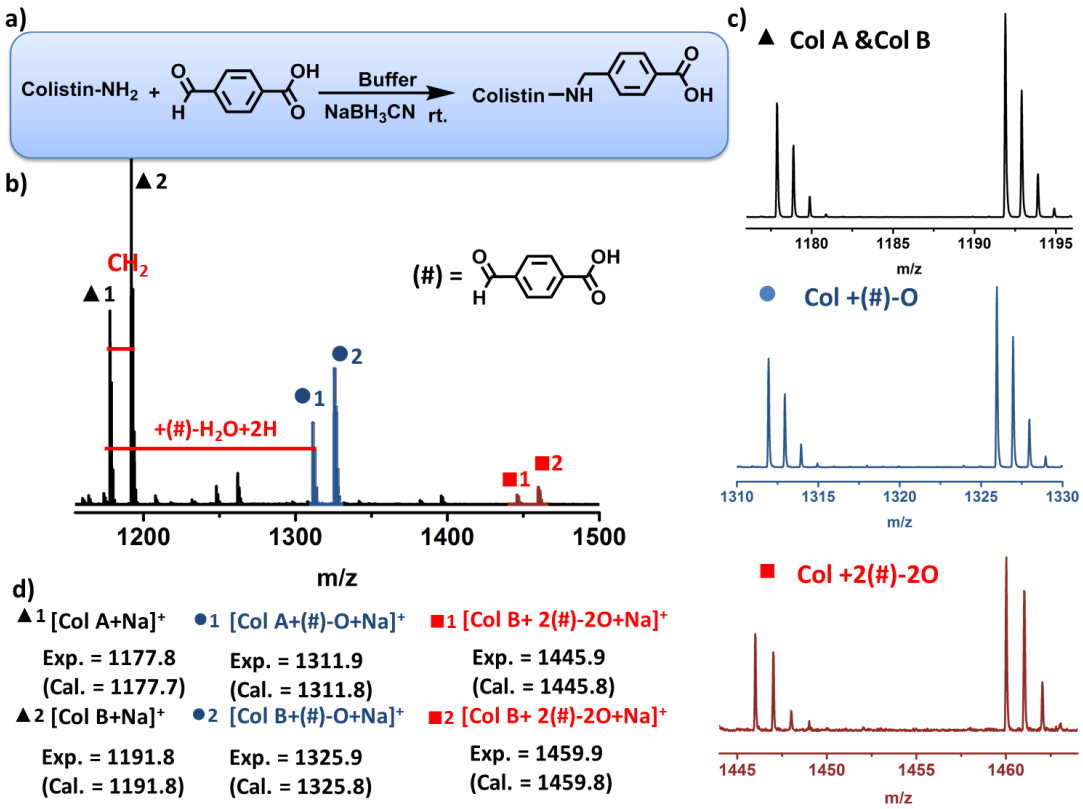

Figure 2.4 MALDI-ToF MS analysis of the colistin-FBA conjugate from the mixture. a) Synthesis of colistin-FBA conjugate. b) MALDI-ToF MS analysis of the reaction mixture. c) The set of peaks for colistin and the conjugate.

In place of FPy, 4-formylbenzoic acid (FBA) was chosen as the aldehyde model to modify the colistin. The carboxyl group on FBA can help the solubility of the

colistin after modification under basic conditions, preventing the precipitation of the product. Instead of using the excess of the aldehyde, FBA and colistin at 1:1 ratio was mixed in the reaction solution to examine the selectivity of FBA for the colistin amines. This reaction was again carried out in a pH = 10 buffer to promote the formation of the colistin-FBA imine conjugates. With $NaBH_3CN$ as the reducing agent, the unstable colistin-FBA imine conjugates were fixed as the stable reduced form. When a 1:1 ratio of FBA and colistin was used, clear patterns corresponding to the mono-adduct and di-adduct on both colistin A and B, along with the unmodified colistin were identified by MALDI-ToF MS of the dialysed reaction mixture due to the similarity of colistin five amines (Figure 2.4). The distance between each double-peaks pattern is 134 Da, suggesting the addition of FBA onto the colistin with a C-N bond instead of C=N bond.

2.2.1.3 Synthesis and characterisation of the aldehyde-terminated mPEG (mPEG-FBA) modification of colistin

Based on the studies of small molecule models described above, a FBA modified mPEG (mPEG-FBA) was synthesised for the PEGylation of colistin (Figure 2.5). The FBA unit was introduced onto mPEG through the Steglich esterification. Although the attachment of FBA onto mPEG through the esterification would cause a mass increase of 132 Da, the peak overlapped with the mPEG with the extra three $–CH_2CH_2O-$ units (44 Da for each unit). Thus, it showed an exact mass pattern as the original mPEG although the average mass increased slightly from the MALDI-ToF MS analysis. Therefore, other characterisation including ^{1}H-NMR, ^{13}C-NMR and Fourier transform infrared spectrometry (FTIR) were used to test the purity of the product. As shown in

Figure 2.5, all these characterisation suggested the formation of an ester bond and the successful introduction of FBA unit onto mPEG.

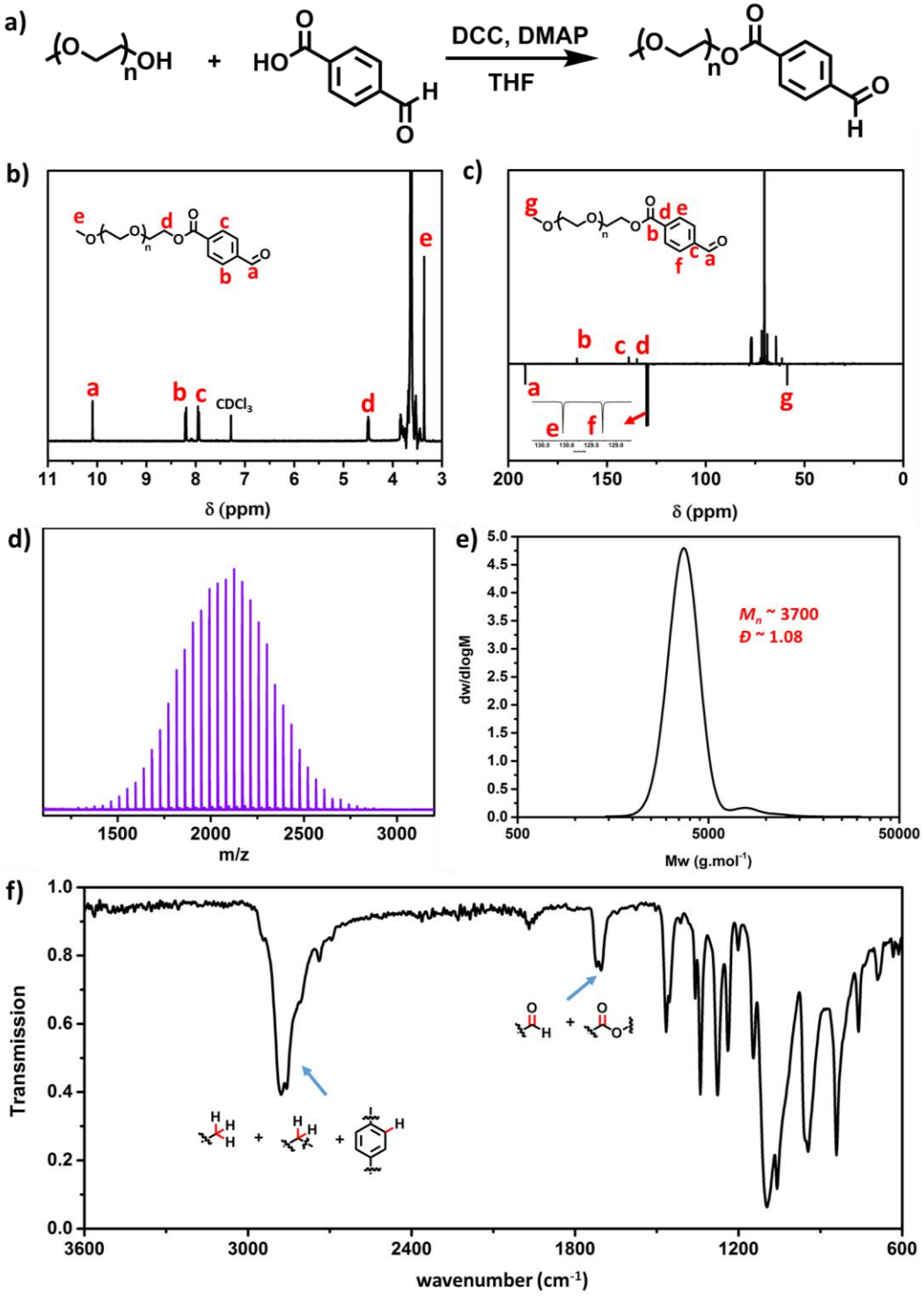

Figure 2.5 a) Synthesis of mPEG-FBA and its characterisations including b) ^{1}H-NMR, c) ^{13}C-NMR, d) MALDI-ToF MS, e) tetrahydrofuran (THF) GPC and f) FTIR.

Gel permeation chromatography (GPC) analysis was also performed to check if any cross-linking reaction had happened during the modification. Although a small high molecular weight peak was observed due to the double PEG modification from the potential impurity (terephthalic acid), the high molecular weight impurty cannot react with amine and the dispersity index of the product remained low ($Đ$ ~ 1.08). Thus, it was then used for the PEGylation of colistin.

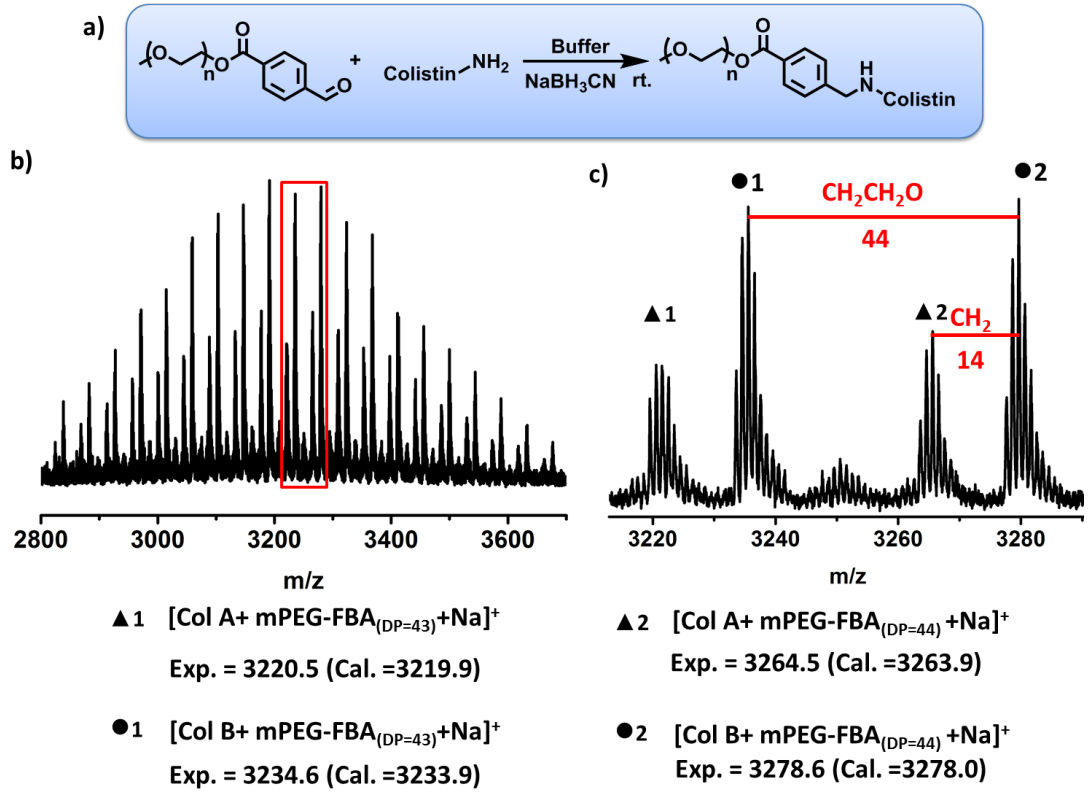

Figure 2.6 MALDI-ToF MS analysis (partial) of the colistin-mPEG-FBA conjugate from the reaction mixture. a) Synthesis of the colistin polymer conjugate. b) MALDI-ToF MS analysis of the colistin polymer conjugate. c) The zoom-in MALDI-ToF MS data of the colistin-mPEG-FBA conjugate.

Due to the presence of a labile ester bond in mPEG-FBA, the reaction to achieve the reduced colistin mPEG-FBA conjugate was conducted at pH = 8.5 rather than pH = 10. Through the MALDI-ToF MS analysis of the reaction mixture, a distribution of PEGylated species was observed around 3200 Da from the reaction mixture, indicating the successful addition of mono mPEG-FBA (M_n ~ 2000 Da) onto colistin (Figure

2.6b). The double-peak pattern along with the repeating unit of 44 Da implied the mPEG-FBA conjugated to both colistin A and B (Figure 2.6c). No higher degree of modification were observed from MALDI-ToF MS due to signal suppression by the mono-modification peaks.

To quantify and separate the obtained amount of mono-PEGylated colistin, HPLC was then applied to identify the composition in the reaction mixture (Figure 2.7). Apart from the original double peaks that belong to the unreacted native colistin, multiple broad new peaks between 16 min to 23 min were observed through the HPLC analysis of the reaction mixture, indicating the formation of the reduced conjugates with mPEG-FBA (Figure 2.7 top trace).

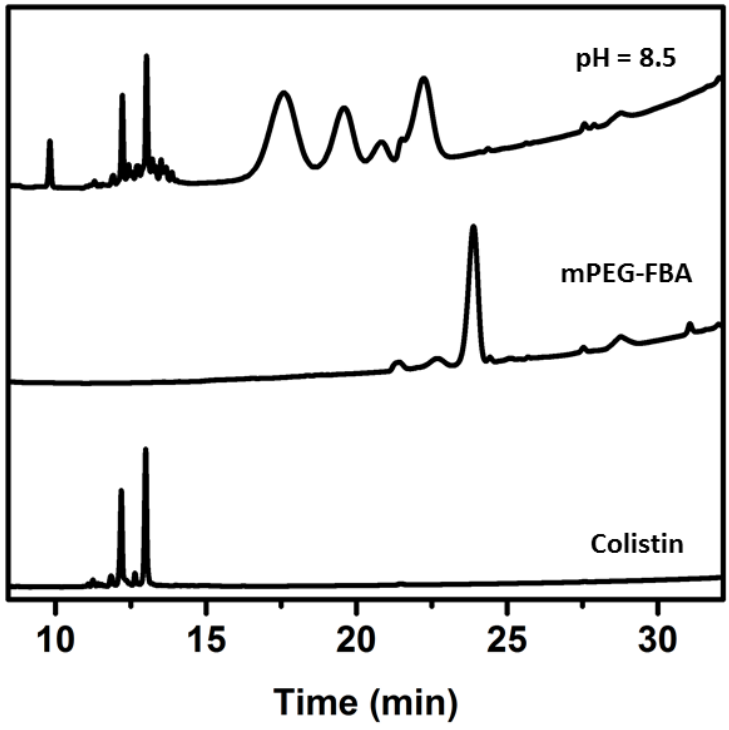

Figure 2.7 HPLC traces of the colistin-mPEG-FBA conjugate (obtained from pH = 8.5 buffer) and the starting materials.

To get a better understanding of the composition of the conjugation product, these multiple broad new peaks from the reaction mixture (pH = 8.5 buffer) were then isolated by HPLC under optimized conditions, collected with a fraction collector and

identified by MALDI-ToF MS (Figure 2.8). The peaks in 11-13 min that eluted at the same time of the pure colistin from HPLC (Figure 2.7 top trace and Figure 2.8a) showed the same mass from MALDI-ToF MS (Figure 2.8c1), suggested they belonged to the unreacted colistin A and B. The peaks between 16 to 22 min (peak ② to ⑤) from HPLC all showed a double-peak pattern and a distribution with the repeating unit of 44 Da although with different molecular weight ranges, indicating they belonged to the colistin-mPEG-FBA conjugates attached with different numbers of mPEG-FBA (Figure 2.8c2-c5). Thus, peak ② was the mono PEGylation product and the accurate molecular weight further confirmed the generation of the conjugate was linked *via* C-N single bond derived from the parent imine formed *in situ*.

As shown in the middle trace of Figure 2.7, the HPLC of the reaction showed that the peak of the original mPEG-FBA completely disappeared after one-day reaction, suggesting the reaction proceeded to completion. However, in addition to being involved in the formation of conjugates with colistin, several side reactions including reduction and hydrolysis processes, were also found to be responsible for the consumption of mPEG-FBA. The MALDI-ToF MS analysis of the peak ⑥ at 22.5 min showed a polymer pattern of a molecular weight distribution around 2000 Da with a repeating unit of 44 Da, suggested it was the reduction product of mPEG-FBA by $NaBH_3CN$ (Figure 2.8c6). The hydrolysis of the mPEG-FBA at this pH was also observed in both MALDI-ToF MS (Figure 2.17a-b) and HPLC as a new peak at 9.8 min that belongs to the reduction product from FBA (Figure 2.8 top trace).

Ion-exchange fast protein liquid chromatography (IE-FPLC) was also introduced to isolate the species with different numbers of amine groups in the reaction mixtures using a cationic exchange column and a fraction collector system. Each fraction was then identified by MALDI-ToF MS. (Figure 2.8c1-c3).

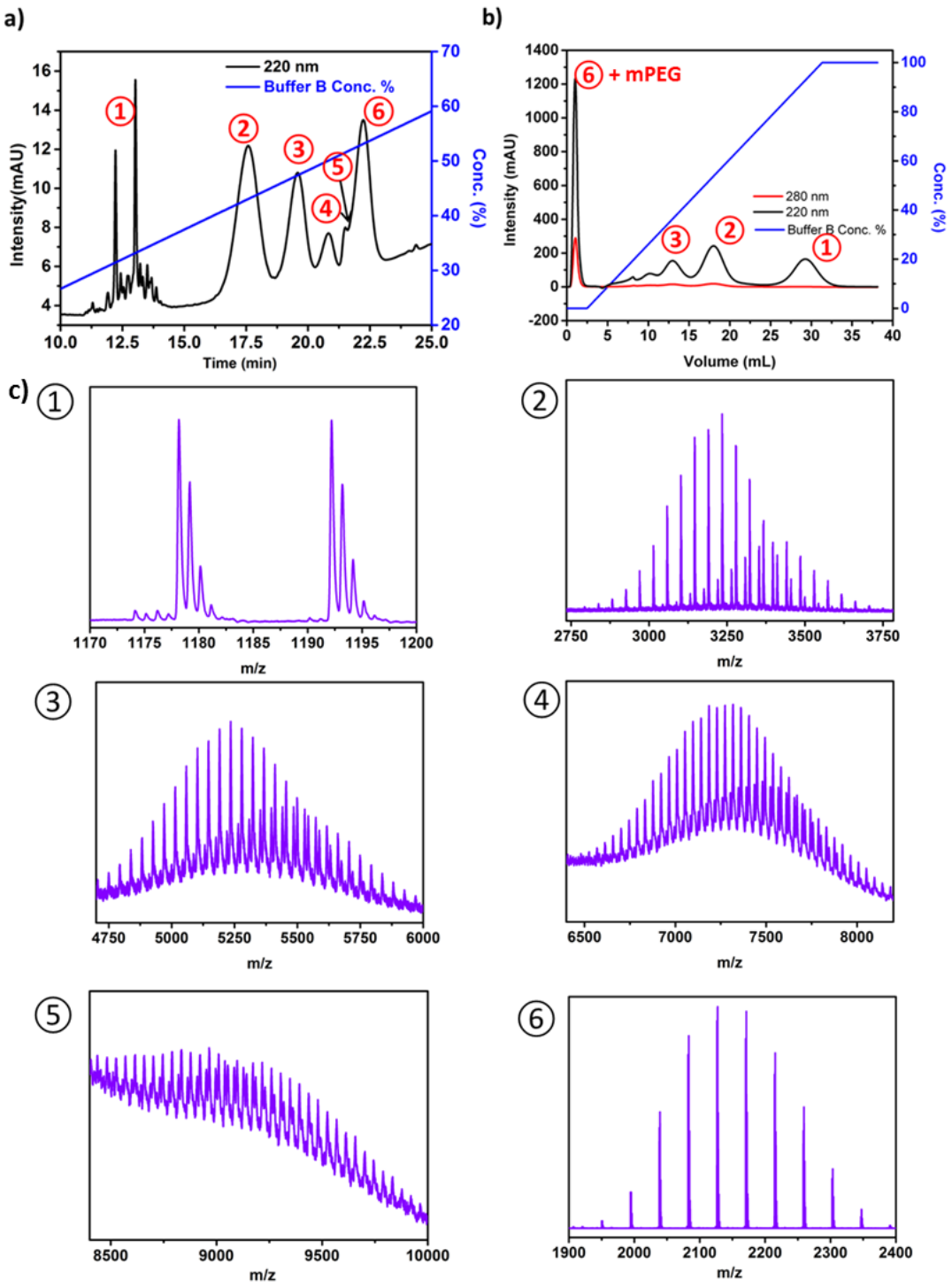

Figure 2.8 The identification of each peak from HPLC and FPLC. A typical RP-HPLC (a) and ion exchange (IE)-FPLC (b) curve of the reduced conjugation mixtures (at pH = 8.5) were shown. c) MALDI-ToF MS of each peak from FPLC (①-③) and HPLC (②-⑥).

The species in the first peak from FPLC were uncharged. The analysis by MALDI-ToF MS showed it was the unmodified mPEG polymers generated from the

hydrolysis (Figure 2.17c-d). The reduced mPEG-FBA should also be present in this peak as it was uncharged. However, it was not observed in this case due to the *in situ* hydrolysis through the purification or the suppression by the strong signal of mPEG.

The elution time from FPLC suggested greater positive charge was present in the compound in peak ② than peak ③ at pH = 4, meaning more amine groups remained on the conjugates in peak ②. The MALDI-ToF MS of the peak ② and peak ③ in FPLC gave similar results as in HPLC, indicating that peak ② contained mainly mono-mPEG-FBA colistin conjugate with four free amine groups whilst the double mPEG-FBA modified colistin conjugate with three amine groups was in peak ③. These data agreed with the result observed from FPLC.

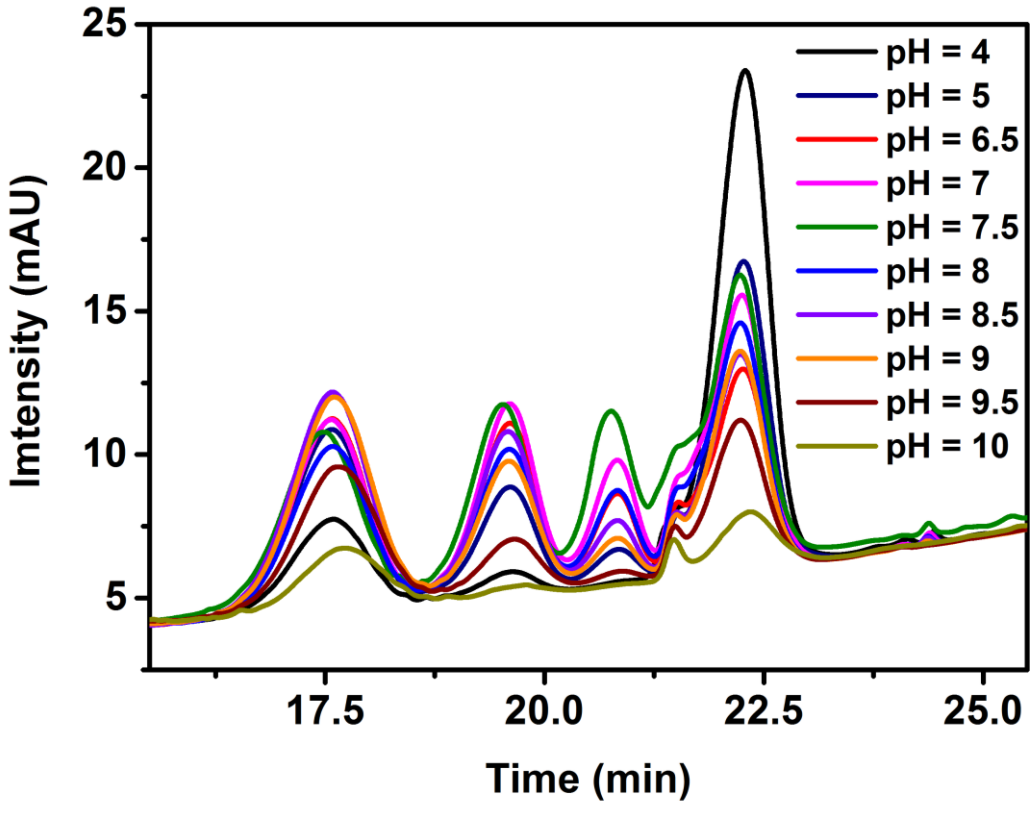

Figure 2.9 HPLC traces (partial) of the colistin-mPEG-FBA conjugates at different pH.

Knowing the compositions of the reaction mixture, the conjugation reaction was then conducted at different pH values for comparison, expecting to find an optimal

condition for the synthesis of mono PEGylated colistin. All of the reaction mixtures were analysed by HPLC as it showed a better separation of the products. As expected, the ratio of each conjugate in the reaction mixture varied with changing the pH. As shown in Figure 2.9, the maximum yield was achieved at pH 8.5-9 when reacting the same mPEG-FBA and colistin. Although the formation and stability of imine bond were favoured at high pH, $NaCNBH_3$ showed less reduction activity at basic condition and the labile ester bond in mPEG-FBA would hydrolyse at this pH, leading to an overall lower yield of the mono PEGylation product. On the other hand, both imine bond and $NaCNBH_3$ are unstable at low pH, mPEG-FBA would be reduced prior to the attachment onto colistin, resulting in the unwanted reducing products.

2.2.2 Antibiotic activity of Dab-modified colistin conjugates

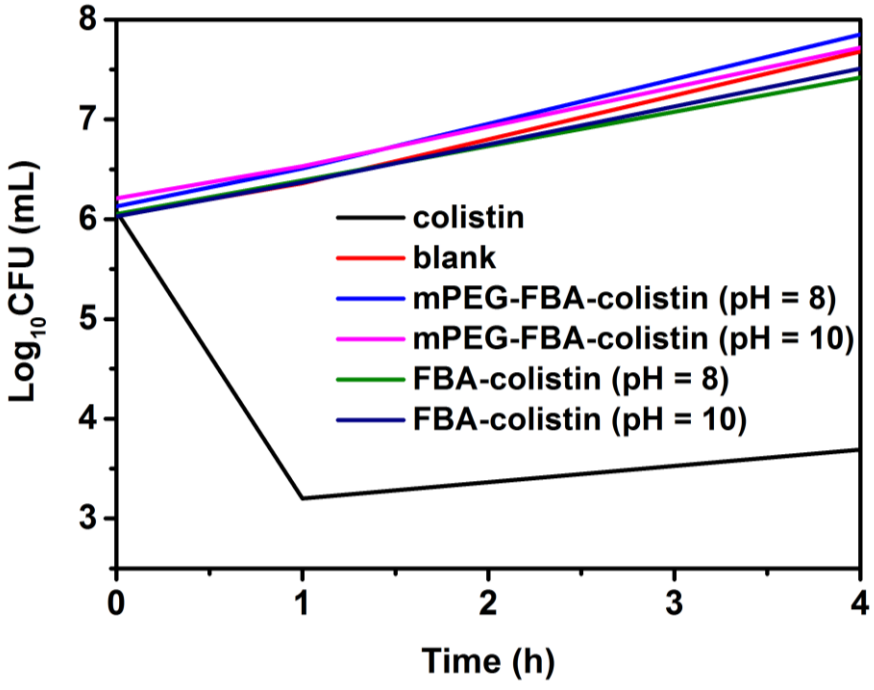

Figure 2.10 The antibiotic activity of the colistin conjugates against *P. aeruginosa* ATCC 27853. Both pH = 8 and 10 buffers were used for the conjugation. CFU: colony-forming unit.

As mentioned previously, the amines on colistin are essential to its antimicrobial activity. However, it was suspected whether the mono PEGylated colistin conjugate still had antimicrobial activity since it retained four unreacted amines. Thus, prior to obtaining the purified mono-conjugate, the antibiotic activity of both small molecule (FBA) and polymer (mPEG-FBA) colistin conjugation reaction mixtures were tested against a MDR Gram-negative strain, *P. aeruginosa* ATCC 27853 (Figure 2.10). Unfortunately, no visible activity was found for the 'time-kill' experiments of all the samples at the concentration of 1 mg/L while the native colistin showed significant suppression of bacterial growth at the same concentration. The number of the colony-forming unit (CFU) decreased dramatically within an hour in the presence of colistin while it increased slightly in all the conjugates samples. Although the ratio of colistin content by weight is less than 50% in the mPEG-FBA colistin conjugation mixture, the activity data obtained from the FBA implied suggesting the modification of colistin on even one of its amine groups with either FBA or mPEG-FBA inhibited the activity of the colistin.

2.2.3 Thiol-acrylate approach for polymyxin analogue (Pol-SH) modification

Although the site-specific modification of native polymyxin is difficult, Pol-SH, a synthetic polymyxin analogue that has a cysteine on position 10, provides an opportunity for the site-specific modification. Several motifs including maleimide and orthopyridyl disulphide, have been widely used for polymer peptide/protein conjugates targeting the cysteine residue.[1, 10-12] However, the synthesis of these functional end-group polymers can be rather complicated. A simple reaction, the thio-michael addition to acrylates (thiol-acrylate reaction) seems to be underestimated in

that field.[13] Unlike other motifs, there is a library of acrylates, most of which are easily synthesized or commercial available. Thus, using small molecule and polymer acryaltes, conjugation at the thiol group on Pol-SH was demonstrated in this section.

2.2.3.1 Pol-SH modification using small molecule acrylate model

Although the thiol-acrylate reaction usually requires a catalyst such as tris(2-carboxyethyl)phosphine (TCEP), triethylamine (TEA) or hexylamine,[14] no additional catalyst in this case was needed since the five primary amines on the peptide will be deprotonated in a basic condition and act as catalyst for this reaction. In order to prove that, small molecule acrylates; 2-hydroxyethyl acrylate (HEA), a glucose acrylate monomer, and poly(ethylene glycol) methyl ether acrylate (M_n ~ 480, $PEGA_{480}$) were tested as models with Pol-SH at both pH = 8 and pH = 9. Slight stoichiometric excess of the acrylates were used to promote the reaction and to minimise the thiol oxidation side reaction.

For glucose acrylate monomers and $PEGA_{480}$, new peaks were observed between the acrylate and Pol-SH at both pH values through the HPLC analysis, while the peaks of starting materials were significantly consumed within 3 h (Figure 2.11b-c), indicating the high efficiency of this thiol-acrylate reaction. Although no new peak was observed for the HEA conjugates due to the similar polarity of the conjugate and Pol-SH, the decrease of the acrylate peak on the HPLC traces implied the successful conjugation was achieved as well (Figure 2.11a). Interestingly, a negligible but observable peak around 10 min was also found in the HPLC of the conjugation mixture. It is thought to be the oxidation product of the Pol-SH into the disulphide form. Although slow, the oxidation of the Pol-SH into the disulphide form can also occur in a basic condition. However, the side reaction can be suppressed at a higher

pH due to the faster thiol-acrylate reaction catalysed by colistin amines in higher pH, thus, it is less visible at pH = 9 than pH = 8.

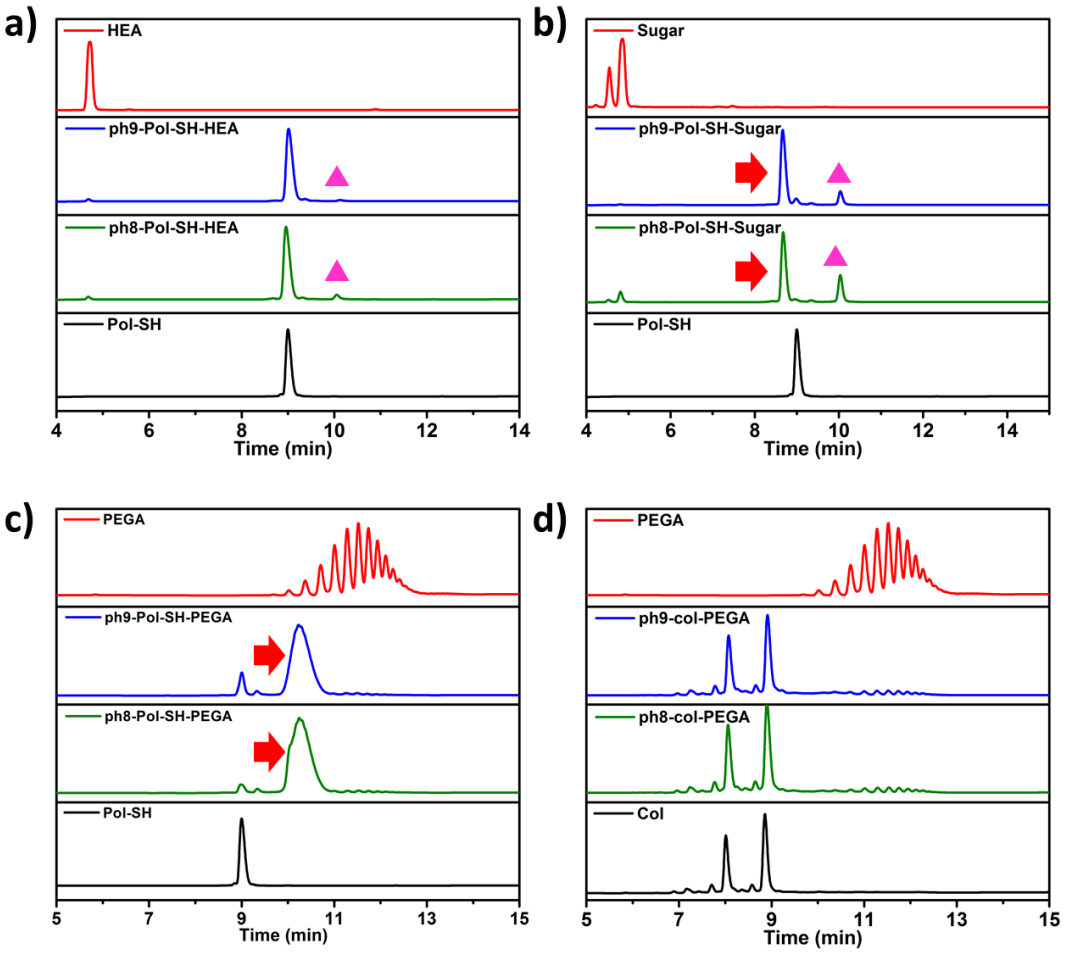

Figure 2.11 The modification of Pol-SH using small molecules. HPLC traces from top to bottom in each graph is 1) small molecular acrylates (red traces): a) HEA, b) glucose acrylate monomer, c-d) $PEGA_{480}$; 2) reaction mixture in pH = 9 after 3 h (blue traces); 3) reaction mixture in pH = 8 after 3 h (green traces); and 4) Pol-SH (a-c) or colistin (d) (black traces). The thiol-addition products and the oxidized side products were labeled with red arrows and triangles, respectively.

Although the addition of the acrylate onto the thiol group is expected to be much faster than onto the amine (or aza-michael addition), a control experiment was conducted to investigate this phenomenon. $PEGA_{480}$ was again used to conjugate with the native colistin which has no thiol group. After 3 h, no decrease of the starting material peaks or new product peak was observed (Figure 2.11d), impling that the

conjugation between Pol-SH and acrylates occured only at the thiol group, and not at the amine groups on the same time scale.

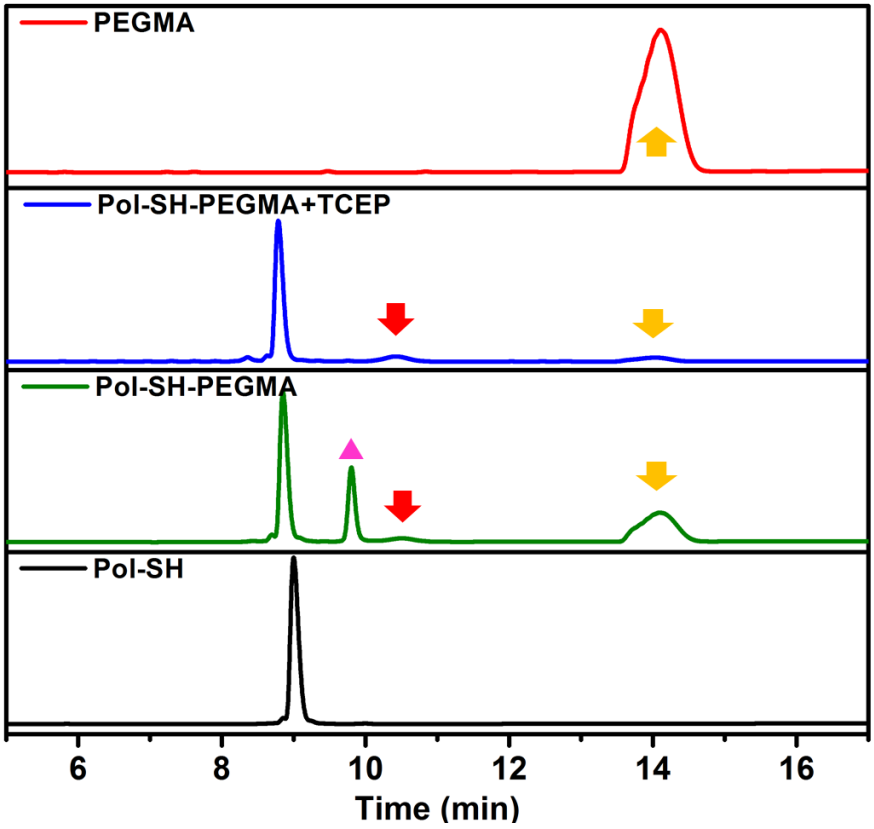

Figure 2.12 HPLC traces of the attempt addition of $PEGMA_{480}$ (red trace) on Pol-SH (black trace) with TCEP (blue trace) or without (green trace) at pH = 8 buffer. The starting material $PEGMA_{480}$, the thiol-addition products and the oxidized side products were labeled with yellow arrows, red arrows and triangles, respectively.

To explore the applicability of this reaction, a poly(ethylene glycol) methyl ether methacrylate (M_n ~ 480, $PEGMA_{480}$) was also tested under the similar condition (Figure 2.12). However, only a small peak was observed at around 10.5 min from HPLC was found while all the starting material peaks remained high, indicating the reaction was much slower and was greatly hindered by the extra methyl group of the methacrylate group, which fitted the observation of this reaction in organic solvents from previous reports.[14] An attempt to accelerated this procoss was then conducted by adding a water-soluble catalyst as well as a reducing agent, TCEP. As shown in Figure

2.12, although more $PEGMA_{480}$ was reacted during the same reaction time and the oxidation side product of Pol-SH disappeared completely in this case, both starting materials were still not consumed completely due to the hindered structure of the $PEGMA_{480}$.

2.2.3.2 Pol-SH modification using acrylate modified mPEG derivatives (PEGA)

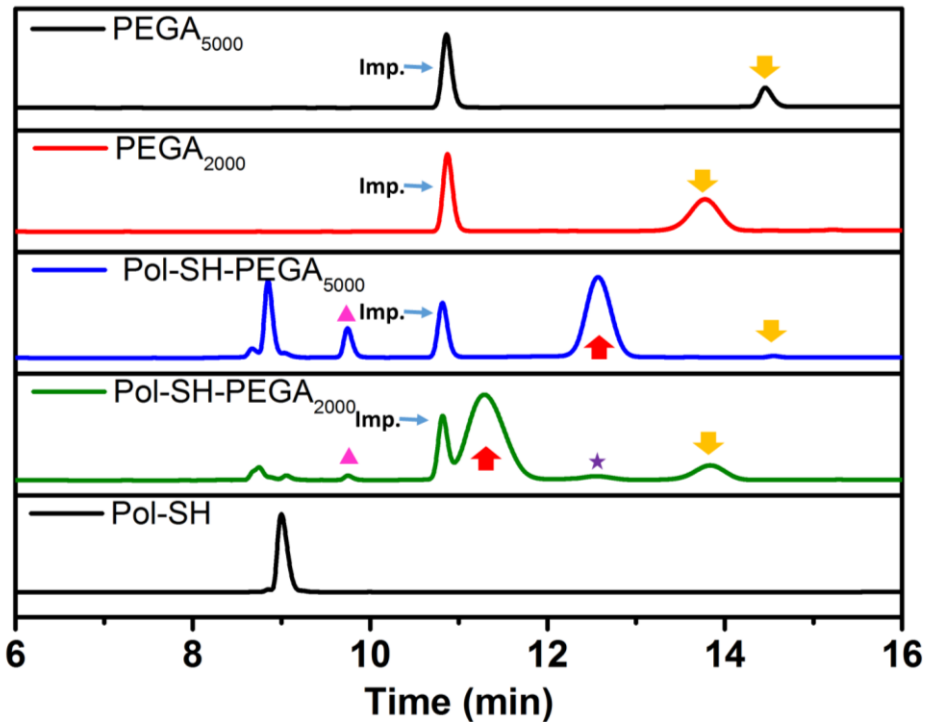

Figure 2.13 HPLC results of the PEGA Pol-SH conjugates and the starting materials. The conponents in each reaction mixture was labled as followed: the formed conjugates (red arrows); the starting polymers (yellow arrows); the oxidised side product (pink triangles) and the potential amine-addition side product (purple stars). The high UV absorbent peak (labelled as Imp.) in the starting material of $PEGA_{2000}$ and $PEGA_{5000}$ was considered to be the inhibitor added commercially although more characterisations were required to confirm this.

Given a better understanding of the thiol-acrylate addition through the small molecule model, the polymer conjugation was then tested using two commercial available polymer acrylates, $PEGA_{2000}$ and $PEGA_{5000}$. TCEP was not added in both

cases to simplify the system. Although a longer reaction time was required in both systems due to the larger size of polymers, similar results were obtained as the small molecule models after 18 h (Figure 2.13). The decrease of the starting polymers and the new peak eluting between the starting polymers and peptide from the HPLC indicated the formation of the PEGylated Pol-SH conjugates. However, the longer reaction time, because of the slower reaction rate of the thiol-acrylate addition to larger polymers, also led to more side reactions. A second polymer containing peak around 12.5 min from HPLC was also observed from the reaction mixture of Pol-SH with $PEGA_{2000}$, which was likely to be due to the amine addition of the acrylate. The oxidation product of Pol-SH was also more significant especially in the case of $PEGA_{5000}$.

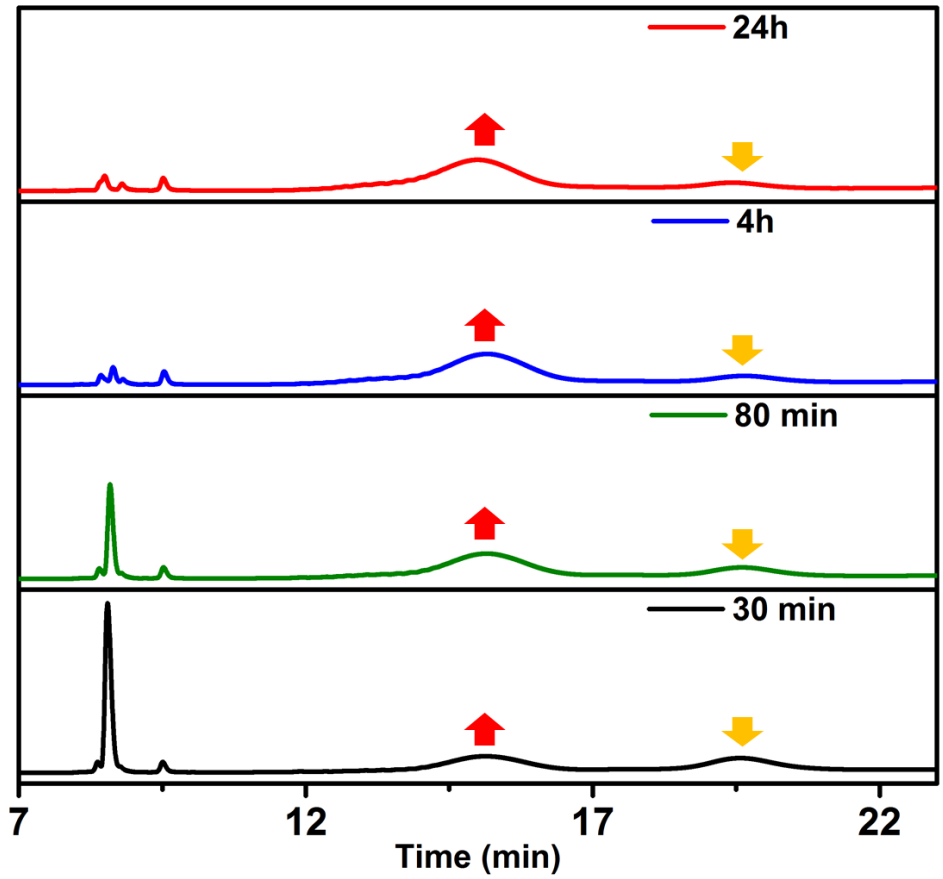

Figure 2.14 The monitoring of the conjugation between APPEGA and Pol-SH using HPLC. The thiol-addition product and APPEGA polymer were labeled with red and yellow arrows, respectively.

Although side reactions were observed using larger PEGA, it may be partially attributed to the lack of acrylate material caused by the impurities in the commercial PEGA (only half or less of the functionalised end group was found in commercial $PEGA_{2000}$ and $PEGA_{5000}$ through ^{1}H-NMR analysis, Figure 2.18). Thus, instead of using the commercial PEGA, an acrylate modified poly($PEGA_{480}$) polymer (APPEGA) was also synthesized *via* aqueous SET-LRP to conjugate with Pol-SH. The reaction was again monitored by HPLC (Figure 2.14). It turned out that the conjugate was formed within 30 min (Figure 2.14, the peak appeared around 15 min), with the reaction reaching completion within 4 h. Negligible amounts of oxidation product were observed, indicating that the thiol-acrylate addition was the dominant reaction even with high molecular weight species, at least with the comb-like polyPEG structure.

2.2.4 Antibiotic activity of Pol-SH polymer conjugates and their native form

Table 2.1 MIC experiments of the peptides, polymers and peptide-polymer conjugates against three bacterial strains (*P. aeruginosa* ATCC 27853, *A. baumannii* ATCC 19606, *K. pneumoniae* ATCC 13883).

MIC (mg/L)	*Pa* ATCC 27853	*Ab* ATCC 19606	*Kp* ATCC 13883
APPEGA	>32	>32	>32
$PEGA_{5000}$	>32	>32	>32
Pol-SH-APPEG	>32	>32	>32
Pol-SH-$PEGA_{5000}$	>32	>32	>32
PolB	1	0.5	0.5
PolB-SH	8	32	16

To verify whether the Pol-SH retained its antibiotic activity when a polymer was attached on its Cys residue, the $PEGA_{5000}$ and APPEGA polymyxin conjugates were

purified by preparative HPLC and then assessed for antibiotic activity (Table 2.1). Through the minimum inhibitory concentration (MIC) assay, all the polymers and their conjugates showed no activity at a concentration of 32 mg/L while the native polymyxin B and the engineered poly-SH showed activity below that concentration against all three bacterial strains. Notably, although poly-SH showed an antibacterial activity, the MIC of it is much higher than the native polymyxin B, indicating the change, even a small one, on native polymyxins can dramatically reduce their antibacterial activity. Thus, it implied the permanent attachment of a polymer onto polymyxin is not suitable for a potential drug candidate as it hindered polymyxin antimicrobial activity.

2.3 Conclusions

Two PEGylation approaches, imine reduction and thiol-acrylate addition reactions, have been developed to achieve the mono PEGylation of colistin and Pol-SH, respectively. Through the small molecule models, it was found the imine bond is unstable in aqueous media although it can be enforced by a basic environment. Therefore, it is not practical to form colistin conjugates directly through imine formation, but it was interesting to find that the small molecule 2-formylpyridine (FPy) can modify colistin forming a precipitate without the reduction process at pH = 10. With the help of $NaCNBH_3$, both small molecules and polymer aldehyde can be successfully attached onto colistin although it ended up with a mixture of products with different degrees of modification. Through the fine tuning of the reaction pH, the highest yield of the mono PEGylation product can be obtained at pH around 8.5-9.

The thiol-acrylate addition, on the other hand, can achieve a targeted modification on the Cys residue onto the engineered peptide (Pol-SH) with an easily

acquired or commercially available acrylate monomer or polymer. As colistin amines can act as a catalyst for the efficient addition reaction, the modification of Pol-SH by the acrylates can be achieved under basic aqueous media without additional catalysts, although TCEP was suggested that can reduce the side reactions and accelerate the addition process.

Both mono PEGylated conjugates showed no antimicrobial activity against the selected MDR Gram-negative bacteria even though most or all of the amines were retained through the modification. It was probably due to the steric hindrance caused by the bulky polymer on its reactive site(s). Although the polymer conjugates have proven not to be the good candidates for antimicrobial application, they have potential in other applications that required a stable linker. Also, the chemistry developed in this work can still be applied in other polymer peptide/protein conjugation that targeting primary amines with high K_b or thiol residue.

2.4 Experimental

2.4.1 Materials

2.4.1.1 Chemicals

All reagents were purchased from Aldrich or VWR international and used without further purification unless otherwise stated. All solvents were purchased from Fisher Chemicals. The dialysis membranes were purchased from Spectrum® Laboratories, Inc. Colistin (A&B mixture) and Pol-SH were kindly provided by Monash Institute of Pharmaceutical Sciences and stored at 4 ^{o}C. $PEGA_{480}$ was passed through the basic aluminium column to remove the inhibitor before being used in the

polymerisation. Tris[2-(dimethylamino)ethyl]amine (Me_6TREN),[15] 2-(2-hydroxyethoxy)ethyl 2-bromo-2-methylpropanoate,[17] and the glucose acrylate monomer[18] were synthesised as described in the literature.

2.4.1.2 Bacterial strains

Bacterial strains of *P. aeruginosa* ATCC 27853, *A. baumannii* ATCC 19606 and *K. pneumoniae* ATCC 13883 (American Type Culture Collection, Manassas, VA) were used in this study. The strains were stored at -80 °C in a cryovial storage container (Simport Plastics, Quebec, Canada). Fresh isolates were sub cultured on nutrient agar (Media Preparation Unit, The University of Melbourne, Parkville, Australia) and incubated at 37 °C for 24 h prior to each experiment. Cation-adjusted Mueller-Hinton broth (CAMHB; Oxoid, Hampshire, England) was used as culture medium.

2.4.2 Instruments

2.4.2.1 Nuclear magnetic resonance (NMR) spectroscopy

^{1}H-NMR and ^{13}C-NMR spectra were recorded on Bruker DPX-250, HD 300, HD 400 and HD 500 spectrometers using deuterated solvents obtained from Aldrich.

2.4.2.2 Fourier transform infrared (FTIR) spectrometry

FTIR spectra were recorder on a Bruker VECTOR-22 FTIR spectrometer using a Golden Gate diamond attenuated total reflection (ATR) cell.

2.4.2.3 Gel permeation chromatography (GPC)

GPC was performed on a Varian 390-LC MDS system equipped with a PL-AS RT/MT autosampler, a PL-gel 3 μm (50 x 7.5 mm) guard column, two PL-gel 5 μm (300 x 7.5 mm) mixed-D columns equipped with a differential refractive index using THF (+ 2% triethylamine (TEA) + 0.01% butylated hydroxytoluene (BHT)) as the eluent with a flow rate of 1.0 mL min^{-1} at 30 ^{o}C. The calibration was fitted with a 3rd order polynomial using narrow molecular weight standards of both poly(methyl methacrylate) (PMMA, between 200 and 467,400 g mol^{-1}).

2.4.2.4 Matrix-assisted laser desorption/ionisation-time of flight mass spectrometry (MALDI-ToF MS)

MALDI-ToF MS was acquired from a Bruker Daltonics Autoflex MALDI-ToF mass spectrometer or Bruker Daltonics Ultraflex MALDI-ToF mass spectrometer. The MALDI-ToF samples were prepared by mixing a solution of α-cyano-4-hydroxycinnamic acid (CHCA) or *trans*-2-[3-(4-tert-Butylphenyl)-2-methyl-2-propenylidene] malononitrile (DCTB) as a matrix (20 mg/mL in THF) and sample (1-2 mg/mL in THF) at 1:1 ratio. 0.5 μL of this mixture was spotted to the target plate. Spectra were recorded in reflector mode calibrating with PEG or mPEG at a similar average molecular weight of each sample.

2.4.2.5 Reversed phase HPLC (RP-HPLC)

2.4.2.5.1 Analytical HPLC

The analytical HPLC system used was an Agilent 1260 infinity series stack equipped with an Agilent 1260 binary pump and a degasser. 50 μL of samples were injected using Agilent 1260 autosampler. The HPLC was fitted with a phenomenex

Lunar C_{18} column (250 x 4.6 mm) 5 micron packing (100Å). Detection was achieved using an Agilent 1260 variable wavelength detector connected in series with UV detection monitored at 225 nm. The method to separate each conjugate varies for different conjugates (typically 5%-70% B) while the total flow rate was set to 1.0 mL/min.

The mobile phases were as followed.

Mobile phase A: 100% water, 0.04% trifluoroacetic acid (TFA);

Mobile phase B: 100% acetonitrile (ACN), 0.04% TFA.

HPLC water and 'far UV' HPLC ACN were used as solvents and HPLC TFA was used as additive.

2.4.2.5.2 Preparative HPLC (PREP HPLC)

The PREP HPLC system used was an Agilent 1260 infinity series stack equipped with a 1260 Quat Pump VL, a degasser and a fraction collector (FC-AS). Samples were injected using Agilent 1260 autosampler with a 100 µl injection volume. The HPLC was fitted with a Jupiter C_{18} column (250 x 21.2 mm) 5 micron packing (300Å). Detection was achieved using an Agilent 1260 TCC detector with UV detection monitored at 225 nm. The method to separate each conjugate varies for different conjugates (typically 30%-45% B) while the total flow rate was set to 8.0 mL/min.

The mobile phases were as followed.

Mobile phase A: 100% water, 0.04% TFA;

Mobile phase B: 100% ACN, 0.04% TFA.

HPLC water and 'far UV' HPLC ACN were used as solvents and HPLC TFA was used as additive.

2.4.2.6 Ion exchange-fast protein liquid chromatography (IE-FPLC)

IE-FPLC (Pharmacia Äkta Purifier) was performed using a cation exchange column, HiTrap SP FF column and eluted in sodium acetate-acetic acid (NaAc-AcOH) buffer at 1 mL/min as the flow rate. The elution of protein fractions was monitored at both 220 nm and 280 nm and the fractions were collected each 0.5 mL.

The details of the mobile phases and the gradient method are showed below:

Mobile phase A: NaAc-AcOH buffer (pH = 4, 20 mM);

Mobile phase B: NaAc-AcOH buffer (pH = 4, 20 mM) + 0.5 M NaCl;

The method for elution started with 100% A, equilibrated with 5 CV, delayed the gradient for 2 mL and gradient eluted for 30 CV to reach 100% B, and washed with 100% B for 5 CV.

The column need to be washed with HPLC water before and after use, and stored in 0.1% sodium azide solution.

2.4.3 Synthesis

2.4.3.1 Synthesis of mPEG-FBA

The synthesis of mPEG-FBA was based on the previous report.[16] Briefly, $mPEG_{2000}$ (4.0 g, 2 mmol, 1 equiv.) was first dissolved with toluene in a 200 mL round bottom flask and the solvent was then evaporated under the vacuum to remove the remaining water in the starting material. FBA (0.60 g, 4 mmol, 2 equiv.), and DMAP

(24.4 mg, 0.2 mmol, 0.1 equiv.) were then added and fully dissolved with 100 mL dry THF under N_2. DCC (0.824 g, 4 mmol, 2 equiv.) was then added into the solution and the reaction mixture was kept stirring overnight. After the removal of the formed precipitation from the reaction mixture, the polymer was obtained after repeated dissolution in THF and precipitation in diethyl ether for three times. The total yield is around 80% with end-group functionality above 95%.

^{1}H-NMR (400 MHz, $CDCl_3$, 298 K) δ (ppm) = 10.08 (-C<u>H</u>O), 8.20 (d, J = 8.3 Hz, -C<u>H</u>CCHO), 7.94 (d, J = 8.3 Hz, -C<u>H</u>CHCCHO), 4.48 (-COOC<u>H</u>$_2$), 3.85-3.40 (-OC<u>H</u>$_2$C<u>H</u>$_2$-), 3.35 (-OC<u>H</u>$_3$).

^{13}C-NMR (126 MHz, $CDCl_3$, 298 K) δ (ppm) = 191.45 (-<u>C</u>HO), 165.27 (-<u>C</u>OO-), 138.97 (-<u>C</u>CHO), 134.84 (-COO<u>C</u>-), 130.08 (-COOC<u>C</u>H-), 129.27 (-<u>C</u>HCCHO), 74.00-66.00 (-O<u>C</u>H$_2$<u>C</u>H$_2$-), 64.44 (-O<u>C</u>H$_3$).

Other characterisations including MALDI-ToF, GPC and FTIR were shown in Figure 2.5. $M_{n\text{MALDI}}$ = 2125.2 (DP =44, $[M+Na]^+$)

2.4.3.2 Synthesis of acrylate modified poly(PEGA$_{480}$) (APPEGA)

2.4.3.2.1 Synthesis of poly(PEGA$_{480}$) with a hydroxyl end group (poly(PEGA$_{480}$)-OH)

The synthesis of poly(PEGA$_{480}$)-OH was carried out using the copper-mediated photoinduced living radical polymerisation (CP-LRP) technique.[19] Filtered PEGA$_{480}$ (2 g, 4.16 mmol, 12 equiv.), the initiator, 2-(2-hydroxyethoxy)ethyl 2-bromo-2-methylpropanoate (88.1 mg, 0.345 mmol, 1 equiv.), $CuBr_2$ (1.5 mg, 6.9 μmol, 0.02 equiv.), Me_6TREN (8.9 mg, 0.0414 mmol, 0.12 equiv.) and DMSO (2 mL) were added to a sealed vial and degassed by purging with nitrogen for 15 min. Polymerisation was conducted under the UV lamp and left overnight. The product was dialysed against

water for 2 days using the dialysis membrane (1000 MWCO) and freeze-dried to obtain the product as an oil with a degree of polymerisation (DP) of 14.

^{1}H-NMR (700 MHz, $CDCl_3$, 298 K) δ (ppm) = 1.08-1.17 (-OC(O)C(C$\underline{H}_3$)$_2$-), 1.30-2.80 (polymer backbone, br, -C$\underline{H}_2$C$\underline{H}$-), 3.35 (br, C$\underline{H}_3$O-), 3.40-3.85 (-OC$\underline{H}_2$C$\underline{H}_2$O-), 4.05-4.40 (-OCH$_2$C$\underline{H}_2$OC(O)C(CH$_3$)$_2$- and -CHC(O)OC$\underline{H}_2$CH$_2$O-) , 5.80-6.00 (br, $\underline{H}$OCH$_2$CH$_2$)

^{13}C-NMR (176 MHz, $CDCl_3$, 298 K) δ (ppm) = 24.50-26.00 (multiple peaks), 32.00-38.00 (br), 39.90-40.20 (br), 40.70-41.50 (br), 59.00, 61.56, 63.20-63.80(multiple peaks), 64.99, 68.55-69.15 (multiple peaks), 70.25-70.75 (multiple peaks), 71.89, 72.50, 169.18, 169.30, 169.37, 173.5-174.5 (multiple peaks), 175.45, 177.05

IR (neat) ν/cm^{-1}: 2865 (CH_2, CH_3), 1731(C=O), 1091 (C-O-C).

$M_{n\mathrm{NMR}}$ ~ 6720 g mol^{-1}. $M_{n\mathrm{GPC}}$ ~ 7200 g mol^{-1}. $Đ$ ~ 1.14 (Figure 2.15 black line).

2.4.3.2.2 Synthesis of APPEGA

Poly(PEGA$_{480}$)-OH (0.5 g, 0.744 mmol, 1 equiv.) and TEA (70 µL, 5.03 mmol 7 equiv.) were dissolved in 2 mL dry DCM. Acryloyl chloride (40 µL, 4.92 mmol, 6.5 equiv.) was then added in to the reaction mixture and the system was stirred for 1 day at ambient temperature. The product was dialysed against water for 2 days using the dialysis membrane (1000 MWCO) and freeze-dried to obtain the product. The yield of the end-group modification (~87%) is calculated using the vinyl peaks (δ = 5.7 - 6.6 ppm) and the methyl peaks on the initiator (δ = 1.0 - 1.2 ppm).

^{1}H-NMR (700 MHz, $CDCl_3$, 298 K) δ (ppm) = 1.08 - 1.17 (-OC(O)C(C$\underline{H}_3$)$_2$-), 1.30 - 2.80 (polymer backbone, br, -C$\underline{H}_2$C$\underline{H}$-), 3.35 (br, C$\underline{H}_3$O-), 3.40 - 3.85 (-OC$\underline{H}_2$C$\underline{H}_2$O-), 4.05 - 4.40 (CH$_2$=CHC(O)OC$\underline{H}_2$-, -OCH$_2$C$\underline{H}_2$OC(O)C(CH$_3$)$_2$- and -

CHC(O)OC$\underline{H_2}$CH$_2$O-), 5.83 (CH$_{cis}\underline{H}_{trans}$=CHC(O)OCH$_2$-, dd, J_1 = 10.54, J_2 = 1.25 Hz) 6.13 (CH$_2$=C$\underline{H}$C(O)OCH$_2$-, dd, J_1 = 17.32, J_2 = 10.04 Hz) 6.40 (C$\underline{H}_{cis}$H$_{trans}$=CHC(O)OCH$_2$-, J_1 = 17.32, J_2 = 1.25 Hz)

^{13}C-NMR (176 MHz, CDCl$_3$, 298 K) δ (ppm) = 24.50 - 26.00 (multiple peaks), 32.00 - 38.00 (br), 39.90 - 40.20 (br), 40.70 - 41.50 (br), 58.99, 61.56, 63.20 - 63.80(multiple peaks), 64.98, 68.55 - 69.15 (multiple peaks), 70.25 - 70.75 (multiple peaks), 71.88, 128.21, 131.13, 166.05, 169.17, 169.29, 169.39, 173.5 - 174.5 (multiple peaks), 175.34, 176.95

IR (neat) ν/cm^{-1}: 2865 (CH$_2$, CH$_3$), 1731(C=O), 1091 (C-O-C).

$M_{n\text{GPC}}$ ~ 7400 g mol^{-1}. $Đ$ ~ 1.15. (Figure 2.15 red line)

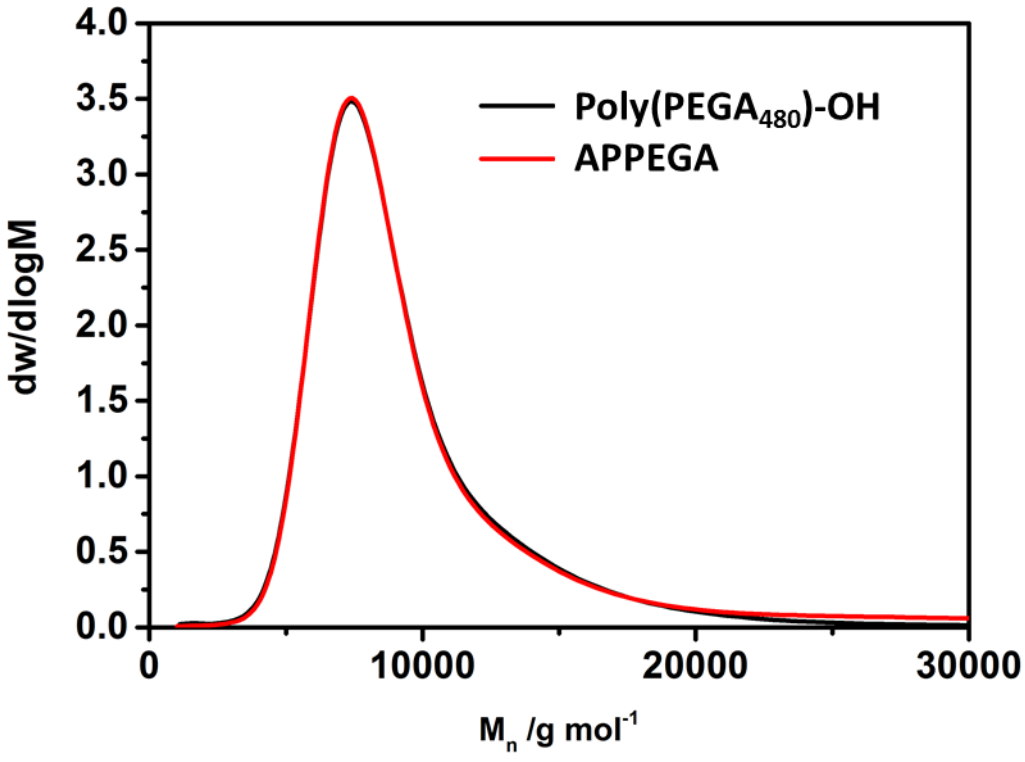

Figure 2.15 THF GPC traces for poly(PEGA$_{480}$)-OH and APPEGA.

2.4.3.3 Synthesis of the colistin-FPy schiff base

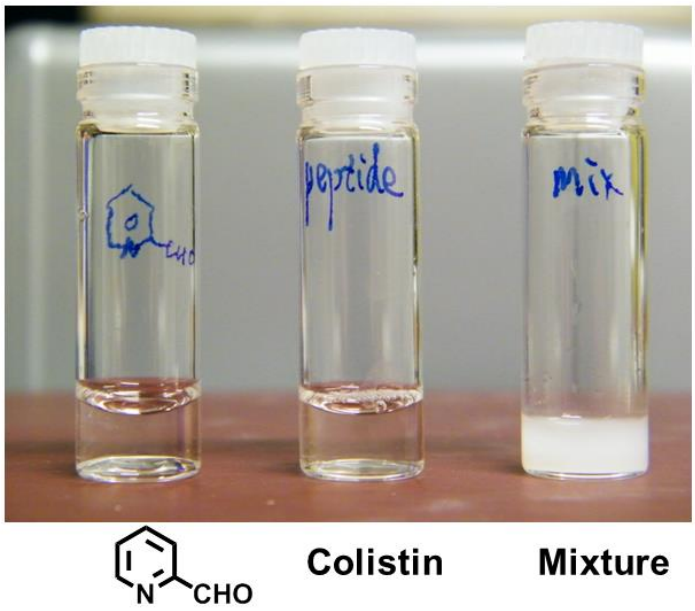

Figure 2.16 Image of the FPy modification within 30 s.

5 mg of colistin (4.7 µmol, 1 equiv.) and 2.5 mg of FPy (23.4 µmol, 5 equiv.) were separately dissolved in 800 µL water and 200 µL pH = 10 Na_2CO_3-$NaHCO_3$ buffers (500 mM). 500 µL of both solution were then mixed together. A precipitate formed within 30 s (Figure 2.16) and was collected for MALDI-ToF MS (Figure 2.3).

2.4.3.4 Synthesis of colistin conjugates using the imine reduction approach

Colistin FBA conjugates: 10 mg of colistin (9.5 µmol, 1 equiv.) and 1.4 mg of FBA (9.3 µmol, 1 equiv.) were dissolved in 900 µL pH = 10 Na_2CO_3-$NaHCO_3$ buffers (500 mM). The reaction mixture was stirring for 1 day and 100 µL 200 mg/mL $NaBH_3CN$ solution (31.7 mmol, 33 equiv.) was added. The sample for MALDI-ToF MS test was dialysed against water to remove salts and small molecules using the dialysis membrane (500 MWCO) (Figure 2.4). The time-kill tests for the obtained products were shown in Figure 2.10.

Colistin mPEG-FBA conjugates: 2 mg of colistin (1.9 μmol, 1 equiv.) and 4 mg of mPEG-FBA (2 μmol, 1 equiv.) were dissolved in 900 μL different pH buffers (100 mM). The reaction mixture was stirring for 1 day and 6.3 mg $NaBH_3CN$ (0.1 mmol, 50 equiv.) in 100 μL buffer was added. The reaction mixture was then stirring for a further day and samples were taken out for HPLC analysis. The sample for FPLC and MALDI-ToF MS was dialysed against water to remove the salt and small molecules using the dialysis membrane (500 MWCO) before the test. The HPLC, FPLC, and MALDI-ToF MS characterisations for the mixtures were shown in Figure 2.7-2.9. The time-kill tests for the obtained products were shown in Figure 2.10.

2.4.3.5 Synthesis of Pol-SH conjugates using thiol-acrylate addition approach

1 mg of Pol-SH TFA salt (5.68 μmol, 1 equiv.) and 1 equiv. of small molecules were dissolved in HPLC vials with 1 mL buffer (pH = 8 or 9). The reaction mixtures were directly sampled after 3 h for HPLC. The polymer modification was carried out under the similar condition while 4 equiv. of $PEGA_{2000}$ or $PEGA_{5000}$ were used instead since ^{1}H-NMR showed only half of the commercial $PEGA_{2000}$ and $PEGA_{5000}$ have the vinyl groups (Figure 2.18). For antibiotic tests, the synthesis is scaled up to 10 mg of peptide. 1.1 equiv. of APPEGA and 2.2 equiv. of $PEGA_{5000}$ were used to minimize the side reactions. The HPLC characterisations of the conjugates were shown in Figure 2.13-2.14.

2.4.4 Methods

2.4.4.1 The stability test of the imine bond

Dissolved 44 μL (47.2 mg, 0.448 mmol) 2-(2-aminoethoxy)ethanol (AEE) in 3 mL D_2O (solution A). Dissolved 40 μL (46.8 mg, 0.437 mmol) 2-pyridinecarboxaldehyde (FPy) into another 3mL D_2O (solution B). Mixed 2 mL of solution A and solution B to get the schiff base solution (solution C). Add 200 μL of solution C into 300 μL different buffers (pH = 4.0, 5.0, 6.5, 7.0, 7.5, 8.5, 9.0, 9.5, 10.0, 100 mM prepared from either acetate, phosphate or carbonate buffers) for ^{1}H-NMR spectrum. Starting materials were sampled in the similar method. Add 100 μL of solution A or B, 100 μL D_2O into 300 μL different buffers (pH = 4.0 or 10.0, 100 mM).

2.4.4.2 Minimum inhibitory concentration (MIC) test

MICs were determined in accordance to the recommendations of the Clinical and Laboratory Standards Institute.[20] *P. aeruginosa* ATCC 27853, *A. baumannii* ATCC 19606 and *K. pneumoniae* ATCC 13883 were used for the tests. Experiments were performed with CAMHB in 96-well polystyrene microtiter plates. Wells were inoculated with 100 μL of bacterial suspension prepared in CAMHB (containing ~ 10^6 CFU/mL) and 100 μL of CAMHB containing increasing concentrations of colistin polymer conjugates (0 − 32 mg/L). The MIC measurements were carried out in duplicates with the MIC being defined as the lowest concentration at which visible growth was inhibited following 18 − 20 h of incubation at 37 °C.

2.4.4.3 Time-kill test

The time-kill kinetics of the colistin samples were examined against *P. aeruginosa* ATCC 27853 at 1 mg/mL. Briefly, 20 mg of each test sample was added into a 50 mL Eppendorf tube loaded with 20 mL of a logarithmic-phase bacteria containing broth culture of approximately 10^6 CFU/mL. The tubes were incubated in a shaking water bath at 37 ^{o}C. The samples were taken at 0, 1 and 4 h. Subcultures for viable counts were performed on nutrient agar (Oxoid) using WASP2 Spiral Plater (Don Whitley Scientific) and incubated at 37 °C for 24 h. Viable counts were determined by either manual counting or using ProtoCol3 Colony Counter (Don Whitley Scientific).

2.4.5 Others

2.4.5.1 MALDI-ToF MS analysis of the hydrolysis product of mPEG-FBA found in reaction mixture

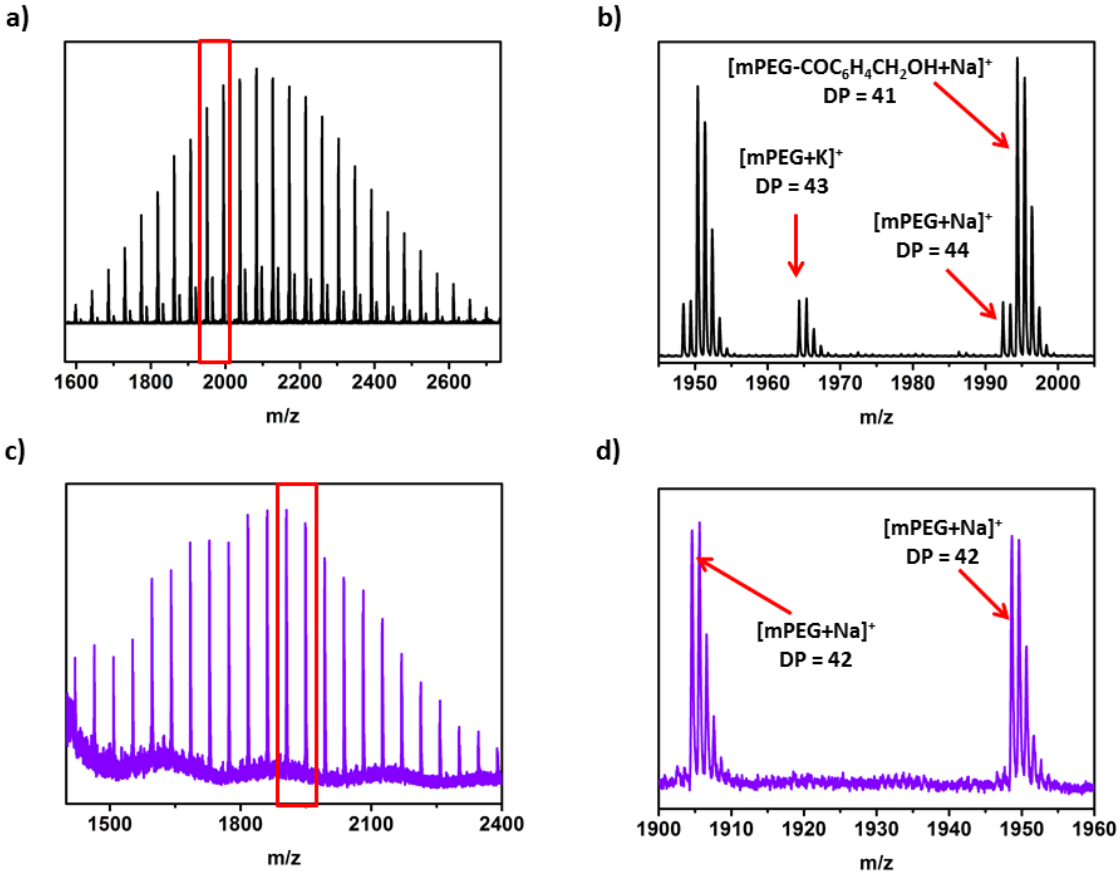

Figure 2.17 MALDI-ToF MS data (partial) of the reaction mixture and FPLC fraction. a) The reaction mixture. b) Partial enlargement in the region around 1945-2005 Da. c) Peak ⑥ in FPLC. d) Partial enlargement in the region around 1900-1960 Da.

2.4.5.2 ^{1}H-NMR spectra of the commerial PEGA$_{2000}$ and PEGA$_{5000}$

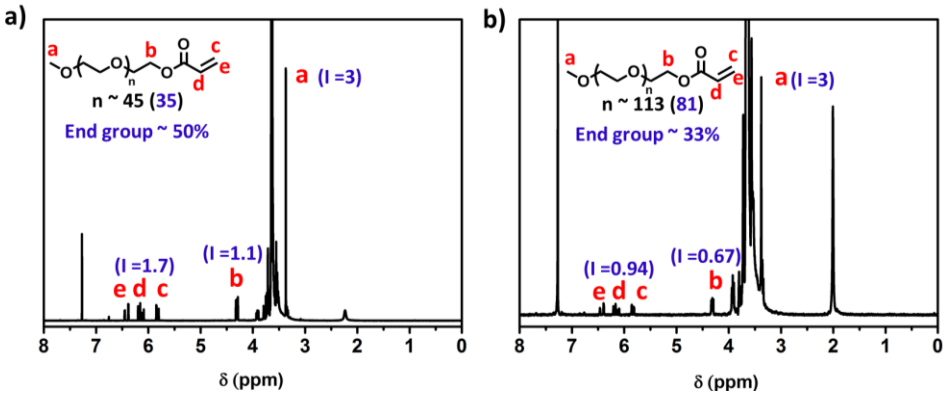

Figure 2.18 ^{1}H-NMR spectra of commercial PEGA$_{2000}$ (a) and PEGA$_{5000}$ (b) in $CDCl_3$. The DP and the functionalised end group was calculated by the integration of each peak. The integration (I) of the methyl group on the ω-end of PEGA was set for 3.

2.5 References

1. M. J. Roberts, M. D. Bentley and J. M. Harris, *Adv. Drug Deliv. Rev.*, 2012, **64**, 116-127.
2. F. M. Veronese and G. Pasut, *Drug Discov. Today*, 2005, **10**, 1451-1458.
3. J. M. Harris and R. B. Chess, *Nat. Rev. Drug Discov.*, 2003, **2**, 214-221.
4. T. Xu, N. Zhao, F. Ren, R. Hourani, M. T. Lee, J. Y. Shu, S. Mao and B. A. Helms, *ACS nano*, 2011, **5**, 1376-1384.
5. M. Danial, C. My-Nhi Tran, P. G. Young, S. Perrier and K. A. Jolliffe, *Nat. Commun.*, 2013, **4**, 2780.
6. B. M. Blunden , R. Chapman, M. Danial, H. Lu, K. A. Jolliffe, S. Perrier and M. H. Stenzel, *Chem. Eur. J.*, 2014, **20**, 12745-12749.
7. L. Tao, G. Mantovani, F. Lecolley and D. M. Haddleton, *J. Am. Chem. Soc.*, 2004, **126**, 13220-13221.
8. A. B. Hughes, *Amino Acids, Peptides and Proteins in Organic Chemistry, Analysis and Function of Amino Acids and Peptides*, John Wiley & Sons, 2013.
9. G. D. Fasman and H. A. Sober, *Handbook of biochemistry and molecular biology*, CRC press Cleveland, 1977.
10. L. Tao, J. Liu, J. Xu and T. P. Davis, *Chem. Commun.*, 2009, 6560-6562.

11. G. Mantovani, F. Lecolley, L. Tao, D. M. Haddleton, J. Clerx, J. J. L. M. Cornelissen and K. Velonia, *J. Am. Chem. Soc.*, 2005, **127**, 2966-2973.

12. M. W. Jones, R. A. Strickland, F. F. Schumacher, S. Caddick, J. R. Baker, M. I. Gibson and D. M. Haddleton, *J. Am. Chem. Soc.*, 2012, **134**, 1847-1852.

13. W. M. Hussein, T.-Y. Liu, P. Maruthayanar, S. Mukaida, P. M. Moyle, J. W. Wells, I. Toth and M. Skwarczynski, *Chem. Sci.*, 2016, **7**, 2308-2321.

14. G.-Z. Li, R. K. Randev, A. H. Soeriyadi, G. Rees, C. Boyer, Z. Tong, T. P. Davis, C. R. Becer and D. M. Haddleton, *Polymer Chemistry*, 2010, **1**, 1196-1204.

15. J. Queffelec, S. G. Gaynor and K. Matyjaszewski, *Macromolecules*, 2000, **33**, 8629-8639.

16. C. Zhu, B. Yang, Y. Zhao, C. Fu, L. Tao and Y. Wei, *Polymer Chemistry*, 2013, **4**, 5395-5400.

17. M. W. Jones, R. A. Strickland, F. F. Schumacher, S. Caddick, J. R. Baker, M. I. Gibson and D. M. Haddleton, *Chem. Commun.*, 2012, **48**, 4064-4066.

18. Q. Zhang, J. Collins, A. Anastasaki, R. Wallis, D. A. Mitchell, C. R. Becer and D. M. Haddleton, *Angew. Chem. Int. Ed.*, 2013, **52**, 4435-4439.

19. A. Anastasaki, V. Nikolaou, Q. Zhang, J. Burns, S. R. Samanta, C. Waldron, A. J. Haddleton, R. McHale, D. Fox, V. Percec, P. Wilson and D. M. Haddleton, *J. Am. Chem. Soc.*, 2014, **136**, 1141-1149.

20. CLSI, *Performance Standards for Antimicrobial Susceptibility Testing: Twentieth Informational Supplement (M100-S20)*, CLSI, Wayne, PA, USA, 2010.

Chapter 3 *A Traceless Reversible Polymeric Colistin Prodrug to Combat Multidrug-resistant (MDR) Gram-negative Bacteria*

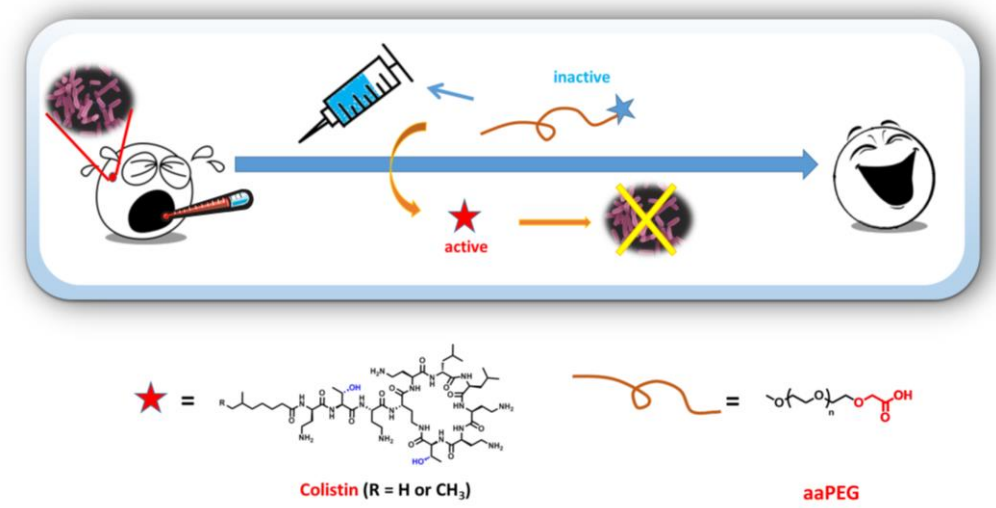

A PEGylated colistin prodrug with a cleavable linker (col-aaPEG) has been developed as a potential alternative for the current colistin prodrug (CMS). This PEGylated prodrug was linked by a labile ester introduced through an acetic acid terminated poly (ethylene glycol) methyl ether (aaPEG) onto the Thr residue of colistin. Due to the labile ester linker, this prodrug can be converted back into active colistin in vitro within 24 h. Compared to CMS, it showed a similar or better antimicrobial performance against two MDR Gram-negative bacteria through in vitro disk diffusion, broth dilution and time-kill studies. In a mouse infection model, col-aaPEG displayed acceptable bacterial killing against P. aeruginosa ATCC 27853 and no nephrotoxicity was found after systemic administration.

3.1 Introduction

The major issue of colistin systematic administration is its high incidence of nephrotoxicity. Although the irreversible PEGylation of colistin has been proven to hinder it antibacterial activity in the previous chapter, formulating colistin into a prodrug form using a releasable linker can potentially improve the *in vitro* and *in vivo* performance of colistin while remaining its activity against the MDR Gram-negative bacteria. A successful example using releasable modification is the current colistin prodrug, colistimethate sodium (CMS). It has become the only colistin treatment for systemic administration. Although CMS is approved by FDA, the slow and variable colistin release rates from CMS complicate its pharmacokinetics, resulting in variable treatment outcomes for patients.[1-3] A further concerning feature of the prodrug is the heterogeneity of the methanesulfonate modification which leads to supplier to supplier and batch to batch structural variation in the prodrug form.[4] Therefore, an alternative prodrug to CMS is highly desirable.

In order to address this, we designed a PEGylated colistin prodrug with a site-specific, traceless, releasable linker. Instead of modifying the five Dab residues of colistin as in case of CMS, the two threonine (Thr) residues were targeted here as it can greatly reduce the site-diversity of the modification products. A relatively labile ester linkage was chosen to build up the colistin prodrug using an acetic acid terminated mPEG (aaPEG) considering the ester is base and enzyme (i.e. lipase) hydrolysable bond that can be cleaved easily in the human body. A commercial mPEG acid with a succinic acid (saPEG) was also applied to achieve colistin conjugation for comparison. *In vitro* degradation studies were performed to investigate colistin release rate. The effect upon the number of mPEG attachments and different linkages on

colistin were also evaluated through the degradation studies. Moreover, the antibacterial activity of the PEGylated colistin prodrug was systematically studied through disk diffusion, broth dilution and time-kill experiments. It turned out to exhibit a similar or better antibacterial activity to the commercial CMS prodrug in all these tests. In addition, a mouse thigh infection model was used to compare the activity performance and toxicity of the PEGylated colistin prodrug with colistin *in vivo*, suggesting the PEGylated colistin demonstrated both low systematic and nephrotoxicity.

3.2 Results and Discussion

3.2.1 Synthesis of reversibly PEGylated colistin

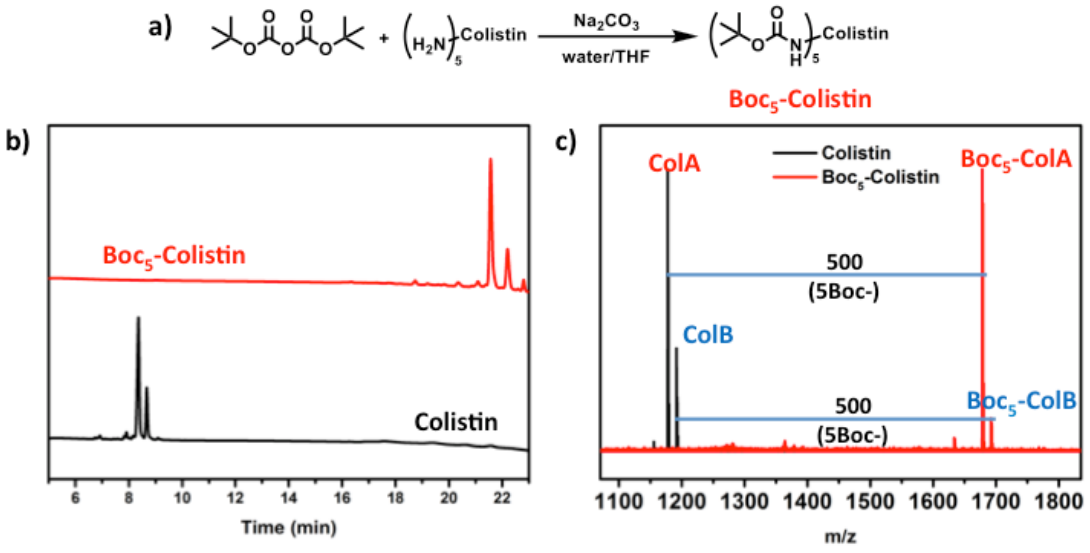

Figure 3.1 a) Synthesis of the Boc_5-colistin. Both HPLC (b) and MALDI-ToF MS (c) of the native colistin and the Boc-modified one showed a fully modified Boc_5-colistin was achieved.

For the site-specific modification of polymyxin we targeted the Thr residues. However, since the amines of the Dab residues in colistin are more chemically reactive than the hydroxyl groups of Thr residues, it was necessary to first protect each of the

amine groups prior to the conjugation of the polymer. A well-developed amine-protection approach using tert-butyloxycarbonyl (Boc) protecting groups was therefore applied (Figure 3.1a). In order to ensure that all the five amines were fully protected, an excess of di-*tert*-butyl dicarbonate (Boc_2O) was used with the addition of potassium carbonate (K_2CO_3) during the modification. The reaction was carried out in a water/ tetrahydrofuran (THF) mixed solvent system so as to prevent further reaction of Boc_2O with the Thr residues. As commercial colistin has two major components (colistin A and colistin B), a double-peak pattern was observed during HPLC analysis of the native lipopeptide (Figure 3.1b, black trace). An identical pattern, but at a higher retention time, was found following reaction with Boc_2O, indicating the protecting groups were successfully introduced onto the amines, rendering the colistin more hydrophobic (Figure 3.1b, red trace). Furthermore, a careful comparison by MALDI-ToF MS of the modified polymyxin to the native colistin measurements (Figure 3.1c), revealed a 500 Da molecular weight increase confirming that all five amines were modified whilst both hydroxyl groups of the Thr residues remained intact.

As hydrolysis was to be used as the mechanism to release the native polymyxin from the prodrug form, aaPEG was chosen since the electron-withdrawing nature of the oxygen bonded to the α-carbon of the carboxyl group makes it a better leaving group thus rendering the ester bond formed less stable and more hydrolytically labile. The synthesis of aaPEG was following a developed method *via* Williamson ether synthesis.[5] mPEG was first deprotonated by a strong base (potassium *tert*-butoxide, tBuOK) in anhydrous *tert*-butanol (tBuOH). The formed reactive oxygen anion on mPEG then attacked a primary alkyl halide, replacing the halide to form an ether bond. As the carboxylic acid group can also react with oxygen anion, an ethyl protected

halide, ethyl bromoacetate, was used in this reaction. After the formation of ether bond, the ethyl protecting group was then hydrolysed under a basic condition and protonated to recover the acid group of aaPEG (Figure 3.2a).

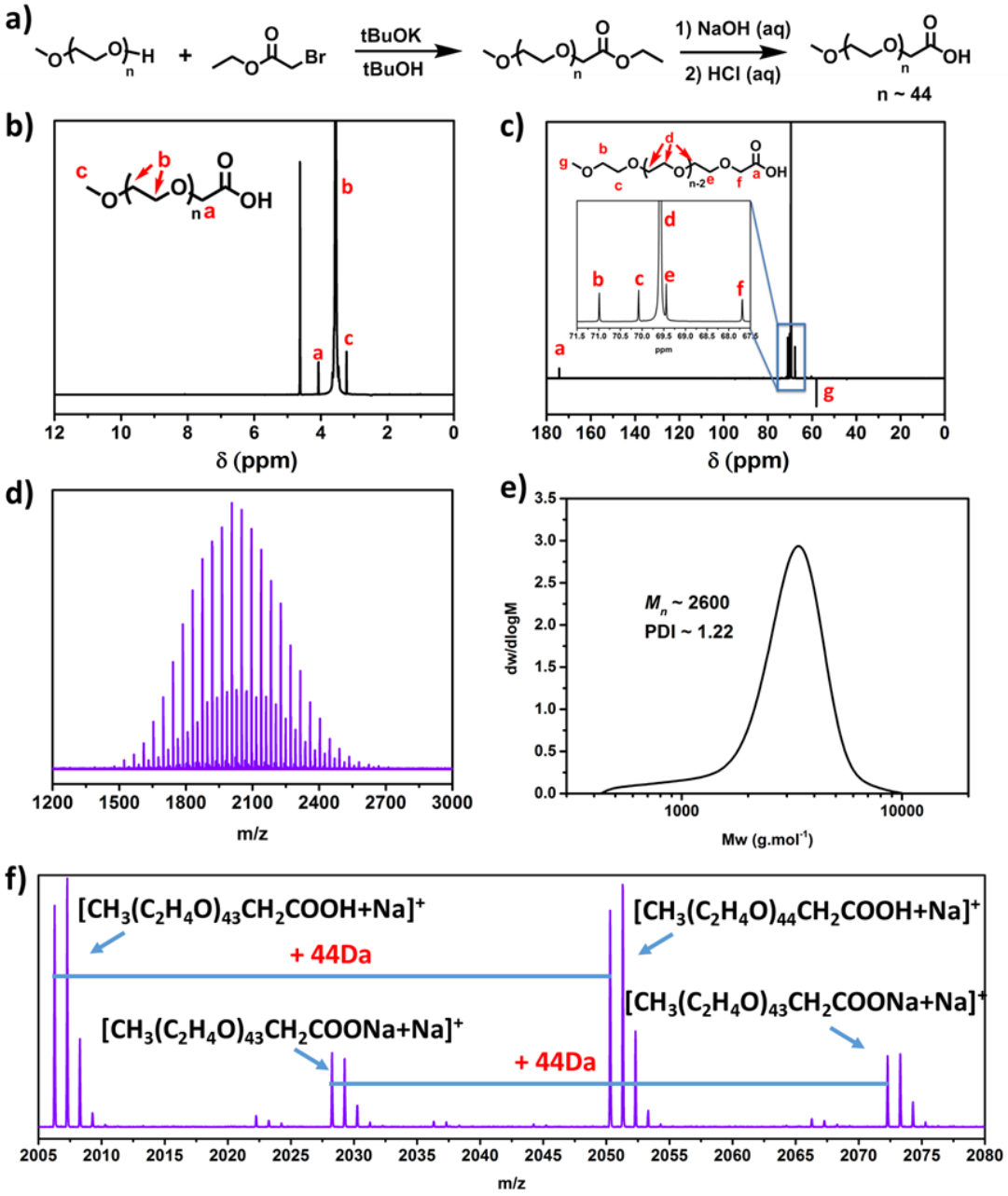

Figure 3.2 a) Synthesis procedure of the aaPEG. b) ^{1}H-NMR and c) ^{13}C-NMR of aaPEG using D_2O as solvent. d) MALDI-ToF MS and e) THF GPC analysis of aaPEG. f) The zoom-in data of (d).

The product was then characterised by NMR, MALDI-ToF MS, and GPC (Figure 3.2b-f). The integration of the original methyl end group (δ = 3.35 ppm) on

mPEG and the formed methylene group next to the carboxyl group (δ = 4.20 ppm) from ^{1}H-NMR while no signal of the ethyl group was found in the both ^{1}H-NMR and ^{13}C-NMR, indicating a successful cleavage of the protecting ethyl group and a complete modification of the acetic acid on the hydroxyl group of mPEG was achieved (Figure 3.2b,c). Although the GPC trace was less symmetrical and had a low molecular weight tailing due to the potential interaction between the acid group of aaPEG and the GPC column, only one molecular weight distribution of around 2000 Da was found in both MALDI-ToF and GPC analyses, suggesting the modification occurred on the end group of mPEG and did not cause the cross-linking of mPEG or the damage to the polymer chain.

Although two main distributions that both have a repeating unit of 44 Da were found through the MALDI-ToF MS (Figure 3.2f), they were considered to be the H^{+}/Na^{+} ion substitution during the sample analysis rather than incomplete protonation through the aaPEG synthesis as only one signal of the formed carboxyl group (δ = 174.3 ppm) can be clearly seen from the ^{13}C-NMR (Figure 3.2c).

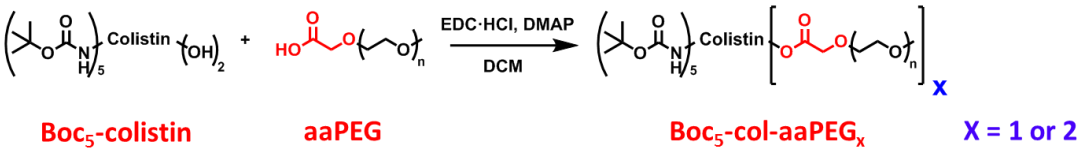

Scheme 3.1 Synthesis of the Boc protected PEGylated colistin conjugates (Boc_5-col-aaPEG_x, x = 1, 2) *via* Steglich esterification.

After the pure aaPEG was obtained and well characterised, it was then used to PEGylate the Thr residues on Boc-protected colistin *via* Steglich esterification (Scheme 3.1). With the help of dehydrating agent, *N*-(3-dimethylaminopropyl)-*N*′-ethylcarbodiimide hydrochloride (EDC·HCl), and the catalyst, 4-

dimethylaminopyridine (DMAP), aaPEG was attached onto Boc-protected colistin at ambient temperature.

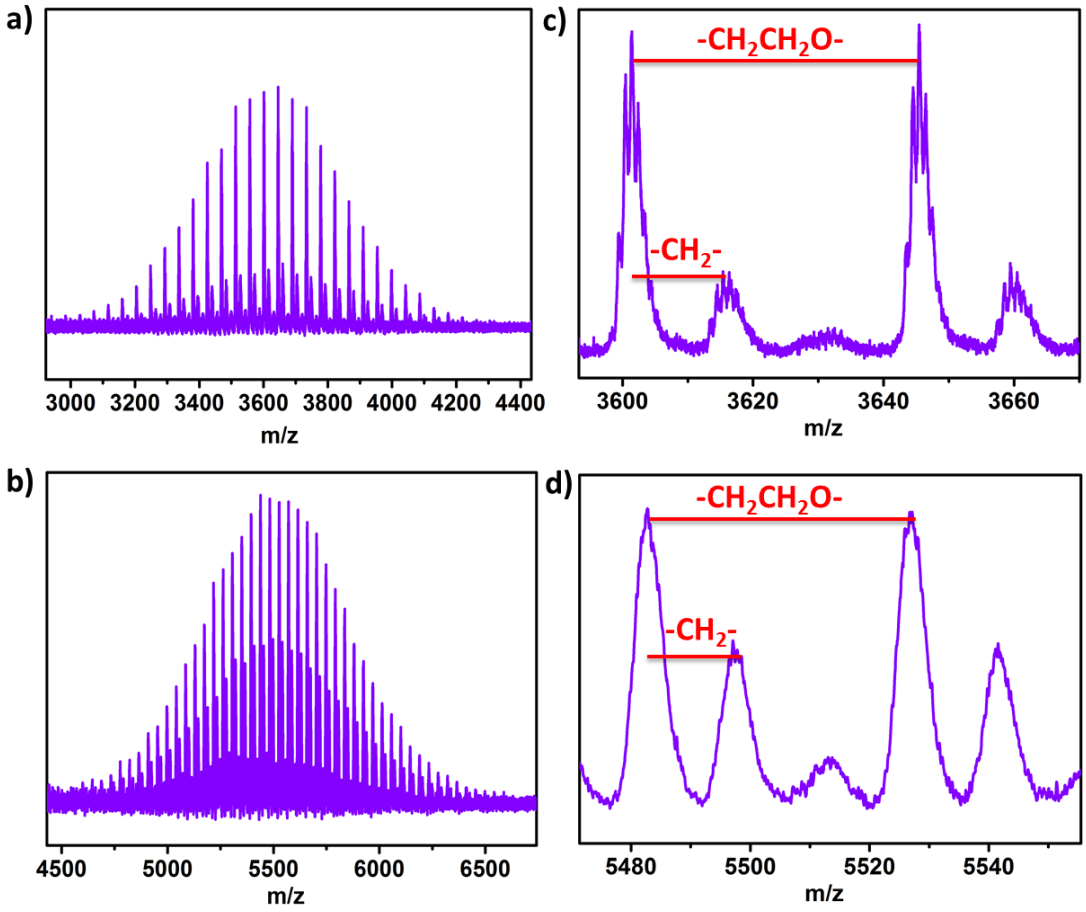

Figure 3.3 MALDI-ToF MS results (a-b) and the related zoom-in data (c-d) of the purified Boc protected conjugation products, Boc_5-col-aaPEG (a, c) and Boc_5-col-$aaPEG_2$ (b, d).

Since there are two hydroxyl groups on the Boc_5-colistin, two products with different molecular weight distributions, a mono-mPEG adduct (Boc_5-col-aaPEG, $M_{n\ \text{Theory}}$ ~ 3.7 kDa, $M_{n\ \text{MALDI}}$ ~ 3.6 kDa, Figure 3.3a) and a bis-mPEG adduct (Boc_5-col-$aaPEG_2$, $M_{n\ \text{Theory}}$ ~ 5.7 kDa, $M_{n\ \text{MALDI}}$ ~ 5.5 kDa, Figure 3.3b), were obtained and isolated by HPLC from the reaction mixture at 20-22 min (Figure 3.4b, black trace) and 18-20 min (Figure 3.4b, green trace), respectively. A polymeric distribution with a typical PEG repeating unit of 44 Da and the double-peak pattern of colistin A and B

can be observed from the MALDI-ToF MS data of both adducts (Figure 3.3c-d), suggesting the successful attachment of aaPEG onto colistin.

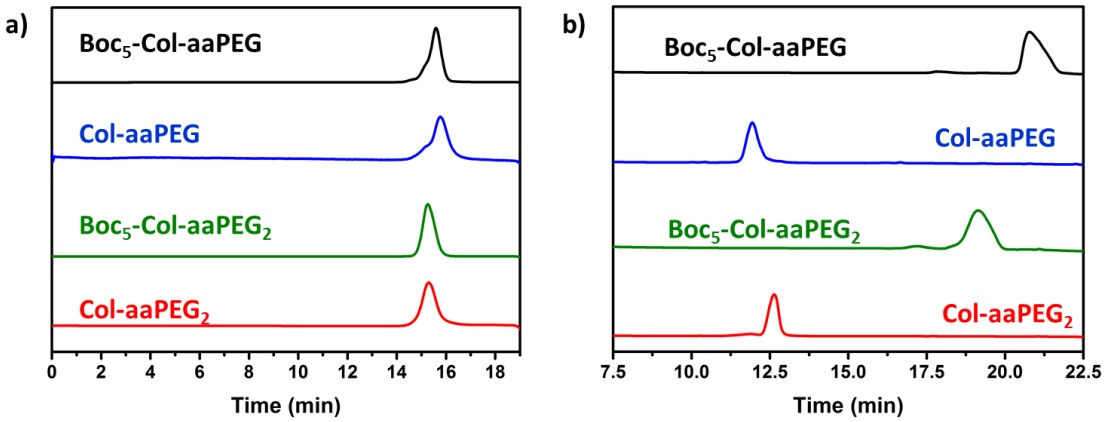

c)

	$M_{n\ \text{Theory}}$	$M_{n\ \text{MALDI}}$*	$M_{n\ \text{GPC}}$	Đ
Boc_5-col-aaPEG	3663	3622	6400	1.10
col-aaPEG	3163	3165	4900	1.21
Boc_5-col-aaPEG$_2$	5663	5527	7800	1.06
col-aaPEG$_2$	5163	5178	7100	1.14

Figure 3.4 The dimethylformamide (DMF) GPC (a) and HPLC (b) traces of the four aaPEG colistin conjugates (Boc_5-col-aaPEG, col-aaPEG, Boc_5-col-aaPEG$_2$ and col-aaPEG$_2$). c) A summary of the theoretical mass, the mass analysed from MALDI-ToF MS and DMF GPC analysis, and the dispersities of these conjugates.

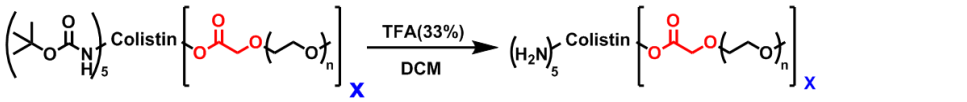

Boc_5-col-aaPEG$_x$ col-aaPEG$_x$

Scheme 3.2 The deprotection of the Boc groups from the Boc_5-col-aaPEG$_x$ (x = 1, 2) conjugates to recover the colistin amines.

The regeneration of the free amines on colistin was conducted under routine conditions for the cleavage of the Boc-protecting groups (Scheme 3.2). After the treatment with 33% trifluoroacetic acid (TFA) in dichloromethane (DCM), the more hydrophilic deprotected products (col-aaPEG and col-aaPEG$_2$) were obtained. A

successful deprotection was indicated by the shift to a shorter retention time during HPLC characterisation when comparing the protected form (Figure 3.4b). Moreover, only a slight decrease in the molecular weight was observed upon GPC characterisation (Figure 3.4a), suggesting the ester bond between colistin and aaPEG remained unaffected during deprotection of both conjugates. Both col-aaPEG ($M_{n\ \text{Theory}}$ ~ 3.2 kDa, $M_{n\ \text{MALDI}}$ ~ 3.2 kDa, Figure 3.5a) and col-aaPEG$_2$ ($M_{n\ \text{Theory}}$ ~ 5.2 kDa, $M_{n\ \text{MALDI}}$ ~ 5.2 kDa, Figure 3.5b) retained the PEG polymeric distribution along with the colistin double-peak pattern through the MALDI-ToF MS data. A molecular weight decrease of 500 Da was observed for the deprotected products, further confirming a full recovery of all the amines on the colistin conjugates.

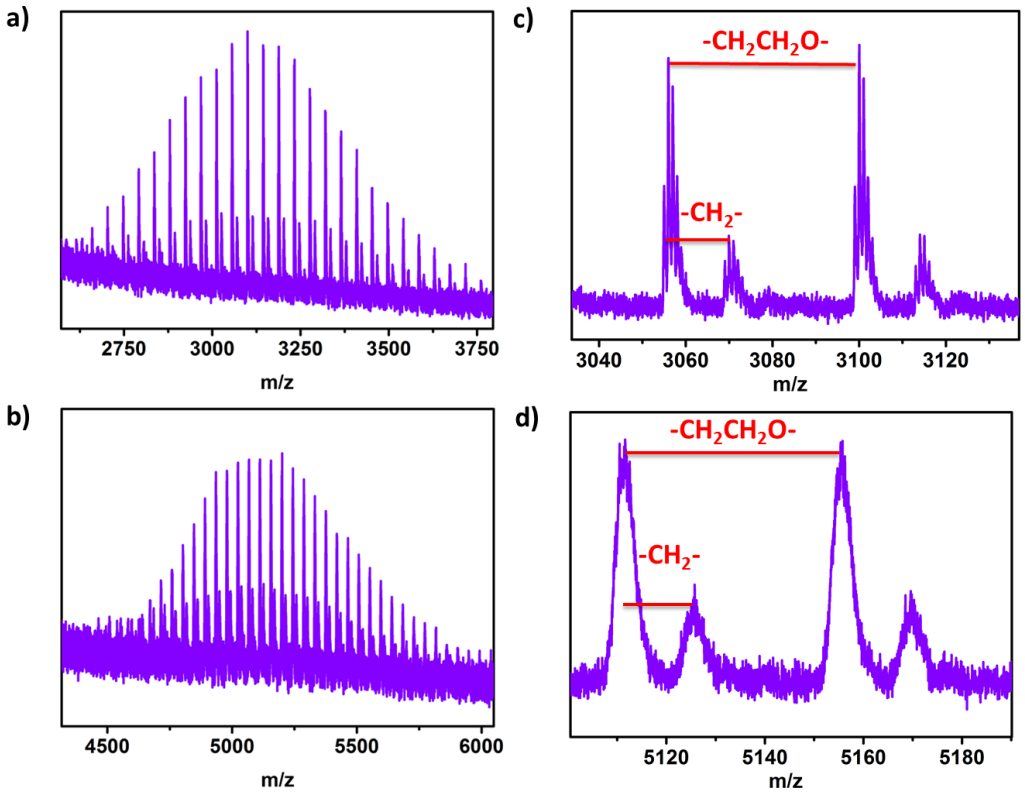

Figure 3.5 MALDI-ToF MS results (a-b) and the related zoom-in data (c-d) of the purified deprocted conjugation products, Boc$_5$-col-aaPEG (a, c) and Boc$_5$-col-aaPEG$_2$ (b, d).

3.2.2 Stability and degradation of the PEGylated colistin conjugates

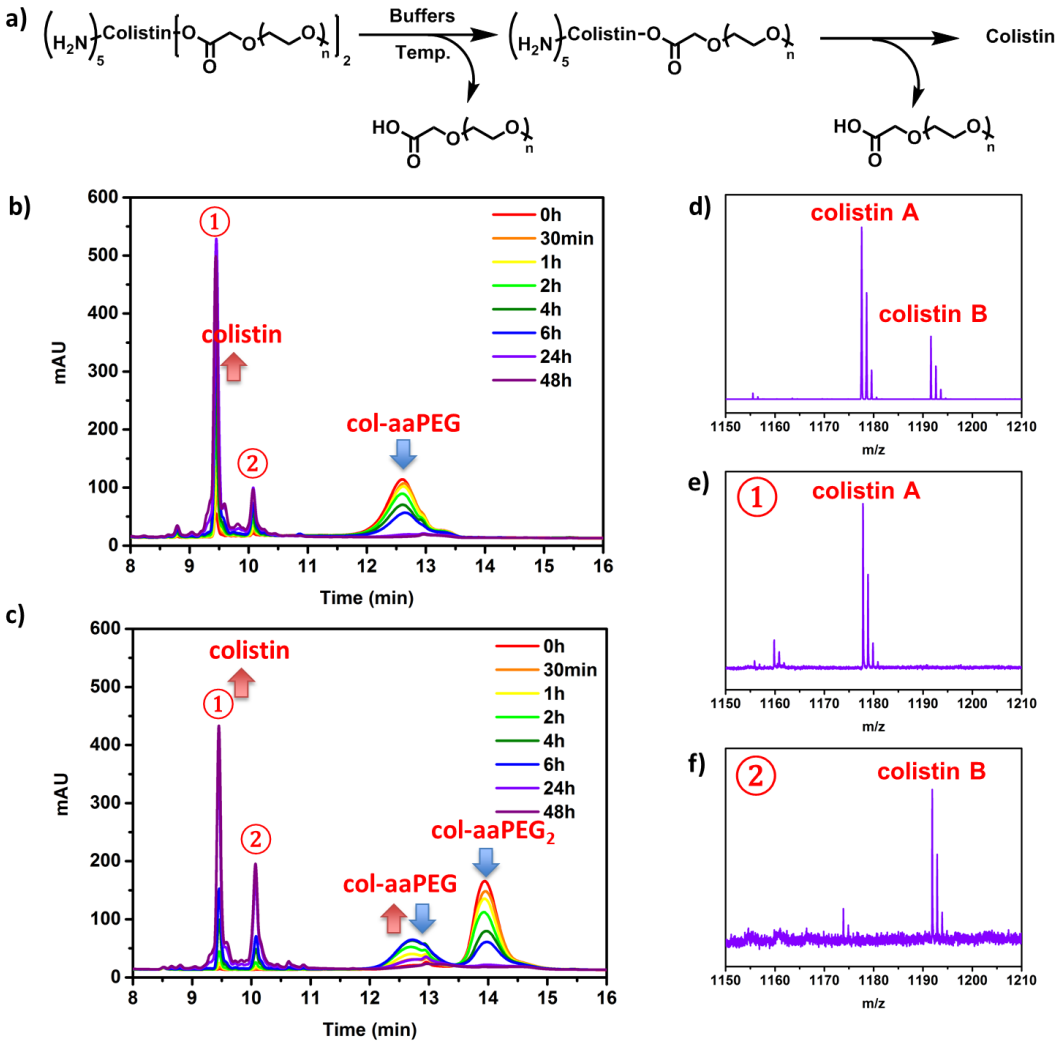

Figure 3.6 a) The proposed mechanism of the colistin release from the col-aaPEG$_2$ conjugate. The ability to release the col-aaPEG (b) and col-aaPEG$_2$ (c) conjugate at 37 ^{o}C in PBS (1X) buffer was monitored by HPLC. MALDI-ToF MS data of the commercial colistin (d) and the isolated colistin peaks (e and f) from the col-aaPEG prodrug solution after the incubation for 2 days.

In order to study the cleavable nature of the ester bond, the degradation of both PEGylated conjugates was performed *in vitro* and monitored by HPLC (Figure 3.6). To mimic physiological condition, the test was conducted at 37 ^{o}C in phosphate buffered saline (PBS, pH = 7.4). For the col-aaPEG form, the signal of the conjugate

decreased continuously with a concomitant appearance and increase in the typical colistin double-peaks up to 48 h (Figure 3.6b). Noticeably, we found that more than 75% colistin can be released from col-aaPEG within 6 h whilst it normally required > 24 h for CMS to achieve a similar extent of colistin release under similar conditions.[4] The two colistin peaks were then collected and analysed *via* MALDI-ToF MS confirming their identity as native colistin A and B (Figure 3.6d-f). This suggested that the released colistin was chemically unchanged and therefore potentially still active. As for col-aaPEG$_2$, although the hydrolysis rate is almost twice as slow compared to col-aaPEG in the first 6 h, a similar pattern was observed when following the reaction by HPLC with the colistin peaks appearing and increasing as a function of time, leading to full release of colistin within 48 h (Figure 3.6c). Interestingly, during degradation a broad peak appeared at 12-13.5 min, which coincided with the col-aaPEG conjugate. The intensity of this peak initially increased during the first 4 h and then decreased along with the full consumption of col-aaPEG$_2$ to furnish the native lipopeptides. This indicates that the release of colistin from col-aaPEG$_2$ undergoes a stepwise degradation process, proceeding *via* a col-aaPEG as an intermediate product (Figure 3.6a). Regardless, this also confirmed that the two aaPEGs which are attached onto the different Thr residues can both be hydrolysed during the degradation process to fully liberate native polymyxins.

To investigate the effect of the traceless linker between mPEG and colistin, a second PEGylated colistin with a different ester bond was synthesized by the same protocol using a commercial available succinic acid terminated mPEG (saPEG) (Figure 3.7a). Lacking an electron-withdrawing oxygen bonded to the α-carbon, saPEG was expected to form a more stable conjugate. It was observed that colistin is still released from both mono- and bis-saPEG modified products through the same

hydrolysis protocol although the amount of the released colistin is nearly twice slower than from the corresponding colistin aaPEG conjugates in the first 6 h (Figure 3.7b-c).

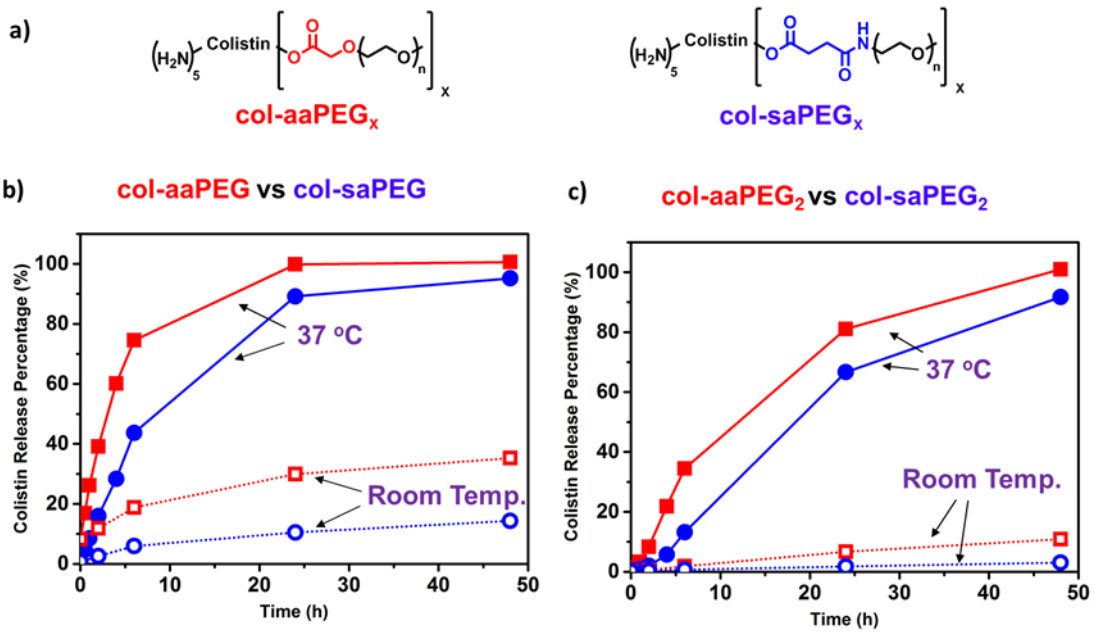

Figure 3.7 a) The chemical structures of the aaPEG modified colistin prodrugs (left) and saPEG modified ones (right). The colistin release profiles of the mono PEGylated prodrugs (b) and double modified prodrugs (c) from PBS solution. Red lines: aaPEG modified produrgs (left: col-aaPEG and right: col-aaPEG$_2$); blue lines: saPEG modified produrgs (left: col-saPEG and right: col-saPEG$_2$); solid lines: 37 °C and dotted lines: ambient temperature.

A similar degradation study was conducted at ambient temperature to evaluate the influence of temperature on the conjugate release (Figure 3.7b-c). As expected, the rate of hydrolysis for all the colistin conjugates was retarded compared to those at body temperature. In particular, the double-modified conjugates showed much slower release compared to the mono-adducts due to the stepwise nature of the hydrolysis process. All of the results implied that both ester linkers were temperature sensitive with regards to stability.

3.2.3 *In vitro* antimicrobial activity test of the PEGylated colistin conjugates

The antibiotic activity of the PEGylated conjugates was subsequently tested against two different MDR Gram-negative bacterial strains (*P. aeruginosa* ATCC 27853 and *A. baumannii* ATCC 19606). A disk diffusion assay was first conducted using colistin and CMS as positive controls. 20 μg of each conjugates was applied onto a blank disc (Ø = 0.6 cm) before placed on a bacterial inoculated agar plate. The potency of each conjugates was estimated through the measurement of their diameter of zone of inhibition (ZoI) (Table 3.1).

Table 3.1 The diameter of zone of inhibition (ZOI) results of the conjugates against two different Gram-negative bacterial through disk diffusion assay (20 μg, 24 h).

	Diameter of Zone of Inhibition (ZOI) (mm)							
	Colistin	CMS	aaPEG	Col-aaPEG	Col-aaPEG$_2$	Col-saPEG	Col-saPEG$_2$	H_2O
Pa ATCC 27853	19.0	17.5	0	14.5	9.0	12.5	0	0
Ab ATCC 19606	20.5	19.5	0	13.0	9.5	11.5	0	0

Overall, aaPEG alone showed no antibiotic activity whereas both aaPEG modified colistin conjugates showed a clear ZoI. This indicated that the colistin conjugates exhibited antimicrobial activity and crucially that the activity did not occur as a result of the cleaved polymer but rather, from the released native colistin. Owing to the larger molecular weight and a slower colistin release rate, col-aaPEG$_2$ showed a smaller ZOI compared to col-aaPEG at the same loading amount (20 μg). Conversely, both saPEG modified colistin conjugates showed a smaller ZOI compared to the corresponding aaPEG modified colistin conjugates which is in agreement with the observed colistin release profiles. Notably, col-saPEG$_2$ revealed no activity

through the disk diffusion assay, indicating the attachment of PEG inhibited the activity of colistin and highlighting the need for a more labile, cleavable linker for the desired prodrug to maintain its activity over a time scale relevant to microbial proliferation.

Table 3.2 The minimum inhibitory concentration of the conjugates against two different Gram-negative bacteria on a weight and molar basis.

	Minimum Inhibitory Concentration (MIC) (mg/L; μmmol/L)						
	Colistin	CMS	aaPEG	Col-aaPEG	Col-aaPEG$_2$	Col-scPEG	Col-scPEG$_2$
Pa ATCC 27853	2; 1.4	8; 4.6	>128; >64	4; 1.3	64; 12	16; 5.0	>128; >25
Ab ATCC 19606	1; 0.7	16;9.2	>128; >64	8; 2.5	32; 6.1	16; 5.0	>128; >25

To obtain a more accurate comparison of the relative activities of the prepared conjugates, minimum inhibitory concentration (MIC) assays were performed using *P. aeruginosa* ATCC 27853 and *A. baumannii* ATCC 19606 (Table 3.2). In general, each sample was dissolved and serial diluted to the test concentration with a bacteria containing broth. The dilutions were then examined for the visible growth of the bacteria after overnight incubation. The potency of each sample can be determined by the lowest concentration, or MIC, that inhibiting the bacterial growth.

The results revealed that the col-aaPEG conjugate behaved similarly to the native colistin in terms of the molar activity. This suggests that nearly full cleavage can be achieved from this colistin conjugate. Furthermore, the released colistin was chemically identical to native colistin, as confirmed during chemical characterisation (Figure 3.6d-f), and crucially that activity of the released polymyxin was retained. More interestingly, even though the molecular weight of the col-aaPEG are nearly twice that of the commercial prodrug CMS ($M_{n\,\mathrm{CMS}}$ ~ 1743 g mol^{-1}), less material was required to inhibit the bacteria, indicating that the colistin release profile of the col-

aaPEG prodrug is more efficient than of CMS in the selected bacterial growth media. In agreement with the colistin release profiles (Figure 3.7b) and disk diffusion assay (Table 3.1), the col-saPEG conjugate showed a lower activity (2-4 times) than the aaPEG conjugate, highlighting the need for faster colistin release to inhibit the growth of bacteria. Conversely, both double PEGylated prodrugs exhibited less activity against both bacterial strains on both mass and molar basis due to the molecular weight of the prodrugs as well as the slower degradation process. Especially col-saPEG$_2$ showed no activity in the selected concentration range, confirming the inhibition of the bacterial growth results from the release of colistin rather than from the prodrug itself.

As the antimicrobial activity of colistin is concentration dependent, different 'killing' rates will be obtained from different concentrations. The amount of active colistin of the PEGylated conjugates released at each time point can be obtained through a comparison of their 'killing' kinetics. In order to determine a better understanding of the "killing" kinetics of the prodrug conjugates, time-kill studies were subsequently conducted by incubating *A. baumannii* ATCC 19606 bacterial strain as a model with colistin, CMS and colistin-aaPEG conjugates. The time-kill curves for selected dosage regimen are shown in Figure 3.8. Three different doses (0.5 x MIC, 1 x MIC, and 2 x MIC, referring to mass based MICs of each compound) were initially tested. At the lower dose (0.5 x MIC), neither CMS nor aaPEG prodrugs exhibited inhibition with the killing curves essentially indistinguishable from those of the control, whereas colistin showed antibacterial killing in the first 6 h (Figure 3.8a). By increasing the dose to 1 x MIC and 2 x MIC of both CMS and col-aaPEG, antimicrobial activity was observed with col-aaPEG performing better at both doses than CMS (Figure 3.8b-c). Particularly, col-aaPEG could inhibit the growth of bacteria

to below the detection limit within 30 min at 2 x MIC, whilst it takes 4 h for CMS to control the bacterial growth close to the detection limit. At all three dosage regimens, col-aaPEG$_2$ did not show any inhibition against the bacteria which is possibly due to the slower degradation rate compared to the bacterial growth rate. However, it still showed an antibacterial killing at 30 min up to 4 h with regrowth occurring at 24 h when using a higher dose (8 x MIC) (Figure 3.8d, purple trace).

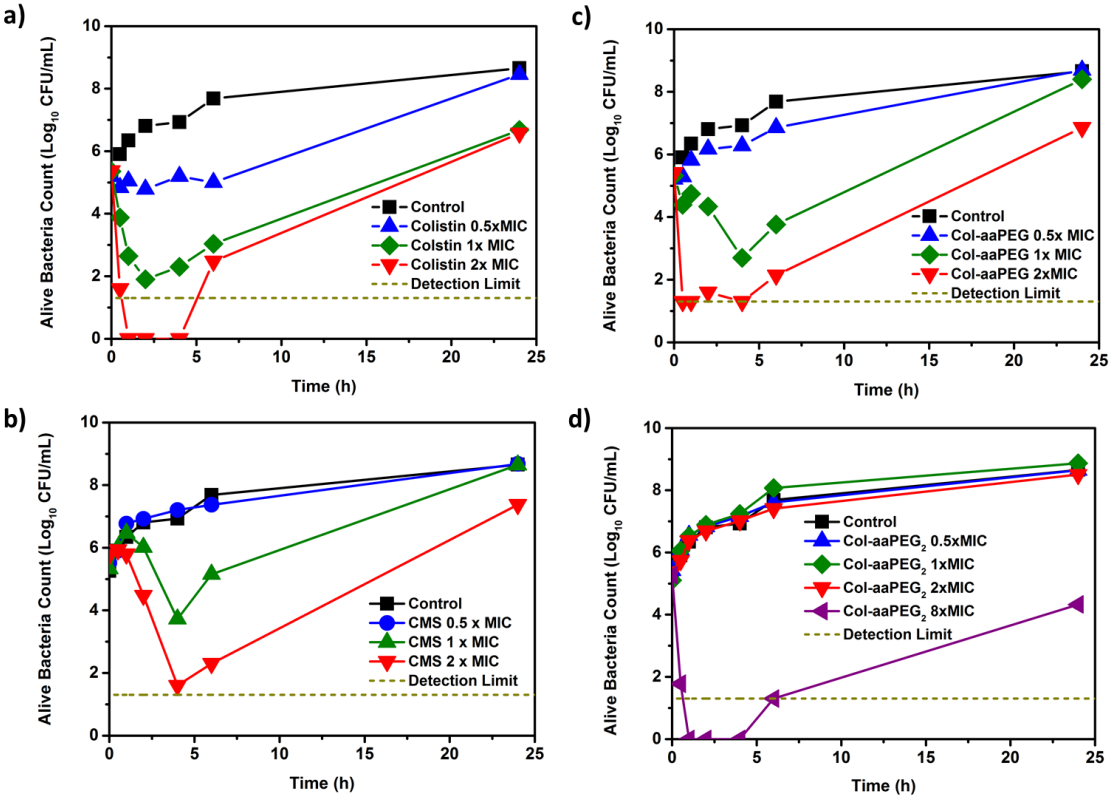

Figure 3.8 *In vitro* time-kill studies of colistin (a), col-aaPEG (b), CMS (c), col-aaPEG$_2$ (d). The dashed line indicates the lower limit of detection of bacterial growth.

3.2.4 *In vivo* antimicrobial activity and toxicity evaluation of the PEGylated colistin conjugates

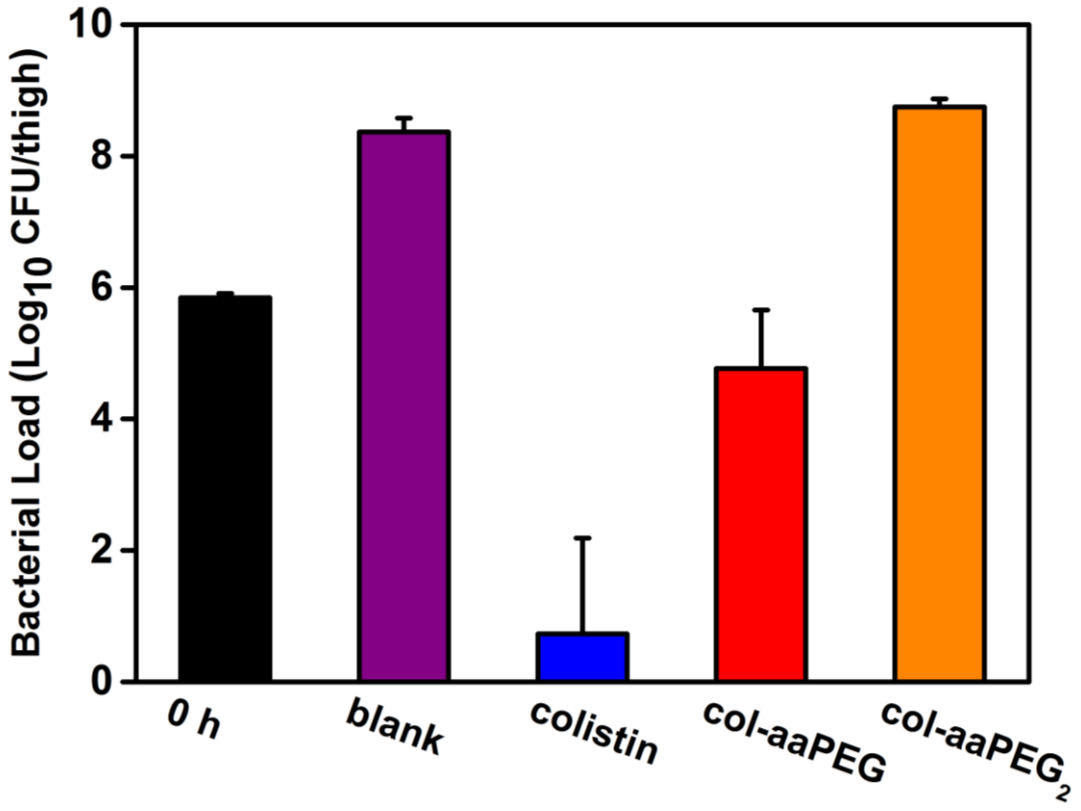

Figure 3.9 *In vivo* activity of colistin and prodrugs (col-aaPEG and col-aaPEG$_2$) against *P. aeruginosa* ATCC 27853 using a mouse thigh infection model. (n = 4)

Due to the encouraging *in vitro* performance from the col-aaPEG prodrugs, the *in vivo* efficacy of these two labile ester based conjugates (col-aaPEG and col-aaPEG$_2$) was investigated in comparison to native colistin treatment against *P. aeruginosa* ATCC 27853 in a neutropenic mouse thigh infection model. Colistin was employed as the comparator as the highly variable release and inter-batch heterogeneity of CMS yields large data fluctuations. After 18 h administration of colistin and the aaPEG prodrugs (40 mg colistin base/kg), a significant reduction in the bacterial burden was observed for both colistin (mean $\log_{10}$ CFU/thigh 0.73±1.46) and col-aaPEG (mean $\log_{10}$ CFU/thigh 4.77±0.89) compared to the 0 h (mean $\log_{10}$ CFU/thigh 5.85±0.06, >

91.6% bacteria kill). However, col-aaPEG$_2$ failed to produce sufficient bacterial killing *in vivo* (mean $\log_{10}$ CFU/thigh 8.75±0.12) (Figure 3.9).

a)

Sample Name	Histology Kidney Scoring
Control 0h	**GRADE 0**
Control 28h	**GRADE 0**
Colistin	**GRADE 1**
Col-aaPEG	**GRADE 0**
Col-aaPEG$_2$	**GRADE 1**

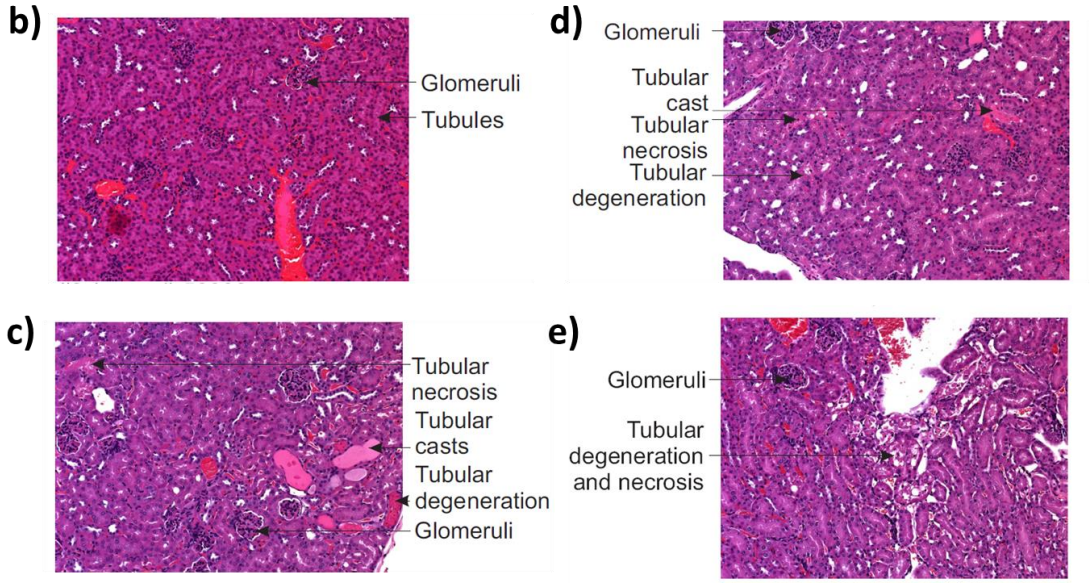

Figure 3.10 a) Summary of histology kidney scoring from each sample. b)-e) Microscopic image of the cortex section of the kidneys of mice treated with saline control, colistin, prodrugs col-aaPEG and col-aaPEG$_2$ (accumulated dose 40 mg colistin base/kg). b) Control (0 h) (SQR score 0); c) colistin (SQR score 1); d) col-aaPEG (SQR score 0), e) col-aaPEG$_2$ (SQR score 1).

Nephrotoxicity remains a dose-limiting issue with the broader application of polymyxin therapy as it impacts the ability of clinicians to increase the dose.[6-12] Therefore, in the present study, the *in vivo* apoptotic effect of col-aaPEG and col-aaPEG$_2$ was examined through the histological examination of the kidneys from mice subcutaneously administered either colistin or PEGylated colistin prodrugs at an accumulated dose of 40 mg colistin base/kg (Figure 3.10a). The kidneys of mice

administered with the saline control had no observable histological damage (semi quantitative SQR score of 0, Figure 3.10b). In comparison, the histological examination of the kidneys from the mice treated with colistin, col-aaPEG$_2$ showed comparable mild histological damage with tubule damage, i.e. tubular dilation and degeneration (semi quantitative SQR score of 1, Figure 3.10c, e). Encouragingly, the kidneys of mice treated with col-aaPEG had no significant histological damage and were essentially comparable to the saline control (grade 0 histology kidney scoring; Figure 3.10d). These results demonstrate that colistin and col-aaPEG$_2$ (both grade 1 histology kidney scoring) appears to be more nephrotoxic than col-aaPEG.

3.3 Conclusions

In this chapter, fully characterised mono- and bis-mPEG modified colistin conjugates with two different ester linkages on the Thr residue(s) of colistin were synthesised *via* Boc-protection/deprotection and Steglich esterification. All of the prodrug candidates were tested through the *in vitro* degradation studies and revealed native colistin can be released smoothly from all the colistin conjugates and that the colistin release rate from the PEGylated conjugates can be altered by the number of mPEG attachment and the lability of the linker. Studies also showed the degradation process is temperature sensitive and the prodrugs are relatively stable at ambient temperature. Among them, the col-aaPEG showed the fastest colistin release rate, achieving near full colistin release within 24 h, which makes it a viable prodrug candidate. All *in vitro* antimicrobial activity tests suggested col-aaPEG performs with a similar or better activity relative to the commercial prodrug CMS or colistin on both molar and mass basis. In comparison to colistin, col-aaPEG showed acceptable bacterial killing in an *in vivo* mouse model against *P. aeruginosa* ATCC 27853 and

displayed no nephrotoxicity through the histological examination of the kidneys. Although further evaluation is needed to determine whether this activity profile of col-aaPEG *in vivo* extends to other Gram-negative species, we believe that due to the enhanced specificity confirmed by targeting Thr residues without loss of antibacterial activity, col-aaPEG has the potential candidate to become a potent alternative prodrug to CMS.

3.4 Experimental

3.4.1 Materials

3.4.1.1 Chemicals

All chemicals were purchased from Sigma-Aldrich and used directly unless otherwise stated. HPLC solvents are obtained from VWR international, LLC. The acetic acid functional mPEG (aaPEG, M_n ~ 2kDa) was synthesised based on the previous report.[5] The succinic acid functional mPEG (saPEG, M_n ~ 2kDa; commercial name: CH_3O-PEG-NHCO-C_2H_4-COOH; reference number: 122000-3) was purchased from Rapp Polymere GmbH.

3.4.1.2 Bacterial strains

Bacterial strains of *P. aeruginosa* ATCC 27853 and *A. baumannii* ATCC 19606 (American Type Culture Collection, Manassas, VA) were used in this study. The strains were stored at -80 °C in a cryovial storage container (Simport Plastics, Quebec, Canada). Fresh isolates were sub cultured on Nutrient agar (Media Preparation Unit, The University of Melbourne, Parkville, Australia) and incubated at 37 °C for 24 h

prior to each experiment. CAMHB (Oxoid, Hampshire, England) was used as culture medium.

3.4.2 Instruments

3.4.2.1 MALDI-ToF MS

MALDI-ToF MS was acquired from a Bruker Daltonics Autoflex MALDI-ToF mass spectrometer. The MALDI-ToF samples were prepared by mixing a solution of CHCA or DCTB as a matrix (20 mg/mL in THF) and sample (1-2 mg/mL in THF) at 1:1 ratio. 0.5 μL of this mixture was spotted to the target plate. Spectra were recorded in reflector mode calibrating with PEG or mPEG at a similar average molecular weight of each sample.

3.4.2.2 GPC

DMF GPC was performed on an Agilent PL50 equipped with 2 Agilent Polargel M Columns and a differential refractive index detector eluting with DMF (0.1 M LiBr) with a flow rate of 1.0 mL min^{-1} at 50 ^{o}C. THF GPC was performed on a Varian 390-LC MDS system equipped with a PL-AS RT/MT autosampler, a PL-gel 3 μm (50 x 7.5 mm) guard column, two PL-gel 5 μm (300 x 7.5 mm) mixed-D columns equipped with a differential refractive index using THF (+ 2% triethylamine (TEA) + 0.01% butylated hydroxytoluene (BHT)) as the eluent with a flow rate of 1.0 mL min^{-1} at 30 ^{o}C. The calibration was fitted with a 3rd order polynomial using narrow molecular weight standards of PMMA (between 200 and 467,400 g mol^{-1}).

3.4.2.3 HPLC

3.4.2.3.1 Analytical HPLC

The HPLC system used was an Agilent 1260 infinity series stack equipped with an Agilent 1260 binary pump and a degasser. Samples (10 – 70 μL) were injected using Agilent 1260 autosampler. The HPLC was fitted with a Phenomenex Lunar C_{18} column (250 x 4.6 mm) 5 micron packing (100Å). Detection was achieved using an Agilent 1260 variable wavelength detector connected in series with UV detection monitored at 214 nm.

The mobile phase condition is as follows.

Mobile phase A: 100% water, 0.04% TFA;

Mobile phase B: 100% ACN, 0.04% TFA.

HPLC water and 'far UV' HPLC ACN were used as solvents and HPLC TFA was used as additive.

The standard analysis method is as followed: 0-24 min 10%-80% B; 24-25 min 80-10%B; 25-40 min 10% B. The total flow rate was set to 1.0 mL/min and the temperature for the column is set to 40 ^{o}C.

3.4.2.3.2 PREP HPLC

The PREP HPLC system used was an Agilent 1260 infinity series stack equipped with a 1260 Quat Pump VL, a degasser and a fraction collector (FC-AS). Samples were injected using Agilent 1260 auto-sampler with a 100 μL injection volume. The HPLC was fitted with a phenomenex Lunar C_{18} column (250 x 4.6 mm) 5 micron packing (100Å) for more precise separation. Detection was achieved using an Agilent 1260 TCC detector with UV detection monitored at 214 nm.

The mobile phase condition is as follows.

Mobile phase A: 100% water, 0.04% TFA;

Mobile phase B: 100% ACN, 0.04% TFA.

HPLC water and 'far UV' HPLC ACN were used as solvents and HPLC TFA was used as additive.

The standard preparative method is as followed: 0-20 min 5%-100% B; 20-25 min 100% B; 25-30 min 100%-5% B; 30-40 min 5% B. The total flow rate was set to 1.0 mL/min and the temperature for the column is set to 40 ^{o}C.

3.4.3 Synthesis

3.4.3.1 Synthesis of Boc$_5$-colistin

The synthesis of Boc$_5$-colistin was as follows. Colistin sulphate (0.56 g, 0.4 mmol, 1 equiv.) was dissolved with 20 mL water in a 100 mL round bottom flask. Boc_2O (2.18 g, 10 mmol, 25 equiv.) was dissolved with 25 mL THF in a 50 mL Eppendorf tube before adding into the 100 mL round bottom flask. The reaction mixture was stirred vigorously at ambient temperature for 5 min. Sequentially, K_2CO_3 (1.38 g, 10 mmol, 25 equiv.) were dissolved in 5 mL of water and the solution was added slowly into the reaction mixture. The reaction mixture would become creamy once the base was added. The mixture was then kept stirring overnight. After that, the mixture was transferred into a separating funnel along with 30 mL saturated sodium chloride solution and 30 mL THF. The mixture was then let stand for around 30 min until two layers was observed. The upper layer was collected and the bottom layer was extracted with 30 mL THF twice. The combined organic solution was dried with $MgSO_4$ and concentrated under the vacuum. The further purification can be done by

the flash column (0% -10% MeOH in DCM).The final product is a fine pale yellow powder with a total yield of 78%. The MALDI-ToF MS and HPLC analyses were shown in Figure 3.1. $M_{n\text{MALDI}}$ = 1678.1 (colA), 1692.1 (colB) ($[M+Na]^+$).

3.4.3.2 Synthesis of Boc_5-col-aaPEG_x (x = 1,2)

The synthesis of the Boc_5-col-aaPEG_x was modified from the standard Steglich esterification. aaPEG (M_n ~ 2kDa, 120 mg, 60 µmol, 1.5 equiv.), Boc_5-colistin (66.0 mg, 40 µmol, 1 equiv.), and DMAP (24.4 mg, 0.2 mmol, 5 equiv.) were fully dissolved in 6 mL of dry DCM. EDC·HCl (76.7 mg, 0.4 mmol, 10 equiv.) was added afterwards and the reaction mixture was kept stirring overnight. The crude product was obtained after the removal of DCM and used directly for the next step. The further separation of Boc_5-col-aaPEG and Boc_5-col-aaPEG_2 can be done by diluting the crude product using ACN and purifying by RP-HPLC. The ratio between Boc_5-col-aaPEG and Boc_5-col-aaPEG_2 is around 1:1. The standard preparative method was used. Boc_5-col-aaPEG_2 appears around 18-20 min and Boc_5-col-aaPEG appeared around 20-22 min. The detailed MALDI-ToF MS, GPC and HPLC characterisations of the products were shown in Figure 3.3-3.4.

3.4.3.3 Synthesis of col-aaPEG_x (x = 1,2)

The deprotection of the Boc groups was followed the typical Boc cleavage procedure. 6 mL 33% TFA in DCM was added slowly into the crude Boc_5-col-aaPEG_x (x = 1,2). [Be caution of the release of gas!] After most gas was released, the reaction mixture was sealed and kept stirring at ambient temperature overnight. After the removal of solvents, the crude product was diluted by ACN and separated by RP-HPLC. The standard preparative method was used. Col-aaPEG appears around 11.4 -

12.2 min and col-aaPEG$_2$ appeared around 12.2 - 13 min. The detailed MALDI-ToF MS, GPC and HPLC characterisations of the products were shown in Figure 3.4-3.5.

3.4.4 Methods

3.4.4.1 Protocol for in vitro release of PEGylated colistin prodrugs

The degradation of the PEGylated colistin prodrugs were conducted in 7 mL vials using 2 mL PBS (1X). 1 mg of the mono PEGylated prodrugs and 2 mg of the double PEGylated prodrugs were used for the test. 500 μL of each prodrug solution was taken into another vial and stirred at ambient temperature. The rest of each prodrug solution was stirred and incubated in an oil bath at 37 ^{o}C. Samples (100 μL each time) were taken periodically and frozen by liquid nitrogen before the analysis. The analysis was conducted by RP-HPLC using the standard analysis conditions. The colistin release percentage was calculated through the following method.

The integration (I_t) of colistin double-peak of the sample at each time point (T = t) was recorded. As the absorbance and concentration of colistin at 214 nm in the measuring concentration range follows the Beer-Lambert law, the concentration of colistin in the solution at each time point (c_t) is proportional to its integration (I_t) from the HPLC chromatograph at 214 nm, meaning $c_t = A \times I_t$ where A is constant. The total amount of colistin released at T = t (m_t) from the prodrug, which is $m_t = m_{sample} + m_{remain} = m_{sample} + V_{remain} \times c_t = m_{sample} + V_{remain} \times A \times I_t$ where; m_{sample} means the amount of colistin taken for analysis before T = t; m_{remian} the remaining colistin amount in the solution; V_{remain}means the remaining volume at T = t. As the volume taken for each sample at each time is the same ($V_{sample} = 100$ μL), $m_{sample} = \sum_{T=0}^{T=t-1}(cV)_T = V_{sample} \times \sum_{T=0}^{T=t-1} c_T = 100\mu L \times$

$A \times \sum_{T=0}^{T=t-1} I_T$,where t-1 means the last time point before T = t. Therefore, $m_t = V_{remain} \times A \times I_t + 100\mu L \times A \times \sum_{T=0}^{T=t-1} I_T = A \times (V_{remain} \times I_t + 100\mu L \times \sum_{T=0}^{T=t-1} I_T)$.

Thus, the colistin release percentage at T = t can be calculated as follows:

$$\text{Percentage}\ (\%) = 100 \times \frac{m_t}{m_{Final}} = 100 \times \frac{V_{remain} \times I_t + 100\mu L \times \sum_{T=0}^{T=t-1} I_T}{V_{Final} \times I_{Final} + 100\mu L \times \sum_{T=0}^{T=48h} I_T}$$

where m_{Final}, V_{Final} and I_{Final} are the mass, volume, and integration of the final sample. The final sample was taken from each sample incubated at 37 ºC for 5 days.

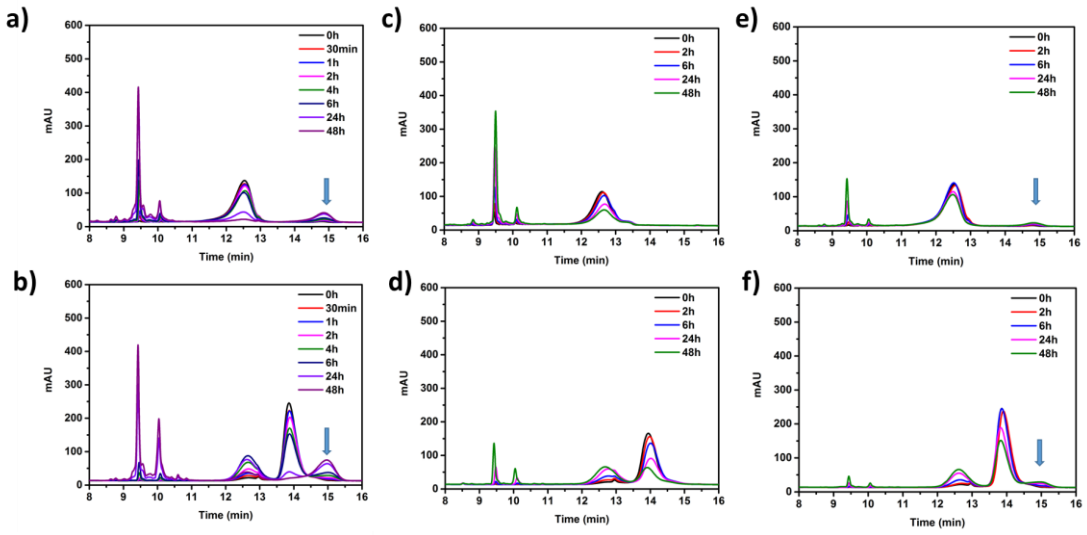

Figure 3.11 HPLC traces of the release profile from the prodrugs. a) col-saPEG, 37 ºC; b) col-saPEG$_2$, 37 ºC; c) col- aaPEG, ambient temperature; d) col- aaPEG$_2$, ambient temperature; e) col- saPEG, ambient temperature; f) col- saPEG$_2$, ambient temperature. The release polymer from col-saPEG and col-saPEG$_2$ (labeled with blue arrow) can be seen from the HPLC traces as it absorbed at 214 nm.

3.4.4.2 Disk diffusion assay

According to the EUCAST guidelines,[13] inoculum was standardised in saline to the density of a McFarland 0.50±0.02 standard, corresponding to ~10^8 CFU/mL of each isolate. A freshly prepared suspension was evenly inoculated onto plates and disks were applied within 15 min and incubated for 18 h at 37 °C. Plates were

examined for satisfactory streaked suspension and evenly distributed growth to achieve uniformly circular inhibition zones within the quality control limits.

3.4.4.3 MIC test

MICs were determined in accordance to the recommendations of the Clinical and Laboratory Standards Institute.[14] *P. aeruginosa* ATCC 27853 and *A. baumannii* ATCC 19606 were used for the tests. Experiments were performed with CAMHB in 96-well polystyrene microtiter plates. Wells were inoculated with 100 μL of bacterial suspension prepared in CAMHB (containing ~ 10^6 CFU/mL) and 100 μL of CAMHB containing increasing concentrations of colistin, CMS and PEGylated colistin prodrugs (0 − 128 mg/L). The MIC measurements were carried out in duplicates with the MIC being defined as the lowest concentration at which visible growth was inhibited following 18 − 20 h of incubation at 37 °C.

3.4.4.4 Time-kill test

The time-kill kinetics of the PEGylated colistin prodrugs at 0.5, 1, and 2 x MIC were examined against *A. baumannii* ATCC 19606. Briefly, each test sample was added into a 50 mL Eppendorf tube loaded with 20 mL of a logarithmic-phase broth culture of approximately 10^6 CFU/mL to yield concentrations of 0, 0.5, 1, and 2 x MIC (8 x MIC was also tested for col-aaPEG_2) of the isolate. The tubes were incubated in a shaking water bath at 37 ºC. The samples were taken at 0 min, 30 min and 1, 2, 4, 6 and 24 h. Subcultures for viable counts were performed on nutrient agar (Oxoid) using WASP2 Spiral Plater (Don Whitley Scientific) and incubated at 37 °C for 24 h (48 h for plates with small colonies). Viable counts were determined by either manual counting or using ProtoCol3 Colony Counter (Don Whitley Scientific).

3.4.4.5 In vivo efficacy study using a neutropenic mouse thigh infection model

All animal experiments were approved by the Monash Institute of Pharmaceutical Sciences Animal Ethics Committee (ID: MIPS.2010.35) and were in conductance with the Australian Code for Care and Use of Animals for Scientific Purposes (8th Edition 2013).

The polymyxin-susceptible strain *P. aeruginosa* ATCC 27853 was cultured on nutrient agar plates. One colony was randomly selected and incubated overnight at 37 °C. An aliquot of 0.2 mL of the overnight culture was dispersed in 20 mL CAMHB and incubated for the production of an early log-phase culture. Bacteria suspension was concentrated *via* centrifugation (3220 × g for 10 min) and the resuspended in 0.9% sterile saline for inoculation onto mice. The bacterial concentration of $2x10^5$ CFU/50 µL per mouse was estimated by determining the optical density (OD) at 600 nm and confirmed *via* plating onto agar.

Swiss mice were rendered neutropenic *via* two intraperitoneally i.p. doses of cyclophosphamide, 4 days (150 mg/kg) and 1 day (100 mg/kg) prior to infection. Thigh infection was established by injecting i.v. bolus of 50 µL of the bacterial suspension ($2x10^5$ CFU/50 µL per mouse). Solutions for colistin, col-aaPEG and col-aaPEG$_2$ were prepared at 1 mg/mL in sterile saline solution (0.9%). At 2 h after inoculation, the mice were treated with 40 mg colistin base/kg of each compound or the same volume of saline, respectively, for the control group. At 0 h and 18 h after administration of either the compound or the control, the animals were sacrificed by an inhalation of isoflurane. The skin was disinfected with 70% ethanol and blood was collected *via* cardia puncture using a 1 mL syringe rinsed with 5,000 IU/mL heparin,

diluted serially in sterile 0.9% saline and plated on nutrient agar plates using WASP2 Spiral Plater (Don Whitley Scientific) and incubated at 37 °C for 24 h (48 h for plates with small colonies). Viable counts were determined by either manual counting or using ProtoCol3 Colony Counter (Don Whitley Scientific). The bacterial load (log_{10} CFU/mL) was calculated for each mouse. Experiments were conducted in duplicates and a mean and standard deviation (SD) was calculated.

3.4.4.6 Measurement of nephrotoxicity in mice

All animal experiments were approved by the Monash Institute of Pharmaceutical Sciences Animal Ethics Committee. Mice were subcutaneously administered with either colistin or PEGylated colistin prodrugs at an accumulated dose of 40 mg colistin base/kg was achieved. At 20 h after the last dose, mice were euthanized by inhalation of an overdose of isoflurane. Immediately after sampling the blood by cardiac puncture (above) the right kidney of each mouse was collected and placed into 10% buffered formalin at pH 7.4 (Sigma, Australia) and stored in a 5 mL plastic tube. The formalin-fixed kidneys were subjected to histological examination at the Australian Phenomics Network, Histopathology and Organ Pathology (The University of Melbourne, Parkville, Australia). Samples were examined by a pathologist who was blind to the treatment groups. The nature and severity of the histological changes was graded as follows: (i) grade 1, mild acute tubular damage with tubular dilation, prominent nuclei and a few pale tubular casts; (ii) grade 2, severe acute tubular damage with necrosis; (iii) grade 3, acute necrosis/infarction.

The overall kidney histology score was calculated as a product of percentage score and grade score.[15] The SQR score (range: 0-5) was assigned as follows: (0): no

significant change; (1): mild damage; (2): mild to moderate damage; (3): moderate damage; (4): moderate to severe damage; (5): severe damage.

3.5 References

1. P. J. Bergen, J. Li, C. R. Rayner and R. L. Nation, *Antimicrob. Agents Chemother.*, 2006, **50**, 1953-1958.

2. P. Koomanachai, C. B. Landersdorfer, G. Chen, H. J. Lee, A. Jitmuang, S. Wasuwattakul, S. Sritippayawan, J. Li, R. L. Nation and V. Thamlikitkul, *Antimicrob. Agents Chemother.*, 2014, **58**, 440-446.

3. A. S. Michalopoulos and M. E. Falagas, *Ann. Intensive Care*, 2011, **1**, 30.

4. J. Li, R. W. Milne, R. L. Nation, J. D. Turnidge and K. Coulthard, *Antimicrob. Agents Chemother.*, 2003, **47**, 1364-1370.

5. F. M. Veronese, P. Caliceti, A. Pastorino, O. Schiavon, L. Sartore, L. Banci and L. M. Scolaro, *J. Control. Release*, 1989, **10**, 145-154.

6. D. Landman, C. Georgescu, D. A. Martin and J. Quale, *Clin. Microbiol. Rev.*, 2008, **21**, 449-465.

7. J. D. Hartzell, R. Neff, J. Ake, R. Howard, S. Olson, K. Paolino, M. Vishnepolsky, A. Weintrob and G. Wortmann, *Clin. Infect. Dis.*, 2009, **48**, 1724-1728.

8. C. J. Kubin, T. M. Ellman, V. Phadke, L. J. Haynes, D. P. Calfee and M. T. Yin, *J. Infect.*, 2012, **65**, 80-87.

9. D. S. Akajagbor, S. L. Wilson, K. D. Shere-Wolfe, P. Dakum, M. E. Charurat and B. L. Gilliam, *Clin. Infect. Dis.*, 2013, **57**, 1300-1303.

10. M. H. Rigatto, T. F. Behle, D. R. Falci, T. Freitas, N. T. Lopes, M. Nunes, L. W. Costa and A. P. Zavascki, *J. Antimicrob. Chemother.*, 2015, **70**, 1552-1557.

11. R. V. Dudhani, J. D. Turnidge, R. L. Nation and J. Li, *J. Antimicrob. Chemother.*, 2010, **65**, 1984-1990.

12. S. Garonzik, J. Li, V. Thamlikitkul, D. Paterson, S. Shoham, J. Jacob, F. Silveira, A. Forrest and R. Nation, *Antimicrob. Agents Chemother.*, 2011, **55**, 3284-3294.

13. *Disk Diffusion Method for Antimicrobial Susceptibility Testing, Version 5.0* E.C.o.A.S.T. EUCAST (Ed.), 2015.

14. CLSI, *Performance Standards for Antimicrobial Susceptibility Testing: Twentieth Informational Supplement (M100-S20)*, CLSI, Wayne, PA, USA, 2010.

15. K. D. Roberts, M. A. Azad, J. Wang, A. S. Horne, P. E. Thompson, R. L. Nation, T. Velkov and J. Li, *ACS Infect. Dis.*, 2015, **1**, 568-575.

Chapter 4 *A Poly(PEGA$_{480}$) Colistin Prodrug for Antimicrobial Treatment*

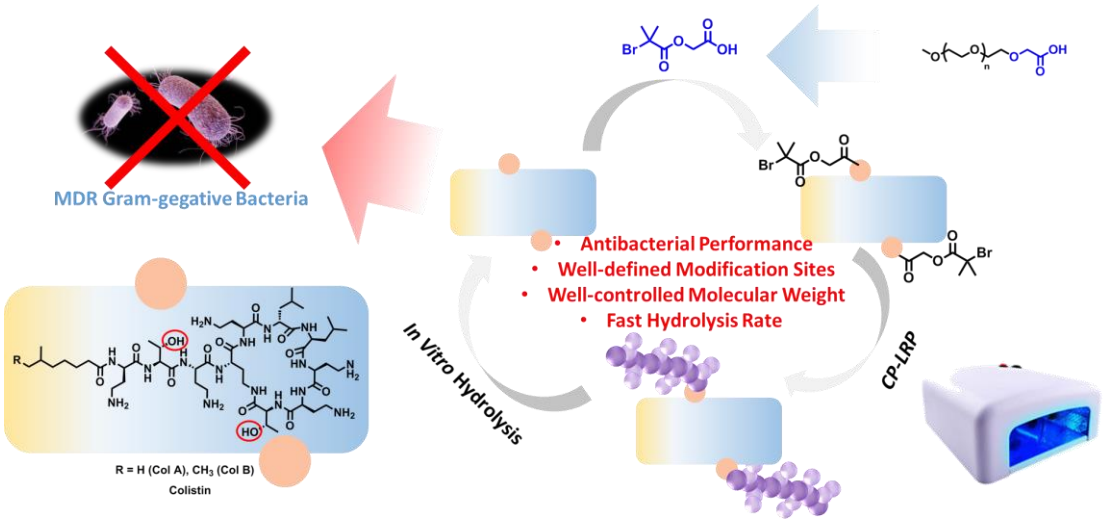

Novel polymeric colistin prodrugs with three different lengths of polymer have been developed. Through the modification of a cleavable initiator linker, 2-(2-bromo-2-methylpropanoyloxy) acetic acid (BMPAA), on both Thr residues of colistin, the polymer-colistin conjugates (col-PPEGA) with two cleavable poly(PEGA$_{480}$) chains were achieved by the polymerisation of PEGA$_{480}$ monomer via the recent developed copper-mediated photoinduced living radical polymerisation (CP-LRP). Thanks to the nature of the linker, most of the active colistin can be recovered from the conjugates in vitro within 2 days. Further in vitro biological analyses including disk diffusion, broth dilution and time-kill studies suggested all the conjugates have the ability to inhibit the growth of MDR Gram-negative bacteria, of which col-PPEGA DP5 and DP10 showed similar antibacterial performance as CMS, indicating their potential as an alternative treatment for CMS.

4.1 Introduction

As demonstrated in chapter 3, the PEGylated colistin conjugate showed an encouraging *in vitro* and *in vivo* performance compared to CMS and revealed no systematic toxicity nor nephrotoxicity. However, this modification approach still has its limitation despite PEGylation being an established method to improve the biological drug performance. In order to obtain better pharmaceutical properties for the conjugate, a high molecular weight PEG modification is sometimes necessary. As a 'grafting-to' approach, the conjugation efficiency of PEGylation can vary depending on the molecular weight of the PEG and normally reduces dramatically when a high molecular weight PEG is used.[1] The purification of the conjugate from the PEG starting material is also sometimes problematic. In addition, the attachment of a high molecular weight PEG increases the overall viscosity of the PEGylated conjugate, making it not suitable for intravenous administration.[2] Furthermore, the high molecular weight PEG is a crystalline polymer that can also accumulate in the human body, causing damage to human kidney and/or liver, which is not ideal for drug delivery system.[3] Moreover, due to the structure configuration, PEG normally acts like a random coil in the aqueous solution, which can hinder the hydrolysis of the linker between the polymer and peptide. Thus, the bis-PEG modification colistin conjugate described in chapter 3 (col-aaPEG$_2$), which is modified on both Thr residues, showed a much slower hydrolysis profile, resulting a less active product compared to col-aaPEG.

Alternatively, polyPEG is a comb-like PEG-based biocompatible polymer that has similar properties to PEG.[3] Synthesized from the PEG (meth)acrylate monomer, polyPEG is a non-crystalline material and the comb-like structure makes it act as a

rigid rod in aqueous solution, therefore, it normally has a lower viscosity compared to linear PEG at the same molecular weight. With the recent development of new polymerisation techniques, such as living/controlled radical polymerisation, polyPEG can now be attached to biological drugs through the 'grafting from' approach of PEG (meth)acrylate monomer with a controlled molecular weight range and a narrow dispersity (*Đ*) under a mild conditions, leading to an efficient conjugation and easy purification.[4, 5]

In present work, the possibility of introducing poly($PEGA_{480}$) onto both Thr residues of colistin, transferring it into a polymeric prodrug has been demonstrated and discussed. With the attachment of a hydrolysable initiator precursor, the $PEGA_{480}$ monomer can be grown evenly from both Thr residues of colistin *via* copper-mediated photoinduced controlled radical polymerisation. The colistin conjugates were prepared with various degrees of polymerisation with low dispersities. *In vitro* hydrolysis studies were conducted to investigate the effect of increasing the degree of polymerisation and therefore the molecular weight on the colistin release rate. Further biological evaluation including disk diffusion, broth dilution and time-kill experiments were also performed to analyse the effect of polymer length on colistin antimicrobial activity.

4.2 Results and Discussion

4.2.1 Design of the initiator linker for colistin conjugation

As the colistin release rate from the polymeric prodrug will greatly affect the final antimicrobial activity, the design of linker between the colistin and the initiating group is imperative to the proposed 'grafting from' approach for formation of a

suitable prodrug candidate. To obtain a better performance and a faster colistin release rate, a labile linker comparable to that present in aaPEG (chapter 3) would be required in order to afford a suitable hydrolysis rate whilst counteracting the two-step hydrolysis effect.

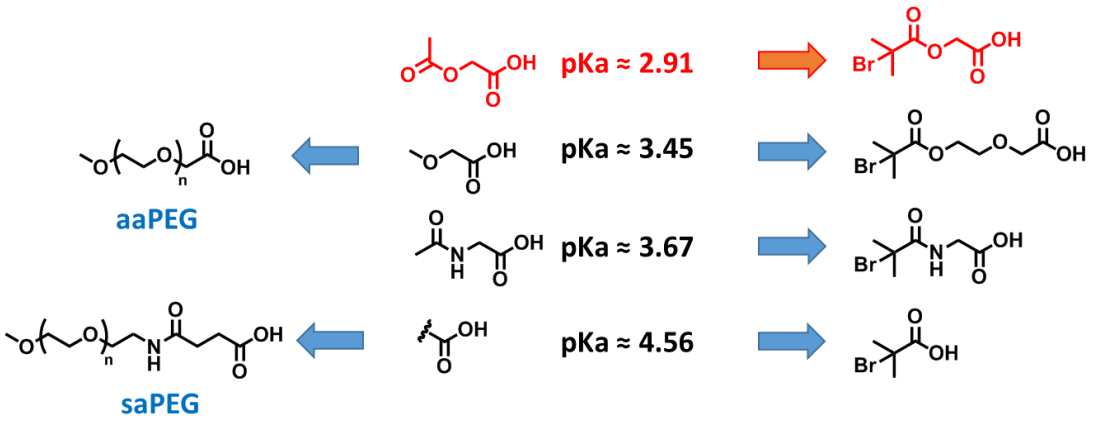

Scheme 4.1 The acid dissociation constant at logarithmic scale (p*K*a) of the acids with different side group and their relative initiator linker.

The stability of an ester is influenced by the different side groups attached on the carboxyl group. A more acidic group (quantified by the acid dissociation constant K_a) which normally has a stronger electron withdrawing group, can act as a better leaving group, leads to a faster ester hydrolysis rate. Due to the same reason, col-saPEG hydrolysed slower than col-aaPEG as demonstrated in chapter 3. Thus, 2-(2-bromo-2-methylpropanoyloxy) acetic acid (BMPAA) was synthesised and chosen as the initiator linker (Scheme 4.1).

Prior to the attachment of this initiator linker to colistin, a Boc_5-colistin was synthesized using *tert*-butyloxycarbonyl (Boc) amine protecting group following the procedure developed in chapter 3 to protect all the amine residues on colistin. The initiator linker was then introduced onto both colistin Thr residues using standard Steglich esterification (Figure 4.1a). A clear molecular weight increase (414 Da) was observed from the modified product (Boc_5-colistin-ini_2) compared to Boc_5-colistin

through MALDI-ToF MS analysis, indicating two initiator linkers were attached (Figure 4.1b). The isotope pattern from the Boc protected colistin initiator also suggested this product contains two bromine atoms (Figure 4.1c), further confirming the successful attachment of two initiators on Boc_5-colistin and both bromines of the initiators were stable under the reaction conditions.

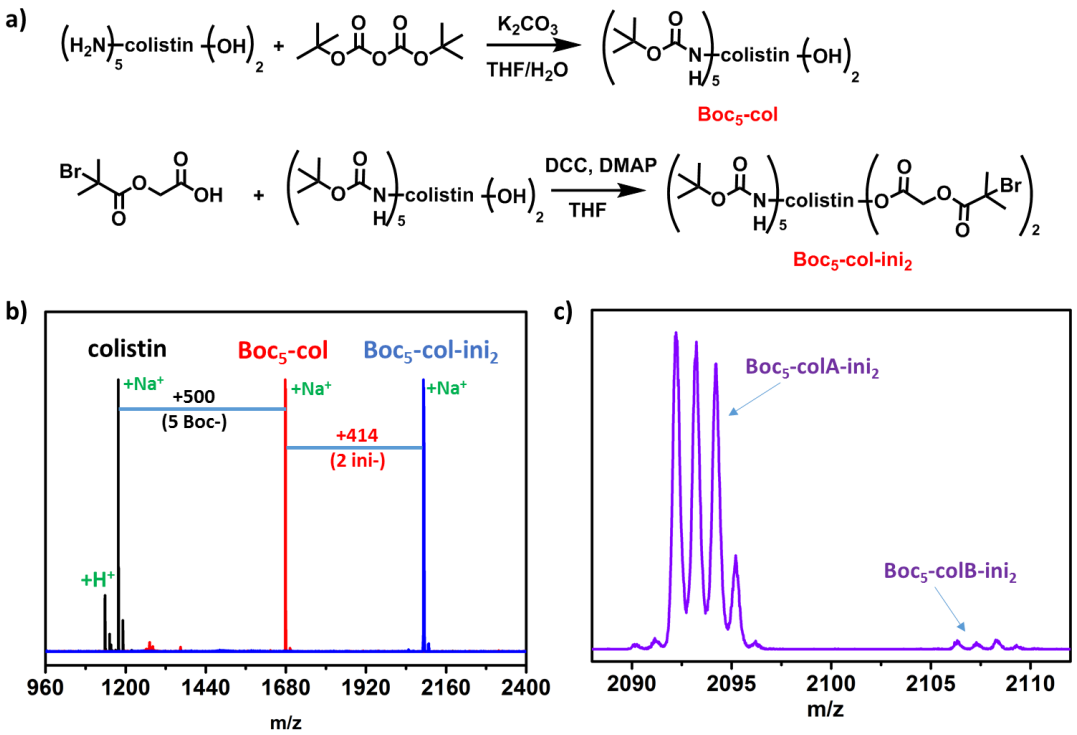

Figure 4.1 a) The Boc-protection reaction on colistin Dab amines and the subsequent modification of the labile BMPAA initiator on colistin Thr groups. b) MALDI-ToF MS data of native colistin (black), Boc_5-colistin (red), Boc_5-colistin-ini_2 (blue). c) The zoom-in data of Boc_5-colistin-ini_2.

4.2.2 Polymerisation of $PEGA_{480}$ from colistin intiator

Due to the hydrolytic and heat sensitive features of both colistin and the labile initiator linker, a compatible polymerisation system with a non-aqueous solvent and a low temperature was required. The recent developed copper-mediated photoinduced living radical polymerisation (CP-LRP) was subsequently explored to achieve polymerisation from the colistin initiator.

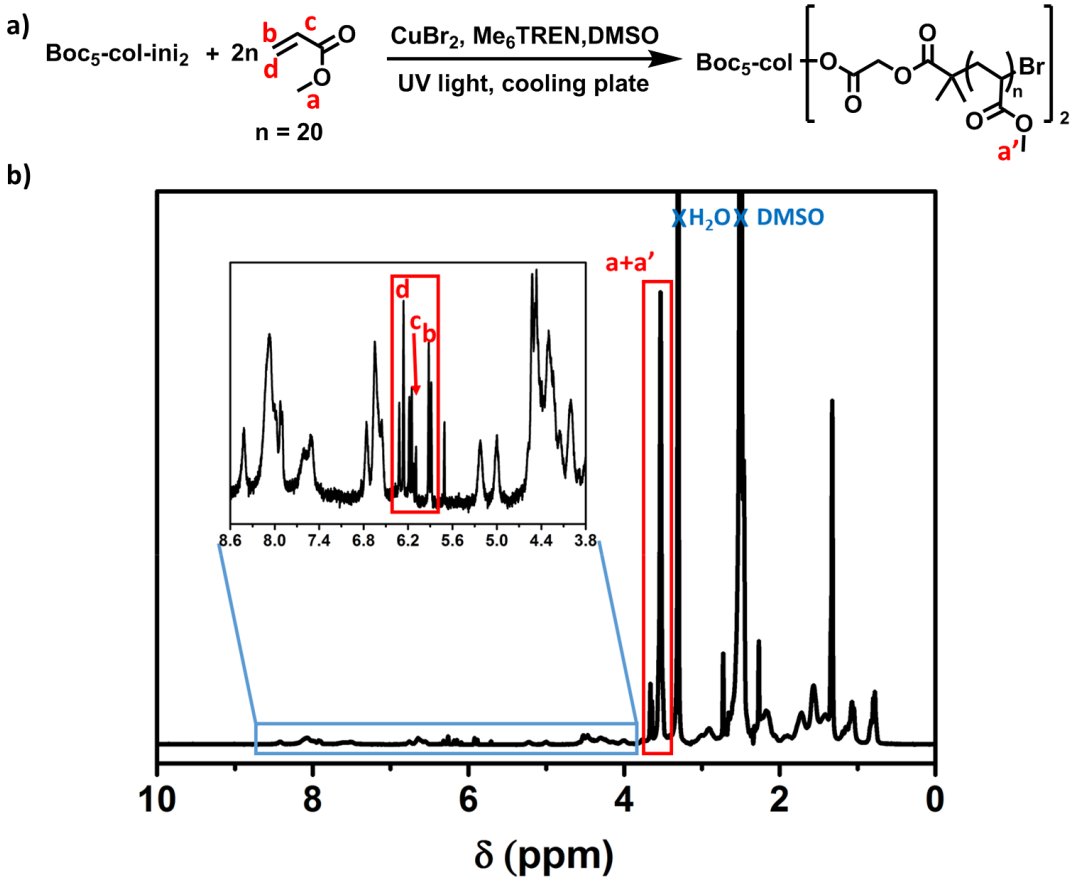

Figure 4.2 a) Scheme of the polymerisation of MA using the colistin initiator *via* CP-LRP. b) ^{1}H-NMR spectrum of the reaction mixture. The spectrum was acquired using d_6-DMSO as solvent.

Although this technique has shown to be a versatile and robust platform, a peptide-based initiator has not been investigated and it was not certain whether the UV would damage the peptide itself. Methyl acrylate (MA) was first used as a model monomer to study the feasibility of the polymerisation (Figure 4.2). Degrees of polymerisation (DP) was set to 20 for each initiator (e.g., DP = 40 for each Boc_5-colistin-ini_2) to achieve a better resolution from both NMR and MALDI-ToF MS analyses. The reaction was conducted under the UV light (λ_{max} ~ 360 nm) with copper(II) bromide ($CuBr_2$) and the ligand (Me_6TREN) at a ratio of 0.02:0.12:1 to the colistin initiator. Anhydrous DMSO was used to prevent the initiator hydrolysis during the polymerisation. A cooling plate was also applied to maintain the reaction temperature (~ 15 ^{o}C), further minimising any side reactions. The conversion of MA

was measured through ^{1}H-NMR analysis of the reaction mixture, comparing the vinyl groups (δ = 5.70 - 6.35 ppm, Figure 4.2b, peak b-d) against the signal of methyl group on both the unreacted monomer and the formed polymer (δ = 3.48 -3.68 ppm, Figure 4.2b, peak a and a'). This revealed that around 96% of the methyl acrylate was converted into polymer after 4 h polymerisation. A monomodal peak with narrow dispersity ($Đ$ ~ 1.12) was observed through GPC analysis (Figure 4.3b, black trace), suggesting that the MA monomer polymerised successfully from the colistin initiator and that the polymerisation was controlled. This also indicated the colistin peptide structure did not disrupt the polymerisation process.

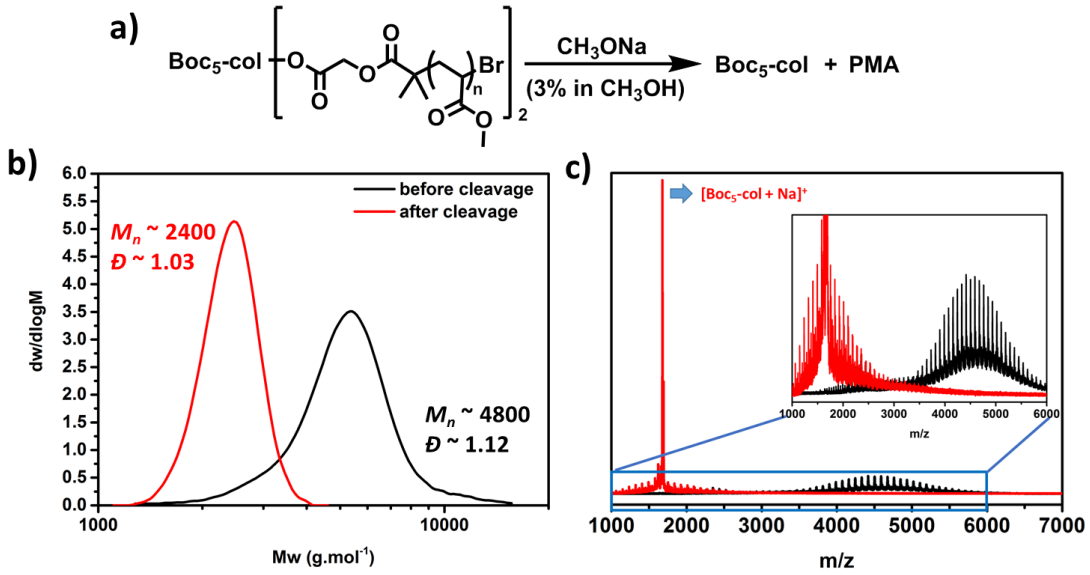

Figure 4.3 a) Scheme of the cleavage of PMA colistin conjugate using NaOMe (3% in MeOH). b) DMF GPC and c) MALDI-ToF MS of the Boc_5-colistin-PMA conjugate before (black traces) and after (red traces) treating with NaOMe.

As there were two initiating sites in the colistin initiator, a further cleavage experiment was performed on the PMA colistin conjugate (Boc_5-colistin-PMA) under a basic condition (3 wt% sodium methoxide, NaOMe) in order to investigate whether the polymerisation had occurred from both sites (Figure 4.3a). The cleaved product was found to be monomodal with approximately half the molecular weight of the

initial polymer colistin conjugate through both the GPC and MALDI-ToF MS analysis, confirming the polymer was grown evenly from both sides of the colistin initiator. Moreover, the peaks that belonging to Boc_5-colistin were also observed via MALDI-ToF MS (Figure 4.3c, red trace), indicating the colistin structure was undamaged through the polymerisation.

The $PEGA_{480}$ monomer was then polymerised at three different DPs (DP = 5, 10 and 20 of each initiator) under the similar condition (Scheme 4.2). As expected, most of the $PEGA_{480}$ was consumed after 2-4 h and all the final products retained narrow dispersities (Figure 4.4a-c and Table 4.3), suggesting the successful synthesis of all the polymers in a controlled manner.

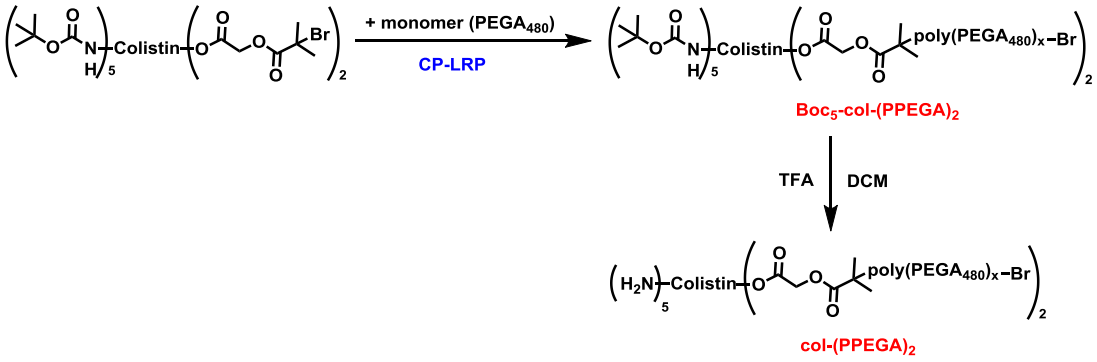

Scheme 4.2 Polymerisation of $PEGA_{480}$ using CP-LRP and the cleavage of the Boc groups on the polymer.

After the purification, the polymers were then treated with trifluoroacetic acid (TFA, 20% in dichloromethane, DCM), removing all the Boc groups on colistin to recover the amine residues. A clear shift to a shorter retention time was observed in all three polymers through HPLC analysis, suggesting a full removal of all the Boc groups (Figure 4.4d). The GPC analysis revealed that a similar molecular weight and dispersity were obtained from the polymers before and after the TFA cleavage process (Figure 4.4a-c), indicating the successful synthesis of the conjugates between colistin and PPEGA polymer with three different DPs (col-PPEGA DP5, DP10 and DP20)

with both ester bonds from the initiator linker being stable to the deprotection conditions.

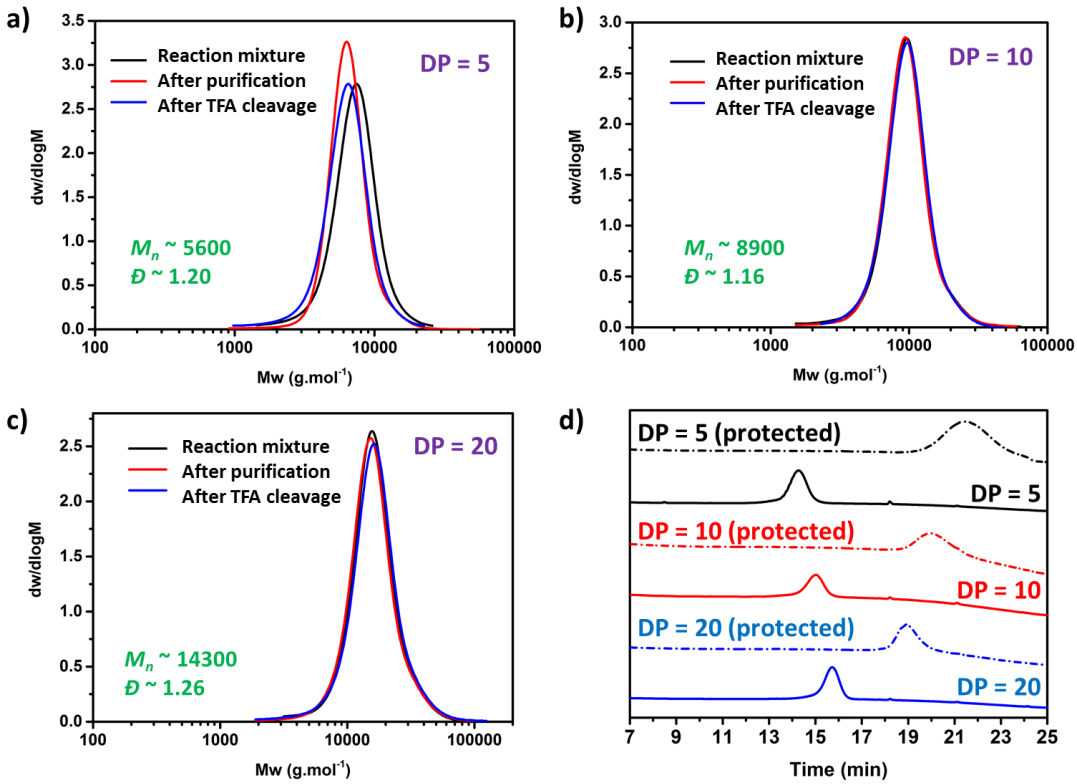

Figure 4.4 DMF GPC (a-c) traces of the col-PPEGA conjugates with different DPs in reaction mixture, after purification and after TFA cleavage. a) DP = 5, b) DP = 10, and c) DP = 20. d) HPLC traces of the col-PPEGA conjugates before and after the Boc groups cleavage.

4.2.3 Hydrolysis test of col-PPEGA conjugates

After obtaining the pure col-PPEGA conjugates, the hydrolytic nature of the linkers was investigated at both body and ambient temperature through the developed hydrolysis method described in chapter 3 (Figure 4.5a). Phosphate-buffered saline (PBS, 1X, pH = 7.4) was again used to mimic physiological conditions. The degradation of the col-PPEGA conjugates can be monitored by HPLC. A similar two-step degradation process was observed in all three conjugates. Typically, the col-PPEGA conjugate peak (varied from 14 - 16 min depending on the DP of polymers)

reduced gradually over the time and two peaks (9.8 - 10.6 min) that belonged to colistin A and B appeared and increased accordingly. An intermediate peak, with a retention time approximately 1.5 min earlier than that of the conjugate peak, was attributed to the mono-cleaved col-PPEGA conjugate. These peaks appeared and increased over the first 6 h and then decreased accordingly as a result of further cleavage. The cleaved PPEGA was also observed through the HPLC but the signal was relatively low owing to the weak absorbance of PPEGA at 214 nm (Figure 4.5b).

The released colistin peaks were then collected and analysed from MALDI-ToF MS. It revealed the released colistin had a same molecular weight as the native colistin, suggesting the chemical structure of the released colistin was unchanged through both the polymerisation and the TFA cleavage process. Moreover, it confirmed that the initiator linkers were cleaved completely from colistin and that the hydrolysis occurred at the ester bond to the colistin rather than the ester bond to the PPEGA polymer.

In general, the colistin release rates of each conjugate were similar, suggesting the hydrolysis of the cleavable linker was not hindered greatly by the large polymers, owing to the comb-like structure of the attached polymers. However, a slow-down of the colistin release rate (5-10%) can still be observed when the DP and the molecular weight of the attached polymers increased, which could have an effect on their antimicrobial activity.

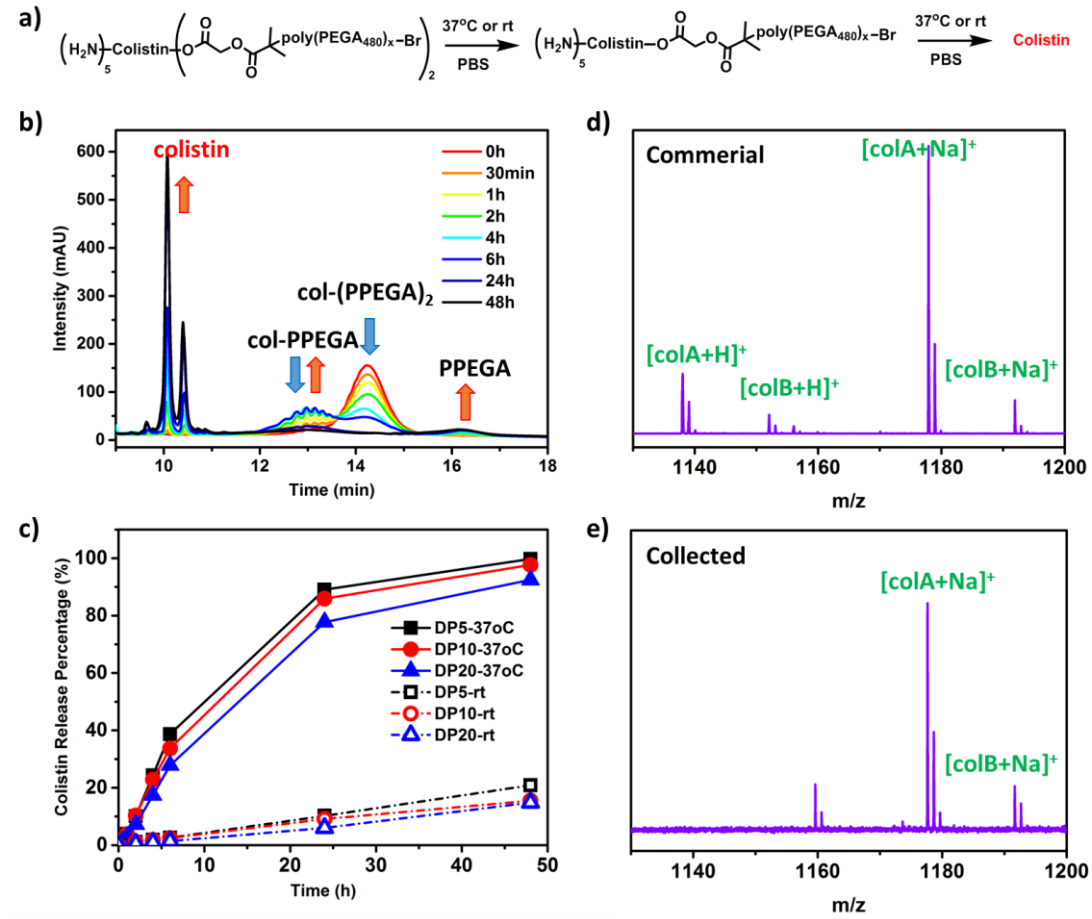

Figure 4.5 a) Scheme of the hydrolysis process of the col-PPEGA conjugates. b) The degradation of col-PPEGA conjugates (DP = 5) at 37 ºC in PBS (1X) monitoring by HPLC. c) Different colistin release profiles obtained from col-PPEGA conjugates with different DPs at 37 ºC or ambient temperature. MALDI-ToF MS of the commercial colistin (d) and the released colistin from the degradation of col-PPEGA conjugates (e).

4.2.4 Disk diffusion assay for *in vitro* antimicrobial activity evalutaion of the col-PPEGA conjugates with various DPs

In order to evaluate the antibiotic activity of each col-PPEGA conjugates, two MDR Gram-negative bacterial strains, *P. aeruginosa* ATCC 27853 and *A. baumannii* ATCC 19606, were first tested through disk diffusion assay. Thus, 20 µg of each conjugate was applied onto a blank disc (Ø = 0.6 cm) before being placed on a bacteria inoculated agar plate. Colistin and CMS was also tested as positive controls and saline

as a negative control. The potency of each conjugate was estimated through the measurement of their diameter of zone of inhibition (ZoI) (Table 4.1).

Table 4.1 The diameter of zone of inhibition (ZOI) results of the colistin-PPEGA conjugates against two different Gram-negative bacteria through disk diffusion assay (24 h).

	Diameter of Zone of Inhibition (ZOI) (cm)					
	saline	colistin	CMS	Col-PPEGA DP5	Col-PPEGA DP10	Col-PPEGA DP20
Pa ATCC 27853	0	1.8	1.7	1	0.8	0
Ab ATCC 19606	0	1.8	1.8	1.1	0.9	0.65

As the PEG has been proven to have no antibiotic activity and the molecular weight of each col-PPEGA conjugate (Table 4.3) is at least 5 times larger than colistin and CMS, it is expected that they would show much less activity with the same mass. For this reason, col-PPEGA DP20 did not show a significant activity during the test. Surprisingly, the other two col-PPEGA conjugates still showed a clear ZoI, indicating the potency of these colistin conjugates resulted from the released colistin. Although the ZoIs are smaller than the ones obtained from colistin and CMS, the observant antimicrobial activity obtained from col-PPEGA DP5 and DP10 suggested the cleavable linker can be effectively hydrolysed under physiological conditions and this 'grafting-from' approach for colistin conjugation did not alter the biological activity of the released colistin.

4.2.5 Quantitative *in vitro* antimicrobial activity evaluation of the col-PPEGA conjugates with various DPs *via* broth microdilution method

A further examination for the minimum inhibitory concentration (MIC) of each conjugate was performed through a broth microdilution method to achieve a more

accurate quantitative comparison. Although all the obtained polymer colistin conjugates have a narrow dispersity, an accurate comparison through the molar basis is not possible. Thus, the MIC test was conducted on a mass basis.

As shown in Table 4.2, all the col-PPEGA conjugates have shown antibacterial activity against *Ab ATCC* 19606, indicating active colistin can be released from these colistin conjugates *via* the successful linker cleavage. Particularly, all these conjugates have comparable or better antimicrobial activity than col-aaPEG$_2$ (from chapter 3) even though the molecular weight of these conjugates are all larger than col-aaPEG$_2$. This suggests that the PPEGA polymer with the BMPAA linker released colistin faster than aaPEG and that the molecule weight of the comb-like PPEGA did not greatly hinder the linker hydrolysis which is in agreement to the colistin release profile from previous studies. Furthermore, col-PPEGA DP5 has a similar activity to the commercial prodrug CMS although the average molecular weight is around five times larger, highlighting its potential as a more efficacious alternative to CMS.

Table 4.2 The minimum inhibitory concentration (MIC) of the conjugates against two different Gram-negative bacteria on a mass basis. (Data with* was acquired from chapter 3.)

Minimum inhibitory concentration against *Ab ATCC* 19606 (MIC) (mg/L)						
Colistin	CMS	Col-aaPEG	Col-aaPEG$_2$	Col-PPEGA DP5	Col-PPEGA DP10	Col-PPEGA DP20
1*	16*	8*	32*	16	16-32	16-32

4.2.6 Kinetics of *in vitro* antimicrobial activity of the col-PPEGA conjugates with various DPs

To study the effects of the colistin release rate and the DP of the polymer employed in the col-PPEGA conjugates upon their antibacterial kinetics, time-kill studies of these conjugates were performed against *A. baumannii* ATCC 19606

bacterial strain at three different doses (0.5 x MIC, 1 x MIC, and 4 x MIC, referring to mass based MICs of each compound).

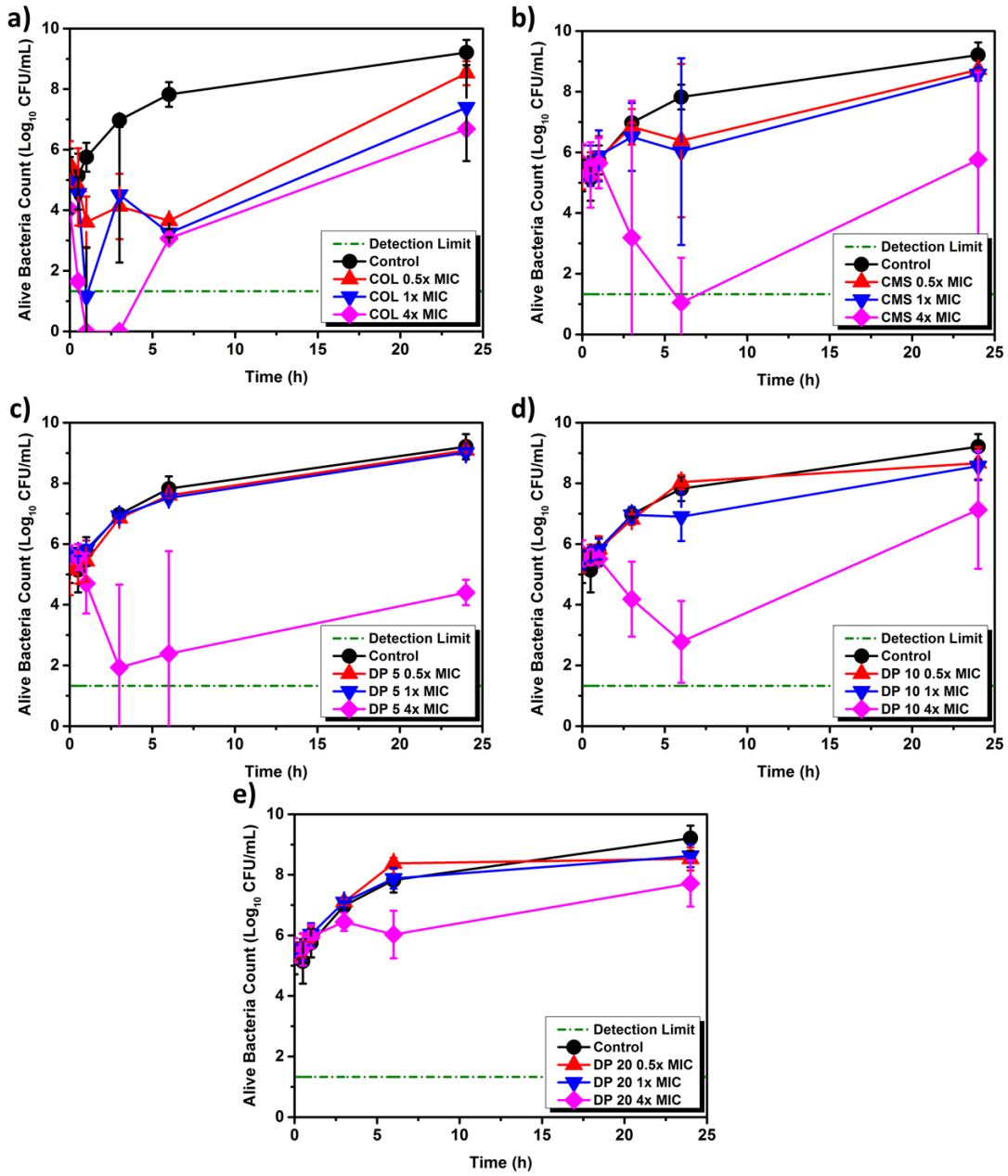

Figure 4.6 The 'time-kill' kinetics with different amount for a) colistin b) CMS and c-e) the col-PPEGA conjugates with DP 5 (c), 10 (d), and 20 (e).

All of the conjugates showed no significant inhibition towards the bacteria at a dose of 0.5 x MIC or 1 x MIC. When applying a higher dose (4 x MIC), both the DP5 and DP10 polymer-colistin conjugates were found to have a similar antibacterial

performance compared to the commercial prodrug CMS, causing a significant decrease of the amount of live bacteria in the broth. Although the DP20 polymer conjugate did not produce a similar effect found from the DP5 and DP10 conjugates, an inhibition of bacterial growth was still observed through the experiment, suggesting antibacterial activity caused by the successful release of colistin.

4.3 Conclusions

In conclusion, col-PPEGA conjugates with different DPs have been successfully achieved through the attachment of a cleavable linker/initiator (BMPAA) on to both Thr residues, followed by the polymerisation of $PEGA_{480}$ monomer using through the CP-LRP technique. All the conjugates were obtained with narrow dispersities. A model PMA polymer synthesis, confirmed that the structure of colistin remained intact during the polymerisation process. The *in vitro* degradation studies suggested most of the native colistin can be recovered from all three conjugates under a mimic physiological condition within 48 hours. The colistin release rate from the three PEGylated conjugates were similar though it slightly decreased with increasing the DP of the attached polymers. It revealed all three conjugates remained active against the tested MDR Gram-negative bacteria through the *in vitro* antimicrobial activity tests. In particular, col-PPEGA DP5 and DP10 showed a similar antibacterial activity to CMS, implying their potential as CMS alternatives. Although these col-PPEGA conjugates required a higher inhibitory concentration and exhibited less active antibacterial performance than the linear PEGylated colistin conjugate (col-aaPEG) described in Chapter 3 on mass basis, they still have some advantages, i.e., the modification sites of these conjugates are well-defined, which are important as prodrug candidates.

4.4 Experimental

4.4.1 Chemicals

All chemicals were purchased from Sigma-Aldrich and used directly unless otherwise stated. HPLC solvents are obtained from VWR international, LLC.

4.4.2 Bacterial strains

Bacterial strains of *P. aeruginosa* ATCC 27853 and *A. baumannii* ATCC 19606 (American Type Culture Collection, Manassas, VA) were used in this study. The strains were stored at -80 °C in a cryovial storage container (Simport Plastics, Quebec, Canada). Fresh isolates were subcultured on nutrient agar (Media Preparation Unit, The University of Melbourne, Parkville, Australia) and incubated at 37 °C for 24 h prior to each experiment. . CAMHB (Oxoid, Hampshire, England) was used as culture medium.

4.4.3 Instruments

4.4.3.1 NMR

^{1}H-NMR and ^{13}C-NMR spectra were recorded on Bruker HD 300 spectrometers and referenced relative to deuterated solvent (Sigma Aldrich) shifts.

4.4.3.2 MALDI-ToF MS

MALDI-ToF MS was performed on a Bruker Daltonics Autoflex MALDI-ToF mass spectrometer. The MALDI-ToF MS samples were prepared by mixing a matrix solution (20 mg/mL DCTB in THF) and a sample solution (1-2 mg/mL in THF) at the

same volume. 0.5 μL of this mixture was spotted to the target plate. Spectra were required from either reflector mode or linear mode calibrating with PEG or mPEG at a similar average molecular weight of each sample.

4.4.3.3 GPC

GPC was performed on an Agilent PL50 equipped with 2 Agilent Polargel M Columns and a differential refractive index detector eluting with DMF (0.1 M LiBr) with a flow rate of 1.0 mL min^{-1} at 50 ^{o}C. The calibration was fitted with a 3rd order polynomial using narrow molecular weight standards of PMMA (between 200 and 467,400 g mol^{-1}).

4.4.3.4 HPLC

Both sample analysis and collection were conducted from a PREP HPLC system (Agilent 1260 infinity series stack) equipped with a 1260 Quat Pump VL, a degasser and a fraction collector (FC-AS). Samples (10-70 μL) were injected using Agilent 1260 auto-sampler. The HPLC was fitted with a Phenomenex Lunar C_{18} column (250 x 4.6 mm) 5 micron packing (100Å). Detection was achieved using an Agilent 1260 variable wavelength detector connected in series with UV detection monitored at 214 nm.

The mobile phase condition is as follows.

Mobile phase A: 100% water with 0.04% TFA;

Mobile phase B: 100% ACN with 0.04% TFA.

The gradient of the mobile phase varied in each analysis. The standard analysis method is as followed: 0-20 min 5%-100% B; 20-25 min 100% B; 25-26 min 100%-

5% B; 26-35 min 5% B. The total flow rate was set to 1.0 mL/min and the temperature for the column is set to 40 ^{o}C.

HPLC water and 'far UV' HPLC ACN were used as solvents and HPLC TFA was used as additive.

4.4.3.5 FTIR

FTIR spectra were recorder on a Bruker VECTOR-22 FTIR spectrometer using a Golden Gate diamond attenuated total reflection (ATR) cell.

4.4.3.6 Electrospray ionisation-mass spectroscopy (ESI-MS)

ESI-MS was done on the Bruker MaXis II instrument (equipped with ESI source) through direct infusion at 1 µL/min. The sample was dissolved and diluted in 50% ACN/water with 0.1% formic acid and run in the positive ion mode.

4.4.4 Methods

4.4.4.1 Disk diffusion assay

According to the EUCAST guidelines,[6] inoculum was standardised in saline to the density of a McFarland 0.50±0.02 standard, corresponding to ~10^8 CFU/mL of each isolate. A freshly prepared suspension was evenly inoculated onto plates and disks were applied within 15 min and incubated for 18 h at 37 °C. Plates were examined for satisfactory streaked suspension and evenly distributed growth to achieve uniformly circular inhibition zones within the quality control limits.

4.4.4.2 MIC test

MICs were determined in accordance to the recommendations of the Clinical and Laboratory Standards Institute.[7] *A. baumannii* ATCC 19606 was used for the tests. Experiments were performed with CAMHB in 96-well polystyrene microtiter plates. Wells were inoculated with 100 μL of bacterial suspension prepared in CAMHB (containing ~ 10^6 CFU/mL) and 100 μL of CAMHB containing increasing concentrations of colistin, CMS and col-PPEGA conjugates (0 − 128 mg/L). The MIC measurements were carried out in duplicates with the MIC being defined as the lowest concentration at which visible growth was inhibited following 18 − 20 h of incubation at 37 °C.

4.4.4.3 Time-kill test

The time-kill kinetics of the col-PPEGA conjugates at 0.5, 1, and 4 x MIC were examined against *A. baumannii* ATCC 19606. Briefly, each test sample was added into a 50 mL Eppendorf tube loaded with 20 mL of a logarithmic-phase broth culture of approximately 10^6 CFU/mL to yield concentrations of 0, 0.5, 1, and 4 x MIC of the isolate. The tubes were incubated in a shaking water bath at 37 ^oC. The samples were taken at 0 min, 30 min and 1, 3, 6 and 24 h. Subcultures for viable counts were performed on nutrient agar (Oxoid) using WASP2 Spiral Plater (Don Whitley Scientific) and incubated at 37 °C for 24 h (48 h for plates with small colonies). Viable counts were determined by either manual counting or using ProtoCol3 Colony Counter (Don Whitley Scientific).

4.4.5 Synthesis

4.4.5.1 Synthesis of initiator precursor, 2-((2-bromo-2-methylpropanoyl)oxy)acetic acid (BMPAA)

Glycolic acid (3.00 g, 40 mmol, 1.0 equiv.) was dissolved with DCM (60 mL) and *N*,*N*-diisopropylethylamine (DIPEA, 8 mL, 45 mmol, 1.125 equiv.) in a 250 mL 3-neck round bottom flask under N_2. The reaction mixture was kept stirring in an ice bath for 30 min before the dropwise addition of α-bromoisobutyryl bromide (6 mL, 50 mmol, 1.25 equiv.) along with DCM (30 mL) through a dropping funnel. After the addition of all the chemicals, the system was gradually warmed up to ambient temperature and left overnight. The solvent was then removed under vacuum and the crude product was extracted by diethyl ether/0.2 M hydrochloric acid (HCl) solution to remove the remaining DIPEA. After the removal of solvent, the product was then purified by Kugelrohr Distillation. The product is normally obtained as a white solid with a slight amount of an acid impurity (which we suspected it to be α-bromoisobutyric acid) at 50 ^{o}C to 100 ^{o}C under $2.2x10^{-2}$ mbar. The purity of the product can be analysed by TLC plate (diethyl ether: AcOH = 400: 1 v/v). A further purification was performed by the recrystallisation from hot hexane. The final product is a white flaky crystal with a yield of 3.6 g (16 mmol, 40%).

^{1}H-NMR (300 MHz, $CDCl_3$, 298 K) δ (ppm) = 1.99 (-C(C$\underline{H}_3$)$_2$Br), 4.76 (-OC$\underline{H}_2$CO-) and 7.83 (br, -COO$\underline{H}$).

^{13}C-NMR (75.5 MHz, $CDCl_3$, 298 K) δ (ppm) = 30.73 (-C(CH_3)$_2$Br), 54.56 (-C(CH_3)$_2$Br), 61.12 (-O$\underline{C}H_2CO$-), 171.21 (-$\underline{C}OOCH_2CO$-), 172.74 (-$OCH_2\underline{C}O$-).

IR (neat) ν/cm^{-1}: 3300-2300 (O-H), 2975, 2865 (CH_2, CH_3), 1724, 1706 (C=O), 1421, 1248, 1147.

ESI-MS (negative mode): m/z (found) 222.9607 (M-H), m/z (calculated) 222.9611 (M-H).

4.4.5.2 Synthesis of Boc_5-colistin-ini_2

The synthesis of Boc_5-colistin-ini_2 was modified from the standard Steglich esterification. 1.00 g of colistin sulphate (0.789 mmol, 1 equiv.) was converted into Boc_5-colistin based on the previous chapter. The crude Boc_5-colistin product (~ 1.10 g) was then dissolved in anhydrous THF (50 mL), following the addition of 2-((2-bromo-2-methylpropanoyl)oxy)acetic acid (885.0 mg, 3.95 mmol, 5 equiv.) and DMAP (48.0 mg, 0.393 mmol, 0.5 equiv.). After the chemicals completely dissolved, *N*,*N'*-dicyclohexylcarbodiimide (DCC, 977.0 mg, 4.74 mmol, 6 equiv.) was added afterwards and the reaction mixture was kept stirring overnight. The reaction mixture was then centrifuged to remove most of insoluble compounds. The solvent was then removed under vacuum and a further purification was performed by the flash column (0% -10% MeOH in DCM).The final product is a fine pale yellow powder with a total yield around 0.96 g (0.463 mmol, 59%).

4.4.5.3 Procedure for the polymerisation of MA using colistin initiator Boc_5-colistin-ini_2

The polymerisation condition of MA was modified from the standard CP-LRP. MA was passed through a short basic aluminium column to remove the inhibitor prior to use. A stock solution of $CuBr_2$ (1 mg/mL in DMSO) and the ligand Me_6TREN (6.5 μL/mL in DMSO) was freshly prepared before the reaction. MA (73 μL, 0.80 mmol,

40 equiv., 20 equiv. per arm), Boc_5-colistin-ini_2 (42 mg, 20 μmol, 1 equiv.), $CuBr_2$ stock solution (90 μL, 0.4 μmol, 0.02 equiv.), Me_6TREN stock solution (100 μL, 2.4 μmol, 0.12 equiv.) were added to a 2 mL vial. 102 μL DMSO was then added to make the monomer/solvent ratio to around 1: 4. The reaction mixture was then stirred until all the compounds were dissolved. The system was then sealed and carefully degassed by purging with N_2 for 15 min (make sure the monomer is not blown off by the N_2). The polymerisation was performed under UV with a cooling plate (CAMLAB, KP283) to maintain the reaction temperature. The reaction was stopped at 4h and the conversion were measured using ^{1}H-NMR. MALDI-ToF MS and GPC analyses were also conducted to evaluate the molecular weight and dispersity of the polymer.

The cleavage of the linker from PMA-Boc_5-colistin conjugate was conducted directly using the crude polymer obtained from previous procedure. 100 μL of the crude polymer was diluted by 1mL 3% NaOMe in MeOH and the reaction mixture was kept stirring at ambient temperature for 1 day. The solvent was then blown off by N_2 and the product were analysis by MALDI-ToF MS and GPC.

4.4.5.4 Polymerisation of $PEGA_{480}$ of different DPs using colistin initiator Boc_5-colistin-ini_2

The polymerisation procedure of $PEGA_{480}$ was similar to MA. The ratio of initiator: $CuBr_2$: ligand was kept the same as the one used in the polymerisation of MA(1: 0.02: 0.12). The $PEGA_{480}$ monomer to initiator ratio was set to 10:1, 20:1, 40:1 for the synthesis of DP5, DP10, and DP20 polymer, respectively. For the synthesis of DP10 and DP20 polymer, 21 mg colistin initiator was used and the monomer/DMSO ratio was changed to 1: 2 so that the reaction time was shorten to 2 h instead of the standard 4h to reach high monomer conversion (> 90%) which can be analysed by ^{1}H-

NMR. To minimise the hydrolysis during the purification steps, the further separation of the polymer and the trace $PEGA_{480}$ monomer was done by diluting the crude using ACN and purifying by RP-HPLC (0-12 min 50%-100% B; 12-20 min 100% B, 20-21 min 100%-50% B; 21-30 min 50% B). The polymer peak would be found from 8-15 min depending on the DP. Once collected from RP-HPLC, the product was frozen by liquid N_2 and the solvents were directly removed under high vacuum. The products before and after the purification were performed by GPC and HPLC analysis to observe whether any change was occurred during the purification step.

4.4.5.5 Deprotection of Boc groups from Boc_5-col-PPEGA conjugates

Table 4.3 ^{1}H-NMR and DMF GPC analysis of the product from the reaction mixture, after purification and after deprotection of the Boc groups.

	DP	Conversion (%)	$M_{nTheory}$ (g·mol^{-1})	M_{nNMR} (g·mol^{-1})	M_{nGPC} (g·mol^{-1})	*Đ*
Before Purification	5	99	6875	6800	6100	1.13
	10	93	11675	11000	8700	1.20
	20	93	21275	19900	14400	1.21
After Purification	5	----	6875	----	6000	1.13
	10	----	11675	----	8700	1.18
	20	----	21275	----	14000	1.23
Deprotection	5	----	6375	----	5600	1.20
	10	----	11175	----	8800	1.16
	20	----	20775	----	14300	1.26

The deprotection of the Boc groups was modified from the typical Boc cleavage procedure. 5 mL 20 % TFA in DCM was added slowly into the purified polymer conjugates. [Be cautious of the release of gas!] After most gas was released, the reaction mixture was sealed and kept stirring at ambient temperature overnight. After the removal of solvents, the product was frozen by liquid N_2 and all the solvents were directly removed under high vacuum. The products were performed by GPC and HPLC analysis for comparison.

4.4.5.6 Protocol for in vitro releasability of col-PPEGA prodrugs

The degradation of the col-PPEGA conjugates was based on the previous chapter. Each conjugate was weighed into a 2 mL vial, followed by the addition of a certain amount of PBS (1X) to make the final concention of 0.4 μmol/mL. 900 μL of each prodrug solution was taken into another vial and incubated in an oil bath with stirring at 37 ºC. The rest of each prodrug solution (> 500 μL) was stirred at ambient temperature. Samples (85 μL each time) were taken periodically and frozen by liquid nitrogen before the analysis. The analysis was conducted by RP-HPLC (injection volume = 70 μL) using the standard analysis condition. The colistin release percentage was calculated based on the reported method.

4.5 References

1. M. J. Roberts, M. D. Bentley and J. M. Harris, *Adv. Drug Deliv. Rev.*, 2012, **64**, 116-127.

2. B. Podobnik, B. Helk, V. Smilović, Š. Škrajnar, K. Fidler, S. Jevševar, A. Godwin and P. Williams, *Bioconjugate Chem.*, 2015, **26**, 452-459.

3. J. Ogden and R. Palmer, available at: http://www.ondrugdelivery.com/publications/Injectable%20Formulations%202011/WEP.pdf, (accessed 1 December, 2017).

4. J. Liu, V. Bulmus, D. L. Herlambang, C. Barner‐Kowollik, M. H. Stenzel and T. P. Davis, *Angew. Chem. Int. Ed.*, 2007, **46**, 3099-3103.

5. B. S. Lele, H. Murata, K. Matyjaszewski and A. J. Russell, *Biomacromolecules*, 2005, **6**, 3380-3387.

6. *Disk Diffusion Method for Antimicrobial Susceptibility Testing, Version 5.0 (January 2015), in: E.C.o.A.S.T. EUCAST (Ed.), 2015*.

7. CLSI, *Performance Standards for Antimicrobial Susceptibility Testing: Twentieth Informational Supplement (M100-S20)*, CLSI, Wayne, PA, USA, 2010.

Chapter 5 *A Hydrogel Based Localised Release of Colistin for Antimicrobial Treatment of Burn Wound Infection*

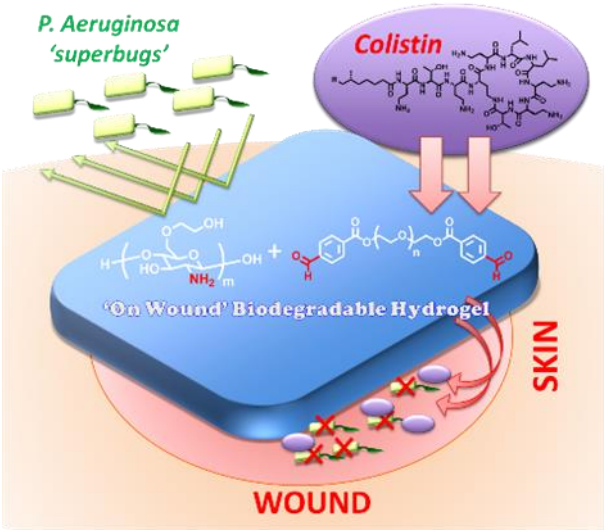

In this chapter, a localised hydrogel-based delivery system for colistin has been developed for a topical delivery regime to demonstrate the possibility to reduce the systemic toxicity caused by colistin treatment. Colistin was incorporated into a self-healable hydrogel (formed via dynamic imine bonds between the amine groups present in glycol chitosan and an aldehyde modified PEG). The storage modulus (G') of the colistin-loaded hydrogel ranged from 1.3 kPa to 5.3 kPa by varying the amount of the cross-linker and colistin loading, providing different options for topical wound care. Most of the colistin is released from the hydrogel within 24 h and remains active as demonstrated by both antibacterial in vitro disk diffusion and time-kill assays. Moreover and pleasingly, the colistin-loaded hydrogel performed almost equally as well as native colistin against both the colistin-sensitive and also colistin-resistant P. aeruginosa strain in the in vivo animal 'burn' infection model despite exhibiting a slower killing profile in vitro.

5.1 Introduction

In the previous two chapters, the possibility of using colistin polymeric prodrugs synthesised through two approaches to reduce colistin toxicity while maintaining its antimicrobial activity during systemic administration has been demonstrated. However, in some cases, such as for treating localised infections like open wounds or burn wound infections, systemic administration of colistin is not necessary and not efficient to achieve a high local concentration to inhibit the growth of bacteria, not to mention that the delicate synthesis and purification steps involved in the synthesis of prodrug would increase the cost of the colistin treatment. It has been demonstrated that the localised application of colistin to the infection site can also reduce its systemic toxicity while maintain its activity.[1] Thus, instead of making any chemical transformations to colistin, focus was switched to colistin formulation in a hydrogel network for localised delivery.

As colistin is a small lipopeptide antibiotic that is sensitive to many thermal, enzymatic and chemical conditions, a hydrogel based delivery platform with facile preparation, easy operation, mild gel formation environment, and high drug loading capacity could be a suitable candidate to deliver colistin in a local and effective manner to wounds. Recently, Wei and co-workers developed an injectable chitosan-based hydrogel through the utilisation of dynamic imine bond chemistry, which exhibits high biocompatibility and allows for the controlled storage and release of proteins, and even cells.[2-4] An inexpensive hydrogel can be formed using commercially available glycol chitosan and an easily prepared low-toxicity aldehyde-modified poly(ethylene glycol) derivative (DF-PEG, the chemical structure of DF-PEG was shown in Scheme 5.1c).[2-4] The resulting hydrogel is a transparent material with self-healing properties; which

can provide better monitoring of the wound through direct observation, and improved adhesion to the wound. The quick and efficient chemistry used allows this hydrogel to be formed either at ambient or body temperatures, which is convenient for topical delivery. More importantly, the starting materials of this hydrogel, as well as colistin, are highly water soluble, suggesting that colistin could be loaded and distributed into the system evenly during the gel formation.

In this chapter, a patch candidate using the dynamic glycol chitosan/DF-PEG hydrogels loaded with colistin was presented. The effects of DF-PEG and colistin concentration on the gel material properties were investigated. The release profile of colistin was determined both in PBS and bacterial growth media by HPLC analysis. Furthermore, the antibacterial activity of the released colistin was evaluated *in vitro via* disk diffusion and time kill experiments. Proof-of-concept *in vivo* experiments were performed using a mouse 'burn' infection model.

5.2 Results and Discussion

5.2.1 Initial attempts to form a colistin/DF-PEG hydrogel

As colistin itself contains five primary amines that are capable of imine formation as demonstrated in chapter 2, initial attempts to prepare a hydrogel were focused on direct mixing of colistin and DF-PEG (20 mg colistin with 500 μL 20% w/w DF-PEG PBS solution, Figure 5.1). However, there was no hydrogel or visible precipitation formed during this process, indicating no effective cross-linking reaction happened between the two materials. This may be attributed to the dynamic reversibility of the imine bonds under these conditions. In order to act as a stable cross-linking point, at least three amines on each colistin need to form imine bonds with DF-

PEG at all times, which is not necessarily easy as the individual imine bond is weak and hydrolytically labile. However, it is more likely to happen with a multi-functional amine-rich material such as glycol chitosan. The viscosity produced by glycol chitosan may hinder the reversibility of the imine bond, which could also promote hydrogel formation. Thus, glycol chitosan is necessary in this system to obtain a stable hydrogel network.

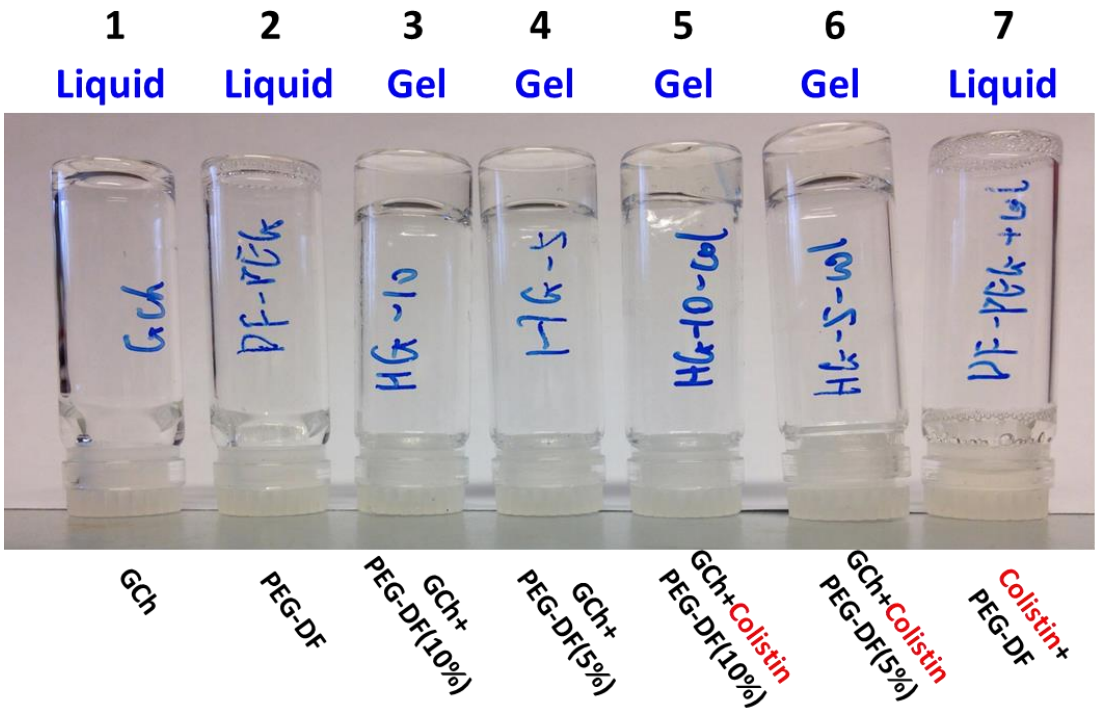

Figure 5.1 The visualisation of the hydrogels using different components. All the hydrogels (vial 3-6) were prepared through the standard condition. Colistin loading amount for each hydrogel sample is 5 mg. GCh: 475 µL 3% glycol chitosan in PBS; DF-PEG: 475 µL 20% w/w DF-PEG PBS solution; colistin+PEG-DF: 20 mg colistin with 500 µL 20% w/w DF-PEG PBS solution.

5.2.2 The formation and characterisation of colistin-loaded hydrogels with different cross-linker ratios

The synthesis of a colistin-loaded hydrogel was achieved by integrating colistin into the glycol chitosan/DF-PEG hydrogel formulation (Scheme 5.1). The original

hydrogel was prepared by mixing an aqueous glycol chitosan solution with an aqueous DF-PEG solution at a volume ratio of 2.8:1. Instead of the established protocol, PBS buffer was used as the solvent in an attempt to more closely mimic the wound environment. To obtain a stronger but not brittle material for patch application, a preliminary study on tuning the concentration of glycol chitosan/DF-PEG was performed. After the optimisation, two types of hydrogels (HG-5 and HG-10) formed from 3% w/w glycol chitosan solution and either 5% or 10% w/w DF-PEG solution were chosen for comparison.

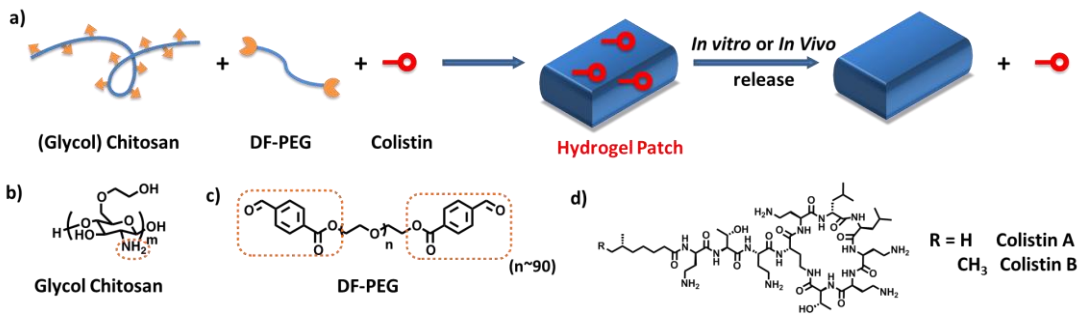

Scheme 5.1 a) Cartoon illustration of the synthesis of colistin-loaded hydrogels. The chemical structure of b) glycol chitosan, c) DF-PEG and d) colistin A and B.

The incorporation of colistin was conducted by the addition of colistin either to the glycol chitosan solution or to the DF-PEG solution, and after mixing the two solutions a transparent hydrogel was formed instantly (typically < 1.6 min) as shown in Figure 5.1. To investigate the effect of colistin upon the hydrogel formation, the gel formation process was then monitoring by the rheological analysis. Both HG-5 and HG-10 were tested. It turned out that the gel formation process of the colistin-loaded hydrogels was not affected by the addition of colistin in both cases, and in fact, the presence of colistin in the formulation accelerated the gelation process compared to the original hydrogels. This effect may be explained by the increased number of amines that can act as catalysts/gelation points in the system (Figure 5.2).

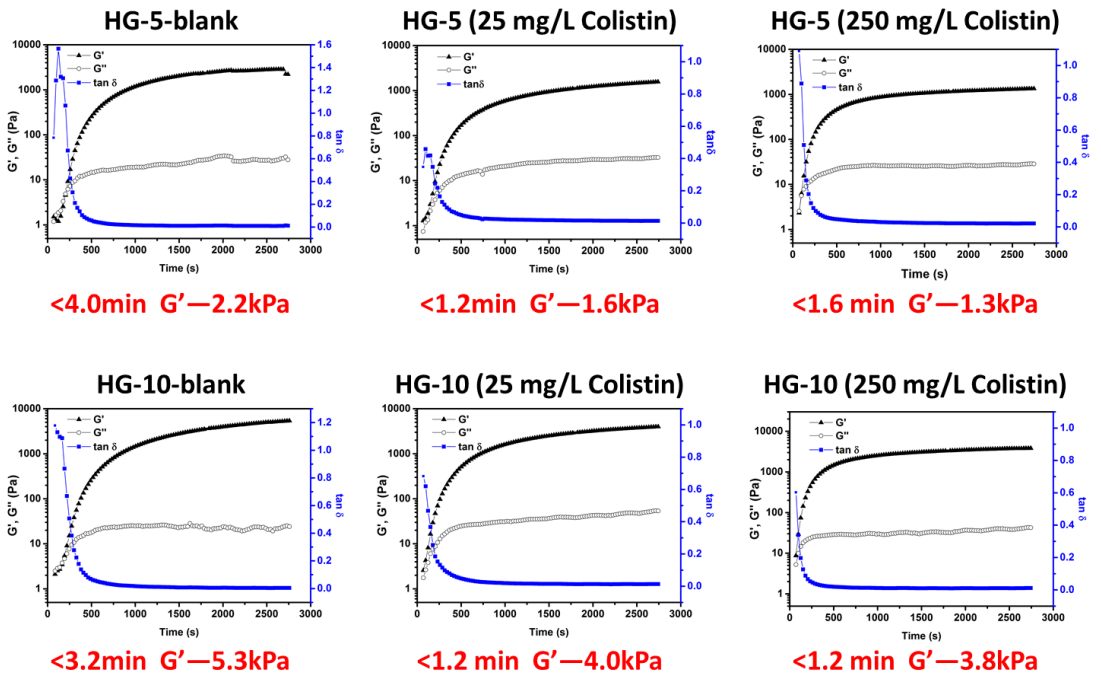

Figure 5.2 Storage modulus G' and loss modulus G'' analyses during gelation process for different hydrogels. (Black: storage modulus; white: loss modulus; blue: phase angle; 37 °C; frequency: 1.0 Hz; strain: 5.0 %).

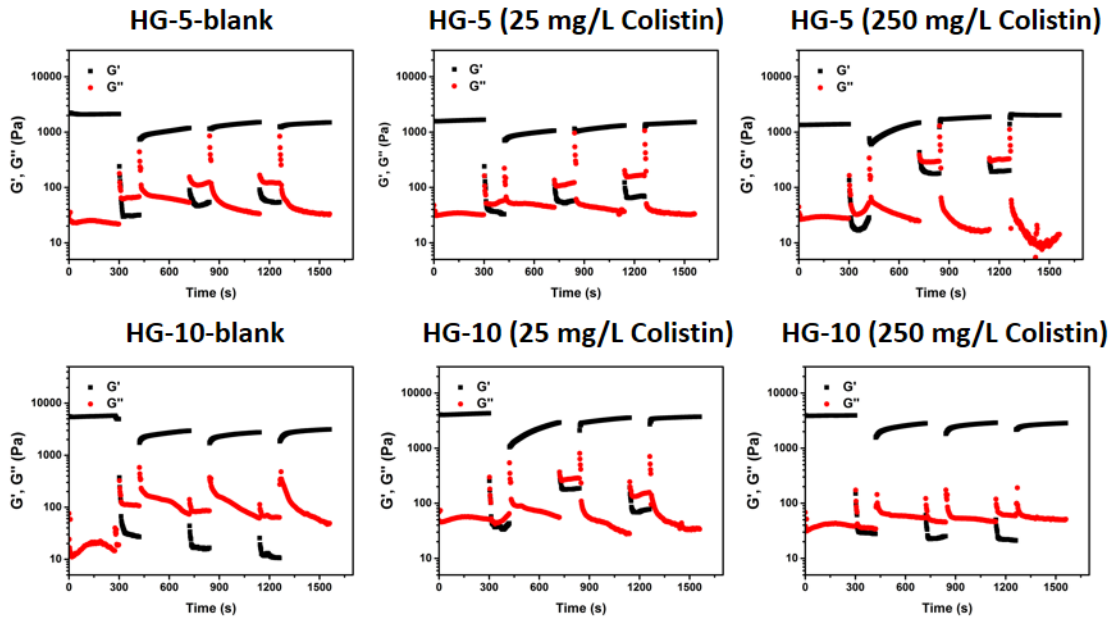

Figure 5.3 Rheology analyses of the hydrogel deformation and recovery with different loading amount of colistin. Black: storage modulus; red: loss modulus. Amplitude oscillatory forces were changed from γ = 250% (last for 2 min) to 1% (last for 5 min) under the same frequency (1.0 Hz) at 37 °C.

Since the hydrogel network is mainly dominated by glycol chitosan and DF-PEG, it is expected that the mechanical properties of the hydrogel can still be tuned by adjusting the amount of the DF-PEG cross-linker in the presence of colistin. Even through a slight decrease of the storage modulus (G') was observed by increasing the loading amount of colistin, the HG-10 hydrogels prepared from a higher concentration DF-PEG solution (10% w/w) all exhibited a larger storage modulus compared to the corresponding HG-5 hydrogels with the same amount of colistin loaded. The G' range of the HG-5 is suitable for application as a topical gel, while the higher G' of HG-10 makes it a suitable candidate for patch processing.

The self-healing property provided by the dynamic imine bond of the original hydrogel has proven to be helpful to tissue repair.[4] To observe whether the self-healable gel would be affected by the addition of colistin, the rheology of the colistin-loaded hydrogels was examined (Figure 5.3). As colistin does not interrupt the formation of the main dynamic cross-linked network of the hydrogels, both hydrogels demonstrated self-healing properties in the presence of colistin whilst the G' of the hydrogels only reduced slightly after three cycles, implying the colistin-loaded hydrogels can still provide similar protection on the wound after suffering some small damage.

5.2.3 Colistin release from the hydrogels

Since the integration of colistin into the hydrogels was successful, the potential for tuning the colistin release was investigated. The release rate of colistin was first tested in PBS (1X) using both HG-5 and HG-10 formulations for comparison. Due to the potency of colistin, the release experiment was then carried out at relatively low concentrations. A high (5 mg colistin per hydrogel; final colistin concentration in

solution, 250 mg/L) and a low dose (0.5 mg colistin per hydrogel; final colistin concentration in solution, 25 mg/L) colistin were loaded into both hydrogels for the test. In order to confirm colistin is incorporated within the hydrogel as opposed to being located at the surface, a washing step was conducted prior to the release study. The recovered wash solutions were systematically analysed by HPLC and revealed no detectable signals, suggesting near quantitative encapsulation of colistin.

Interestingly, although adjusting the amount of the DF-PEG cross-linker is used to tune the physical properties of the hydrogels, it has little impact upon the colistin release rate under the formulation conditions used herein (Figure 5.4). The colistin concentration difference at each sampling time is sufficiently insignificant not to have any biological implication for both hydrogels loaded with the same amount of colistin. We attribute this observation to the dynamic properties of the hydrogel cross-linked network and the weak interactions between colistin and the hydrogel scaffold. The low colistin loading may also be one of the reasons for the little difference of the release rate between the HG-5 and HG-10 formulations.

Similarly, the release of colistin was tested in cation-adjusted Mueller-Hinton (CAMHB) bacterial growth media to evaluate the effect of a complex biological media on the colistin release rate. Even though the CAMHB contains amino acids, proteins and various ions, which is very different to PBS, the release profiles of both colistin-loaded hydrogels were found to be very similar (Figure 5.4). Again, under these conditions the amount of the cross-linker in the hydrogel did not have a great influence on the release of colistin due to similar reasons described above. All of these results suggest that the antibiotic activity between these two colistin-loaded hydrogels should be similar.

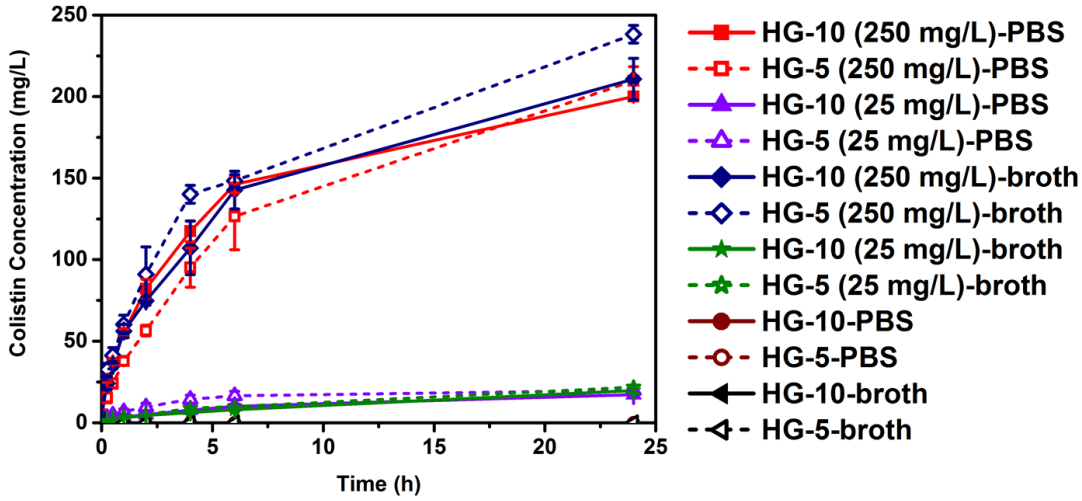

Figure 5.4 The release study in PBS and cation-adjusted Mueller-Hinton broth. The data of HG-5 is described in dash lines and HG-10 in solid lines. (The release traces of the blank hydrogels overlap with the x axis).

5.2.4 *In vitro* bio-activity evaluation of colistin-loaded hydrogels

The activity of the colistin-loaded gels was investigated *in vitro* against two *P. aeruginosa* strains, a colistin-sensitive strain (ATCC 27853, minimum inhibitory concentration (MIC) = 1 mg/L) and a colistin-resistant strain cystic fibrosis isolate (19147 n/m, MIC > 128 mg/L). Firstly, a disk diffusion assay was used to evaluate the release of colistin from the hydrogel through the interface (Figure 5.5). Briefly, the colistin-loaded hydrogels were placed on an agar plate surface that was swabbed with a bacterial isolate solution and the plate was then incubated for 24 h. A clear bacteria-free zone, also known as zone of inhibition (ZoI), would be found from the samples that have antibiotic activity and the larger size of ZoI indicates a higher potency of the sample.

Although the hydrogel *per se* did not show any inhibition against the bacteria, clear ZoIs were found from the colistin-sensitve *P. aeruginosa* strain when colistin-loaded hydrogels were applied (Figure 5.5a, left lane), suggesting that colistin is

effectively released from the colistin-loaded hydrogels to the bacterial interface and more importantly, that the released colistin remains active.

a)

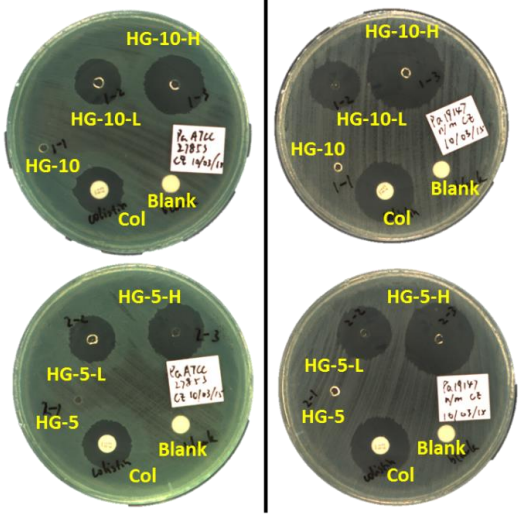

b)

	ATCC 27853		19147 n/m	
	D/cm	ZoI/cm	D/cm	ZoI/cm
Blank	0.60	0	0.60	0
Col (10 µg)	0.60	1.60	0.60	1.93
HG-10 (0 µg)	0.30	0	0.28	0
HG-10-L (10 µg)	0.36	1.52	0.30	1.65
HG-10-H (100 µg)	0.35	1.97	0.31	2.49
Blank	0.60	0	0.60	0
Col (10 µg)	0.60	1.58	0.60	1.94
HG-5(0 µg)	0.27	0	0.34	0
HG-5-L (10 µg)	0.36	1.53	0.30	1.78
HG-5-H (100 µg)	0.31	1.86	0.33	2.36

D: Disk/Hydrogel Diameter
ZoI: Zone of Inhibition

Figure 5.5 a) Disk diffusion assay for the colistin-loaded hydrogels against the colistin-sensitive (left) and colistin-resistant (right) *P. aeruginosa* strains. b) Zone of inhibition (ZoI) results of the colistin-loaded hydrogels. Blank: commercial blank disc; Col: commercial colistin disk (contains 10 µg colistin); HG-10/5: blank hydrogels; HG-10/5-L: hydrogels loaded with 10 µg colistin; HG-10/5-H: hydrogels loaded with 100 µg colistin.

ZoIs of similar size were found between both colistin-loaded hydrogels (HG-5 and HG-10) against the *P. aeruginosa* strain, in accordance with the extent of colistin release after 24 h from the release profile (Figure 5.4), proposing the two colistin-loaded hydrogels have similar antibacterial properties despite the difference in their physical properties. More importantly, the colistin-loaded hydrogels showed similar activity to commercial colistin disks containing the same amount of colistin (10 µg), indicating the released colistin has similiar activity against the *P. aeruginosa* bacteria as the native one and that the hydrogel does not severely hinder or alter the activity of the colistin during loading and whilst encapsulated. Similar results were also found from the colistin-resistant *P. aeruginosa* strain (Figure 5.5a, right lane). Owing to the

high loading capacity of the hydrogel, it was possible to increase the loading of colistin into the hydrogel of the same size. With the higher loading of the colistin (100 μg colistin per hydrogel), the hydrogels showed the expected enhanced antibiotic performance against the bacteria when compared to the commercial disks.

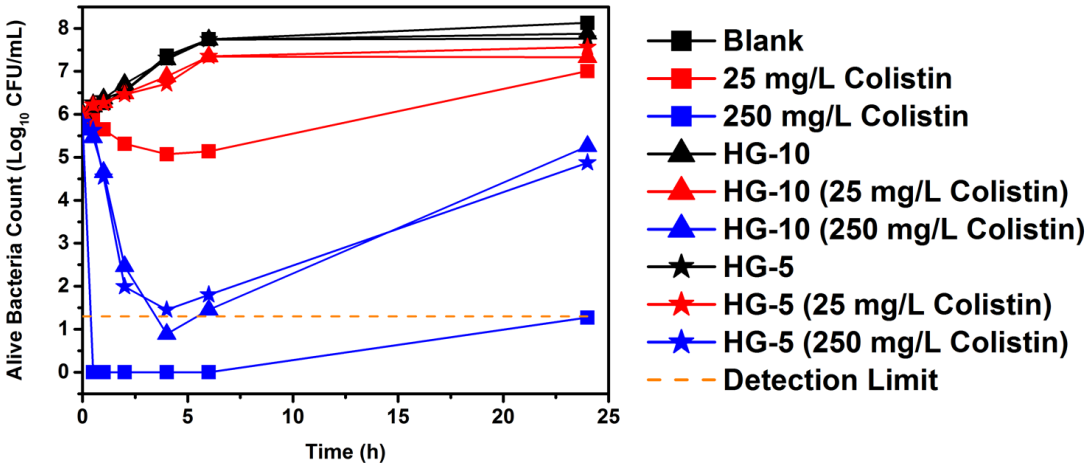

Figure 5.6 Time-kill test of the colistin-loaded hydrogels. Black lines: blank control and blank hydrogels; red lines: samples loaded with 0.5 mg colistin (final concentration: 25 mg/L); blue lines: samples loaded 5 mg colistin (final concentration: 250 mg/L). The detection limit is shown in dash line.

In order to obtain a better understanding of the killing kinetics of the colistin-loaded hydrogels, time-dependent bacterial inhibition experiments (time-kill experiments) were conducted (Figure 5.6). Briefly, the colistin-loaded hydrogels were introduced into the broth containing bacteria at the logarithmic phase of growth and the broth samples were taken periodically for viable counts. As the growth of the colistin-sensitive *P. aeruginosa* strain can be easily inhibited at a very low colistin concentration, only the colistin-resistant strain was investigated in these time-kill studies. Although the MIC of the colistin-resistant strain is greater than 128 mg/L, colistin solution at a final concentration of 25 mg/L inhibited the growth of the bacteria from 0.5-6 h. On the contrary, the lower colistin dose hydrogels (0.5 mg colistin per hydrogel; final colistin concentration in solution, 25 mg/L), showed a lower level of activity. This is mainly due to the different diffusion profiles obtained from the two

solutions and the hydrogel-solution interface. The slower colistin release provided by colistin-loaded hydrogel in the first few hours resulted in a lower local concentration of released colistin, compared with the colistin solution, thus inhibition of the growth of bacteria at that dose is not observed. To increase the initial local colistin concentration, a higher concentration of colistin was loaded into the hydrogels (5 mg colistin per hydrogel; final colistin concentration in solution, 250 mg/L). At this loading, colistin-loaded hydrogels showed a much better performance against the resistant *P. aeruginosa* strain. Akin to the previous colistin release curve (Figure 5.4), the difference of the killing profiles between HG-5 and HG-10 were again very subtle, indicating similar concentrations of colistin with similar antibiotic ability were released from both colistin-loaded hydrogels. Although a slightly slower killing profile was still observed compared to a solution containing the same amount colistin due to the reduced initial local concentration provided from the hydrogels, the survival bacteria number was significantly decreased (Figure 5.6).

5.2.5 *In vivo* animal 'burn' infection model test of colistin-loaded hydrogels

An animal 'burn' infection model was also developed to evaluate the gel performance *in vivo* (**see section 4.4 Experimental for the details**). Both the colistin-sensitive strain and the resistant strain were tested. Although colistin-loaded hydrogels were quite stable in vitro, a visible weight loss was found in both blank and colistin-loaded hydrogels during the test due to the biodegradability of the hydrogels (Figure 5.7). Notably, no matter if colistin was loaded, HG-5 degraded much faster compared to HG-10, leading to a complete degradation after being applied onto the wound for 24 h. Since the HG-5 hydrogel required a longer gelation time and it exhibited a faster

degradation rate *in vivo*, only the HG-10 formulation was examined in the following *in vivo* test.

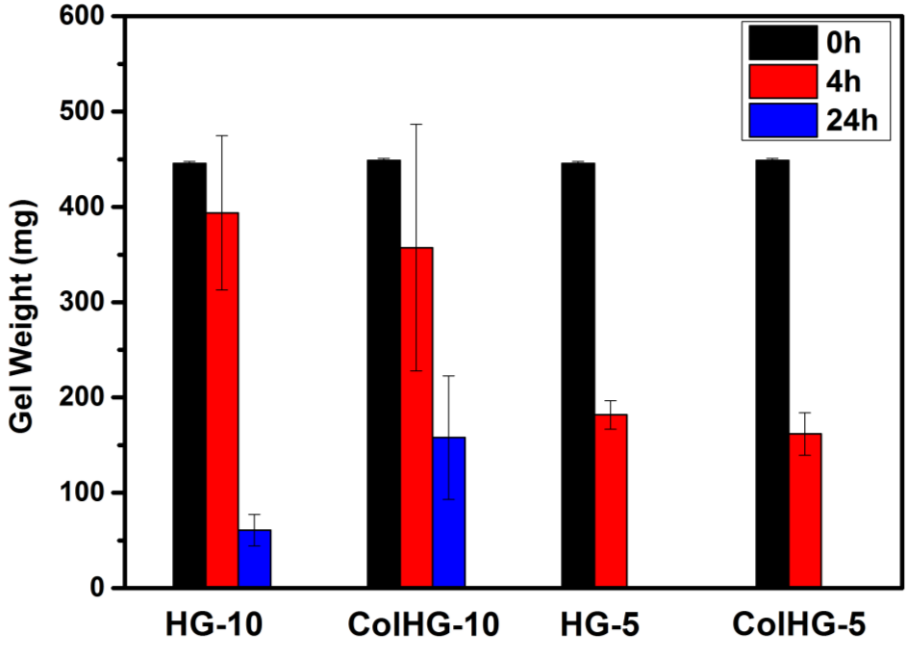

Figure 5.7 The weight loss of the colistin-loaded hydrogels *in vivo* over the time. ColHG-10 and ColHG-5 were the corresponding hydrogels loaded with 0.3 mg colistin.

100 μL 10^9 CFU/mL of bacteria at the early logarithmic growth phase was inoculated onto the wound (1 cm^2) of each mouse, two hours in advance of the test. Then patches made from colistin solution, colistin-loaded hydrogel or blank hydrogels were applied onto the wound at time = 0 h. Colistin (0.3 mg) was loaded into the hydrogel to kill the colistin-sensitive strain. Surprisingly, in spite of the slower colistin release in vitro, the colistin-loaded hydrogel performed as efficiently as the colistin solution *in vivo* (Figure 5.8).

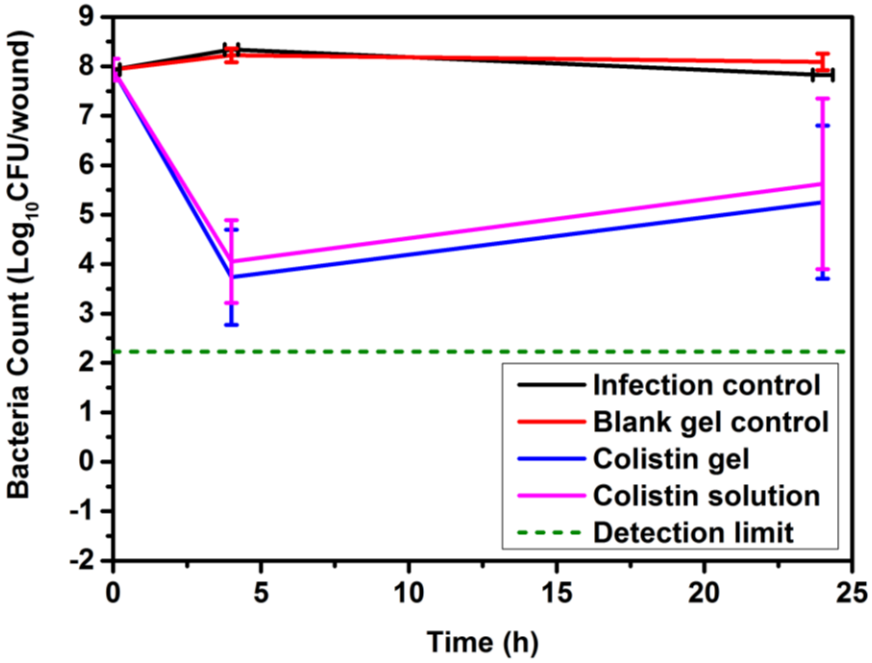

Figure 5.8 The 'burn' infection model test of the colistin-loaded hydrogel against colistin-sensitive *P. aeruginosa* strain. Black line: blank infection control; red line: blank HG-10 hydrogel; blue line: HG-10 with colistin (0.3 mg/wound); pink line: colistin solution (0.3 mg/wound). The detection limit is shown in dash line.

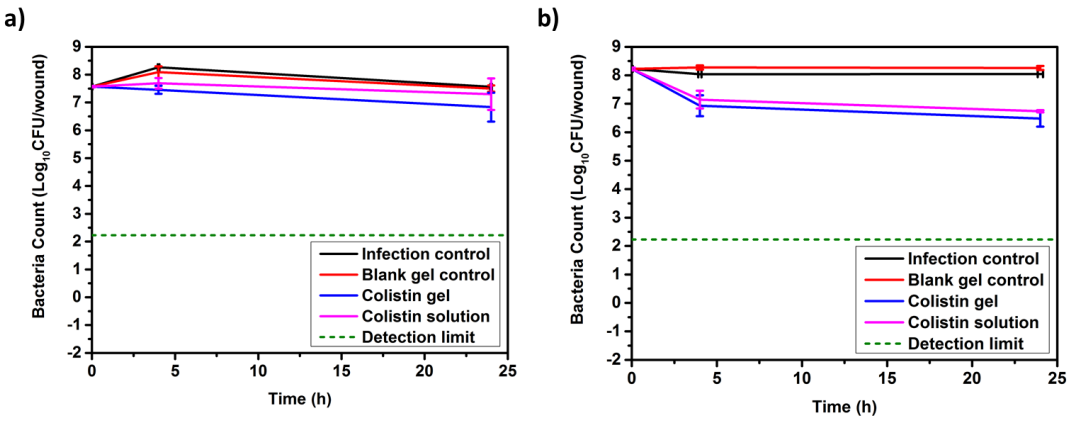

Figure 5.9 The 'burn' infection model test of the colistin-loaded hydrogel against colistin-resistant *P. aeruginosa* strain. Black line: blank infection control; red line: blank HG-10 hydrogel; blue line: HG-10 with colistin (a: 0.3 mg/wound and b: 1.5 mg/wound); pink line: colistin solution (a: 0.3 mg/wound and b: 1.5 mg/wound). The detection limit is shown in dash line.

In the case of the resistant strain, the colistin concentration was not sufficient to kill the bacteria whether it was applied in the hydrogel or as a solution (Figure 5.9a).

Therefore, a higher dose (1.5 mg colistin) was used instead to kill the resistant strain. Although the killing profile is slower due to the nature of the resistant strain, the colistin-loaded hydrogel again showed a similar activity as the colistin solution, leading to approximately 2 logarithm reductions of the bacteria population (i.e. ~99% bacteria population was killed) (Figure 5.9b). This implies that the hydrogel formulation did not inhibit the activity of the colistin *in vivo* even though it has a slower release rate than that observed in the time-kill study. This may partially be attributed to the similar diffusion profile occurring at the wound interface but also through the enhanced degradation of the hydrogel in the biologically complex local wound environment. Moreover, since the colistin-loaded hydrogels were applied directly onto the burn wound, it appears that the local concentration on the wound was high enough to kill the bacteria whilst all the tested mice survived suggesting the overall systemic concentration and toxicity remained low.

5.3 Conclusions

In summary, self-healing colistin-loaded hydrogels by incorporating colistin into an inexpensive, biocompatible and biodegradable chitosan hydrogel has been successfully prepared. The hydrogel structure was not affected by the addition of the colistin lipopeptide and the colistin-loaded hydrogels inherited all of the properties from the original hydrogel without disrupting their desired physical properties. Interestingly, the hydrogel formation process could be accelerated in the presence of the colistin. Colistin is released from the hydrogel at a similar rate at body temperature in different buffers. The disk diffusion assay showed that the released colistin remained active and had comparable antibacterial activity as the colistin solution. Although the colistin-loaded hydrogels showed a slower killing profile *in vitro*

compared with the colistin solution, it performed as well as the colistin solution *in vivo* thanks to the biodegradable and dynamic nature of this glycol chitosan hydrogel. Furthermore, a wide range of colistin loading was easily achievable, thus allowing the tuning of the release of colistin for different applications. Indeed, even the colistin resistant *P. aeruginosa* strains can easily be killed *in vivo* in a mouse burn infection model. Finally, this hydrogel system can achieve the localized release of active colistin without causing any toxicity to the mice. This colistin-loaded hydrogel holds significant potential for the treatment of chronic wound infections caused by problematic Gram-negative 'superbugs'.

5.4 Experimental

5.4.1 Materials

5.4.1.1 Chemicals

All chemicals were purchased from Sigma-Aldrich and used directly unless otherwise stated. Colistin sulfate salt (≥ 15,000 U/mg) was used as colistin source in all the experiments. HPLC solvents are obtained from VWR international, LLC.

5.4.1.2 Bacterial strains

Bacterial strains of *P. aeruginosa* ATCC 27853 (American Type Culture Collection, Manassas, VA) and *P. aeruginosa* 19147 n/m (MIC > 128 μg/L, clinical isolate) were used in this study. The strain was stored at -80 °C in a cryovial storage container (Simport Plastics, Quebec, Canada). Fresh isolates were subcultured on Nutrient agar (Media Preparation Unit, The University of Melbourne, Parkville,

Australia) and incubated at 35°C for 24 h prior to each experiment. CAMHB (Oxoid, Hampshire, England) was used as culture medium.

5.4.2 Instruments

5.4.2.1 NMR

^{1}H-NMR spectra were recorded on Bruker HD 500 spectrometers and referenced relative to deuterated solvent shifts using deuterated solvents obtained from Aldrich.

5.4.2.2 HPLC

HPLC was performed using an Agilent 1260 infinity series stack equipped with a binary pump and degasser. The HPLC was fitted with a Phenomenex Lunar C_{18} column (250 x 4.6 mm) with 5 micron packing (100Å). Samples were injected using Agilent 1260 autosampler. UV detection was monitored at λ = 214 or 225 nm. The flow rate was set to 1.0 mL/min. The condition for the detection of colistin release is shown below:

Mobile phase A: 100% water, 0.04% TFA.

Mobile phase B: 100% ACN, 0.04% TFA.

Programmed Gradient: 10%-80% B (0-30 min); 80% B (30-35 min); 80%-10% B (35-36 min); 10% B (36-50 min).

5.4.2.3 Rheometer

Rheology analysis was performed using a Kinexus Rheometer (Kinexus Ultra, Malvern Instruments. Inc, MA, USA) with a JULABO heating module (CF-41, JULABO USA, Inc.).

5.4.3 Synthesis

5.4.3.1 Synthesis of difunctionalized PEG (DF-PEG)

The synthesis of DF-PEG was adapted from literature using PEG_{4000}.[2, 3] PEG_{4000} (12.0 g, 3 mmol, 1 equiv.), FBA (1.80 g, 12 mmol, 4 equiv.), and DMAP (0.36 g, 3 mmol, 1 equiv.) were fully dissolved in 200 mL of dry THF under N_2. DCC (5.85 g, 0.28 mmol, 9.5 equiv.) was then added into the solution and the reaction mixture was kept stirring overnight. The white precipitation was filtered and the filtrate was concentrated under vacuum. The polymer was obtained after repeated dissolution in THF and precipitation in diethyl ether for three times. The total yield is around 89% with end-group functionality above 93%.

^{1}H-NMR (400 MHz, $CDCl_3$, 298 K) δ (ppm) = 10.11 (s, 2H, CHO), 8.22 (d, J = 8.0 Hz, 4H, CHCCHO), 7.96 (d, J = 8.3 Hz, 4H, CHCHCCHO), 4.51 (m, 4H, $COOCH_2$), 3.86-3.55 (m, 364H, OCH_2CH_2O).

5.4.3.2 Synthesis of colistin-hydrogels

The synthesis of the colistin-hydrogels was modified from previous report.[2, 3] Briefly, 125 μL freshly prepared solution B was added into 350 μL solution A, mixing properly to form a hydrogel. The hydrogel usually can be formed with 2 min (Size around 0.5 cm^3). The gel size can be scaled-up or down by simply increase or decrease the volume of solution A and B. The details of solution A and B are shown below.

[Solution A] Prepare 3% glycol chitosan in PBS.

A 3% (w/w) glycol chitosan solution was prepared by dissolving 88 mg glycol-chitosan in 2.8 mL PBS (1X) solution. The mixture was kept stirring overnight until a

clear viscous solution was obtained. Filtration sterilisation was applied to the solution before biological tests.

[Solution B] Prepare 5% or 10% DF-PEG solution with different amount of colistin.

Typically, a 5% or 10% (w/w) DF-PEG solution was obtained by dissolving a certain amount of the DF-PEG (26.3 mg for 5% and 52.6 mg for 10%) into 500 μL PBS (1X) or PBS (1X) contains colistin. A syringe filter was used to sterilise the solution before biological test.

5.4.4 Methods

5.4.4.1 Rheology analysis

A series of hydrogels were prepared with different colistin loading amount to test their mechanical properties followed by the protocol described above. As a typical operation, glycol chitosan solution (280 μL, 3% in PBS) was spread on a parallel plate (diameter: 20 mm). Then, DF-PEG aqueous solution (100 μL, with different amount of colistin) was evenly added dropwise onto the glycol chitosan solution surface at 37°C. The storage moduli G' and loss moduli G'' were measured as a function of time for 45 min at constant frequency (1 Hz) and strain (5%) as the monitoring of the gel formation process (Figure 5.2). For the self-healing property of the colistin gel, the profile of G' and G'' values to different amplitude were tested subsequently. Amplitude oscillatory forces were changed from $\gamma = 250\%$ (last for 2 min) to 1% (last for 3 min) under the same frequency (1.0 Hz) at 37 ^{o}C. This process was repeated twice (Figure 5.3).

5.4.4.2 In vitro release

The release of the colistin-loaded hydrogel was conducted in 50 mL Eppendorf tubes using 20 mL buffers (PBS or CAMHB). The hydrogels were prepared according to the standard protocol *in situ* in the tubes. The solution A and B were sequentially added into the bottom of each tube and the tube was then immediately centrifuged at 5000 rpm at 37 ^{o}C using a horizontal centrifuge for 10 min to make sure the hydrogel can stick to the bottom of the tube. The hydrogels were washed gently with 6 mL PBS 3 times before the test. 20 mL buffer was then carefully introduced and the tubes were incubated in a shaking water bath at 37 ^{o}C. Samples (200 μL each time) were taken periodically for analysis. The hydrogels should stay at the bottom of the tubes during the test otherwise the surface area would change, leading a faster release. The release from PBS was analysed by RP-HPLC and the released from CAMHB was analysed by LC-MS using the method adapted from literature.[5]

To investigate the integration of the hydrogel network during the release, the experiment was conducted under a concentrated condition (size of gel is twice as the standard one with 10 mg colistin loading). The release was conducted in 5 mL PBS and samples were taken from the release solution for HPLC analysis (Figure 5.10).Even though the hydrogels were cross-linked through the dynamic imine bonds, the signal of DF-PEG cross-linker was hardly detectable and stayed low during the release. Thus, the main hydrogel structure stayed intact even after 2 days.

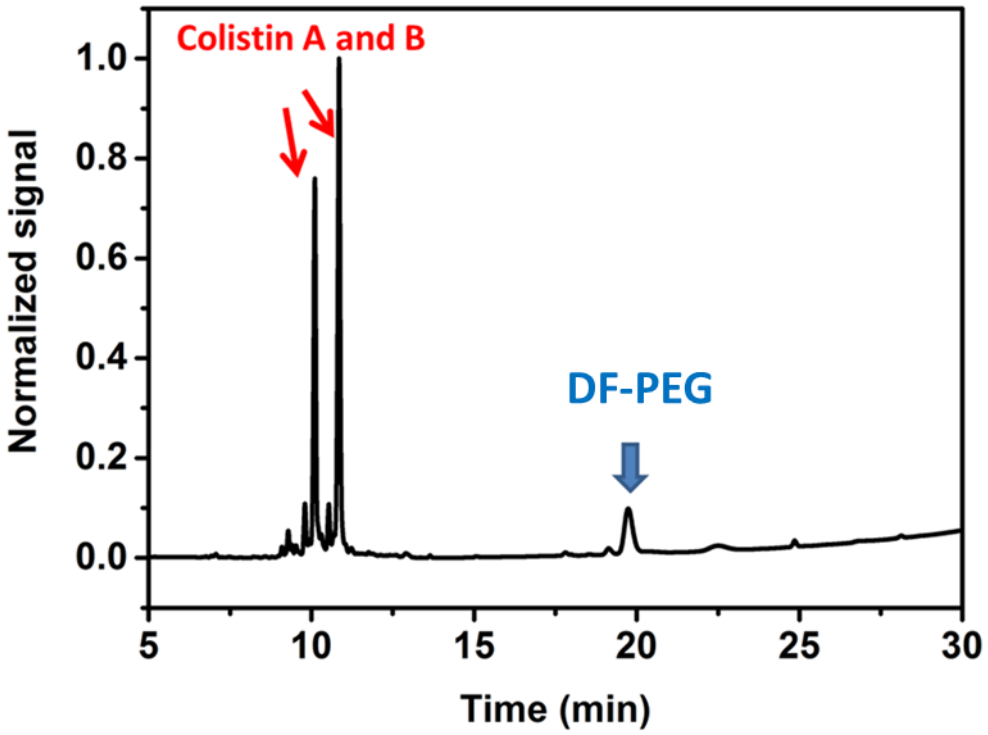

Figure 5.10 The typical HPLC trace of the released solution from PBS. (UV detector: λ = 225 nm).

5.4.4.3 Disk diffusion assay

Test isolates were matched to a 0.5 McFarland standard before being swabbed onto nutrient agar. The experimental materials (disks or hydrogels) were applied after allowing the surface of the agar to dry at ambient temperature for 20 minutes (agar side down). The agar plates were then inverted and incubated at 37 ºC for 24h and recorded using Plate Counter (ProtoCol3 Colony Counter, Don Whitley Scientific). Controls used were: Commercial colistin disk (contains 10 μg colistin) and blank disk (contains 10 μL F/S MQ H_2O). The hydrogels were prepared at a small scale based on the standard procedure described above (2.5 μL for solution B and 7 μL for solution A). The low-dosing and high-dosing colistin-loaded hydrogels contain 10 μg and 100 μg colistin, respectively.

5.4.4.4 Time kill test

The time-kill kinetics of the colistin-loaded hydrogels against *P. aeruginosa* 19147 n/m were examined according to the developed method.[6] For the hydrogel samples, the testing hydrogels were pre-prepared in a similar way as the ones from *in vitro* release. 20 mL of a logarithmic-phase broth culture of approximately 10^6 CFU/mL was carefully added into each tube at 37 ^oC without stirring up the hydrogels. The tubes were incubated in a shaking water bath at 37 ^oC. The samples were taken at 0 min, 30 min and 1, 2, 4, 6 and 24 h. Subcultures (50 μL sample) for viable counts were performed on nutrient agar (Oxoid) using WASP2 Spiral Plater (Don Whitley Scientific) and incubated at 37 °C for 24 h (48 h for plates with small colonies). Viable counts were determined by either manual counting or using ProtoCol3 Colony Counter (Don Whitley Scientific).

5.4.4.5 Animal 'burn' infection model test

Animal experiments were approved by the institutional animal ethics committee and animals were maintained in accordance with the criteria of the Australian code of practice for the care and use of animals for scientific purposes.

Neutropenic mice were rendered and maintained as previous report[7] and a burn wound with the size of 1.4 cm^2 was introduced onto each posterior thigh skin.[8, 9] The details of creating the burn wound are shown below. The neutropenic mice was then placed in an induction chamber for initiation of anesthesia. A mouse mask will be used for delivery of isoflurane for maintaining anesthesia afterwards. The hair on the dorsal skin of mice will be shaved and residual hair removed using Nair hair removal cream. Bupivacaine (Marcaine 0.5%, 0.1 mL, single dose, local anesthetics/analgesia) will be injected under the dorsal skin over the shoulder (i.e. the burn area) to prevent pain.

While the mouse is still under anesthesia, an iron bolt will be placed in boiling water (100 °C) for more than 5 min and then be taken out of the boiling water and quickly fixed on a see-saw like device. The touch pressure of the bolt on the skin will be controlled by moving the balance weight on the other side of the see-saw like device. The height of the bottom end of the heated bolt will be adjusted to touch (within 10 seconds after out of boiling water) the dorsal skin over the shoulder for 5 seconds to deliver a full-thickness skin burn. (Diameter = 1.4 cm, two-degree burn wound)

Burn infection was produced by swabbing 100 μL of an early-logarithmic-phase bacterial suspension (10^9 CFU/mL) of either *P. aeruginosa* ATCC 27853 or *P. aeruginosa* 19147 n/m) onto each wound. The colistin-loaded treatment was conducted 2 h after inoculation, by which time an infection was reproducibly established.

Single-dose pharmacodynamics studies were performed with neutropenic burn-infected mice after applying the colistin solution or colistin-loaded hydrogel (HG-10 was used here. 0.3 mg/wound colistin was used for *P. aeruginosa* ATCC 27853 and 1.5 mg/wound colistin for *P. aeruginosa* 19147 n/m) onto the wound. For the appliance of colistin-containing sample, a mouse was anaesthetised by gaseous isoflurane. Colistin solution was dropped to the surface of burn wound. The mouse was kept under anaesthesia for a while until the applied solution was absorbed by wound tissue. The colistin hydrogel samples were applied

The blank hydrogel was also tested for comparison. The animals were humanely killed at different time point (0h, 4h, and 24h), and the hydrogel was re-collected and weighed (Figure 5.7). The wound tissue samples were collected at the same time, destructed and mixed with 8 mL saline to obtain the homogenate. 50 μL homogenate was then plated on nutrient agar (Oxoid) using WASP2 Spiral Plater (Don Whitley

Scientific) and incubated at 37 °C for 24 h (48 h for plates with small colonies). Viable counts were determined by either manual counting or using ProtoCol3 Colony Counter (Don Whitley Scientific).

5.5 Reference

1. M. E. Falagas, I. I. Siempos, P. I. Rafailidis, I. P. Korbila, E. Ioannidou and A. Michalopoulos, *Respir. Med.*, 2009, **103**, 707-713.

2. Y. Zhang, L. Tao, S. Li and Y. Wei, *Biomacromolecules*, 2011, **12**, 2894-2901.

3. B. Yang, Y. Zhang, X. Zhang, L. Tao, S. Li and Y. Wei, *Polymer Chemistry*, 2012, **3**, 3235-3238.

4. T. C. Tseng, L. Tao, F. Y. Hsieh, Y. Wei, I. M. Chiu and S. h. Hsu, *Adv. Mater.*, 2015, **27**, 3518-3524.

5. S.-E. Cheah, J. B. Bulitta, J. Li and R. L. Nation, *J. Pharm. Biomed. Anal.*, 2014, **92**, 177-182.

6. P. J. Bergen, A. Forrest, J. B. Bulitta, B. T. Tsuji, H. E. Sidjabat, D. L. Paterson, J. Li and R. L. Nation, *Antimicrob. Agents Chemother.*, 2011, **55**, 5134-5142.

7. R. V. Dudhani, J. D. Turnidge, K. Coulthard, R. W. Milne, C. R. Rayner, J. Li and R. L. Nation, *Antimicrob. Agents Chemother.*, 2010, **54**, 1117-1124.

8. T. Dai, Y.-Y. Huang, S. K Sharma, J. T Hashmi, D. B Kurup and M. R Hamblin, *Recent Pat. Antiinfect. Drug Discov.*, 2010, **5**, 124-151.

9. E. J. Stevens, C. M. Ryan, J. S. Friedberg, R. L. Barnhill, M. L. Yarmush and R. G. Tompkins, *J. Burn Care Res.*, 1994, **15**, 232-235.

Chapter 6 *PEGylation Nystatin Prodrug for Antifungal Treatment*

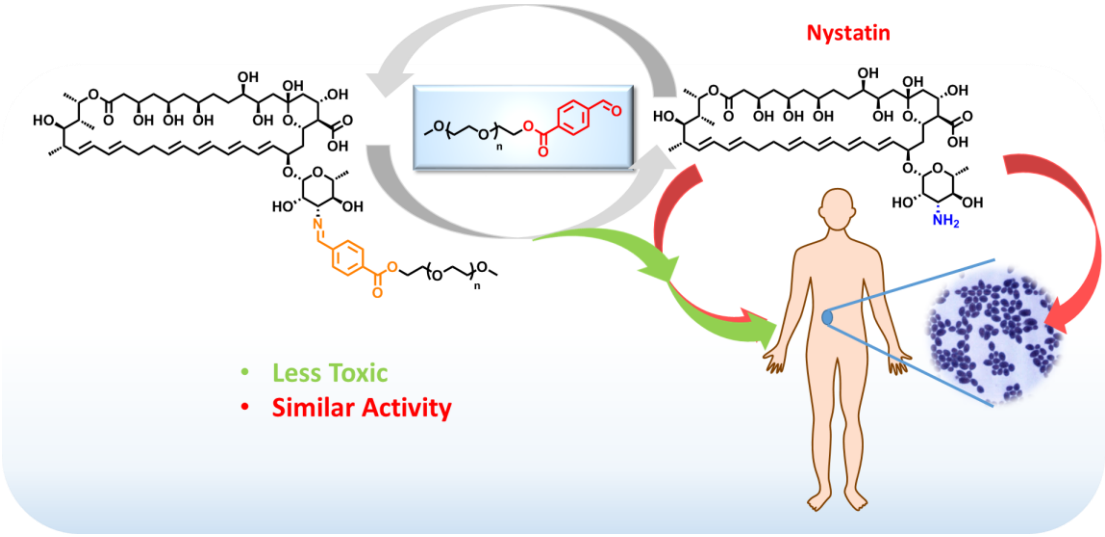

A PEGylated Nys conjugate has been prepared using an aldehyde modified mPEG (mPEG-FBA) via a labile imine bond. The conjugate can be obtained nearly quantitatively in organic media with or without the addition of dehydrating agent, Na_2SO_4. Due to the labile nature of the imine bond, this conjugate was prone to hydrolysis in the presence of water, which proved problematic for its purification. However, the solubility of Nys in the crude conjugate is much better than the native Nys, and more importantly, the conjugate showed an excellent antifungal performance against the human pathogen, Candida albicans, through the in vitro antifungal tests while the more stable PEGylated Nys obtained through reductive amination showed nearly no activity. More importantly, unlike the native Nys, this mPEG-FBA Nys conjugate showed no visible acute cytotoxicity towards the model mice cell, highlighting its potential as an alternative formulation for delivery of Nys for intravenous treatment of antifungal treatments.

6.1 Introduction

Nystatin (Nys) and amphotericin B (AmB) are important polyene antifungal agents used to combat many pathogenic fungi. Although potent, their use is limited due to concerns regarding their poor aqueous solubility and the potential toxicity to humans. Amongst all the fungal infections, systemic fungal infections are one of the most obnoxious and normally difficult to treat.[1] So far, only AmB has been formulated for intravenous treatment while no Nys formulation has been approved by the FDA.[2-4] Compared to AmB, Nys is less toxic and also exhibits activity against some fungi that are resistant to AmB.[3, 5, 6] Considering the increasing population of the drug-resistant human pathogens, the development of Nys for systemic application is timely and relevant.

As mentioned previously, prodrug formulations could potentially reduce the toxicity of Nys as well to improve its aqueous solubility. Due to the small size of Nys, the attachment of PEG *via* an irreversible linker could potentially hinder its antifungal activity. Therefore, a single-site PEGylation of Nys through a labile imine bond was developed in this work. With the help of an aldehyde functionalised mPEG (mPEG-FBA), a PEGylated Nys conjugate (mPEG-FBA Nys) targeting its sugar amine has been achieved. Through the formed water-sensitive imine bond, the conjugate can be stable in an anhydrous organic medium but is able to release the free native Nys in the presence of water. Thanks to the labile linker, this conjugate has been demonstrated to have a similar antifungal activity as native Nys against a fungal infection model, *Aspergillus carbonarius* CICC 41254. More importantly, it exhibited a much less toxicity to the human cells comparing to the native Nys and the mPEG/Nys mixture, suggesting its potential as a Nys formulation for systemic treatments.

6.2 Results and Discussion

6.2.1 Evaluation of the imine bond under physiological conditions through a small molecule model

Although demonstrated in chapter 2, the stability of the imine bond formation in aqueous media is unstable and prone to hydrolysis, depending on the aldehyde and amine. As the amine on nystatin is a glycosylamine which has a lower K_b[7] than other primary amines due to the hydroxyl groups on the neighbouring carbons, it behaves similar to the protein terminal amine. Therefore, it is possible to form a relatively stable imine bond with aldehydes at a lower pH, i.e., physiological pH. To test the feasibility of PEGylating Nys *via* dynamic imine chemistry, the mPEG-FBA, as described in chapter 2 was again used as a model aldehyde. Due to the complexity and the poor aqueous/organic solubility of Nys, a small molecule sugar amine model (glucosamine) was employed as a Nys model, mimicking the glycosylamine on Nys, to investigate the stabililty of the formed imine bond. The formation of a conjugate between the polymer and glucosamine were conducted at a 1 : 1 ratio in aqueous solution and the stability of the formed imine bond was measured at different pH values (pH = 4.2, 6.8, 7.4, 8.2, 10.2), monitored by ^{1}H-NMR (Figure 6.1).

The formation of the imine bond (δ = 8.45 ppm) was observed when the two compounds were mixed at neutral and basic condition through ^{1}H-NMR analysis along with the decrease of the aldehyde peaks of the starting material, mPEG-FBA (δ = 10.02 ppm). The formation of imine bond increased as a function of pH, consistent with the observation in chapter 2, suggesting the imine bond is more stable at a basic condition. The conversion of the imine bond was approximately 33% at physiological pH (pH =

7.4) indicating the imine bond can be formed under physiological condition although it is not as stable (Figure 6.1). Apart from the instability of imine bond in aqueous system, the low yield was also partially due to the formation of a hydrate peak (around $\delta = 6.07$ ppm, < 10% in all the pH range tested), which is mainly the product obtained through the reaction of mPEG-FBA with water. Interestingly, the hydrolysis of the ester bond linking the mPEG and FBA occurred at a basic pH, confirming by the split of the aldehyde and imine peak on the ^{1}H-NMR (Figure 6.11), suggesting degradability of mPEG-FBA.

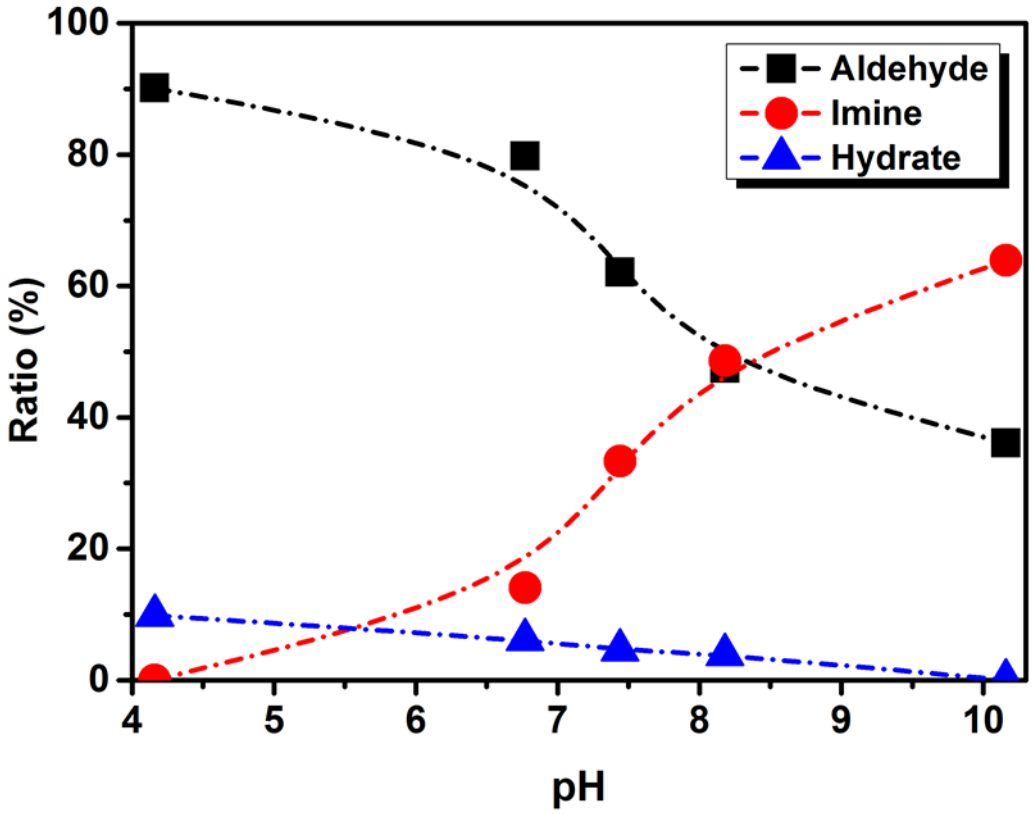

Figure 6.1 The ratio of the main products (unreacted aldehyde, formed imine, and side product acetal) obtained through mPEG-FBA and glucosamine in aqueous media under various pH conditions.

6.2.2 Conjugation of mPEG-FBA onto Nys through a labile imine bond

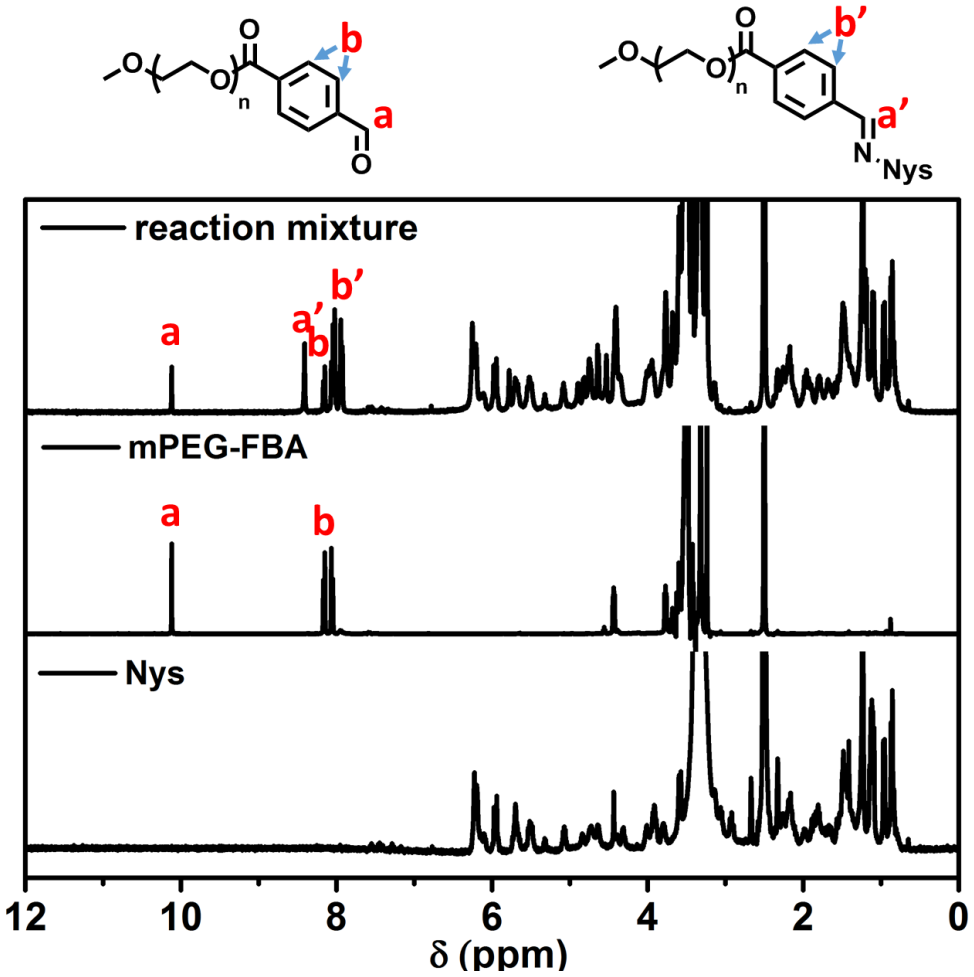

Figure 6.2 ^{1}H-NMR spectra showing the reaction between Nys and mPEG-FBA using d_6-DMSO as solvent.

As the imine bond is not very stable in the presence of water, the conjugation between Nys and mPEG-FBA was conducted in an organic solvent. Due to the poor solubility, Nys can only be dissolved above 1 mg/mL for reaction in a few polar solvents such as DMSO, DMF, and DMAc. Therefore, the conjugation of Nys and mPEG-FBA was performed in deuterated DMSO (d_6-DMSO) by mixing the two materials at 1:1 ratio for ^{1}H-NMR analysis (Figure 6.2). Since the imine formation generates one equivalent of water, a dehydrating agent, anhydrous Na_2SO_4, was also

added to effectively remove the water by-product as well as any remaining water in the solvent, to promote the formation of the imine bond. The imine proton (δ = 8.41 ppm) and the shifts of the aromatic ring protons affected by the imine bond can be observed while the aldehyde peak of mPEG-FBA (δ = 10.12 ppm) decreased, suggesting the formation of PEGylated Nys. Through the integration of the formed imine bond and the original aldehyde peak, it revealed > 75% of mPEG-FBA was conjugated onto Nys. However, due to the complex structure of Nys, more accurate calculation of the imine conversion was difficult to be obtained.

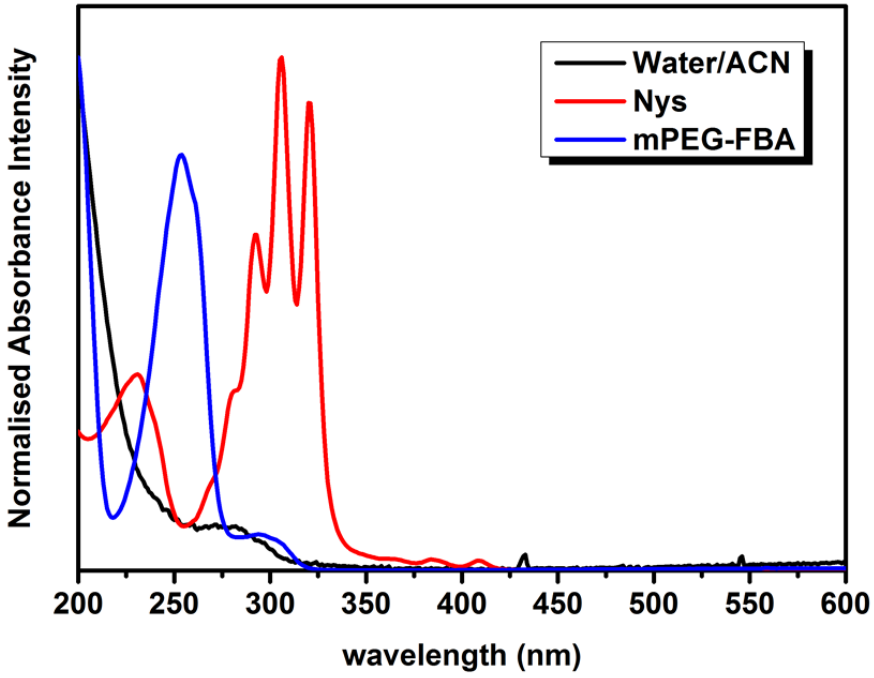

Figure 6.3 a) UV-Vis spectra of Nys and mPEG-FBA in a 50:50 water/ACN mixture ranging from 200-600 nm. The signals are normalised for comparison. The actually UV absorbance of the water/ACN solvent is below 0.2 Abs.

In order to further characterise the conjugate, HPLC analysis was also performed. As the imine bond is not as stable in standard HPLC eluents that containing TFA, a basic HPLC eluent using triethylamine (TEA) as an additive was selected for the detection of the formation of Nys-PEG conjugates. To choose the right wavelength

for HPLC detection, the ultraviolet–visible (UV-Vis) spectra of the starting materials were recorded in a water-acetonitrile (ACN) mixture (Figure 6.3). Although Nys has a strong and unique pattern of UV absorbance from 280 nm to 350 nm, mPEG-FBA has nearly no absorbance at that range. Therefore, to detect both starting materials, 260 nm was then used. As Nys is a fluorescent molecule, a fluorescence detector was also set for the detection of Nys and mPEG-FBA Nys conjugates. As shown in Figure 6.4, both Nys (~ 4.9 min) and mPEG-FBA (~ 7.5 min) peaks decreased and a new peak (~ 6.2 min) appeared between the starting materials from the HPLC. This peak can was detected in both UV and fluorescence detectors, suggesting the mPEG-FBA Nys conjugate was obtained with a high efficiency.

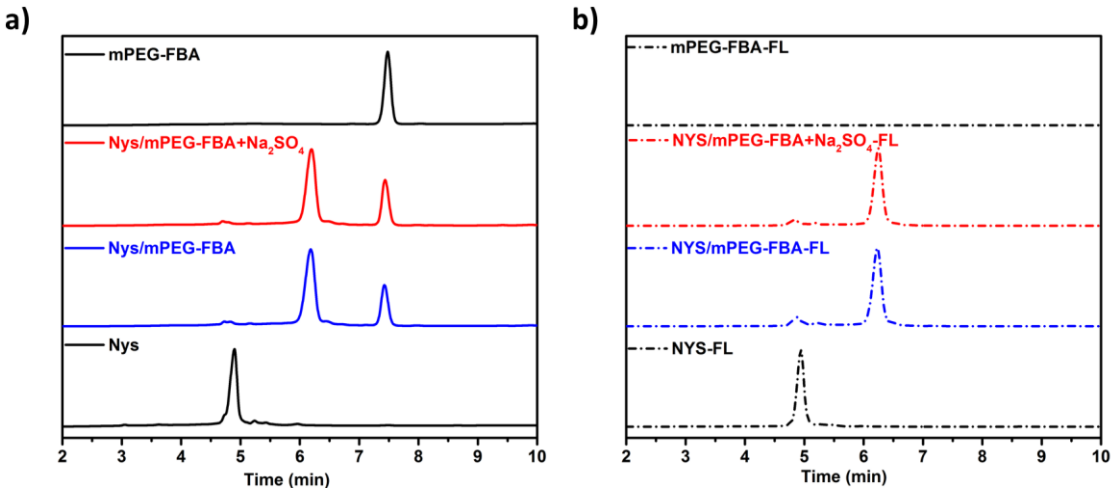

Figure 6.4 HPLC traces of the starting materials and their reaction mixture with or without Na_2SO_4, recorded by UV (a) and fluorescence (b) detector.

To observe the necessity of the dehydrating agent, a comparison of the reaction with and without Na_2SO_4 was also conducted. Surprisingly, no visible difference was observed over the reaction time scale through HPLC analysis (Figure 6.4), suggesting the imine bond is stable in an organic medium in the presence of a small amounts of water.

A small peak between 5-6 min, attributed to Nys was observed in both UV and fluorescence traces. To test if the reaction could be promoted to reach higher conversions, the stoichiometry of mPEG-FBA was increased (2 or 4 equivalents) (Figure 6.5). However, apart from the increased signal generated from the addition of more mPEG-FBA starting material, no significant change was observed through both UV and fluorescence detectors. This indicated that the conjugation reaction was complete by mixing both starting materials at the same ratio and the remained peak could be the amine-lacking impurities from the Nys.

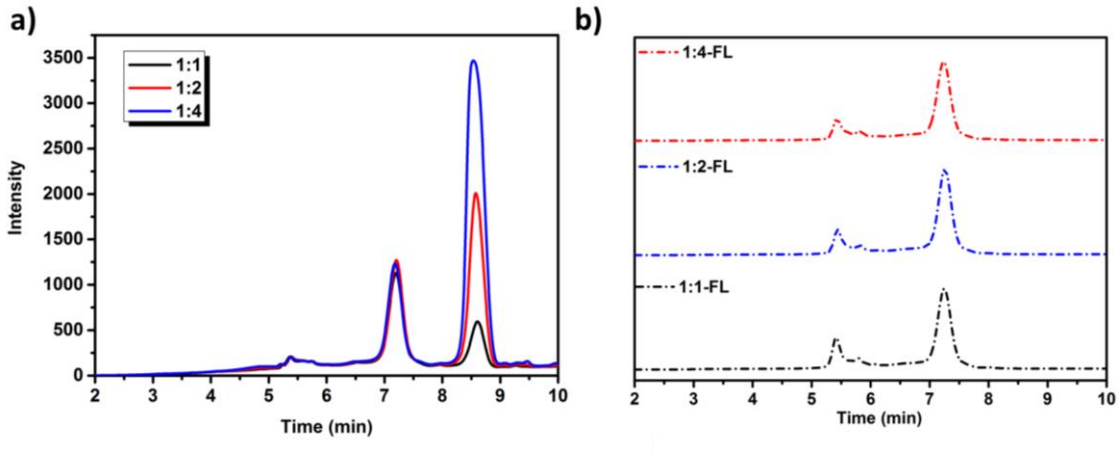

Figure 6.5 The a) UV and b) fluorescence traces through the HPLC analysis from the reactions between Nys and mPEG-FBA with different ratios.

To remove the excess of mPEG-FBA and other impurities, PREP HPLC was conducted using a multiple wavelength UV detector. Both 260 nm and 300 nm were used for the identification of the starting materials and the PEGylated conjugate. After the collection of the conjugation product from 10.2-11.4 min of the HPLC trace, the product was injected directly into the system to analyse its purity. Unfortunately, instead of a single peak of the conjugate, three peaks which were assigned to both starting materials and the conjugate were observed and the ratio of the conjugates was much lower than the reaction mixture (Figure 6.6). This suggests that the imine bond

was hydrolysed gradually in the water/ACN mixture with the TEA as additive during the purification process even though a single peak was observed during the analysis. Thus, the conjugate cannot be purified through this method.

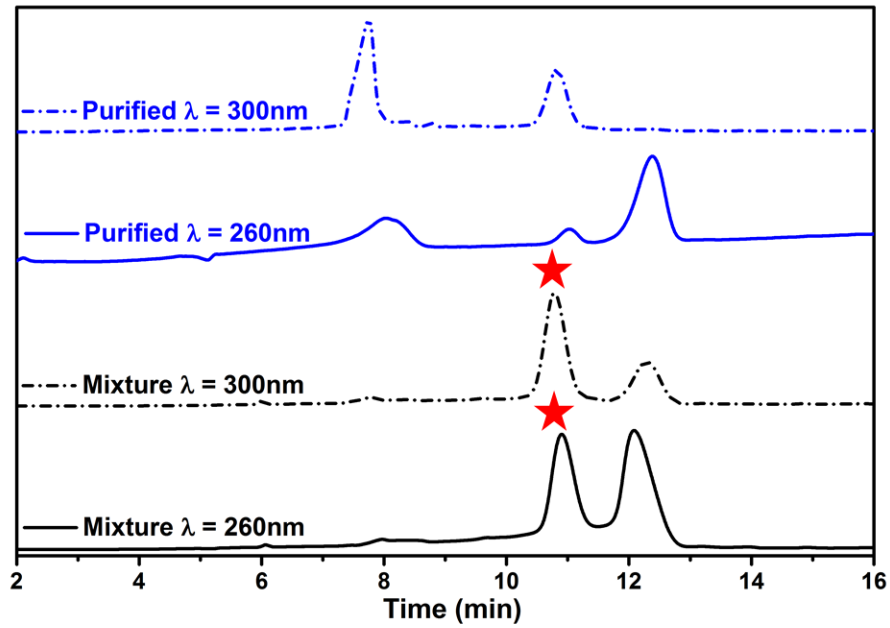

Figure 6.6 UV traces of the reaction mixture (black) and the collected peak (blue) from the PREP HPLC (λ = 260 nm and 300 nm). The collected peak from the reaction mixture is highlighted with a red star.

Instead of further purification, the reaction mixture was then precipitated directly and washed with diethyl ether to remove the reaction solvent. However, it was found that the product had hydrolysed slightly after the precipitation as an increase in the Nys peak (~ 8.0 min from λ = 260 nm) was observed in the HPLC traces (Figure 6.7). Although no further evidence has been obtained to date, it was considered that the trace of water presented in the atmosphere or in the solvent used for precipitation was the reason for the hydrolysis.

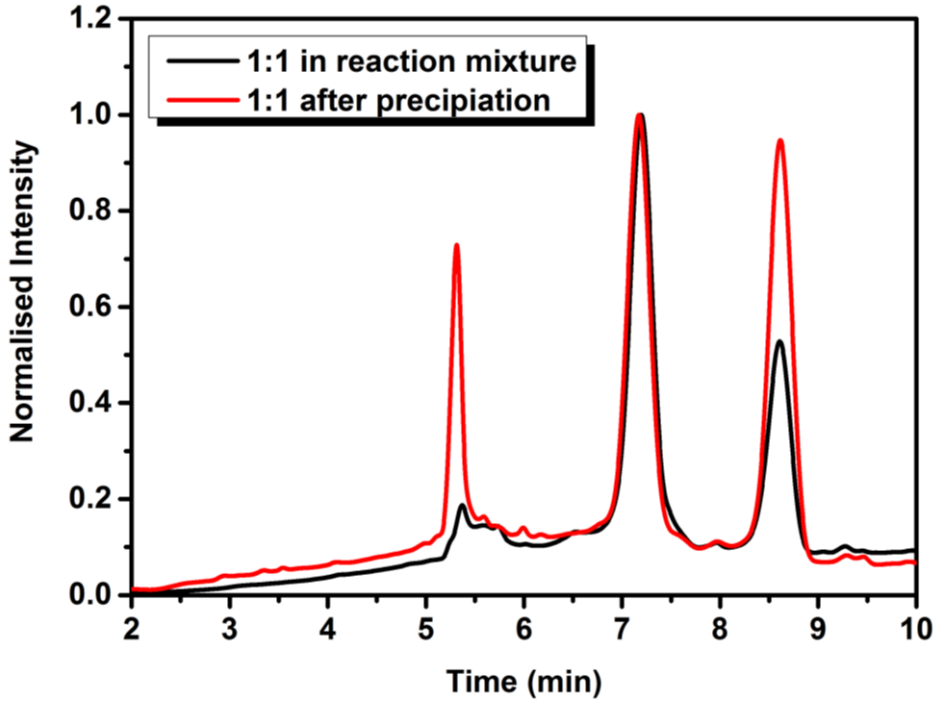

Figure 6.7 HPLC traces of the reaction mixture (black) and the precipitate (red).

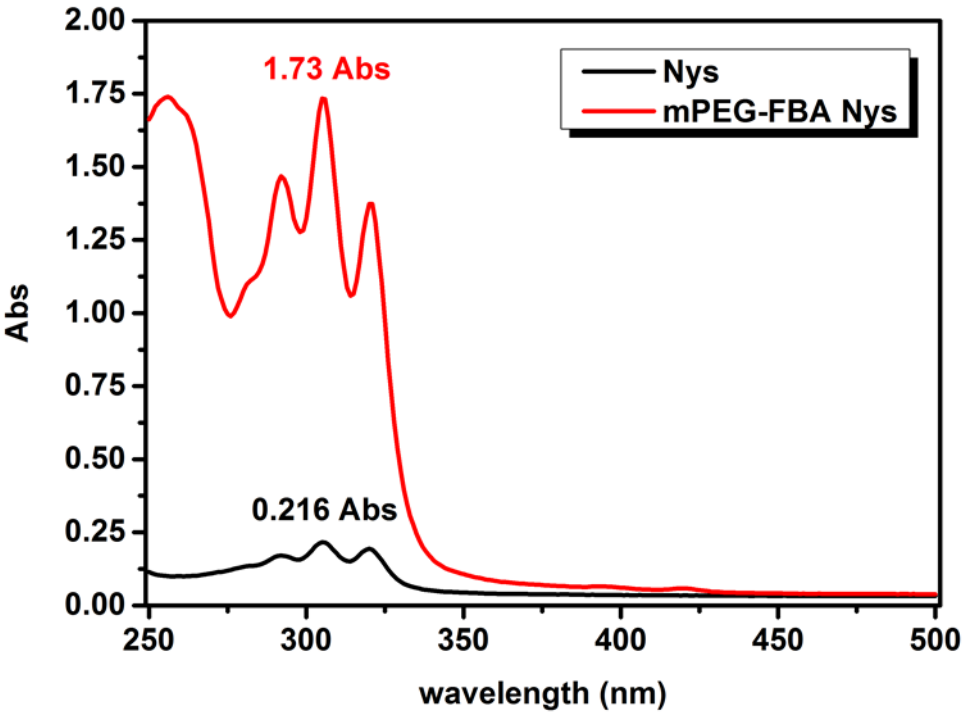

Figure 6.8 The difference between the UV absorbance of Nys and mPEG-Nys in PBS (1X) after 1 day.

The solubility of the mPEG-Nys conjugate was then tested *via* a UV-Vis analysis as Nys has a unique UV absorbance pattern at a range of 280 - 350 nm. Although the precipitation of Nys was observed over the time due to the labile imine

linkage, the typical UV absorbance peak (λ = 305 nm) belonging to Nys from the mPEG-FBA Nys conjugate in water after a day was still 8 times larger than the native Nys, indicating the attachment of mPEG-FBA can provide a better solubility to Nys (Figure 6.8).

An irreversibly modified conjugate was also synthesized by reductive amination in the presence of excess reducing agent ($NaBH_3CN$) for comparison. MeOH was used as the solvent since it guaranteed a high reductive activity of $NaBH_3CN$. Due to the poor solubility of Nys, the formation of the reduced conjugate did not reach full conversion when mixing the starting materials at near 1:1 ratio (Figure 6.9).

As no further procedures could be made to improve the purity of the labile imine PEGylated product and the purities between the imine product and its reduced conjugate were similar, both products were used and evaluated for biological tests directly.

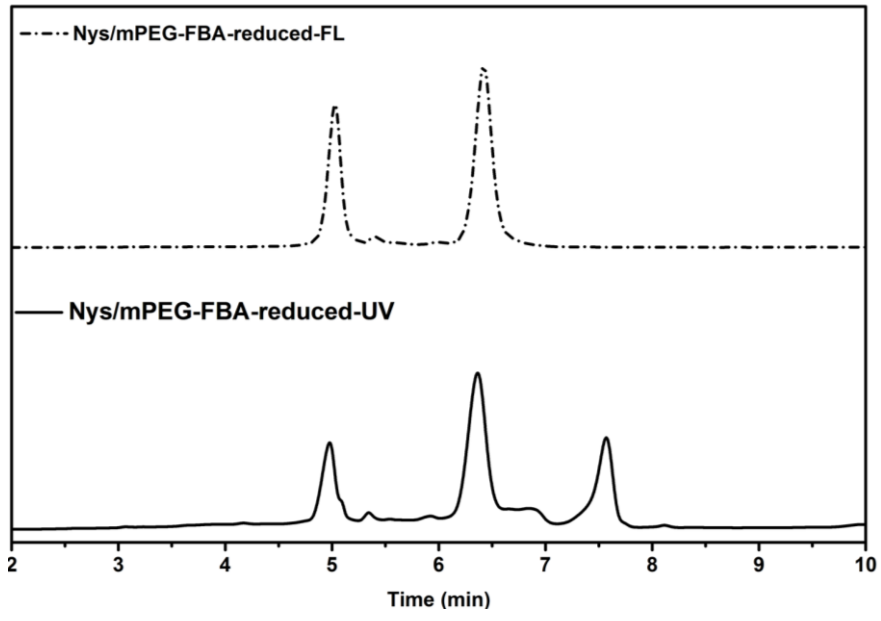

Figure 6.9 HPLC traces of the reduced PEGylated Nys. Solid line: UV trace and dotted line: fluorescence trace.

6.2.3 The antifungal activity and the potential cytotoxicity of the labile PEGylated Nys (mPEG-FBA Nys)

In order to evaluate the antifungal activity of the labile mPEG-FBA Nys conjugate, the minimum inhibitory concentration (MIC) and the minimum fungicidal concentration (MFC) assays were performed to determine its fungistatic and fungicidal endpoints. The reduced PEGylated Nys, the starting materials and a mixture of Nys and mPEG at a ratio of 1:1 were also tested for comparison. As *Candida albicans* is a human pathogen, *Aspergillus carbonarius* CICC 41254 was selected as a model for the tests.

Both the labile mPEG-FBA Nys conjugate and the Nys/mPEG mixture showed a comparable antifungal activity to native Nys while neither the reduced PEG-Nys conjugate nor mPEG-FBA showed a reliable antifungal activity against *Aspergillus carbonarius* CICC 41254 (Table 6.1). The reduced PEG-Nys conjugate only showed some inhibition towards *Aspergillus carbonarius* CICC 41254 at 128 mg/L, which may be attributed to the remaining Nys impurity in the samples. This indicated the irreversible PEGylation of Nys would hinder the function of Nys, thus, the labile linkage between PEG and Nys is necessary to maintain the antifungal activity of Nys.

Table 6.1 The MIC and MFC test of the labile mPEG-FBA-Nys conjugate, its reduced analogue and starting mateials.

Sample name	Nys	mPEG-FBA Nys	mPEG/Nys	Reduced mPEG-FBA Nys	mPEG-FBA
MIC (mg/L)	≤ 2	≤ 2	≤ 2	128	> 512
MFC (mg/L)	≤ 2	≤ 2	≤ 2	128	> 512

Although labile ligation can effectively release Nys *in vitro*, the concern of its potential toxicity has also been raised because the resulting conjugate would hydrolyse very rapidly and therefore not significantly reduce the toxicity of Nys. To investigate

the acute cytotoxicity of the mPEG-FBA Nys conjugate, a cytotoxicity experiment was then conducted using a mouse fibroblast cell line, L929, as a model. The cell viability was recorded through a cell count kit-8 (CCK-8) assay and the cytotoxicity of each compound was represented by the lethal concentration of 20% cell death (LC_{20}). It turned out the mPEG-FBA Nys conjugate showed much less toxicity (LC_{20} > 500 μg/mL) towards the L929 cell while both Nys and the Nys/mPEG mixture showed a significant toxicity at the same concentration (Figure 6.10).

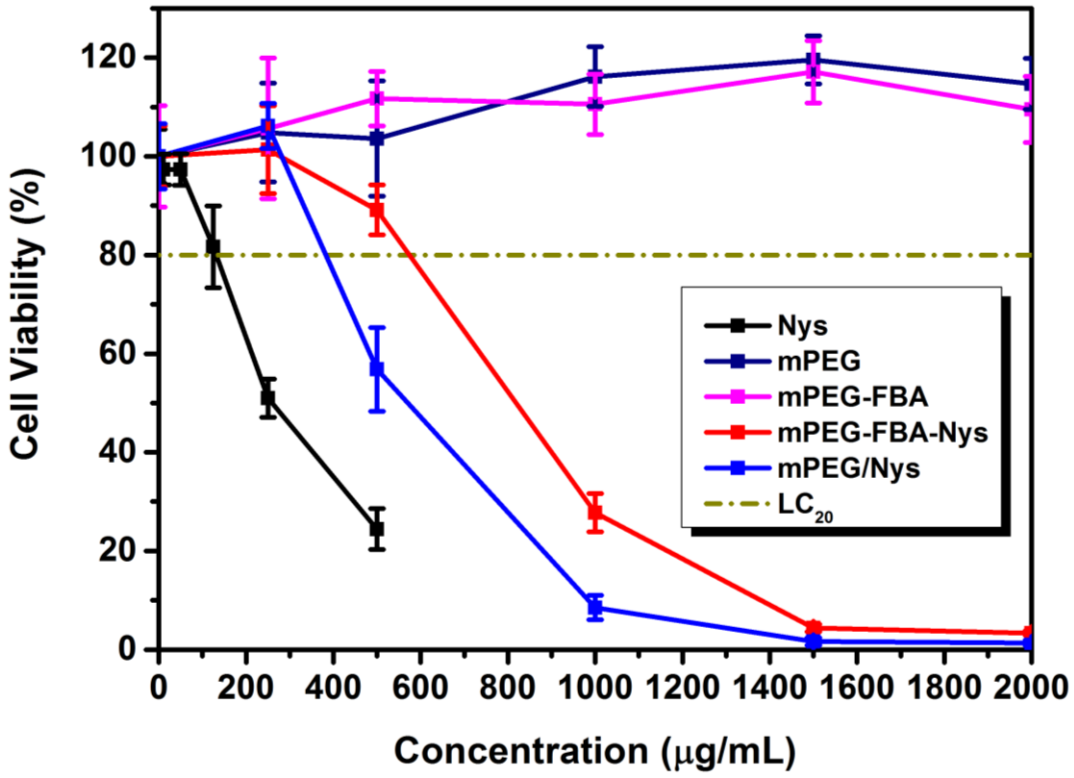

Figure 6.10 The acute cytotoxicity of Nys, mPEG-FBA Nys conjugate and mPEG/Nys 1:1 mixture.

It can be estimated that the LC_{20} of Nys is around 125 μg/mL and the Nys/mPEG mixture is around 380 μg/mL. Considering there is only 1/3 of the mass belonging to Nys, it suggested the mPEG itself cannot reduce the toxicity of Nys, implying even though the linkage between Nys and mPEG-FBA is labile under physiological condition, the FBA unit on mPEG is important to reduce the acute cytotoxicity of Nys. As the poor solubility of Nys can act as the hydrophobic part when coupled to the

hydrophilic mPEG-FBA, the surfactant structure of mPEG-FBA Nys conjugate is likely to cause self-assembly in aqueous medium. This would limit the exposure of the labile imine linkage to the aqueous media and encapsulate unbound Nys remaining in the crude reaction mixture, leading to the reduction of the toxicity of Nys.

6.3 Conclusions

Thus far, an mPEG-FBA modified Nys conjugate was successfully synthesized through a dynamic imine bond. A small molecule model suggested the imine bond could form, although with limited stability, at physiological pH. The mPEG-FBA Nys conjugate was relatively stable in an anhydrous organic medium and can be characterised using HPLC with the help of a basic additive, TEA. Although the purification of this mPEG-FBA Nys conjugate was difficult due to the labile imine bond, it greatly improved the solubility of Nys. Furthermore, an excellent antifungal performance was found from the mPEG-FBA Nys conjugate that is close to the native Nys *via* the *in vitro* antifungal analysis against *Aspergillus carbonarius* compared to its analogue from reductive amination. Through the acute cytotoxicity experiments, it has proven that the FBA unit is crucial for the conjugate to reduce the overall toxicity of Nys. Although further evaluation is required to evaluate its toxicity to human cells, the mPEG-FBA-Nys conjugate with a labile imine linkage can increase the solubility for Nys and can be a potential formulation for Nys intravenous treatment.

6.4 Experimental

6.4.1 Materials

6.4.1.1 Chemicals

All chemicals were purchased from Sigma-Aldrich and used directly unless otherwise stated. HPLC solvents are obtained from VWR international, LLC. The synthesis and characterisation of mPEG-FBA was described in chapter 2.

6.4.2 Cell line and fungal species

Cell line: L929 fibroblast-like cell from mouse was used for the cytotoxicity tests. Cell culture was maintained in a 37ºC incubator with 5% CO_2, L929 cells was cultured in RPMI 1640 medium included 10% fetal bovine serum (FBS) and 1% penicillin and streptomycin. Culture medium was changed every one or two days.

Fungus strain: *Aspergillus carbonarius* CICC 41254 (Institute of Microbiology Chinese Academy of Sciences, CICC) was used as a fungal infection model in this study. The culture of the isolates and the related MIC and MFC tests against *Aspergillus carbonarius* CICC 41254 were conducted following the developed precedure. [8]

6.4.3 Instruments

6.4.3.1 NMR

^{1}H-NMR spectra were recorded on Bruker HD 400 spectrometers and referenced relative to deuterated solvent shifts using deuterated solvents obtained from Aldrich.

6.4.3.2 HPLC

HPLC analysis was acquired from the Agilent 1260 infinity series stack equipped with an Agilent 1260 binary pump and a degasser. Samples (10-70 µL) were injected using Agilent 1260 auto-sampler. The HPLC was fitted with a ZORBAX Eclipse Plus C_{18} (4.6 x 100 mm, 3.5 µm). Detection was achieved using an Agilent 1260 variable wavelength detector monitoring at 260 nm and an Agilent 1260 fluorescence detector with fluorescence detection at λ_{ex} = 320 nm; λ_{em} = 410 nm.

The mobile phase condition is as follows.

Mobile phase A: 100% water, 0.2 % TEA;

Mobile phase B: 100% ACN, 0.2% TEA.

HPLC water and 'far UV' HPLC ACN were used as solvents and HPLC TEA was used as additive.

The standard analysis method is as followed: 0-10 min 20%-60% B; 10-12 min 60% B; 12-14 min 60-20% B; 14-30 min 20% B. The total flow rate was set to 1.0 mL/min and the temperature for the column is set to 25 ^{o}C.

For the separation, collection, and analysis of PEGylated Nys peak, a PREP HPLC system (Agilent 1260 infinity series stack) equipped with a 1260 Quat Pump VL, a degasser and a fraction collector (FC-AS) was used. Samples were injected using Agilent 1260 auto-sampler with a 900 µL injection volume. The HPLC was fitted with a ZORBAX Eclipse Plus C_{18} (4.6 x 100 mm, 3.5 µm). Detection was achieved using an Agilent 1260 variable wavelength detector connected in series with UV detection monitored at 260 and 300 nm.

The method for purification is as followed: 0-20 min 20%-60% B; 20-25 min 60% B; 25-26 min 60-20% B; 26-35 min 20% B. The total flow rate was set to 1.0 mL/min and the temperature for the column is set to 25 ºC.

6.4.3.3 Ultraviolet-visible (UV-Vis) spectroscopy

The UV-Vis absorption spectra of Nys and mPEG-FBA were measured on a Perkin Elmer Lambda-35 UV/VIS spectrometer using 1 cm path length quartz cuvettes using 1:1 water-ACN as a reference and solvent.

6.4.4 Synthesis

6.4.4.1 Synthesis of mPEG-FBA Nys conjugate

9.2 mg of colistin (10 µmol, 1 equiv.) and 20 mg of mPEG-FBA (10 µmol, 1 equiv.) were dissolved with 1 mL of solvent (d_6-DMSO or DMF or DMAc) in a 2 mL glass vial with or without the addition of the dehydrating agent (Na_2SO_4, 140 mg). The vial was then sealed and left on a roller mixer (SRT9, Stuart) for 24 h. The crude was then precipitated from 40 mL diethyl ether. The precipitate was collected through centrifugation and washed with another 40 mL diethyl ether to get the product. The NMR, HPLC and UV characterisations of the conjugates were shown in Figure 6.2, 6.4-6.8.

6.4.4.2 Synthesis of reduced mPEG-FBA Nys conjugate

9.2 mg of colistin (10 µmol, 1 equiv.) and 20 mg of mPEG-FBA (10 µmol, 1 equiv.) were added into a 7 mL glass vial along with 5 mL of MeOH. After 5-10 min vortexing, 30 mg $NaBH_3CN$ (477 µmol, 47.7 equiv.) was dissolved in 1 mL of MeOH and added into the system. The reaction was vortexed for another 5-10 min and the

vial was then sealed and left on a roller mixer (SRT9, Stuart) for 24 h. The product was obtained through the same procedure as mPEG-FBA Nys conjugate. The HPLC analysis of the conjugate (6-7 min) was shown in Figure 6.9.

6.4.5 Methods

6.4.5.1 Small molecule model for ^{1}H-NMR analysis

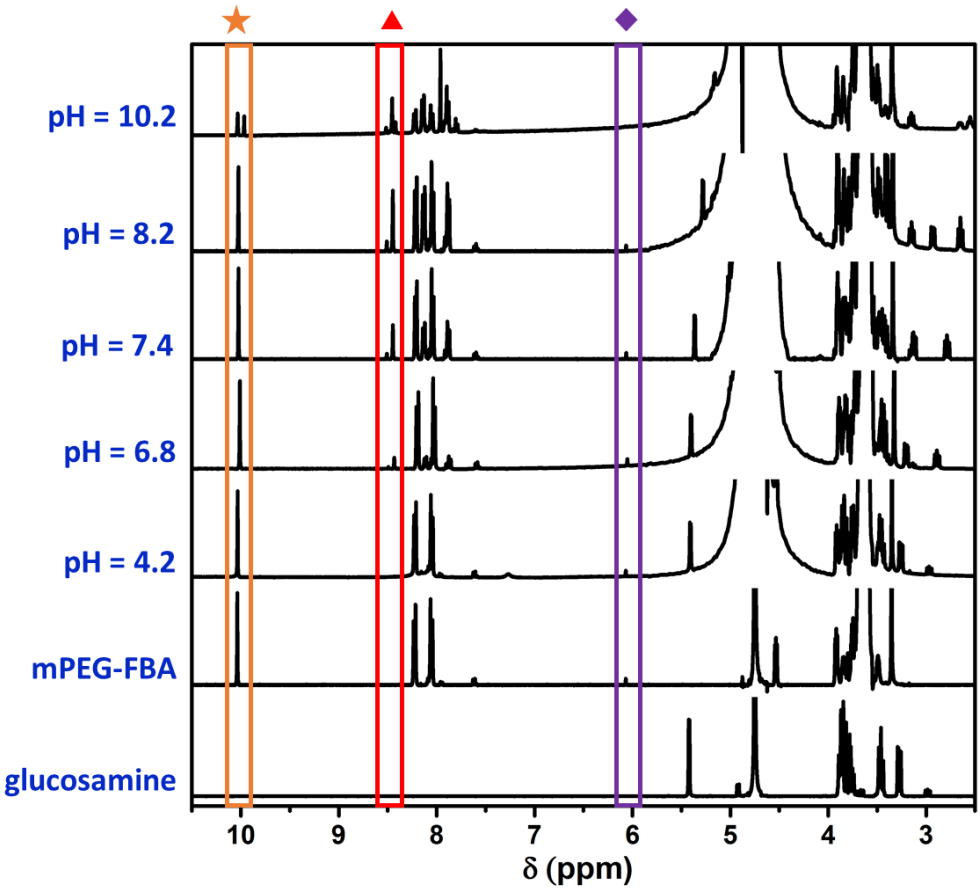

Figure 6.11 ^{1}H-NMR of the mixture of mPEG-FBA and glucosamine at a ratio of 1:1 at various pH and the starting materials in D_2O. The peaks belonged to aldehyde, imine and hydrate product are labled with ★, ▲, and ♦, repectively.

The samples for ^{1}H-NMR analysis were prepared as followed (Figure 6.11). mPEG-FBA (160 mg, 0.08 mmol) and glucosamine·HCl (43 mg, 0.2 mmol) were dissolved in 1 mL D_2O, respectively. 125 µL mPEG-FBA solution and 50 µL

glucosamine solution was mixed together and with 200 μL D_2O adjusted with 200 μL various buffers to desired pH. The pH was tested by a pH probe (Product Code: 10237293, Thermo Scientific Orion) before analysed by ^{1}H-NMR.

6.4.5.2 Cell viability assay

As modified from a developed method,[9] the cytotoxicity of the labile PEGylated Nys conjugate to L929 cells was evaluated. Nys, mPEG-FBA and the mixture of 1:1 Nys and mPEG were also tested for comparison. The cell viability was analysed through CCK-8 assay. Briefly, 100 μL cell suspension were seeded in a 96-well plate at a density of ~ 10^5 cells/mL. After the cell attachment, cells were washed with PBS (1X) and culture with different concentration of each sample in culture media at 37 ºC for 1 h. Due to the poor solubility of Nys, 2% DMSO was added into all culture media to improve the sample solubility. Each well was then washed three times with PBS and incubated with 100 μL culture medium with 10% CCK-8 solution for 2 h. After the incubation, the UV absorbance of each sample was recorded with a microplate reader (VICTORTM X3 PerkinElmer 2030 Multilabel Plate Reader) with a UV wavelength of 450 nm. The cell viability was calculated by comparing to the positive control (cells in pure culture medium, 100% viability) and negative control (pure culture medium without cells, 0% viability). The results were showed as mean ± standard deviation.

6.4.5.3 Aqueous solubility of Nys and mPEG-Nys conjugate determined by UV-Vis

3 mg of mPEG-Nys conjugate and 1 mg of Nys was dissolved in a 2 mL glass vial with 1 mL of HPLC grade water, respectively. The samples were incubated at ambient temperature on a roller mixer (SRT9, Stuart) for 24 h before being centrifuged

at 10000 rpm for 30 min to remove the unsolubilised Nys. The supernatants were then diluted 10 times with PBS 1X. 200 µL of each sample was added into a 96-well plate and the UV scan (λ = 250 – 500 nm) of each sample was performed by a microplate reader (Synergy HTX Multi-Mode Reader) (Figure 6.8).

6.5 References

1. C.-C. Lai, C.-K. Tan, Y.-T. Huang, P.-L. Shao and P.-R. Hsueh, *J. Infect. Chemother.*, 2008, **14**, 77-85.

2. S. Hartsel and J. Bolard, *Trends Pharmacol. Sci.*, 1996, **17**, 445-449.

3. E. M. Johnson, J. O. Ojwang, A. Szekely, T. L. Wallace and D. W. Warnock, *Antimicrob. Agents Chemother.*, 1998, **42**, 1412-1416.

4. M. Bondaryk, W. Kurzątkowski and M. Staniszewska, *Postepy Dermatol. Alergol.*, 2013, **30**, 293-301.

5. M. A. Pfaller, R. N. Jones, S. A. Messer, M. B. Edmond and R. P. Wenzel, *Diagn. Microbiol. Infect. Dis.*, 1998, **31**, 327-332.

6. D. W. Denning and P. Warn, *Antimicrob. Agents Chemother.*, 1999, **43**, 2592-2599.

7. M. Sinnott, *Carbohydrate chemistry and biochemistry: structure and mechanism*, Royal Society of Chemistry, 2007.

8. A. J. Carrillo-Muñoz, G. Quindós, C. Tur, M. T. Ruesga, Y. Miranda, O. d. Valle, P. A. Cossum and T. L. Wallace, *J. Antimicrob. Chemother.*, 1999, **44**, 397-401.

9. H. Zheng and K. L. Audus, *Int. J. Pharm.*, 1994, **101**, 121-126.

Chapter 7 *Micellar Formulation for the Solubility Improvement of Nystatin and Its Potential Target Delivery*

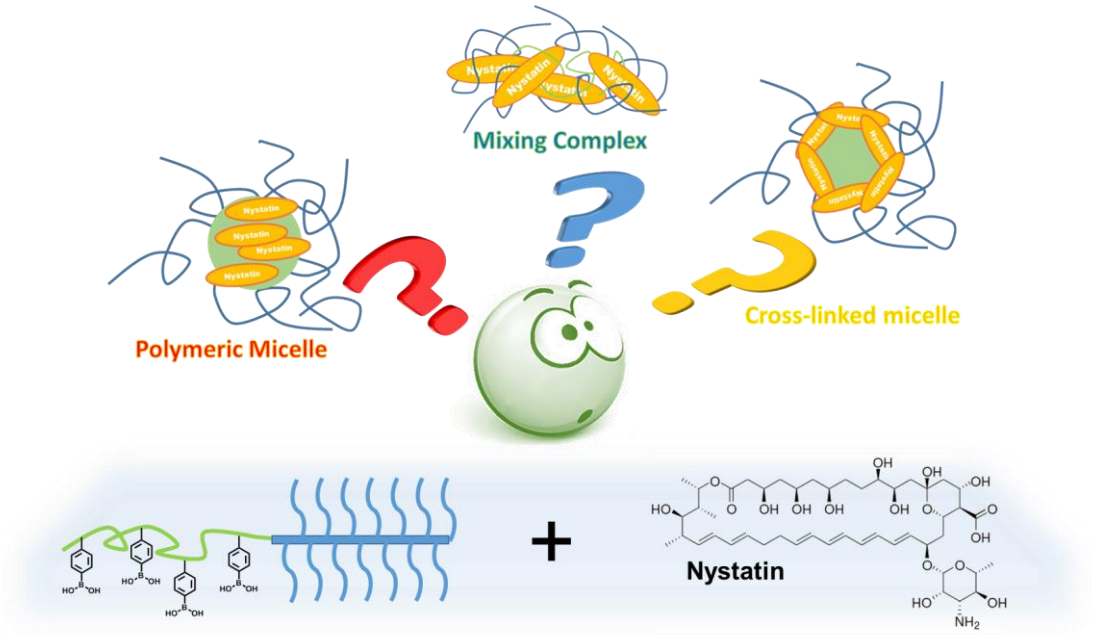

In order to improve the aqueous solubility of Nys for intravenous antifungal applications, amphiphilic block copolymers ($PB_{acid}A_{20}PPEGA_x$) containing boronic acid units on the side chains have been successfully synthesized via CP-LRP using a pinacol protected PBA containing acrylate monomer ($B_{pin}A$) and a biocompatible monomer $PEGA_{480}$. Comparing to the block copolymer analogues without the boronic acid groups generating from BzA monomer ($PBzA_{20}PPEGA_x$), the $PB_{acid}A_{20}PPEGA_x$ can greatly improve the Nys solubility (2.4-9.8 times), showing their potential as a Nys carrier. To develop an applicable Nys delivery system, the ongoing work will be focused on the investigation of the self-assembly and their bio-performances of each polymer in the presence/absence of Nys.

7.1 Introduction

Although a prodrug formulation has been designed and demonstrated to have some potential to increase the solubility of nystatin (Nys), reduce toxicity and maintain activity in chapter 6, the incomplete modification and the difficulties in isolating pure products remain a concern for its application. Furthermore, the reason for the reduced toxicity using Nys 'prodrug' seems to be attributed to the self-assembly of the polymer-Nys complex, indicating the Nys solubility can be in theory improved and the toxicity of Nys can be reduced by the encapsulation of Nys into the right delivery system. Thus, to investigate this concept, the development of a suitable delivery system through encapsulation with targeted covalent attachement of Nys was attempted as discussed in this chapter as the chemical attachment of Nys onto a delivery system can provide a more stable and reliable performance comparing to the physical encapsulation.

As described in chapter 1, the hydroxyl groups on Nys can be the potential modification sites for boronic acid containing compounds. The amphiphilic polymers that contains boronic acid groups can be a possible tool to improve the aqueous solubility of Nys through the formation of a polymer-Nys complex with Nys *via* dynamic boronate ester bonds. The formed boronate esters can be responsive not only to pH change but also to oxidation stress, which may be useful for the target antifungal treatments and has potential to reduce the oxidation stress produced during Nys administration.

Thus, to investigate the possibility of the utilisation of the boronate linkage to covalently attach Nys, a small molecular model was initially tested. After that, the development and synthesis of boronic acid containing amphiphilic polymers was

targeted. With the help of copper-mediated photoinduced living radical polymerisation (CP-LRP), polymers with boronic acid on the side chains have been obtained with controlled molecular weight and narrow dispersities after optimisation. The obtained polymers were further used to test the binding with Nys *via* a UV study, demonstrating the possibility of improving solubility of Nys through the formation of boronate ester bonds. Although a slow response rate was found, the polymer-Nys complex showed a potential responsiveness towards the pH change of the environment.

7.2 Results and Discussion

7.2.1 A small molecule model for the boronate linker through the diol on Nys

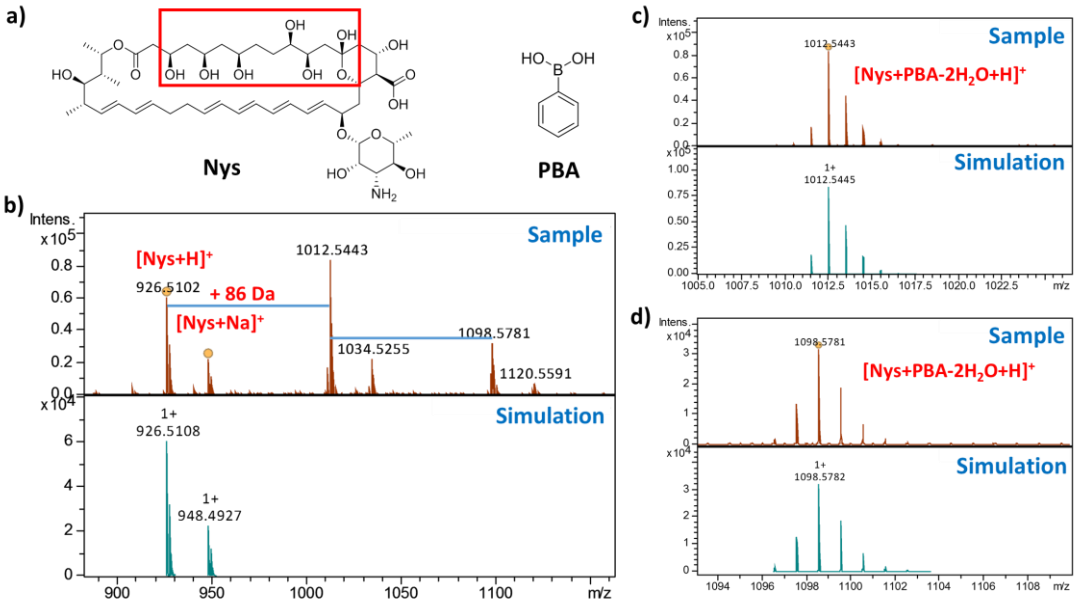

Figure 7.1 a) The chemical structure of Nys (left) and PBA (right). The possible conjugation sites for PBA are highlighted with a red rectangle. b-e) ESI-MS data of the three Nys containing products and their mass simulation found in the reaction mixture of Nys with PBA.

A small molecule model, phenylboronic acid (PBA), was initially reacted with Nys in an organic solvent (DMF) to test the feasibility of the boronate ester linkage formation. Through ESI-MS analysis, two Nys containing products were found from the reaction mixture in addition to unreacted Nys. The mass of each product along with the isotopic pattern indicated that one was the mono adduct and the other a double adduct of PBA on Nys (Figure 7.1). In order to confirm the formation of the PBA adducts and to identify the modification site(s) of the PBA, a further tandem mass spectrometry (ESI-MS/MS) was performed on the products (details of analysis please see Appendix). Indeed it as observed that the two PBA molecules can be attached on the 1,2-diol on position 3, 4 and/or 1,3-diol between positions 1, 3; 7, 9; or 9, 11 (highlighted in Figure 7.1a). The possibility of two molecules of PBA binding to Nys suggests potential use of Nys as a cross-linker for the polymer containing multiple boronic acid side chains.

7.2.2 Synthesis of the block copolymer containing PBA units on the side chains

7.2.2.1 Synthesis of the monomer containing PBA unit for polymerisation

In order to obtain the desired polymer, 4-(hydroxymethyl)phenylboronic acid (HBA) was used as the starting material for the synthesis of the PBA containing monomer suitable for polymerisation (Figure 7.2). The boronic acid group on HBA was protected using pinacol to improve the solubility of the PBA unit in organic solvents as well as to minimise the potential side reaction caused by the boronic acid during the polymerisation. The pinacol protected PBA containing acrylate monomer

($B_{pin}A$) was obtained through the substitution of hydroxyl group on HBA using acryloyl chloride in the presence of TEA. The peaks belonging to pinacol (g in Figure 7.2b and g, i in Figure 7.2c) and the acrylate unit (c, d, e in Figure 7.2b and d, e in Figure 7.2c) have been successfully introduced onto the HBA as shown by ^{1}H-NMR and ^{13}C-NMR. Although the carbon adjacent to the boron atom is not detectable from ^{13}C-NMR due to the splitting by the boron atom, a sharp boron signal obtained from ^{11}B-NMR suggested the retention of the boron atom after the pinacol protection and the acrylate formation. A strong absorbance at 1724 cm^{-1} which belongs to the carbonyl stretch of the ester bond can clearly be found by FTIR, further confirming the formation of acrylate.

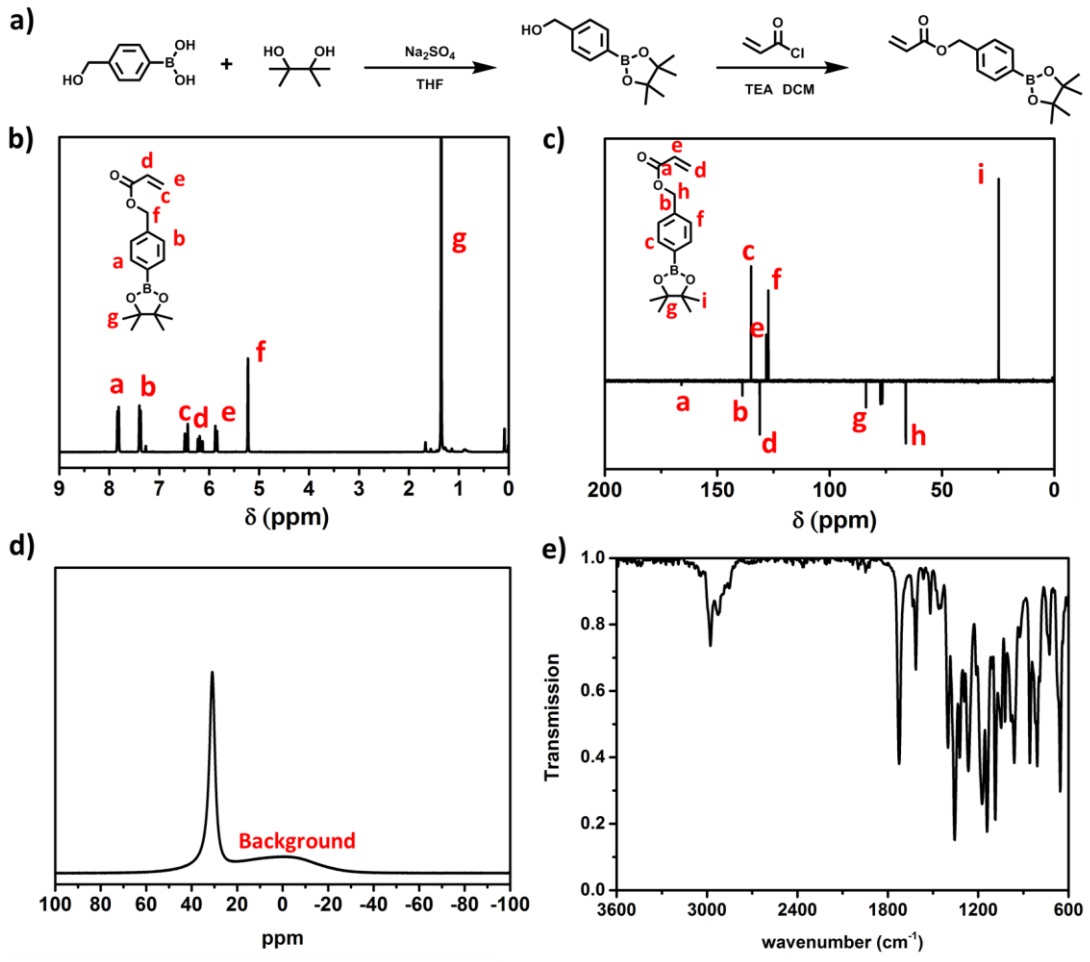

Figure 7.2 Synthesis (a) and characterisation including ^{1}H-NMR (b), ^{13}C-NMR (c), ^{11}B-NMR (d) and FTIR (e) of the $B_{pin}A$ monomer.

7.2.2.2 Synthesis of the PBzA homopolymer using copper-mediated photoinduced living radical polymerisation (CP-LRP)

Although the CP-LRP technique has been well developed and has proven to be applicable to polymerise various monomers with a good compatibility with biological agents as demonstrated in chapter 4,[1] monomers with an aromoatic/phenyl ring have never been explored. It is uncertain whether this technique is feasible to polymerise the monomers with an aromatic ring as the monomer may absorb light which can potentially interfere with the polymerisation. Therefore, a benzyl acrylate (BzA) monomer was first used as a model to verify the possibility of using CP-LRP before the polymerisation of $B_{pin}A$.

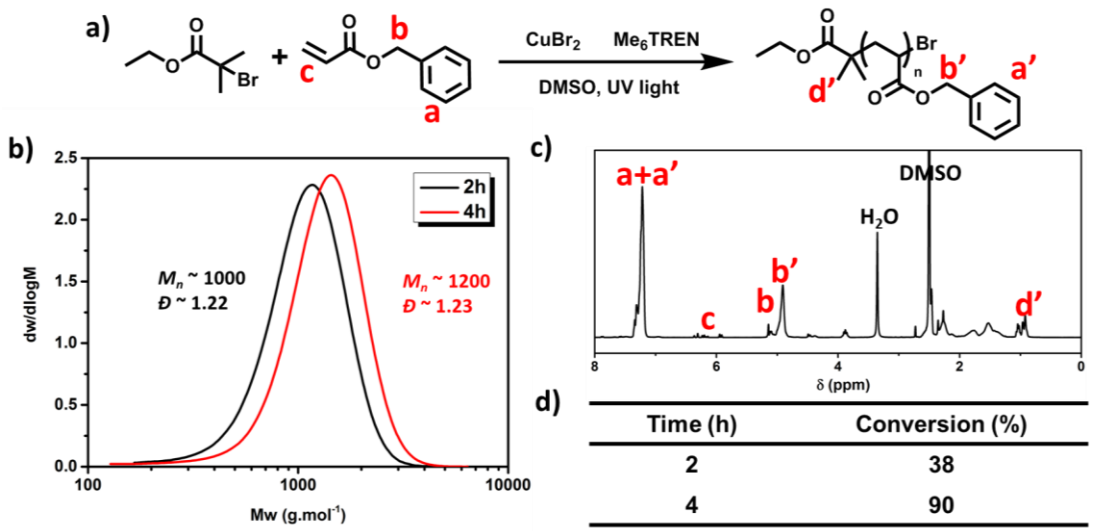

Figure 7.3 a) Synthesis of PBzA using a standard CP-LRP condition. b) DMF GPC traces of the reaction mixture at 2 and 4 h. c) ^{1}H-NMR of the reaction mixture at 4h. d) The conversion of the polymerisation at 2 and 4 h calculated from ^{1}H-NMR.

Using the standard CP-LRP condition, a poly(benzyl acrylate) homopolymer (PBzA) with DP = 10 was synthesised in DMSO under UV irradiation (λ_{max} ~ 360 nm) with the initiator, ethyl α-bromoisobutyrate (EBiB), $CuBr_2$ and the ligand (Me_6TREN) ([BzA]:[EBiB]:[Me6TREN]:[$CuBr_2$] = 10:1:0.12:0.02). Samples were taken from the

reaction mixture at 2 and 4 hours. The polymerisation occurred smoothly and the conversion reached 90% after 4 h (Figure 7.3). The formed polymer stayed with a narrow $Đ$ ($Đ$ < 1.3) during the polymerisation process and an increased molecular weight was observed as a function of conversion, indicating the monomer with an aromatic ring can be polymerised using CP-LRP.

Subsequently, the homopolymerisation of $B_{pin}A$ was conducted under a similar polymerisation condition and left overnight to examine the compatibility of $B_{pin}A$ monomer with CP-LRP. Unfortunately, although the polymerisation did occur, precipitation was obersved during the polymerisation, which was considered to be homopolymer of $B_{pin}A$ ($PB_{pin}A$). Considering the low polarity of the pinacol protection group, the formed polymer may also have a low polarity which makes it immiscible with the DMSO solvent. Io order to obtain confirmation, the precipitate was then collected and dissolved in $CDCl_3$ for ^{1}H-NMR analysis. The typical peaks on the $B_{pin}A$ monomer were all found from the precipitate (Figure 7.4c). The broadening of these peaks however indicated the formation of the $B_{pin}A$ homopolymer. A further GPC analysis revealed a peak with a broad $Đ$ ($Đ$ ~ 1.53) and a high molecular weight tail (Figure 7.4a), suggested the polymerisation lost control during the polymerisation as a result of the precipitation.

Therefore, another trial of the homopolymerisation of $B_{pin}A$ was conducted under a similar polymerisation procedure using DMF as an alternative solvent. This time, no precipitation was found during the polymerisation process and the polymer was obtained with narrow dispersity ($Đ$ ~1.14) analysed from the GPC, suggesting the monomer is compatible with the CP-LRP technique. However, unlike CP-LRP of other acrylate monomers, the conversion was limited to 90% even the reaction was

left overnight, indicating the polymerisation was slower when DMF was used as solvent.

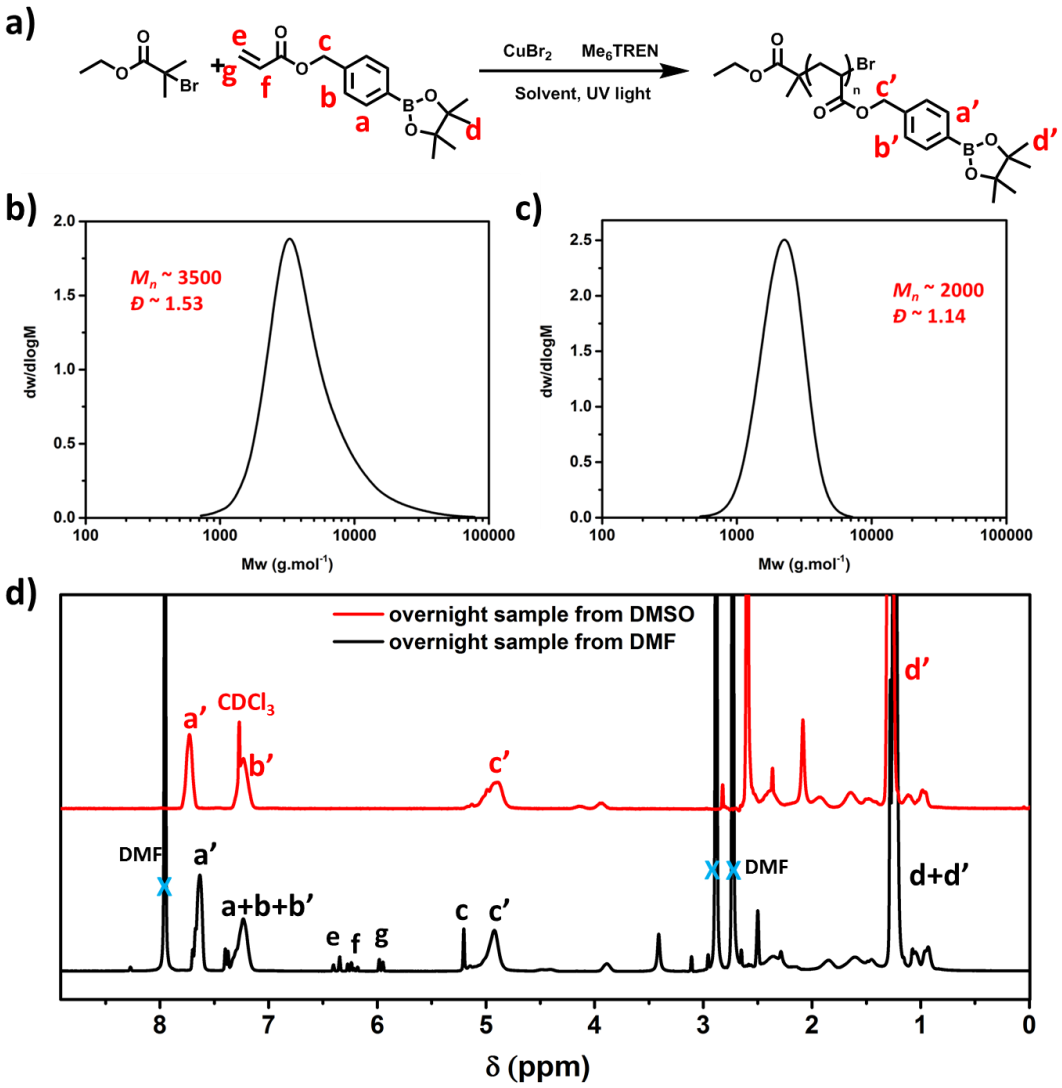

Figure 7.4 a) Homopolymerisation of $PB_{pin}A$. DMF GPC traces of the overnight samples of the polymerisation of $PB_{pin}A$ under the UV light using b) DMSO or c) DMF as solvents. d) ^{1}H-NMR of the overnight sample of the polymerisation of $PB_{pin}A$ in DMSO (red trace, $CDCl_3$ as solvent) and in DMF (black trace, DMSO as solvent).

7.2.2.3 Synthesis of an amphiphilic block copolymer containing PBA units via CP-LRP

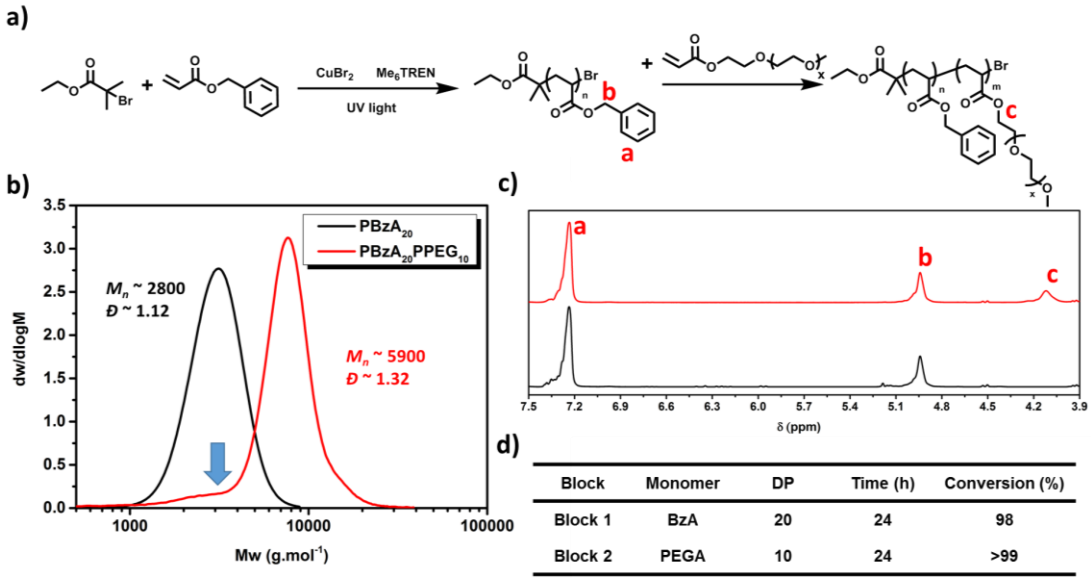

Figure 7.5 a) Synthesis of $PBzA_{20}$- $PPEGA_{10}$ block copolymer. DMF GPC traces (b) and ^{1}H-NMR (c) of the first block (black) and the copolymer (red). d) The conversion of each block calculated from ^{1}H-NMR.

In order to form micelles under physiological condition, the synthesis of an amphiphilic block copolymer was required. The biocompatible water soluble monomer, $PEGA_{480}$, was selected as the hydrophilic part of the molecule. Again, benzyl acrylate was first used to build up the hydrophobic block. DP = 10 and DP = 20 was selected for each block. Due to the poor solubility of $B_{pin}A$ polymer in DMSO, the polymerisation of the block copolymer was performed in DMF. The polymerisation of BzA was first conducted, followed by the one-pot sequential addition of PEGA monomer (Figure 7.5). Due to the slow polymerisation rate in DMF, each block was left overnight to reach high conversion (Figure 7.5d). The disappearance of the protons from the double bonds along with the peak broadening from both monomers from ^{1}H-NMR confirmed both BzA and PEGA were

polymerised during the process (Figure 7.5c). Through the GPC analysis, a clear molecular weight increase was observed after the polymerisation of the second block and the disperisty remained relatively narrow ($Đ$ ~ 1.32), suggesting the successful synthesis of the PBzA-PPEGA block copolymer (Figure 7.5b). However, a notable small molecular weight peak which belonged to the first block remained in the product (Figure 7.5b highlighted by the arrow), suggesting some of the PBzA polymer chains were 'dead' that is unable to be reinitiated before the addition of the second block, which is likely to be attributed to the long reaction time.

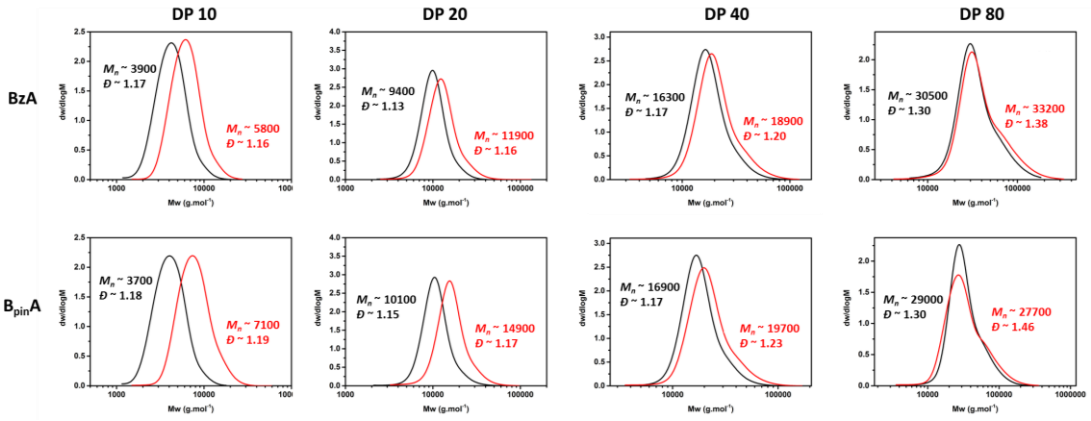

Figure 7.6 DMF GPC traces of the polymerisation of the first block using PEGA with various DPs (black) after 6h and the overnight polymerisation of the second block using hydrophobic monomers (BzA or $B_{pin}A$) for the synthesis of the amphiphilic block copolymers. Black traces: homopolymer (PPEGA), red traces: block copolymers.

To improve the yield of the block copolymer as well as to save the reaction time, DMSO was used for the polymerisation of the block copolymer for both BzA and $B_{pin}A$ monomers with PEGA. Due to the poor solubility of $B_{pin}A$ polymer in DMSO, the sequence of the monomer addition was adjusted so as to form a PPEGA macroinitiator followed by *in situ* chain extension with the hydrophobic monomer (BzA or $B_{pin}A$) to improve the solubility of the formed copolymer during the polymerisation. The DP for the hydrophilic part was varied from DP 10, 20, 40 and

80, while the DP of the hydrophobic monomer was fixed as 20 for comparison. The polymerisation was performed again using the standard CP-LRP condition ([PEGA]:[BzA/B_{pin}A]:[EBiB]:[Me_6TREN]:[$CuBr_2$] = 10/20/40/80:20:1:0.12:0.02), of which the first block was polymerised for 6 h before the addition of the second block and the reaction was left overnight to ensure the high conversion for both blocks. Samples were taken at 6 h and overnight for ^{1}H-NMR and GPC analysis. As shown in Figure 7.6, all the polymerisation were well controlled and relative narrow dispersities ($Đ$ < 1.5) were obtained. The PEGA monomer was consumed nearly quantitatively in the first 6 h in all cases and the conversion of the second hydrophobic monomer was also high (~ 96 – 99%) after the overnight reaction (Table 7.1).

Table 7.1 Summary of ^{1}H-NMR and DMF GPC characterisation of the amphiphilic block copolymers, $PBzA_{20}PPEGA_x$ and $PB_{pin}A_{20}PPEGA_x$.

	DP of PEGA	1st Conversion (%)	2nd Conversion (%)	1st M_{nGPC} (g·mol^{-1})	1st $Đ$	2nd M_{nGPC} (g·mol^{-1})	2nd $Đ$
BzA	10	95	99	3900	1.17	5800	1.16
	20	97	99	9400	1.13	11900	1.16
	40	99	> 99	16300	1.17	18900	1.20
	80	98	96	30500	1.30	33200	1.38
B_{pin}A	10	92	> 99	3700	1.18	7100	1.19
	20	96	99	10100	1.15	14900	1.17
	40	96	98	16900	1.17	19700	1.23
	80	99	96	29000	1.23	27700	1.46

All polymers showed an increase molecular weight after the polymerisation of the second block, with the exception of the copolymer prepared from PPEGA DP80, suggesting a successful polymerisation of the block copolymers. Due to the nature of the PEGA monomer and the large size of PPEGA DP80 macroinitiator, no significant change was observed from the GPC analysis before and after the polymerisation of

the second blocks *via* the addition of the hydrophobic monomers even though the conversions were nearly full (Table 7.1). In order to confirm the formation of the both block copolymers, $PBzA_{20}PPEGA_{80}$ and $PB_{pin}A_{20}PPEGA_{80}$, a diffusion-ordered spectroscopy (DOSY) NMR was obtained. Through DOSY, the mixed compounds can be distinguished by their different diffusion coefficients while one distribution will be found in a block copolymer. As shown in Figure 7.7, the ester signals belonging to $BzA/B_{pin}A$ units (peak a and a' in Figure 7.7) and PEGA units (peak b and b' in Figure 7.7) showed the same diffusion coefficient, indicating both monomers were attached on the same polymer, confirming the formation of a block copolymer.

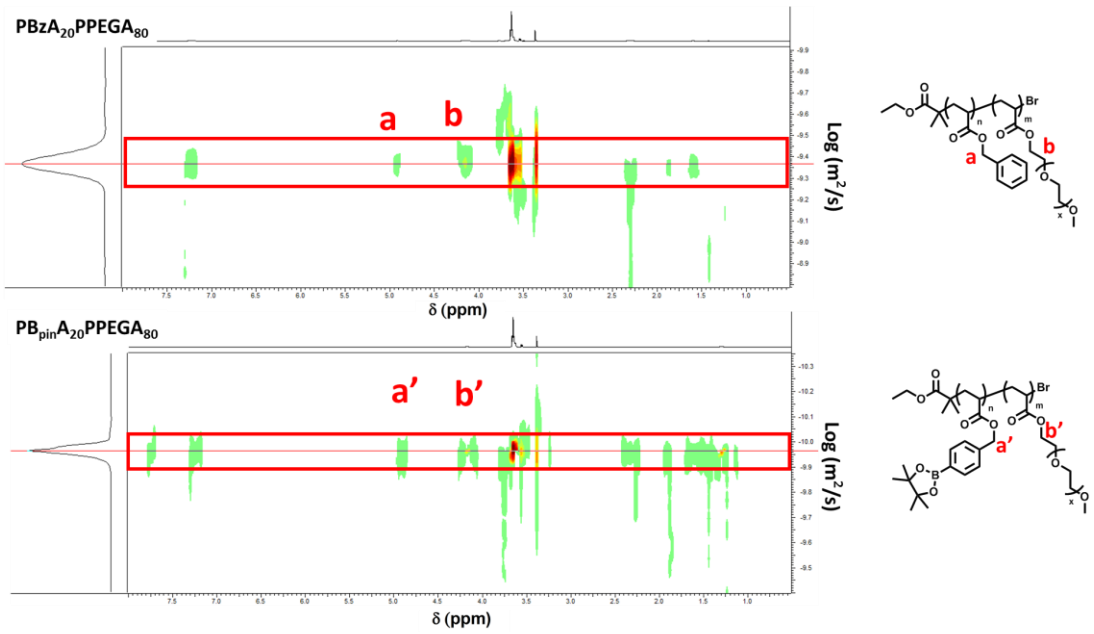

Figure 7.7 DOSY data of $PBzA_{20}PPEGA_{80}$ and $PB_{pin}A_{20}PPEGA_{80}$ (in $CDCl_3$).

7.2.2.4 Recovery of the boronic acid groups from the $PB_{pin}A_{20}PPEGA_x$ block copolymer

To regenerate the boronic acid groups from the pinacol protecting groups, as well to prevent the hydrolysis of the ester bonds on the monomer units, the $B_{pin}A_{20}PPEGA_x$ (x = 10, 20, 40, 80) block copolymers were dialysed separately under

weak acidic conditions (0.12 M HCl in 1:1 water/THF) for 2 days. The deprotected polymers were not very soluble in most of the common organic solvents due to the recovery of the boronic acid groups. In addition to the bulky size of the polymers and their amphiphilic behaviour, no reliable data with good signal-to-noise ratio was acquired from the deprotected polymers through ^{13}C-NMR, ^{11}B-NMR, or GPC analysis.

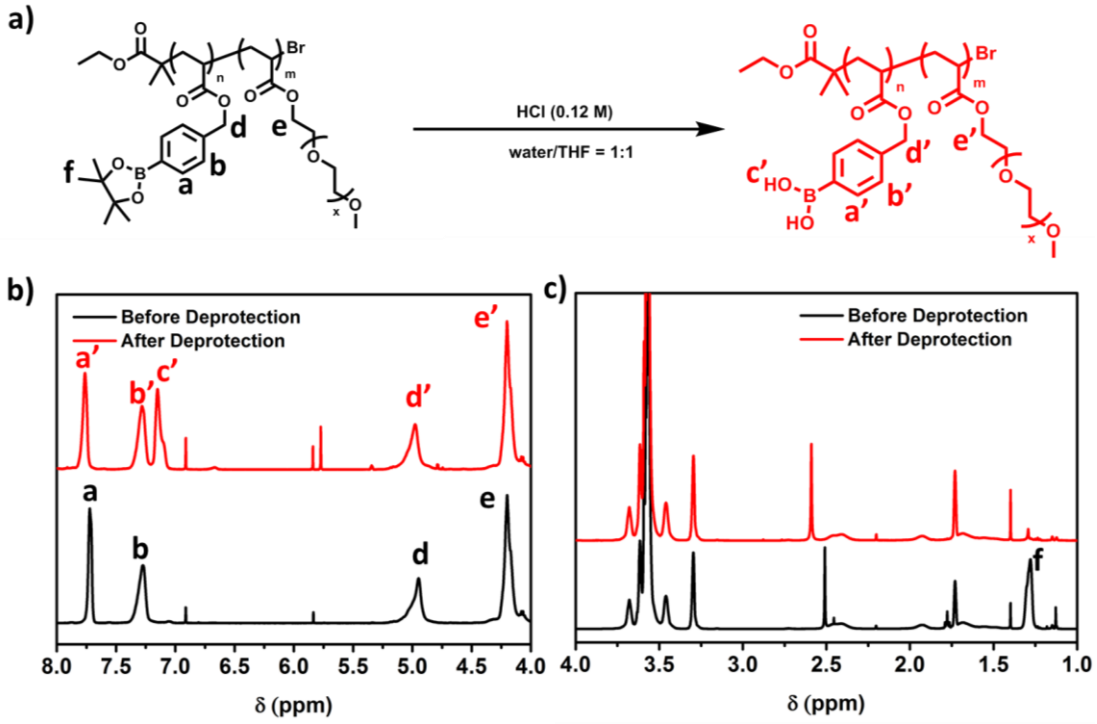

Figure 7.8 a) Removal of the pinacol protection of $BpinA_{20}PPEGA_{40}$ through the dialysis under an acid condition. The zoomed-in ^{1}H-NMR spectra (b, δ = 4 - 8 ppm) and (c, δ = 0 - 4 ppm) of the polymers before and after deprotection process in d_8-THF.

Fortunately, the deprotection efficiency could be determined through ^{1}H-NMR analysis of the obtained polymers in d_8-THF. As shown in Figure 7.8, the main structure of the polymers including both monomer ester bonds (peak d (d'), e (e')) before and after the deprotection process remained unchanged, suggesting the polymer backbone and the ester linkage on the side chains survived during the deprotection process. The original pinacol peaks (peak f in Figure 7.8) disappeared nearly

completely and a new peak which represented to be the boronic acid groups (peak c') appeared along with a slight shift of peak a to peak a', indicating the successful removal of the protection groups.

7.2.3 UV analysis for the interactions between the amphiphilc block copolymers and Nys

7.2.3.1 Investigation on the increased solubility of Nys in the presence of $PB_{acid}A_{20}PPEGA_x$ or $PBzA_{20}PPEGA_x$ through the UV spectroscopy

After obtaining the boronic acid containing polymers, the interaction between Nys and the boronic acid groups on polymers was then investigated. As Nys has a UV absorbance pattern at a range of 280 - 350 nm, the UV absorbance of these peaks could be used to quantify the amount of Nys presented in the aqueous media. Therefore, a binding study was performed on the obtained polymers with Nys *via* UV spectroscopy. Excess of Nys (1-2 mg) was introduced into 1 mL of each polymer solution of the same concentration (10 mg/mL) and mixed well for 24 h. Each sample was then centrifuged (10000 rpm) to remove the non-bounded Nys. The supernatants were then diluted 10 fold by PBS (1X, pH = 7.4) and analysed by UV-Vis spectroscopy. As the block copolymers can be self-assembled into higher-ordered structures (Figure 7.11 and 7.12), Nys can interact with the hydrophobic core of the assembly either through non-covalent encapsulation or through covalent 'cross-linking', resulting in a stronger UV response. As expected, the UV absorbance of Nys solution were all higher in the presence of polymers compared to the pure water (Figure 7.9). Interestingly, the UV aobsorbance of the Nys signal was much higher (2.4 - 9.8 times) in the presence of the

$PB_{acid}A_{20}PPEGA_x$ polymers than the $PBzA_{20}PPEGA_x$ polymers with similar molecular weight. A notable UV shift of the highest peak of Nys (λ_{max} = 305 nm→310 nm) was also observed from the samples with $PB_{acid}A_{20}PPEGA_x$ while it stayed the same as the Nys in water (λ_{max} = 305 nm) for the samples with $PBzA_{20}PPEGA_x$. All these data implied that, beyond the hydrophobic interaction between Nys and the aromatic ring structure, the boronic acid groups on PBA units can react with the hydroxyl groups on Nys, forming a water-soluble Nys-polymer complex ($PB_{acid}A_{20}PPEGA_x$-Nys complex). Notably, less Nys was solubilise in the presence of $PB_{acid}A_{20}PPEGA_{10}$ compared to the other $PB_{acid}A_{20}PPEGA_x$. This can be explained by the large aggregates formed by the unstable self-assembly caused by the short hydrophilic PPEGA DP10 (Figure 7.11).

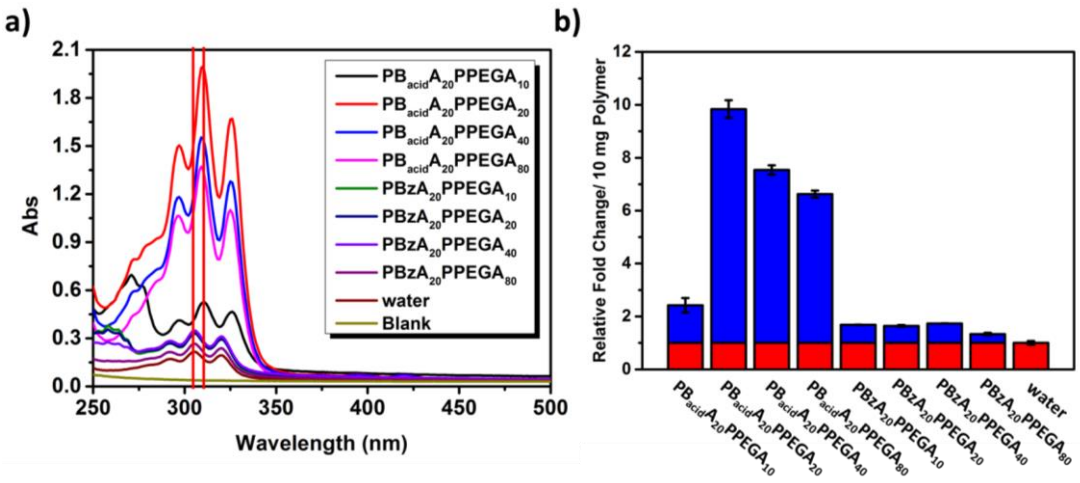

Figure 7.9 a) UV spectra of the Nys in the presence of different polymers in aqueous media. b) The relative solubility of Nys in aqueous media with different polymers.

7.2.3.2 Stimuli release of Nys from $PB_{acid}A_{20}PPEGA_x$-Nys complex in aqueous media

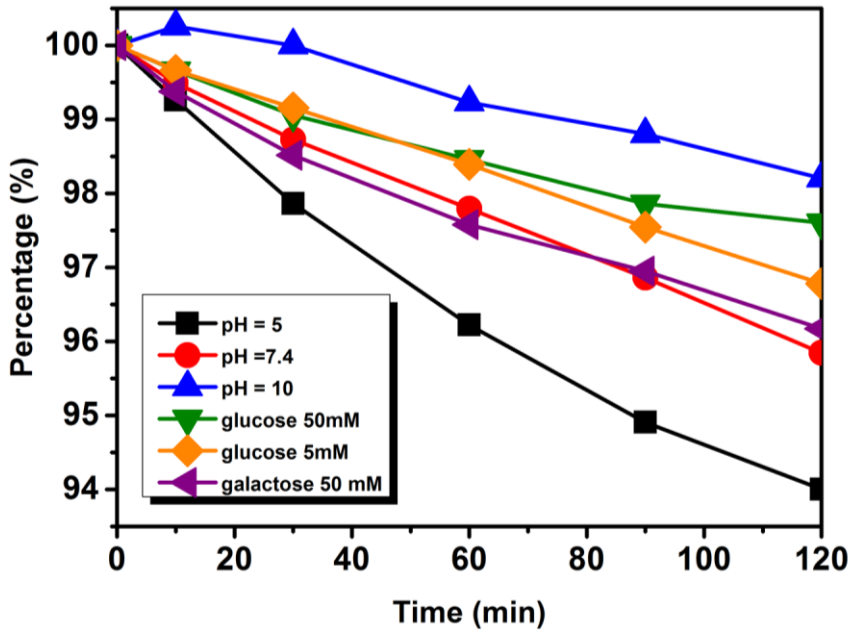

Figure 7.10 Release percentage of Nys from the $PB_{acid}A_{20}PPEGA_{20}$ using different stimuli in aqueous solution monitoring by the UV spectroscopy.

After confirming the formation of $PB_{acid}A_{20}PPEGA_x$-Nys complexes, a further investigation on the responsive release of Nys from the complexes was carried out. As the boronate is more stable in a basic condition rather than an acid pH,[2] the effect of the pH of the environment upon the stability of the complex was conducted using $PB_{acid}A_{20}PPEGA_{20}$-Nys as a model. Acidic pH (pH = 5), physiological pH (pH = 7.4) and a basic pH (pH = 10) were selected for comparison. As shown in Figure 7.10, the signals of Nys in the different pH solutions all decayed over the time, suggesting instability of the formed boronate between Nys and polymers in the presence of water. The decrease rate of the Nys signal was faster at a lower pH, which is consistent with the stability of the boronate bond at various pH. Since the boronate is a dynamic bond responsive to diols such as sugars,[3, 4] two sugars (glucose and galactose, 50 mM) existing in the human body were also tested on $PB_{acid}A_{20}PPEGA_{20}$-Nys complex. A

lower concentration of glucose (5 mM), mimicking the sugar concentration in the human blood was also tested for comparison. Surprisingly, although the Nys signal also decreased over the time, < 4% of the Nys signal decrease was observed during the 2 h test in all cases. Taking account that the release rates are similar to the one from PBS buffer and the difference among the sugars was not significant (< 1%), it was hard to draw a convincing conclusion at this stage. Although further experiments are needed, this may be explained by the fact that the sugar units are very hydrophilic so that it is difficult to interact with the formed boronate bonds between Nys and polymer that are buried in the hydrophobic core.

7.3 Conclusions & Ongoing work

In this chapter, it has been found that chemical reaction forming boronate ester bonds can occur on the hydroxyl groups, either on 1,2-diol or 1,3-diol, of Nys using boronic acid containing compounds. This founding has then been exploited to develop a dynamic delivery system for Nys to increase its aqueous solubility. In order to obtain a suitable boronic acid-rich self-assembly system, CP-LRP was intestigated to polymerise monomers with an aromatic ring. After the optimisation on CP-LRP, amphiphilic block copolymers with boronic acid side chains and various lengths of the hydrophilic part ($PB_{acid}A_{20}PPEGA_x$) have been successfully synthesized. The similar block copolymers without the boronic acid groups ($PBzA_{20}PPEGA_x$) were also synthesized using BzA monomer for comparison. Although both types of block copolymers improved the Nys solubility, the $PB_{acid}A_{20}PPEGA_x$ showed a much greater improvement (2.4-9.8 times to Nys in pure water) thanks to the interaction between Nys and the boronic acid groups on the side chains. Although the Nys release rates from the $PB_{acid}A_{20}PPEGA_x$ polymers remained low at this stage, it showed a

potential to be responsive to some stimuli, at least pH, suggesting the possible targeted delivery of Nys using these polymers. The ongoing work will be focused on the possibility of increasing the release rate of Nys from the polymers and the investigation of the self-assembly and morphology change of each polymer in the presence/absence of Nys. The antifungal activity of each polymer-Nys complex and the related acute cytotoxicity are also needed to be analysis.

7.4 Experimental

7.4.1 Materials

7.4.1.1 Chemicals

All chemicals were purchased from Sigma-Aldrich and used directly unless otherwise stated. BzA monomer (97%, stab. with ca 150 ppm) was purchased from Alfa Aesar and used without purification. HBA was obtained from Apollo Scientific Ltd. HPLC solvents are obtained from VWR international, LLC. The dialysis membranes were purchased from Spectrum® Laboratories, Inc.

7.4.2 Instruments

7.4.2.1 NMR

^{1}H-NMR, ^{11}B-NMR, ^{13}C-NMR spectra were recorded on Bruker HD 400, HD 500 and AV 500 spectrometers and referenced relative to deuterated solvent shifts using deuterated solvents obtained from Aldrich.

7.4.2.2 GPC

GPC was acquired from an Agilent PL50 equipped with two Agilent Polargel Medium Columns eluting with DMF (0.1 M LiBr) as an additive at 50 °C. The flow rate was 1 mL/min and detection was achieved using differential refractive index detector. Molecular weights were calculated relative to narrow PMMA standards.

7.4.2.3 FTIR

Infrared absorption spectra were recorder on a Bruker VECTOR-22 FTIR spectrometer using a Golden Gate diamond attenuated total reflection (ATR) cell.

7.4.2.4 ESI-(tandem) mass spectroscopy (ESI-MS and ESI-MS/MS)

ESI-MS and ESI-MS/MS was done on the Bruker MaXis II instrument (equipped with ESI source) through direct infusion at 1 μL/min. The sample was dissolved and diluted in 50% ACN/water with 0.1% formic acid and run in the positive ion mode.

7.4.2.5 Transmission electron microscopy (TEM)

TEM data was obtained using either JEOL 2000FX TEM or JEOL 2100FX TEM at an acceleration voltage of 200 kV. All TEM samples were prepared on graphene oxide (GO) on lacey carbon (300 mesh) copper grids or GO on holey carbon (300 mesh) copper grids to get high contrast images without staining. Typically, 10 μL sample was pipetted on a grid and left for 1 min before blotted away. Each grid was then air-dried for 15 minutes.

7.4.3 Synthesis

7.4.3.1 Synthesis of $B_{pin}A$ monomer

The synthesis of BpinA monomer was a two-step synthesis adapted from the literature. The pinacol protected HBA (HB_{pin}) was synthesized as followed. HBA (9.14 g, 0.060 mol, 1 equiv.) and pinacol (10.42 g, 0.088 mol, 1.5 equiv.) were dissolved with 70 mL toluene in a 100 mL round-bottle flask and reflexed at 120 ºC using a Dean-Stark apparatus for 24 h until a homogeneous solution was obtained. The reaction solution was then evaporated to remove both toluene and most unreacted pinacol under reduced pressure. A further recrystalisation using hot hexane was conducted to remove the trace pinacol remaining in the products. The final product HB_{pin} was a clear needle-like crystal with a yield of 85% (12.1g, 0.51 mmol).

^{1}H-NMR (500 MHz, $CDCl_3$, 298 K) δ (ppm) = 1.35 (s, C(C$\underline{H}_3$)$_2$), 4.68 (br. s, HOC$\underline{H}_2$-), 7.35 (d, J = 8.1, HOCH$_2$CC$\underline{H}$), 7.80 (d, J = 7.9, -C$\underline{H}$CB).

^{13}C-NMR (125 MHz, $CDCl_3$, 298 K) δ (ppm) = 24.75 (C($\underline{C}$H$_3$)$_2$), 65.06 (HO$\underline{C}$H$_2$-), 83.76 ($\underline{C}$(CH$_3$)), 126.00 (-OCH2C$\underline{C}$H), 134.95 (-$\underline{C}$HCB), 144.00 (HOCH$_2\underline{C}$).

After obtaining the pure HB_{pin}, HB_{pin} (11.7 g, 0.050 mol, 1 equiv.) and 14 mL TEA (0.10 mol, 2 equiv.) was then dissolved with 60 mL anhydrous DCM into a 250 mL round-bottom flask in an ice bath. 6 mL acryloyl chloride (0.075 mol, 1.5 equiv.) in 20 mL anhydrous DCM was added dropwise into the flask in 1 h under nitrigen. The reaction mixture was then stirred at ambient temperature for 24 h. After the reaction, the DCM was removed on a rotary evaporator and the crude mixture was redissolved by diethyl ether followed by the removal of the TEA salt by filtration. The filtrate was then washed with saturated ammonium chloride solution three times and

the organic phase was collected and dried with anhydrous $MgSO_4$. The crude product was purified by flash chromatography (diethyl ether/hexane, 0%-7%). The product was obtained as an off-white solid with the yield of 60% (8.67 g, 0.30 mol). ^{1}H-NMR, ^{13}C-NMR, ^{11}B-NMR and IR were shown in Figure 7.2.

7.4.3.2 Homopolymerisation of the $PBzA_{10}$ and $PB_{pin}A_{10}$ polymer

The polymerisation of BzA and B_{pin}A was conducted using a standard CP-LRP condition. The ratio of initiator (EBiB), $CuBr_2$, ligand (Me_6TREN) and monomer (BzA or B_{pin}A) was set as 1: 0.02: 0.12: 10. DMSO or DMF was used as solvent. 1-2 volume equiv. of solvent was used for the synthesis. The reaction was left under UV with a cooling plate (CAMLAB, KP283, temperature was set to 5 ^{o}C, the actual temperature for the reaction mixture is ~ 20 ^{o}C) under a UV lamp (λ_{max} ~ 360 nm) for 4h or overnight. For example, the synthesis of $PBzA_{10}$ in DMSO was conducted as followed. 1.5 mg $CuBr_2$ (0.0067 mmol, 0.02 equiv.), 10 µL Me_6TREN (0.037 mmol, 0.12 equiv.), and 0.5 mL BzA (3.3 mmol, 10 equiv.) was dissolved in a 7 mL vial with 0.5 mL DMSO. 48 µL EBiB (0.33 mmol, 1 equiv.) was then added and the reaction mixture was sealed, stirred and degassed under nitrogen for 15 min before the exposure to the UV. The characterisation of the products was shown in Figure 7.3 and Figure 7.4.

7.4.3.3 Synthesis of the amphiphilic block copolymer, $PB_{pin}A_{20}PPEGA_x$ and $PBzA_{20}PPEGA_x$

The block copolymer was synthesised in the similar condition as the polymerisation of BzA using a standard CP-LRP condition. 3 volume of DMSO was used in the second block to promote the solubility of B_{pin}A monomer. For example, $PBzA_{20}PPEGA_{10}$ 100 µL $CuBr_2$ stock solution (7.3 mg/mL in DMSO, 0.0033 mmol,

0.02 equiv.), 5.24 µL Me_6TREN (0.020 mmol, 0.12 equiv.), and 784.9 mg PEGA (1.6 mmol, 10 equiv.) was dissolved in a 7 mL vial with 700 mL DMSO. 24 µL EBiB (0.16 mmol, 1 equiv.) then added and the reaction mixture was sealed, stirred and degassed under nitrogen for 15 min before the exposure to the UV. After 6 h reaction, the BzA monomer (500 µL, 3.3 mmol, 20 equiv.) along with 1.5 mL DMSO was degassed and transferred into the sealed vial. The reaction mixture was left under the UV overnight for the completion of the second block. The 6h and overnight samples were taken for GPC and ^{1}H-NMR analysis. The obtained polymers were then collected and dialysed (1000 MWCO) against THF to remove the DMSO and the trace unreacted monomer. The characterisation of the products was shown in Table 7.1 and Figure 7.8 (black trace).

7.4.3.4 The deprotection of the pinacol groups from the $B_{pin}A_{20}PPEGA_x$

The deprotection of the $PB_{pin}A_{20}PPEGA_x$ was conducted in a dialysis tubing. Instead of THF, 4 L 1:1 water/THF mixture with 40 mL concentrated $HCl_{(aq)}$ (37%, ~12 M) was used for dialysis. The solvent was changed every 12 hours. After 2 days dialysis, the products were quenched *via* the dialysis (1000 MWCO) against THF for another 2 days. The products were then collected and the remaining THF was then blowed off under nitrogen. The typical ^{1}H-NMR of the products was shown in Figure 7.8 (red trace).

7.4.4 Methods

7.4.4.1 UV-Vis analysis for determining the increased amount of solubilised Nys in the precence of amphiphilic block copolymers

10 mg of $PBzA_{20}PPEGA_x$ and $PB_{pin}A_{20}PPEGA_x$ polymers was dissolved in a 2 mL glass vial with 1 mL of HPLC grade water, respectively. Excess of Nys (normally 1-2 mg) was added into each vial and all the vials were sealed and incubated at ambient temperature on a roller mixer (SRT9, Stuart) for 18 h. The samples were then collected and centrifuged at 10000 rpm for 30 min to remove the unsolubilised Nys. The supernatants were then diluted 10 times with PBS 1X. 200 µL of each sample was added into a 96-well plate and the UV-Vis scan (λ = 250 – 500 nm) of each sample was performed by a microplate reader (Synergy HTX Multi-Mode Reader).

For the analysis of the responsiveness of the polymer-Nys complex towards stimuli, pH = 5 (NaAc-AcOH, 50 mM), pH = 7.4 (Na_2HPO_4-NaH_2PO_4, 50 mM), and pH = 10 (Na_2CO_3-$NaHCO_3$, 50 mM) buffers and the sugar containing solutions: glucose (5 mM and 50 mM, in water) and galactose (50 mM, in water) were prepared. 100 uL each solution was added into a 96-well plate along with 100 uL of $PB_{pin}A_{20}PPEGA_{20}$ dilute prepared through the aboved procedure. The UV-Vis scan (λ = 250 – 500 nm) of each sample was collected at 0 min, 10 min, 30 min, 60 min, 90 min and 120 min. The UV absorbance at λ = 310 nm was compared to the 0 min sample to obtaine the relative amount Nys remaining in the solution.

7.4.4.2 Sample preparation for the self-assembly of block copolymers for TEM analysis

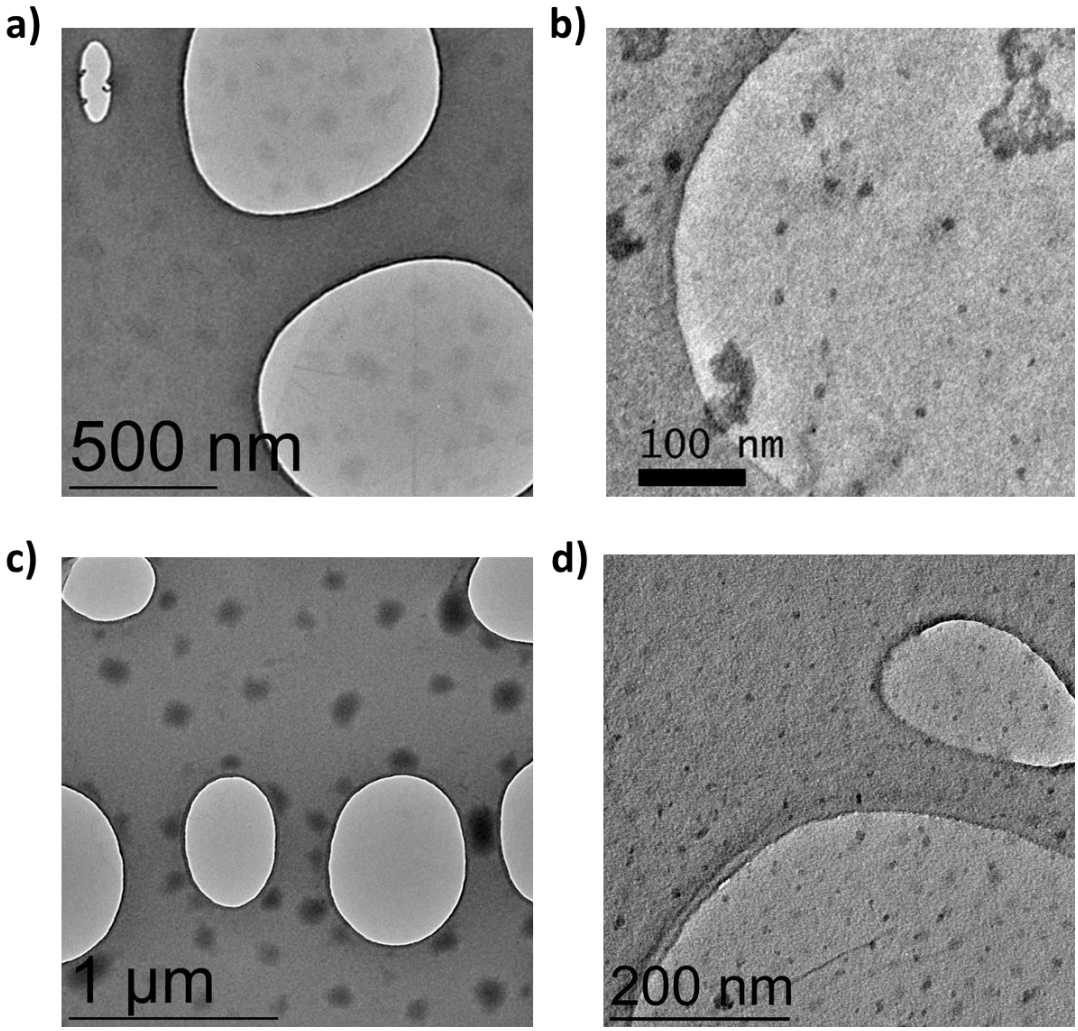

Figure 7.11 TEM images of the two morphology found in the self-assembly of $PBzA_{20}PPEGA_{10}$ (a-b), and $PB_{pin}A_{20}PPEGA_{10}$ (c-d) block copolymers in water (1 mg/mL).

The samples for TEM were prepared by dissolving a certain amount of polymers (typically 5-10 mg) in a 14 mL vial using 1 mL DMF and followed by vigorous stirring (700 rpm) under nitrogen. 9 mL of HPLC grade water was added into the vial at a rate of 0.02 mL/min. Each sample was then dialysed against water (solvent changed 3 times a day) for 2 days. After collecting each sample into a 50 mL Eppendorf tube, a

certain amount of water was added into the tube to reach a desired concentration (typically 5 mg/mL or 1 mg/mL).

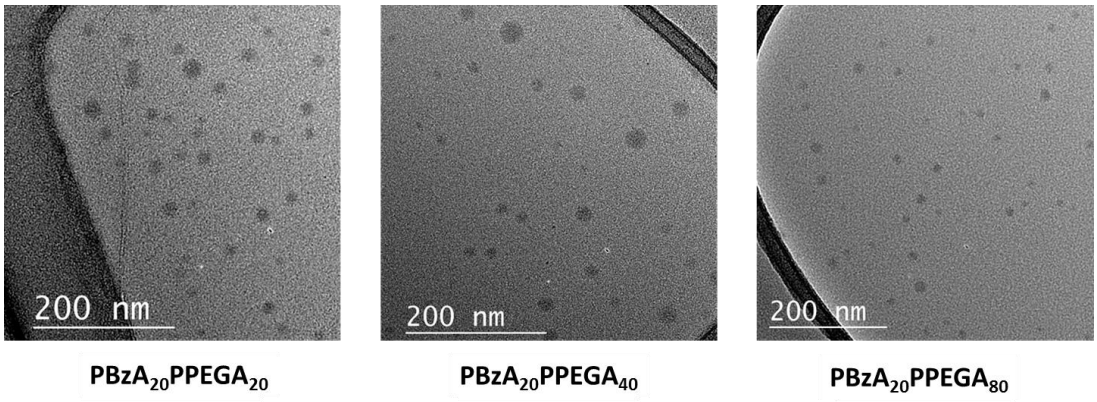

Figure 7.12 TEM images of the self-assembly of $PBzA_{20}PPEGA_{20}$, $PBzA_{20}PPEGA_{40}$, and $PBzA_{20}PPEGA_{80}$ block copolymers in water (5 mg/mL).

7.5 References

1. A. Anastasaki, V. Nikolaou, Q. Zhang, J. Burns, S. R. Samanta, C. Waldron, A. J. Haddleton, R. McHale, D. Fox, V. Percec, P. Wilson and D. M. Haddleton, *J. Am. Chem. Soc.*, 2014, **136**, 1141-1149.

2. L. He, D. E. Fullenkamp, J. G. Rivera and P. B. Messersmith, *Chem. Commun.*, 2011, **47**, 7497-7499.

3. A. P. Bapat, D. Roy, J. G. Ray, D. A. Savin and B. S. Sumerlin, *J. Am. Chem. Soc.*, 2011, **133**, 19832-19838.

4. X. Wu, Z. Li, X.-X. Chen, J. S. Fossey, T. D. James and Y.-B. Jiang, *Chem. Soc. Rev.*, 2013, **42**, 8032-8048.

Chapter 8 *Conclusions & Outlook*

Several strategies for the delivery of two antimicrobial agents, colistin and nystatin (Nys), have been described. It has demonstrated that the potential systemic toxicity of these biological agents to mammals can be reduced while their antimicrobial activity can be retained through the right choices of the polymeric delivery systems.

The main focus of this work has been to modify polymyxin with polymers through a covalent linkage. It has been demonstrated that the polymer (PEG or PPEGA) modification of polymyxins can happen on the Dab or Thr residue(s) of the native colistin or the thiol group of the $Thr^{10} \rightarrow$ Cys polymyxin B (Pol-SH), forming irreversible or releasable bonds under mild conditions. In particular, through a high efficient thiol-acrylate addition reaction, polymers can be introduced onto Pol-SH in aqueous media without the need for a catalyst. It has also been shown that copper-mediated photoinduced living radical polymerisation technique (CP-LRP) is compatibility with polymyxin through the synthesis of polymer-polymyxin conjugates can be achieved through both 'grafting-to' and 'grafting-from' approaches. Due to the large size of the polymers, no antimicrobial activity was observed from the polymyxin conjugates with a single polymer chain attachment through the irreversible modification. However, the antimicrobial activity of polymyxins can be recovered from the colistin polymer conjugates with a releasable linker *via* hydrolysis. It is worth mentioning that the mono PEGylated colistin (col-aaPEG) showed a similar or better antibacterial activity as colistimethate sodium (CMS) and revealed no systemic toxicity, which can be a potential candidate as the alternative for CMS.

To demonstrate the concept that systemic toxicity of colistin can be reduced through a topical administration, a colistin-loaded antibacterial patch for burn wound infections treatment was developed through the encapsulation of colistin with a biocompatible and biodegradable hydrogel (HG-10). Through the dynamic imine bond formation and the 'on-wound' biodegradability of the hydrogel, colistin can be successfully encapsulated into the hydrogel and released effectively under physiological conditions, showing a similar antibacterial activity as the colistin solutions. Furthermore, even colistin-resistant Gram-negative bacterial can be greatly inhibited during the treatment while no overall systemic toxicity was revealed thanks to the localisation delivery of colistin.

The delivery of Nys using polymers has also been described, aiming to improve its poor aqueous solubility and potential toxicity. The sugar amine and the 1,2-/1,3-diol groups of Nys have proven to be possible modification sites for polymer modifications. Through the amine modification of Nys *via* a dynamic imine bond using an mPEG derivative (mPEG-FBA), an mPEG-FBA Nys conjugate can be achieved in an organic medium without a dehydrating agent. Although no pure product has been obtained, the crude mPEG-FBA Nys conjugate exhibited a comparible antifungal activity as native Nys with a reduced cytotoxicity. A polymeric micelle system to improve Nys solubility has also been prepared using a boronic acid containing amphiphilic polymer. Through the labile boronate ester formation between the polymer and the 1,2/1,3-diol groups on Nys, a water soluble Nys polymer complex has been formed and showed a much better solubility (~ 10 times) than native Nys. Although the actual morphology and the biological behaviour of the complex remain unknown, it showed a potential as a formulation to improve Nys chemical and biological performances.

Appendix

The Characterisation of PBA Modification Sites of Nys through Tandem Mass Spectroscopy

The sample for tandem mass spectroscopy was prepared as below. Phenylboronic acid (PBA, 6 mg, 0.049 mmol, 4.5 equiv.) and Nystatin (Nys, 10 mg, 0.011 mmol, 1 equiv.) were dissolved in a 7 mL glass vial with 2 mL DMF. The mixture was left on a roller mixer (SRT9, Stuart) for 18 h before the analysis from the tandem mass spectroscopy. The data and the related analysis were shown below.

Though the ESI-MS data (SFigure 1-3), three Nys containing species charged with both proton and sodium ion were observed from the mixture. The mass of each species fitted perfectly with the Nys, Nys modified with one PBA (PBA_1-Nys) and Nys modified with two PBA (PBA_2-Nys), suggesting the formation of the Nys conjugate with PBA. To confirm that, tandem mass spectroscopy was then conducted.

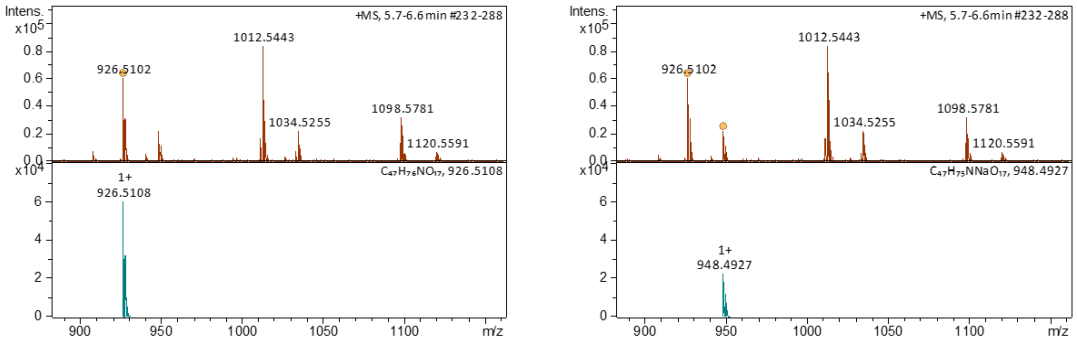

SFigure 1 The ESI-MS data of the mixture (above) and the simulation (below) of the isotopic pattern of Nys peaks, m/z 926 (proton adduct, left) and 948 (sodium adduct, right).

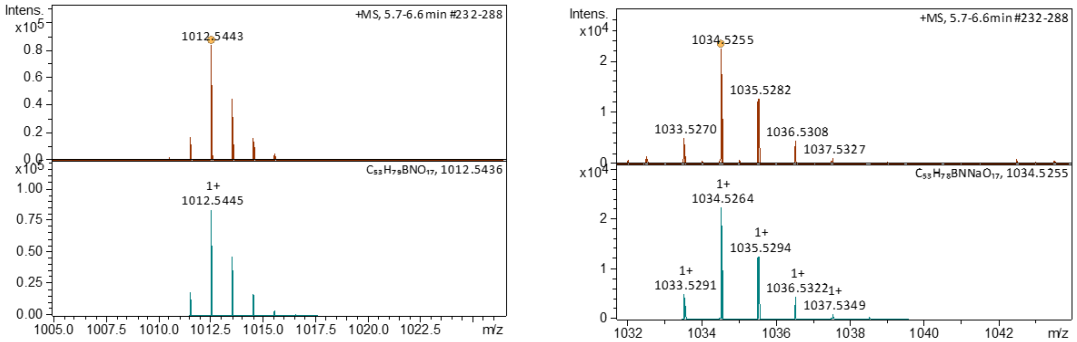

SFigure 2 The ESI-MS data (above) and the simulation (below) of the isotopic pattern of PBA_1-Nys conjugate, m/z 1012 (proton adduct, left), 1034 (sodium adduct, right).

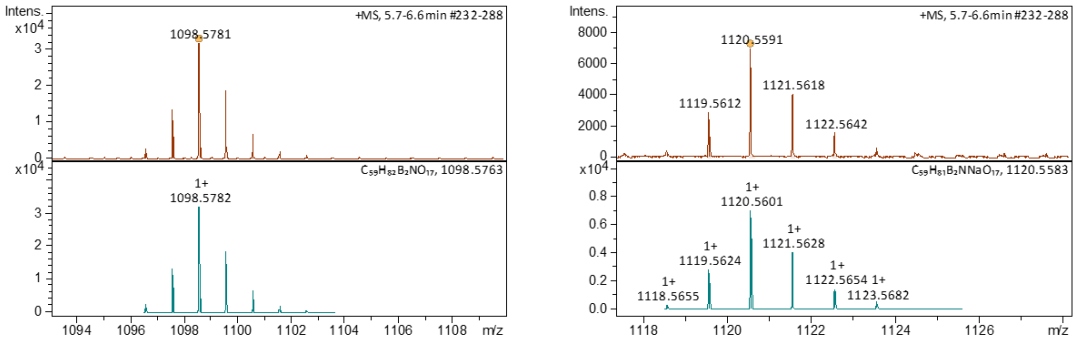

SFigure 3 The ESI-MS data (above) and the simulation (below) of the isotopic pattern of PBA_2- Nys conjugate, m/z 1098 (proton adduct, left), 1120 (sodium adduct, right).

Through the comparison of the ESI-MS/MS data of the three species with proton (m/z 926, 1012, 1098) and sodium ion (m/z 948, 1034, 1120) (SFigure 4-8), it can be seen that similar patterns were observed in all these three species, suggesting all three species contained the structure of Nys. More importantly, extra sets of peaks that shared Nys pattern but with an increased molecular weight of one PBA and two PBA attachments along with a boron and two boron isotopic pattern, respectively, were observed from the MS/MS data of PBA_1-Nys and PBA_2-Nys peaks, suggesting one PBA was covalently attached onto Nys for PBA_1-Nys and two for PBA_2-Nys.

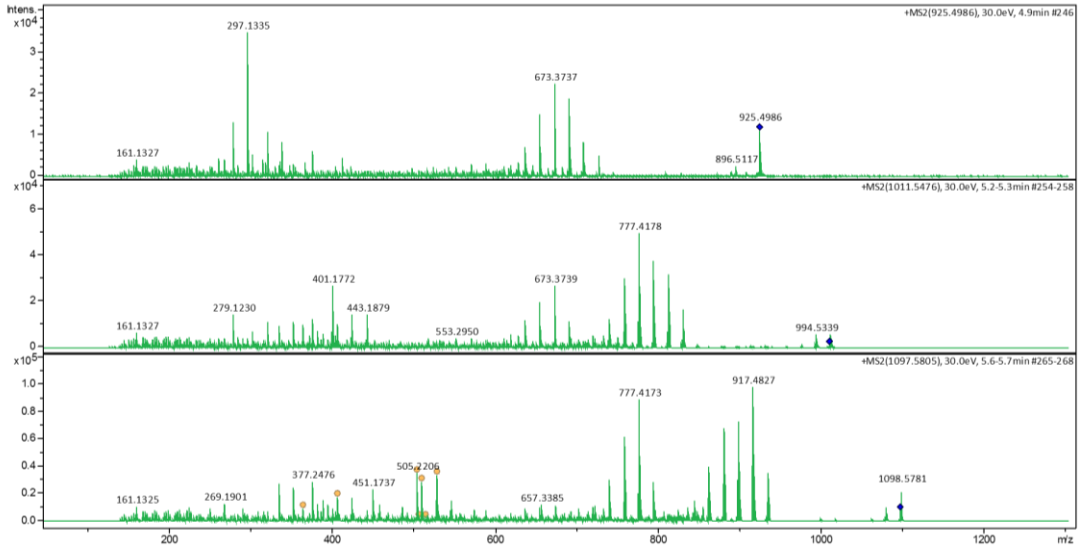

SFigure 4 Comparison of the MS/MS data of m/z 926, 1012, 1098 (full spectra).

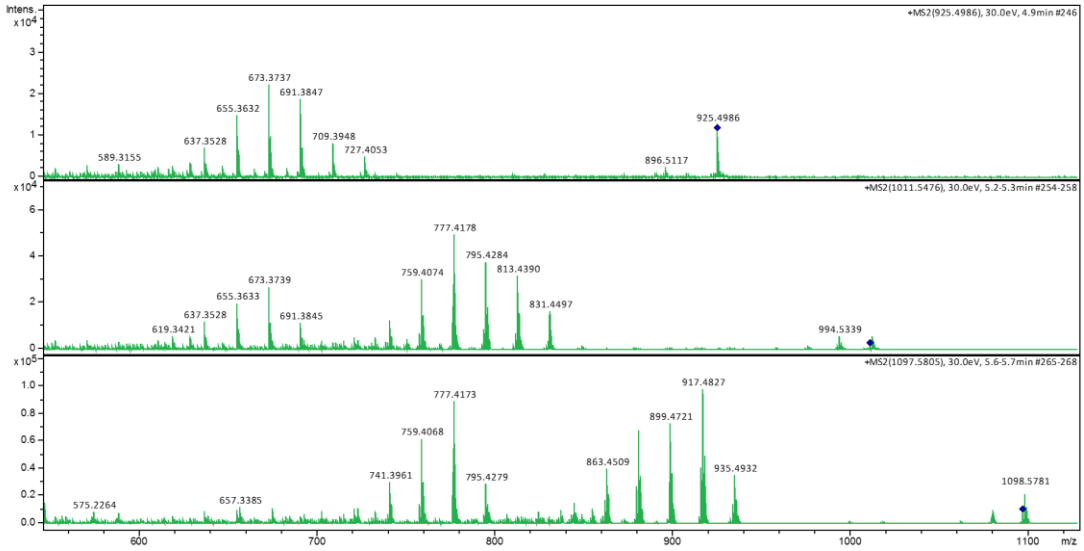

SFigure 5 Comparison of the MS/MS data of m/z 926, 1012, 1098 (zoom-in at high m/z).

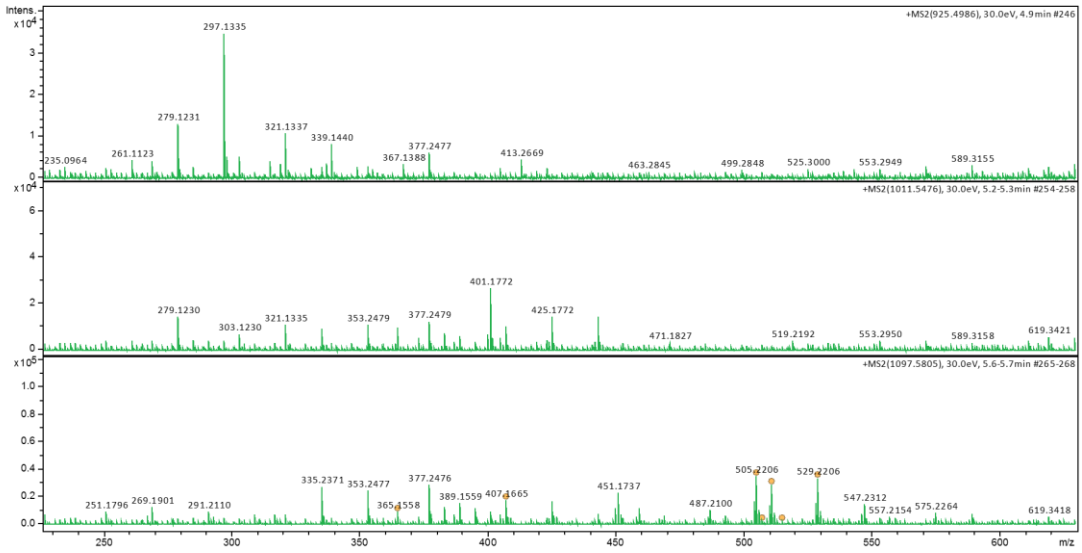

SFigure 6 Comparison of the MS/MS data of m/z 926, 1012, 1098 (zoom-in at low m/z).

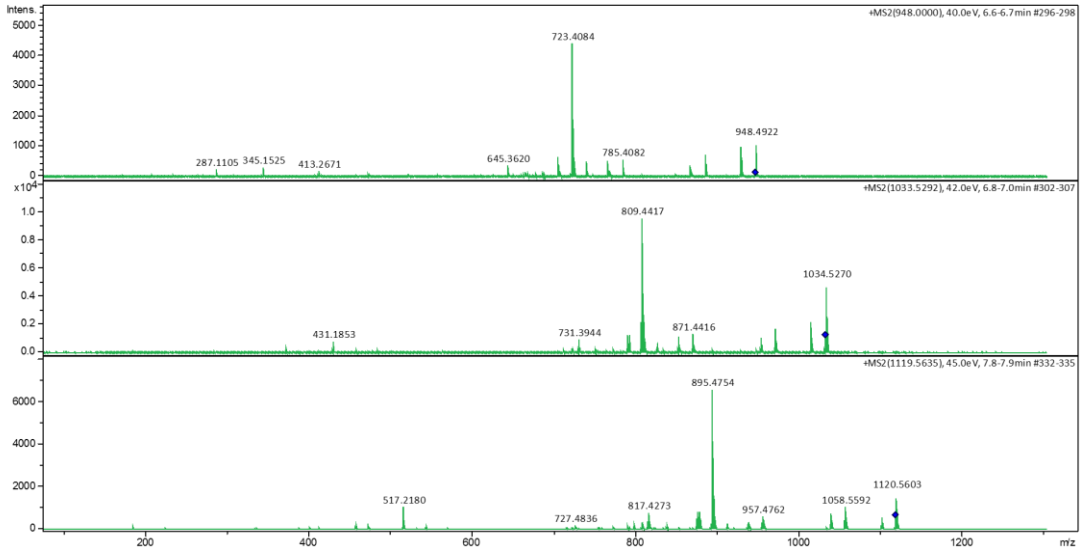

SFigure 7 Comparison of the MS/MS data of m/z 948, 1034, 1120 (full spectra).

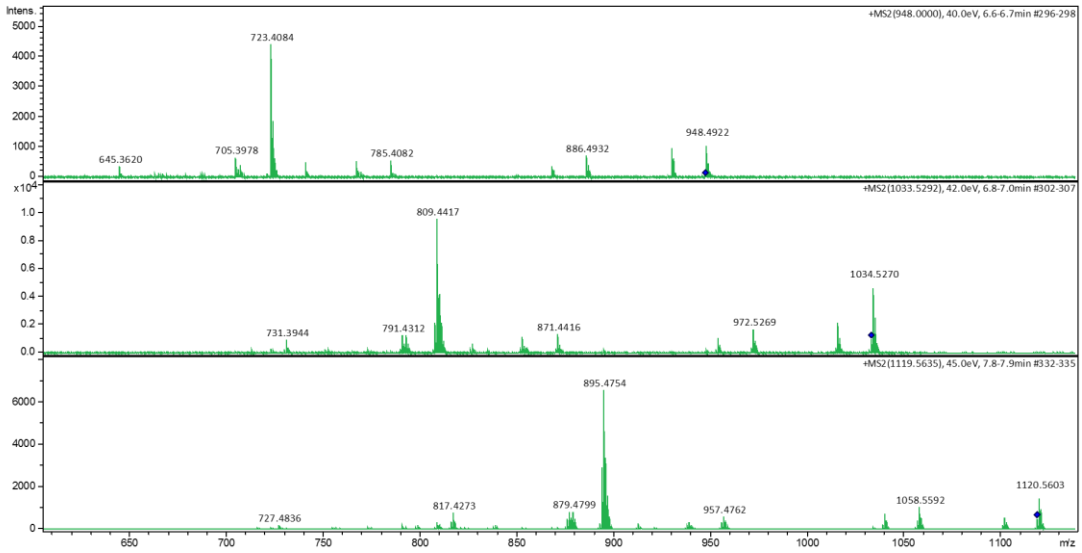

SFigure 8 Comparison of the MS/MS data of m/z 948, 1034, 1120 (zoom-in at high m/z).

As shown in SFigure 9, m/z 723 was found in all the MS/MS data from the sodium adduct of three Nys species. This peak is possibly produced by the loss of the sugar unit, the carboxyl group and one water (can be from any one of the hydroxyl groups) from Nys. This implied that any modification will have to occur elsewhere on the lactone ring, rather than on the amino sugar unit.

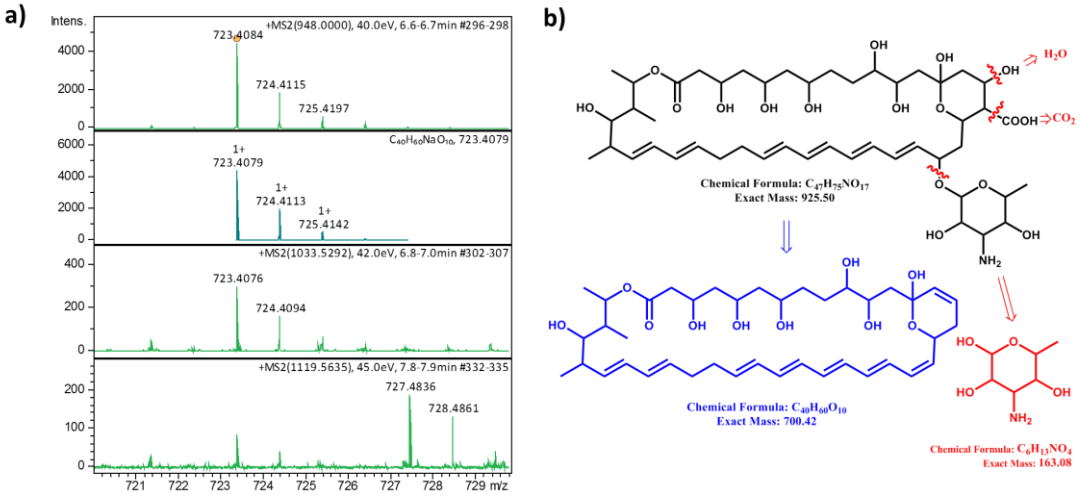

SFigure 9 a) Comparison of the MS/MS data of m/z 948, 1034, 1120 (zoom-in at m/z 723) and the simulation of m/z 723. b) The possible chemical structure of the fragment of m/z 723 (sodium adduct on the blue structure).

The fragment ion m/z 809 was found in both MS/MS data from the sodium adduct of PBA_1-Nys and PBA_2-Nys but not in native Nys (SFigure 10a). The isotopic pattern indicated there was one boron atom in m/z 809. Compared to m/z 723, 86 Da increased from m/z 809, indicating one PBA was attached. The fragment m/z 817 was only found in PBA_2-Nys (SFigure 10b). The isotopic pattern indicated there were two boron atoms in the fragment ion m/z 817. On the other hand, a fragment ion m/z 645 was only found in Nys, which is possible caused by the further loss of a part of the polyene structure ($-C_6H_6$) from m/z 723. The mass difference between m/z 817 and m/z 645 is 172 (= 2 × 86) Da (SFigure 11), implying two PBA were attached on PBA_2-Nys. Furthermore, the fragment m/z 895 with an isotopic pattern containing two boron atoms was only found in PBA_2-Nys, which is 172 Da larger than the fragment ion m/z 723, further confirming PBA_2-Nys was the conjugation between Nys and two PBA.

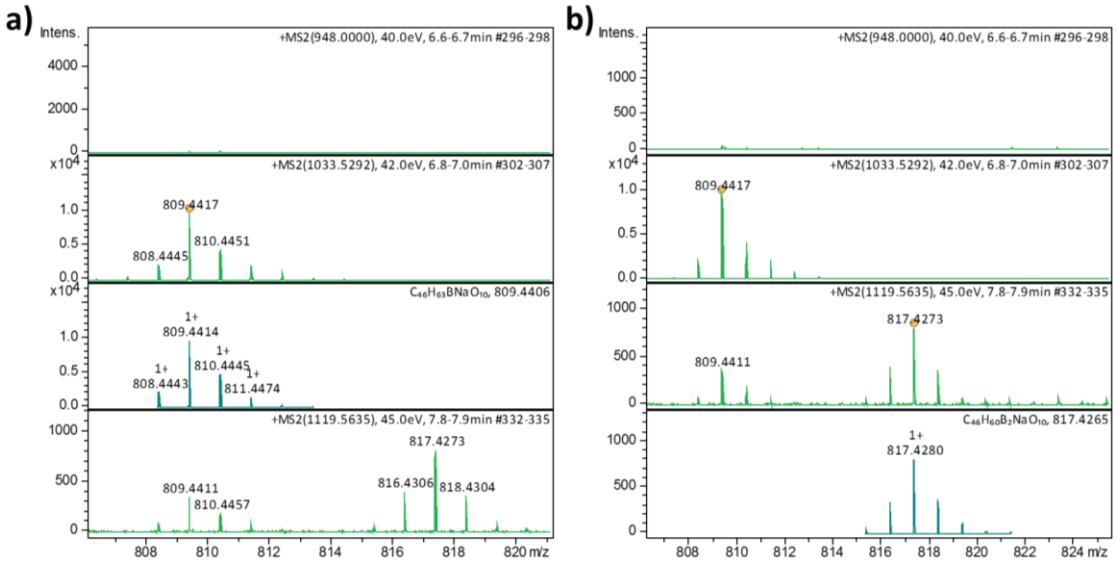

SFigure 10 Comparison of the MS/MS data of m/z 948, 1034, 1120 and the simulation of m/z 809 (a, zoom-in at m/z 809) and m/z 817 (b, zoom-in at m/z 817).

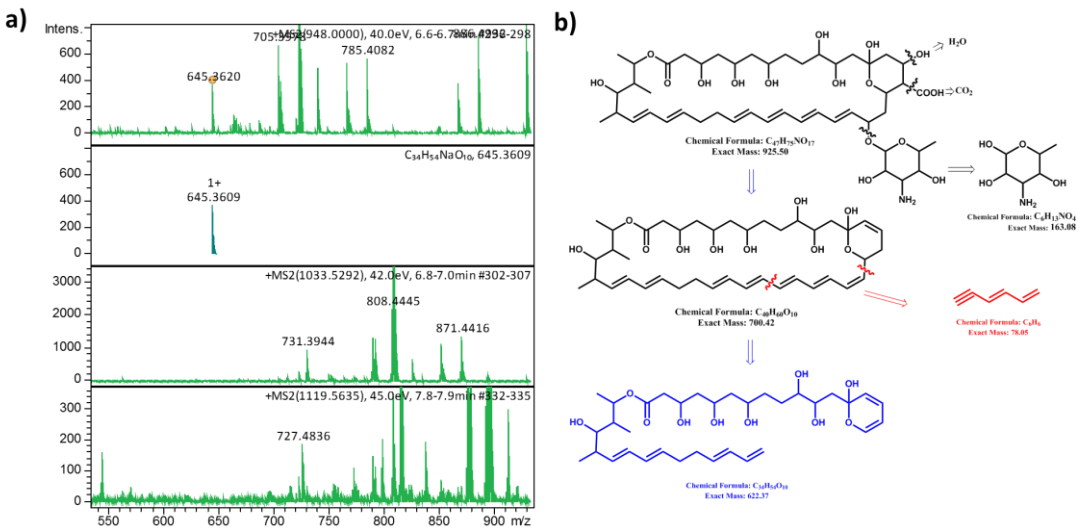

SFigure 11 Comparison of the MS/MS data of m/z 948, 1034, 1120 (zoom-in at m/z 645) and the simulation of m/z 645. b) The possible chemical structure of the fragment of m/z 645 (sodium adduct on the blue structure).

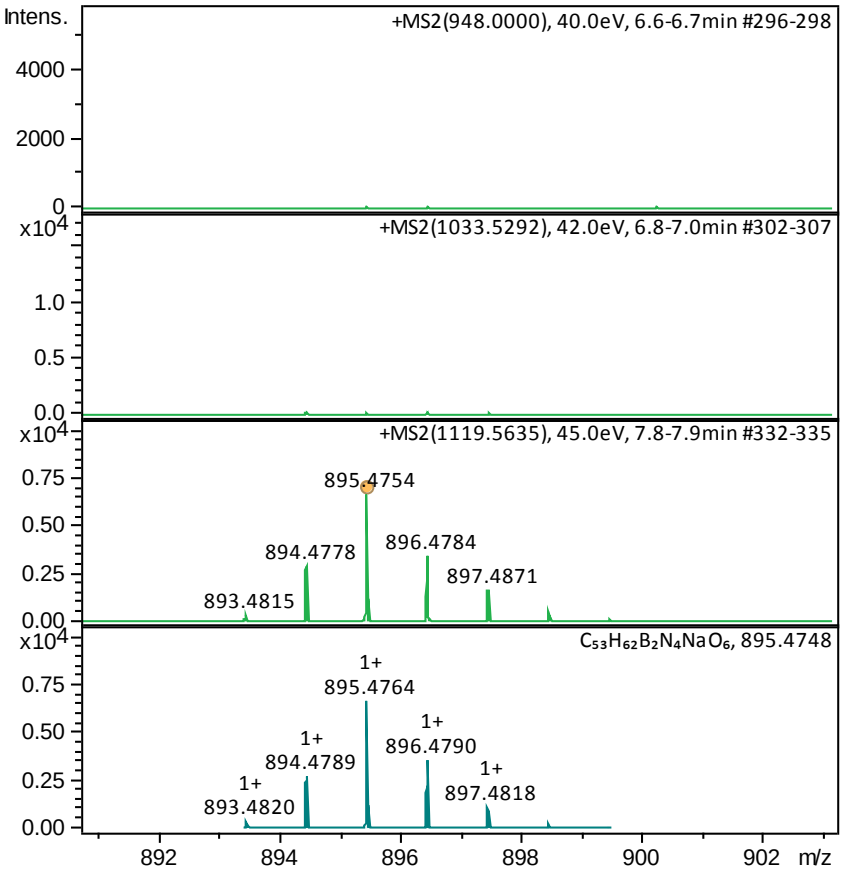

SFigure 12 Comparison of the MS/MS data of m/z 948, 1034, 1120 (zoom-in at m/z 895) and the simulation of m/z 895.

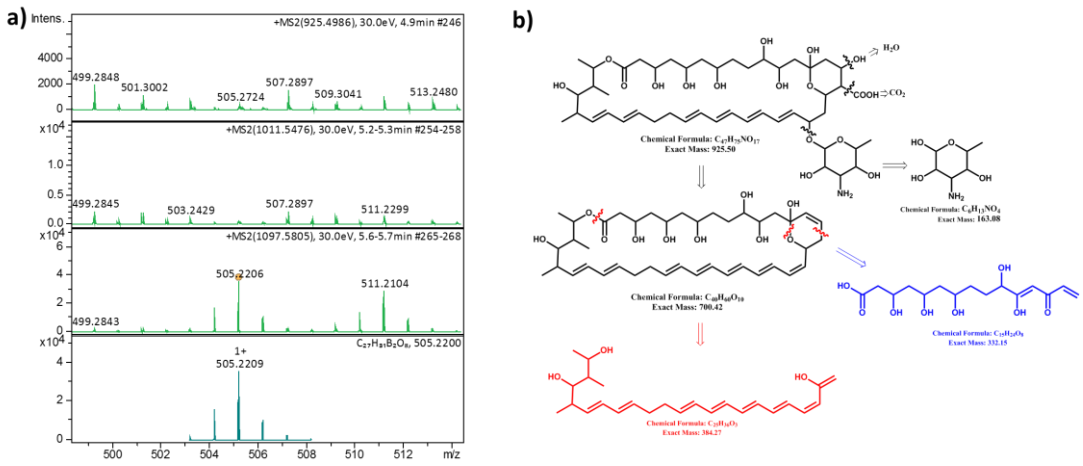

SFigure 13 Comparison of the MS/MS data of m/z 926, 1012, 1098 with the simulation of m/z 505 (a, zoom-in at m/z 505). b) The possible chemical structure of the fragment of m/z 645 (proton adduct with two PBA on the blue structure).

The isotopic pattern indicated there were two boron atoms in the fragment ion m/z 505 (SFigure 13). The most likely chemical formula is $C_{27}H_{31}B_2O_8$. Thus, the chemical formula for the two PBA attachment is $C_{15}H_{24}O_8$. Considering 8 oxygen atoms remain in that structure, the most likely modification is the hydrophilic hydroxyl group-rich part of Nys (highlighted as blue in SFigure 13). As the polyol structure is easy to dehydrate during the analysis and the dehydration could happen on any hydroxyl group. Therefore, a more accurate determination of the modification site was not possible at this stage. However, it can be determined that at most two PBA can be attached on to Nys molecule and the possible modification sites should happen at the hydroxyl groups within the area highlighted in Figure 7.1.

Other m/z patterns with one boron or two boron atoms which were unable to be resolved were listed as below.

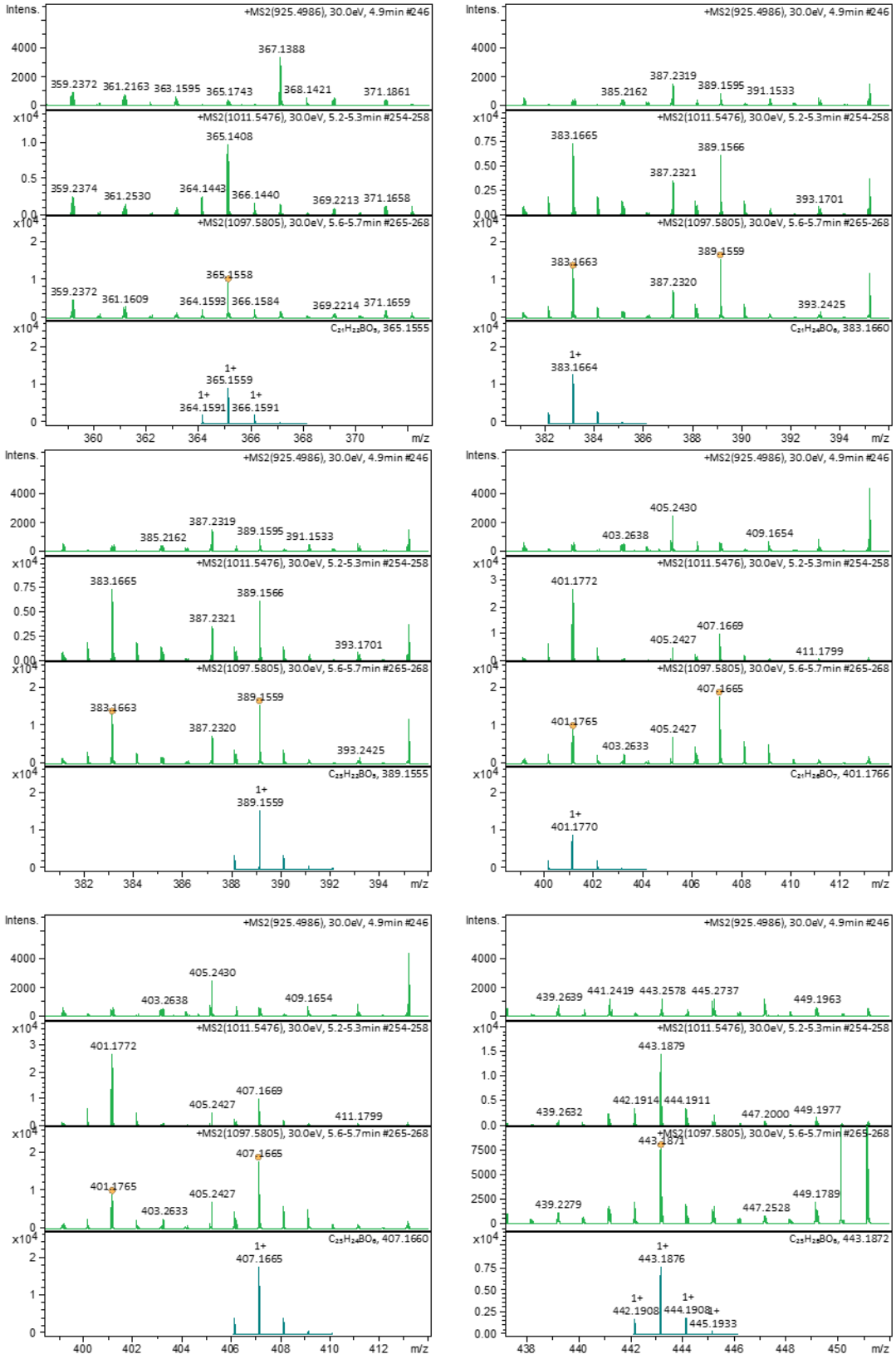

SFigure 14 The fragment ions of m/z 365, 383, 389, 401, 407, 443 found with the isotopic pattern containing one boron atoms from PBA-Nys and PBA_2-Nys.

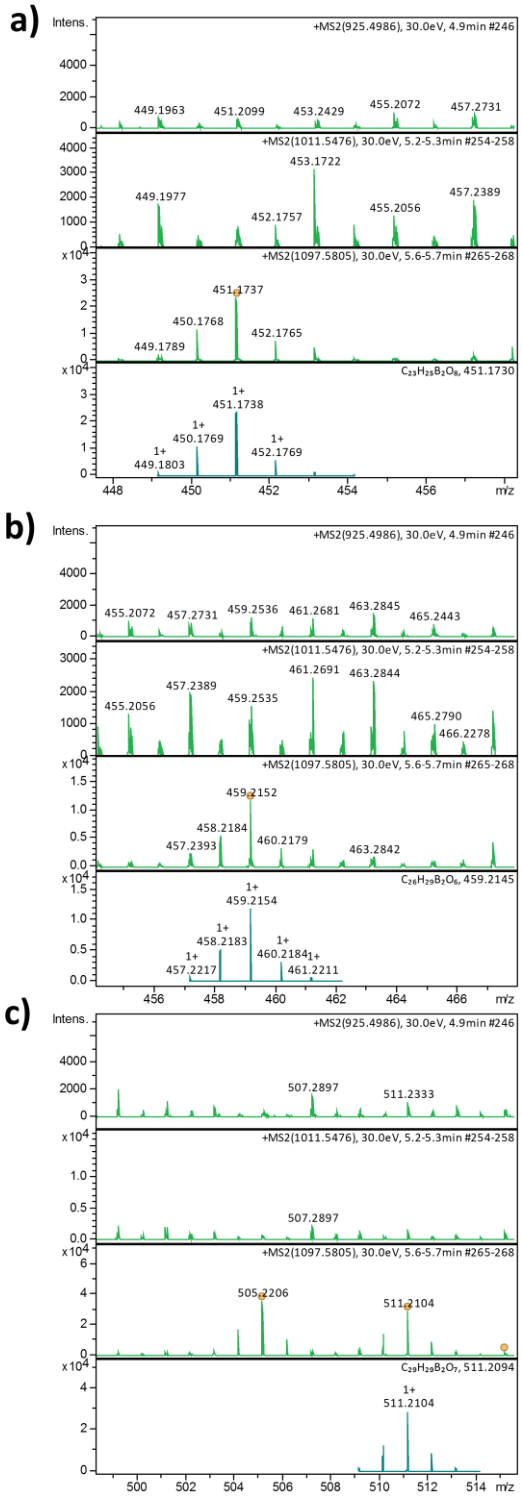

SFigure 15 The fragment ions of m/z 451 (a), 459 (b) and 511 (c) found with the isotopic pattern containing two boron atoms from PBA_2-Nys.